The Role of the CaSR During Development of Cranial Sensory Neurons

A thesis submitted to Cardiff University
for the degree of PhD
2009

Katja Burk

Cardiff School of Biosciences
Cardiff University

ProQuest LLC
789 East Eisenhower Parkway
P.O. Box 1346
Ann Arbor, MI 48106-1346

Index

List of Figures

Acknowledgements

Many thanks to Prof. Alun Davies for his supervision and support over the last few years. Thank you for giving me the opportunity to work in your lab where I gained such valuable experiences.

A big "Thank you" is going to Dr. Sean Wyatt who read this thesis and gave me the opportunity to discuss science in an enthusiastic manner. Thanks for all your support-I owe you a life-long supply of baked beans on toast.

Dr. Thomas Vizard: I want to thank you not only for your support in the lab and helping me with this thesis and project, I also want to thank you for making me laugh, making me think, and for lots of coffee. Ta.

I want to thank all members of the Davies' lab, past and present, who created a relaxed working environment and were always supportive.

Meinen Eltern, Heinz und Angelika Burk, danke ich von ganzem Herzen. Ohne Ihre Unterstützung über all die Jahre und ohne Ihren Glauben an mich wäre ich nicht hier angekommen. Diese Doktorarbeit ist Euch gewidmet.

Estimada Dr. Núria Gavalda, moltíssimes gràcies per haver estar sempre aquí, per tot el teu suport, les converses, la teva paciència inesgotable i, per damunt de tot, la teva amistat i tot el que m'ha comportat. M'ajuda a seguir endavant.

Diolch Yn Fawr, Michelle Lazenby. You where always there to listen. Thanks for making me laugh hysterically and reminding me to wear my corn-flower-blue shirt. Thanks for your support and -most of all- for your friendship.

Dr. Flavio Maina, voglio ringraziarti per tutto il tuo aiuto, il tuo tempo, i tuoi suggerimenti e per aver trovato le soluzioni per quei problemi tanto difficili da risolvere. Je tiens encore à te remecier pour ton soutien, ta patience; pour ton ecoute et pour avoir ete toujours present ce qui signifie pour moi, un monde.

Last but not least I want to thank Fran Martin, Petar Misljen and Trefor Farrimond for discussions covering a range of important issues from different beer types to superheroes. But most of all thanks for giving me a place to come home to.

Für meine Eltern

Abstract

Virtually all studies on the molecular regulation of axonal growth have been carried out on axotomised neurons that regenerate axons in culture and are dependent on neurotrophic factors not only for survival but also for axonal growth. The technical difficulty of obtaining and culturing early, newly differentiated neurons that initiate axonal growth for the first time in culture has meant that developmentally relevant *de novo* axonal growth has been almost ignored. Numerous studies have shown that axonal regeneration from embryonic and postnatal neurotrophic factor-dependent neurons is regulated by a variety of signalling pathways that influence the assembly and stability of key components of the cytoskeleton in growth cones. Depending on neuron type, these can include MEK, PI3 kinase, GSK3, NF-κB and calcium signalling. The extent to which these pathways are important for *de novo* axonal growth, and how their importance changes as axonal growth becomes responsive to neurotrophic factors during early development is not known.

I have used the experimentally advantageous placode-derived sensory neurons of the chicken embryo to study the molecular basis of *de novo*, neurotrophic factor independent axonal growth and to compare this neurotrophic factor-dependent axonal growth at later stages of development. These neurons can be dissected from the earliest stages in their development and cultures can be established in which neurons extend axons for the first time. Previous work has shown that at this stage of development, axonal growth is independent of neurotrophic factors and its rate is correlated with target distance. For example, neurons of the nodose ganglion have the most distant targets, the fastest axonal growth rate and survive longest before becoming dependent on the neurotrophic factor BDNF for survival, whereas neurons of the vestibular ganglion have the nearest targets, slowest axonal growth rate and survive for the shortest time before acquiring BDNF dependence.

My initial studies focused on the role of the extracellular calcium-sensing receptor (CaSR), a G protein coupled receptor that has recently been shown to regulate axonal growth from sympathetic neurons during the stage when neurons are innervating their targets. I found that during the stage of development when the earliest axons of placode-derived sensory neurons are growing to their targets, nodose ganglion neurons (which have the fastest axon growth rates) express the highest levels of the CaSR, and vestibular neurons (which have the slowest axon growth rates) express the lowest levels of the CaSR. Experimental manipulation of CaSR activation in cultured nodose neurons at the stage in development when their axons are normally growing to their targets markedly affects axon growth rate

(enhancing activation increases growth rate whereas reducing activation has the opposite effect). In contrast, similar manipulations of CaSR activation in cultured vestibular neurons have no effects on axonal growth rate. These findings suggest that the CaSR plays an important role in the regulation of *de novo* axonal growth rate. Manipulating CaSR activation in older, BDNF-dependent nodose neurons at the stage in development when these neurons are innervating their targets also demonstrated a role for the CaSR in promoting axonal growth at this stage.

Having demonstrated a role for the CaSR in promoting axonal growth at these two successive stages of development, I then characterised the intracellular signalling pathways that mediate the effects of the CaSR on axonal growth at these stages. Using Western blot analysis and pharmacological inhibitors of PI3-kinase, GSK3 and MEK1/2, I discovered a clear switch in the signalling pathways that are involved in promoting axon elongation between early BDNF-independent stages of *de novo* axon growth to later BDNF-dependent stages of axon growth. Whereas PI3-kinase signalling plays a pivotal role in transducing CaSR-enhanced, neurotrophin-independent axon growth, GSK3 signalling plays a major role in transducing the growth enhancing effects of CaSR activation on BDNF-promoted axonal growth from older BDNF-dependent nodose neurons. My findings suggest that PI3-Kinase and GSK3 signalling are not linked in developing nodose neurons, but are regulated independently of each other. Furthermore, Western analysis also suggests the operation of a novel activation mechanism of GSK3 in axon growth in BDNF-dependent nodose neurons that involves tyrosine phosphorylation of GSK3 rather than serine phosphoryation following CaSR activation. In all, my studies have revealed several novel and unexpected aspects of regulation of axonal growth by the CaSR during the early stages of neuronal development.

Abbreviations

AC	Adenylyl cyclase
ADH	Autosomal dominant hypercalcaemia
Akt	Protein kinase B
APC	Adenomatous polyposis coli protein
BDNF	Brain-derived neurotrophic factor
Ca^{2+}	Calcium Ion
CaSR	Calcium sensing receptor
cDNA	Complemenary DNA
Ci	cubitus interruptus, transcription factor
CK1	Casein Kinase 1
CNS	Central nervous system
Cos	Costal 2
CRMP2	Collapsin response mediator protein 2
DMSO	Dimethylsulphoxide
DN CaSR	Dominant negative calcium sensing receptor
ECD	Extracellular Domain
ElF2B	Initiation factor
FasL	Fas-Ligand
FHH	Familial hypocalciuric hypercalcaemia
Fus	fused
Fzl-r	Frizzled receptor
GAPDH	Glyceraldehyde 3- phosphate dehydrogenase
Grb2	Growth factor receptor- bound protein 2
GSK3	Glycogen- synthase kinase 3
GPCR	G protein coupled receptor
Hsp25/27	Heat shock protein 25/27
IRS 1	Insulin receptor substrate 1
JNK	c-jun N-terminal kinase
LRP 5/6	Low- density lipoproetin receptor related protein
mRNA	Messenger RNA
MAPK	Mitogen- activated Protein Kinase
NGF	Nerve growth factor

NT-3 (4/5)	Neurotrophin – 3 (4/5)
NTC	No template control
PI3-K	Phosphatidylinositol-3-kinase
PBS	Phosphate buffered saline
PCR	Polymerase chain reaction
PDK1	pyruvate dehydrogenase kinase isozyme 1
PKC	Protein Kinase C
PLC	Phospholipase C
PLD	Phospholipase D
PNS	Peripheral nervouse system
PP-1	Protein Phosphatase 1
Ptc	patched receptor
Pten	Phosphatase and Tensin homologue
PTH	Parathyroid hormone
PtdIns	phosphatidylinositol biphosphate/ triphosphate
$p75^{NTR}$	p 75 neurotrophin receptor
RalGDS	ras-related guanine nucleotide dissociation stimulator
RT-PCR	Reverse transcriptase polymerase chain reaction
SCG	Superior cervical ganglion
SFO	Subfornical organ
Smo	smoothed receptor
Trk	Tropomycin- related kinase
Wnt	Wingless + Int 1
WT	Wild type
WT CaSR	Wild type calcium sensing receptor

Chapter 1

Introduction

1.Introduction

The work of this thesis focuses on two key aspects of neuronal development, the regulation of *de novo* axonal growth in early, neurotrophic factor-independent neurons and the control of neuronal growth in axotomized, neurotrophic factor dependent-neurons. This research was carried out on the cranial sensory neurons of the vestibular and nodose ganglia of the embryonic chicken peripheral nervous system. I will therefore begin this introductory chapter with a brief overview of the anatomy and development of the peripheral nervous system, with an emphasis on the cranial sensory neurons. I will describe growth cone structure and function, and provide an overview of some of the key extracellular signalling proteins, especially neurotrophic factors, that influence the growth of neuronal processes and regulate the survival of neurons during development. I will introduce the extracellular calcium sensing receptor (CaSR), as the influence of this receptor on neurite growth forms a major part of the research described in this thesis. Finally, I will outline the main intracellular signalling pathways that mediate the effects of neurotrophic factors and the CaSR, with a particular emphasis on the pathways I have studied in this thesis, namely, the glycogen synthase kinase-3 (GSK3), phosphoinositol 3-kinase (PI 3-kinase) and mitogen-activated protein (MAP-kinase) pathways.

2. Organization of the peripheral nervous system

The peripheral nervous system consists of somatic and autonomic divisions. The somatic division is comprised of sensory neurons and the axons of motoneurons. Sensory neurons, whose cell bodies reside within cranial sensory ganglia and dorsal root ganglia, convey sensory information from skin, muscles, joints and viscera to the CNS. Motoneurons, whose cell bodies reside within the spinal cord and brainstem of the CNS, innervate skeletal muscle. The autonomic division is comprised of three subdivisions: the sympathetic, parasympathetic and enteric nervous systems. The sympathetic and parasympathetic subdivisions use a disynaptic pathway to influence their target tissues. The cell bodies of preganglionic neurons reside within the brainstem and spinal cord. The axons of preganglionic neurons synapse with postganglionic neurons whose cell bodies reside in paravertebral and prevertebral sympathetic ganglia and in terminal and cranial parasympathetic ganglia. The enteric nervous system is comprised of a network of sensory, visceral motor and interneurons that are predominantly embedded in plexi lining the digestive system. Enteric sensory neurons detect intestinal stretch and the chemical composition within the lumen of the digestive system. This information is processed by interneurons that regulate motor neuron functions like peristalsis, control of blood vessel diameter and secretion of digestive enzymes. Although the enteric nervous system

operates in a predominantly autonomous manner, its function is modulated to a certain extent by input from the sympathetic and parasympathetic divisions of the ANS.

Cranial sensory ganglia are associated with 5 of the 12 pairs cranial nerves. The trigeminal ganglion of cranial nerve V (trigeminal nerve) is comprised of neurons that innervate mainly thermoreceptors and nociceptors in the face, oral cavity and nasal cavity and periodontal mechanoreceptors of teeth. Most of the neurons of the geniculate ganglion of cranial nerve VII (facial nerve) innervate taste buds of the anterior two thirds of the tongue, and small number innervate the skin of the external ear. The vestibular and cochlear ganglia (the latter known as the spiral ganglion in mammals) of cranial nerve VIII (vestibulocochlear nerve) innervate the hair cells of the organs of hearing and balance. The petrosal ganglion (inferior glossopharyngeal ganglion) of cranial nerve IX (glossopharyngeal nerve) contains the cell bodies of visceral afferent neurons that innervate the oropharynx, carotid body and the taste buds of the posterior third of the tongue. The superior glossopharyngeal ganglion of cranial nerve IX (vagus nerve) contains somatic sensory neurons that innervate a portion of the skin of the external ear. The nodose ganglion (inferior vagal ganglion) of cranial nerve X contains visceral afferent neurons that innervate the pharynx, larynx and viscera of the thorax and abdomen. The jugular ganglion (superior vagal ganglion) of cranial nerve X contains somatic sensory neurons that innervate the external auditory meatus. In addition to the above cranial sensory ganglia, there are two further populations of primary sensory neurons associated with cranial nerves. These are the olfactory neurons (cranial nerve I) resident within the olfactory epithelium and the proprioceptive neurons of the trigeminal mesencephalic nucleus (cranial nerve V) that innervate the muscles of mastication. The optic nerve (cranial nerve II), although traditionally classified as part of the peripheral nervous system, is more appropriately considered to be a CNS tract as it and the retina originate from the diencephalon during development.

3. Development of the peripheral nervous system

The cells of the peripheral nervous system are derived from two sources: the neural crest and ectodermal thickenings in the cranial region called placodes. The neural crest gives rise to all of the glial cells of the peripheral nervous system, namely, the Schwann cells of peripheral nerves and the satellite cells of peripheral ganglia. All postganglionic autonomic neurons, enteric neurons and the majority of sensory neurons of the peripheral nervous system are derived from the neural crest. Neurogenic placodes only give rise to the neurons in certain cranial sensory ganglia or parts of these

ganglia and to olfactory neurons and their supporting cells in the olfactory and vomeronasal epithelia. Newly born neurons extend axons that are guided to their target organs and tissues by a variety of guidance cues. Shortly after axons reach their targets, a substantial proportion of neurons is eliminated by a phase of cell death that serves to match the number of neurons to the functional requirements of their targets and the circuits in which they participate. After this period of naturally-occurring neuronal death, there is an ongoing phase of growth and elaboration of neural processes, synaptogenesis and refinement of neural connections.

3.1 Neural crest

The neural crest is a transient component of the ectoderm formed during the final stages of neurulation. It is comprised of cells at the margins of the approaching neural folds that do not become incorporated into the neural tube, but migrate away from the dorsal aspect of neural tube following neural tube closure to give rise to wide variety of cell types in addition to neurons and glial cells of the peripheral nervous system. In chick embryos, the neural crest is specified during the early stages of neurulation. Fate mapping experiments designed to reveal the prospective fate of various regions of the chick epiblast (the structure that develops out of the inner cell mass that differentiates into the three layer embryonic disc) have shown that prospective neural crest cells are located in the narrow margin of the epiblast between the prospective neural plate and epidermis (Rosenquist, 1981). The mechanisms by which the precursors of the neural crest cells are formed during development are unknown. One possibility is that some cells, particularly those of the marginal zone between the neural plate and presumptive epidermis, are relatively distant from the neural inducing signals produced by the mesoderm (Rosenquist, 1981) and consequently become assigned to a neural crest cell fate as a result of differential neural induction of the dorsal ectoderm by this underlying mesoderm (Mazzoni et al., 1999). Detailed fate mapping of neural crest cells, predominantly in the chick, has determined that they migrate along characteristic pathways to form specific cell types depending on their rostral-caudal position along the neuroaxis. For example, whereas melanocytes arise from the whole length of the neural crest, various types of peripheral nervous system neurons have distinct levels of origin along the neural axis (Figure 1.1).

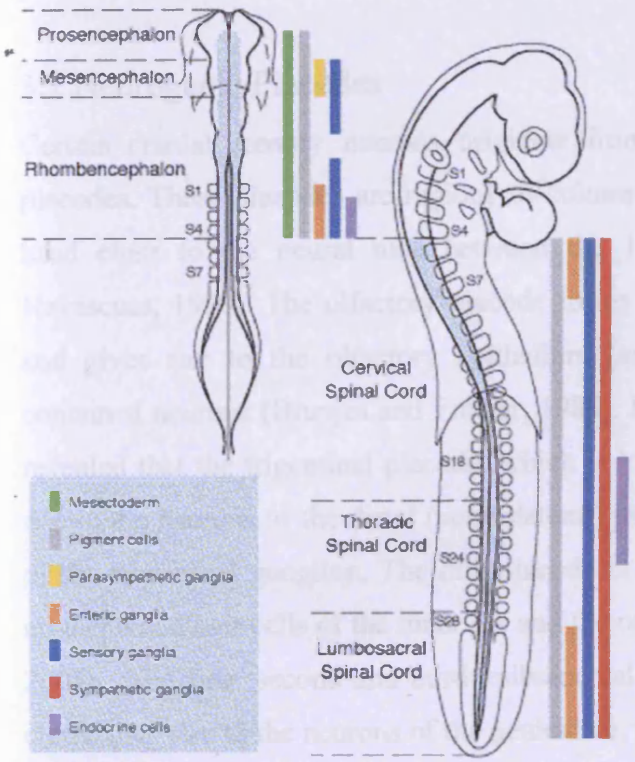

Fig. 1.1: Fate map of the derivates of the neural crest. The levels of origin of the main derivates of the neural crest are indicated along the neural axis at 2 developmental stages: 7 somite stages and 28 somite stages. Illustration adapted from (Le Douarin, 2004)

The molecular regulation of neural crest formation is incompletely understood. Both BMP and FGF signalling have been implicated in neural crest induction (Selleck and Bronner-Fraser, 1995), (D'Amico-Martel and Noden, 1983). A prevailing model for neural crest induction suggests that a gradient of BMP signalling subdivides the ectoderm into different domains: epidermis forms at high levels of BMP signalling, neural plate forms where BMP signalling is low and neural crest form at intermediate levels. Since both the neural crest and the placodes are induced by FGF signalling, an additional signal is considered to divide neural crest cells from placodal ectoderm, namely, the Wnts (Litsiou et al., 2005). Mouse embryos in which β-catenin has been inactivated have malformed neural crest derivates, including the DRG and various craniofacial regions, implicating Wnt signalling in neural crest formation and differentiation (Brault et al., 2001), whereas stabilizing of β-catenin modulates the production of neural crest cells and melanocytes (Voigt and Papalopulu, 2006)

3.2 Neurogenic Placodes

Certain cranial sensory neurons originate from the olfactory, trigeminal, otic and epibranchial placodes. These placodes are regions of columnar epithelium that form at distinct locations in the head close to the neural tube between the 10-30 somite stage of development (Alvarez and Navascues, 1990). The olfactory placode forms in the anterior-most position next to the forebrain, and gives rise to the olfactory epithelium (and vomeronasal epithelium of mammals) and its contained neurons (Brunjes and Frazier, 1986). Fate-mapping experiments in chicken embryos have revealed that the trigeminal placode, which is located near the anterior/mid hindbrain region, gives rise to the neurons of the distal (ventrolateral) parts of the ophthalmic and maxillo-mandibular lobes of the trigeminal ganglion. The otic placode is caudal to the trigeminal placode, and gives rise to epithelia and hair cells of the inner ear and the neurons of the vestibular and cochlear ganglia (Streit, 2001). The first, second and third epibranchial placodes, located in the dorsal region of branchial clefts, give rise to the neurons of the geniculate, petrosal and nodose ganglia, respectively (D'Amico-Martel and Noden, 1983). The cranial sensory neurons of the trigeminal mesencephalic nucleus, the proximal (dorsomedial) parts of the trigeminal ganglion, and the entire jugular and superior glossopharyngeal ganglia are derived from the neural crest.

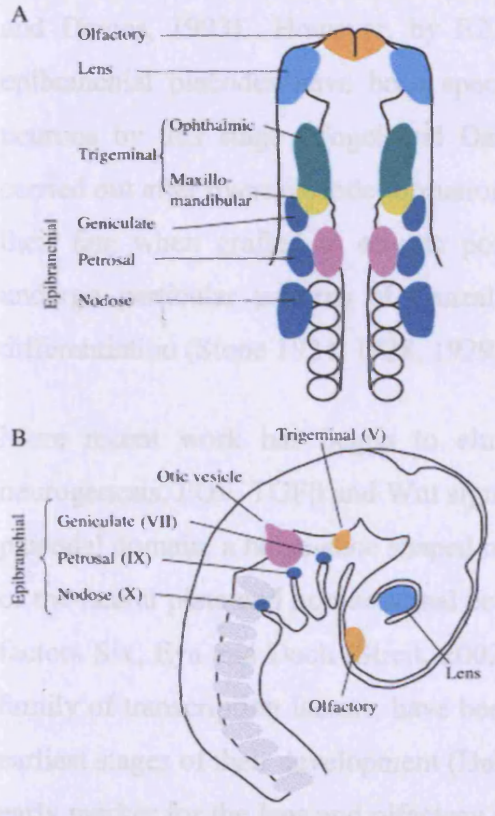

Figure 1.2: Image adapted from (Streit, 2004)

The illustration above shows the position of the cranial placodes in a 1.5- and 3.5-day chick embryo. At the 10- to 13-somite stage precursors for different placodes are segregated and occupy unique positions in the head ectoderm. At 3.5 days in development, all placodes can be recognized morphologically and some have begun to undergo differentiation.

Classically, most of the studies on the cellular interactions that influence the development of placodes and their derivatives have been carried out on amphibian and avian embryos using heterotopic and heterochronic grafting experiments and in vitro tissue recombination experiments. Placode induction begins in late gastrula stages, involving a series of inducers from different embryonic tissues including endoderm, mesoderm and the neural tube (Jacobson, 1963a; Jacobson, 1963b; Jacobson, 1963c). Heterochronic grafting of ectoderm performed at very early stages before placodes have formed has shown that the graft adopts a fate that is appropriate to its new location, suggesting that commitment towards a particular placodal fate has not yet occurred. For example, heterotopic grafting in E1.5 chicken embryos of presumptive placodal ectoderm of the otic and third epibranchial placodes (which give rise to vestibular and nodose neurons, respectively) has demonstrated that the ectoderm is not determined to give rise to neurons of vestibular-type (short-neurotrophin-independent survival and slow axonal growth rate) or nodose-type (long-neurotrophin-independent survival and fast axonal growth rate) at this stage in development, suggesting that placodal cells become specified to particular neuronal fates between E1.5 and E2.5 *in ovo* (Vogel and Davies, 1993). However, by E2.5 the respective neuronal precursors in the otic and third epibranchial placodes have been specified to differentiate into vestibular-type and nodose-type neurons by this stage (Vogel and Davies, 1991). Accordingly, heterotopic grafting experiments carried out after overt placode formation have shown that most placodes are no longer able to change their fate when grafted to ectopic positions, so that ectodermal cells are already determined to undergo particular patterns of central and peripheral target innervation prior to overt neuronal differentiation (Stone 1924, 1928, 1929).

More recent work has begun to elucidate key molecular aspects of placode development and neurogenesis. FGF, TGFβ and Wnt signalling pathways have been implicated in the induction of a pre-placodal domain, a horse-shoe shaped region around the prospective anterior neural plate at the border of the neural plate and non-neuronal ectoderm that, is characterized by expression of the transcription factors Six, Eya and Dach (Streit, 2002; Streit, 2007) Specific markers, such as members of the Pax family of transcription factors, have been identified that are expressed by particular placodes from the earliest stages of their development (Dahl et al., 1997; Mansouri et al., 1996). For example, Pax6 is an early marker for the lens and olfactory placodes, Pax2 is an early marker for the otic and epibranchial

placodes, and Pax3 is an early marker for the ophthalmic trigeminal placode (Favor et al., 1996; Hill et al., 1991; Hogan et al., 1986). Studying Pax gene expression in explant studies and heterotopic grafting experiments between the ophthalmic trigeminal placode and the third epibranchial placode has revealed that at the 3-to 4- somite stage, the ophthalmic trigeminal placode is competent to express epibranchial placode and neuronal markers (Pax2 and Phox2a) when grafted to the nodose region. This competence declines with time as the number of Pax3-expressing cells increases. Competence is mainly lost by stages 14-18 when many cells are already expressing Pax3. Moreover, Pax3 expression within presumptive ophthalmic trigeminal placodal ectoderm correlates at a single cell level both with neuronal specification and with commitment to a trigeminal neuron fate, and it is the Pax3-negative cells in presumptive ophthalmic trigeminal placodal ectoderm that can be induced to express the epibranchial placode marker Pax2 and form *Phox2a*-positive neurons in the nodose ganglion. These findings suggest that neurogenesis in the neurogenic placodes is not a two-step process in which neurons are induced and subsequently specified to a particular fate, but the different placodes are individualized by different cues. While formation of the otic and the epibranchial placodes both require FGF signalling (Sun et al., 2007), other factors may later determine their specific fates. . For example, Wnt, appears to be instructive for the otic placode and repressive for the epibranchial placode (Freter et al., 2008), and BMP signalling is additionally involved in otic placode induction (Kwon and Riley, 2009; Martin and Groves, 2006) neuronal differentiation and neuronal subtype identity seem to be coupled (Baker and Bronner-Fraser, 2000).

4. Growth cones

Once sensory neuronal progenitor cells have migrated to their respective ganglia and differentiated into post-mitotic neurons they begin to extend axons towards their peripheral and central target fields . Since axonal outgrowth and path-finding is an essential mechanism in establishing a functional nervous system, I will discuss the morphology of growth cones, their movements and some aspects of the signalling involved in axonal path-finding.

4.1 Growth cone morphology and motility

The growing tip of axons and dendrites is a specialized structure called the growth cone. The existence of a growth cone was originally proposed by the Spanish histologist Santiago Ramon y Cajal. Cajal first described the growth cone based on histologically fixed cells as "a concentration of protoplasm of conical form endowed with amoeboid movements" (Cajal, S.R. 1890). The sensory, motor, integrative, and adaptive functions of growing axons and dendrites are all contained within this specialized structure. Growth cones have a central region bounded by veils of membrane called lamellipodia from which emerge fine, narrow, cylindrical extensions known as filopodia or microspikes that extend several microns beyond the edge of the growth cone to probe the environment. The membrane surrounding filopodia contains receptors and cell adhesion molecules that are important for axon growth and guidance. Filopodia contain actin filaments cross-linked into bundles by actin-binding proteins that are continuous with a dense actin meshwork in the lamellipodia. Actin filaments are helical polymers composed of F-actin microfilaments. F-actin microfilaments are in turn made up of actin monomers that, in the case of axons, are predominantly β-actin (Pak et al., 2008).

Actin monomers can spontaneously self-assemble into polarised, bi-helical filaments in vitro. This process requires ATP hydrolysis at the rapidly growing "barbed end" of filaments and the dissociation of ADP and inorganic phosphate at the slower growing "pointed end" of filaments. Assembled filaments are dynamic and constantly treadmilling, adding monomers to the barded end and removing them from the pointed end, even in a steady state. (Pak et al., 2008; Pollard and Borisy, 2003). In order to contribute to growth cone motility, actin must be organised into-higher order networks of filaments, often called actin superstructures, that resemble either gels or bundles. In vitro, cell-free, studies have demonstrated that these superstructures are self-organizing, requiring a limited ensemble of actin binding proteins, but not extracellular signals or motor proteins (Cameron et al., 1999; Loisel et al., 1999). The generation of actin superstructures appears to occur in two steps. The first is de-novo actin filament assembly (nucleation), which in the motile cell is enhanced by a

number of different proteins including ARP2/3, formins, spir proteins and cofilin(Andrianantoandro and Pollard, 2006; Mullins et al., 1998; Pruyne et al., 2002; Quinlan et al., 2005). These nucleating proteins are activated by association with activated signalling proteins such as the Rho GTPase, Cdc42, and Wiscott-Aldrich-syndrome proteins (WASPS) (Higgs and Pollard, 2000). The second step is the formation of higher-order structures and requires a multitude of actin binding proteins to both positively regulate actin bundle/gel assembly and to tether them to the plasma membrane. Several actin binding proteins also act to destabilise actin superstructures to allow for the remodelling in actin networks that is required for growth cone guidance (Pak et al., 2008).

In addition to actin filaments, the other major component of the growth cone cytoskeleton is microtubules, which are found in the central region of the growth cone and in the lamellipodia. Microtubules are long, hollow, non-branched cylindrical filaments composed of protofilament polymers of α- and β-tubulin heterodimers (Dent and Gertler, 2003). Tubulin heterodimers are intrinsically polar and associate head to tail in the protofilaments that lie parallel to the microtubule along the axis. The polymerization of tubulin heterodimers into microtubule protofilaments requires the binding and hydrolysis of GTP. The fast growing end of the microtubule that contains tubulin-bound GTP is known as the "plus" end, while the slow growing end, containing tubulin bound GDP, is called the "minus" end (Gordon-Weeks, 2004).

Growth cone motility is driven by a combination of dynamic actin filament assembly and disassembly and microtubule polymerization and depolymerization. Growth cones can extend rapidly, solely by virtue of microtubule polymersization, if actin assembly is inhibited. However, neuritic processes extend in a random, non-targeted fashion under these conditions, suggesting that actin filament assembly is essential for correct growth cone guidance (Bradke and Dotti, 1999; Pak et al., 2008). A number of key signalling cascades regulate microtubule and actin polymerization dynamics in the growth cone in response to attractive (e.g. chemoattractants, neurotrophins) or repellent (e.g. semaphorins, ephrins) guidance molecules. These cascades include MAP-Kinase, PI3-Kinase and GSK3 signalling pathways and their role in regulating growth cone motility will be discussed in detail in section 1.10, below.

5. Axon guidance

Resolving the question of how growing axons accurately follow precise pathways during development to establish the correct synaptic connections to non-neuronal and neuronal targets tissues is an area of intense research. A large body of evidence has emerged suggesting that the growth cones of extending "pioneering" axons contain receptors for specific guidance molecules that are present in the extracellular environment. Once activated, guidance cue receptors initiate intracellular signalling cascades that modulate cytoskeletal dynamics within the growth cone to bring about growth cone extension, retraction, turning or collapse. Guidance cue molecules can be either contact-mediated or diffusible, and can either attract or repel axons. The list of guidance cues elucidated to date includes; netrins (Round and Stein, 2007), semaphorins (Kruger et al., 2005), slits (Dickson and Gilestro, 2006), ephrins (Egea and Klein, 2007), neurotransmitters (Spencer et al., 2000), morphogens from the Wnt and TGFβ families (Charron and Tessier-Lavigne, 2005) neurotrophins, extracellular matrix molecules (Hari et al., 2004) and nitric oxide (Bicker, 2005). Since the roles of netrins, semaphorins, slits and ephrins in regulating axon guidance have been the most thoroughly characterized, I will briefly describe them below.

Netrins are bifunctional guidance cues that can either attract or repel growing axons depending on which netrin receptor is expressed within the growth cone of the axon. For example, Netrin 1 attracts axons that express the receptors DCC or neogenin, but repels axons that express the netrin receptors Unc5a, Unc5b, Unc5c or Unc5d. The cytoplasmic domains of netrin receptors do not contain any identifiable catalytic motifs, but bind, and become phosphorylated by, cytoplasmic tyrosine kinases like FAK, src and fyn following netrin engagment. Tyrosine phosphorylated netrin receptors recruit other cytoplasmic signalling proteins, resulting in the activation of PI3-Kinase, MAP-kinase, PLC-gamma and rac/Cdc42 signalling cascades, which in turn modulate cytoskeletal dynamics to bring about growth cone extension or turning (Round and Stein, 2007).

In most cases, semaphorins act to repel growth cones, resulting in growth cone turning or collapse. Semaphorins are either secreted or membrane associated glycoproteins that have been grouped into eight classes based on sequence and structural homology. Classes 3 to 7 are expressed in vertebrates, and individual semaphorins within each class are identified by a letter code. The most comprehensively characterized semaphorin is probably Sema3A (Kruger et al., 2005). Semaphorins derive their name from a conserved "Sema" domain that is approximately 400 amino acids in size. In addition to the Sema domain, all semaphorins contain a PSI domain that is shared with plexins and integrins. Additional domains may include immunoglobulin and thrombospondin domains. Vertebrate semaphorins in classes 4 to 7 are membrane-associated, whereas class 3 semaphorins are secreted proteins. The main group of semaphorin receptors are the plexins that are in turn divided

into four groups, A to D. The plexins, which also contain "sema" and PSI domains, were first identified as cell adhesion molecules. Class 3 soluble semaphorins, like Sema3A, signal though plexins in group A and require neuropilins as essential plexin co-receptors. The intracellular domains of plexins have constitutively active RasGAP activity in the absence of semaphorin binding, and also contain motifs that bind Rho family GTPases such as Cdc42, Rac and RhoD (Kruger et al., 2005). Semaphorin binding leads to the phosphorylation of tyrosine residues in plexin intracellular domains by cytoplasmic kinases such as Fes and Fyn. In the case of Plexin A1, the binding of Sem3A and subsequent tyrosine phosphorylation by Fes leads to phosphorylation of Collapse Response Mediator Protein-2 (CRMP-2), probably via sequential activation of Cdc42 and GSK3, which in turn plays a role in mediating growth cone collapse. The role of CRMP-2 in mediating the effects of GSK3 signalling pathways on neuronal process outgrowth are discussed further in section 1.10, below. Activated Plexin A1 can also activate MAP-Kinase signalling pathways (Kruger et al., 2005).

Slit proteins have been shown to play a vital role in the guidance of commissural neuron axons. These neurons project axons that cross the midline to connect the two symmetric halves of invertebrate and vertebrate central nervous systems (Dickson and Gilestro, 2006). Mammals possess three slit genes (Slit-1, Slit-2 and Slit-3) that are all expressed in midline cells of the CNS. Studies of transgenic mice and *Drosophila* mutants, and in vitro assays of vertebrate neurons, have demonstrated that slits are repellent guidance cues for commissural axons. Slits exert their repellent effects by binding to Robo receptors that are expressed in the growth cones of commissural neurons. Mammalian genomes encode four Robo receptors, although only three (Robo-1, -2 and -3) are expressed in the CNS. Robo receptors consist of a large extracellular ligand-binding domain, comprising five immunoglobulin like domains and three fibronectin type repeats, a single transmembrane segment and a cytoplasmic domain that appears to be devoid of intrinsic catalytic activity and poorly conserved amongst Robo proteins (Dickson and Gilestro, 2006). Whilst the cytoplasmic domain has been shown to bind a number of SH2/SH3 domain adaptor proteins, the Abl tyrosine kinase and Rho GTPase-activating proteins, signal transduction from Robo receptors is relatively poorly understood at present.

Ephrins are a large family of membrane bound proteins that are divided into two subclasses, A and B. The A subclass (ephrinA1-ephrinA5) are tethered to the plasma membrane by a GPI linkage, whereas the B subclass (ephrinB1-ephrinB3) have a transmembrane domain and a cytoplasmic tail that appears to lack endogenous catalytic activity (Egea and Klein, 2007). Ephrins bind to Eph receptors that are transmembrane tyrosine kinases. Eph receptors are also divided into A- and B-subclasses with 9 and 5 members, respectively, in mammals. Eph-ephrin signalling can mediate either attraction

or repulsion of growth cones and pre- and post-synaptic membranes. Eph-ephrin signalling can also be bi-directional (i.e both can act as ligand or receptor) and interactions between them can be both trans, between adjacent cells, or in cis, on the same cell. The regulation of Eph-ephrin signalling to bring about either the attraction or repulsion of cells/cell membranes is complex and appears to involve the formation of higher-order Eph-ephrin signalling clusters, cleavage of ephrin ectodomains from cell surfaces and the endocytosis of Eph-ephrin complexes (Egea and Klein, 2007). Eph-ephrin signalling has been shown to play an important role in directing retinotopic mapping of retinal axons to the midbrain tectum (Flanagan, 2006) and path-finding of limb motor axons (Helmbacher et al., 2000).

6. Axon growth rate

While there have been innumerable studies on the molecular cues that guide axons to their targets in the developing nervous system, relatively little attention has been given to the regulation of axonal growth rate during the stage of development when axons are growing to their targets. Rather, most studies on the regulation of axonal growth rate have been carried out on embryonic or postnatal neurons at stages of development after the neurons had already innervated their targets and were regenerating axons in culture, as opposed to initiating axon growth for the first time. One of the most detailed studies of de novo axonal growth rate, and the experimental system used for much of the work of this thesis, has been carried out on four populations of placode-derived cranial sensory neurons of the chicken embryo (Davies, 1989). The neurons of the vestibular, geniculate, petrosal and nodose ganglia are born during the same period of development and start extending axons to their peripheral and central targets at approximately the same time, but have different distances to grow to reach their targets. Vestibular neurons have the closest targets, nodose neurons have the most distant targets, and geniculate and petrosal neurons have targets of intermediate distance. The rate at which the axons of these neurons grow to their targets *in vivo* is correlated with target distance: vestibular neurons have the slowest axon growth rates, and nodose neurons the fastest. Importantly, these distinctive differences in axonal growth rate appear to be an intrinsic property of the neurons. When they are cultured at very low density or as isolated single cells at the stage of development when their axons are normally growing to their targets, they extend axons at different rates: the axons of nodose neurons growing faster than those of petrosal neurons, which grow faster than those of geniculate neurons, which grow faster than those of vestibular neurons.

7. Neurotrophins and their receptors

In this section I will focus on the involvement of the neurotrophin family of neurotrophic factors in regulating neuronal survival and axonal growth. My studies have been carried out on early, neurotrophic factor-independent neurons as well as older axotomised, neurotrophic factor-dependent neurons. In the case of axotomised neurons, it is important to consider the regulatory effects of the neurotrophins on the intracellular signalling cascades involved in modulating axon growth when interpreting experimental data.

7.1 Neurotrophic factors of the neurotrophin family regulate neuronal survival

In 1934, Victor Hamburger discovered that removal of the limb bud in the chick embryo resulted in reduced numbers of sensory and motorneurons in the spinal cord.

In 1939, Victor Hamburger demonstrated that transplantation of an extra limb bud caused increased numbers of sensory- and motorneurons in the spinal cord. In 1942, Rita Levi-Montalchini confirmed the loss of neurons after limb bud removal, and proposed that target- derived signals act on the innervating neurons to sustain their survival. In 1948, Elmer Buecker, a former student of Victor Hamburger, implanted tumour cells (Sarcoma 180) into a region of the hind limb to see if these cells would have that same effect on the innervating neuronal populations as transplanting an extra limb bud. Surprisingly, transplantion of these cells increased the size of limb innervating sensory ganglia, but motorneurons remained unaffected. By 1954, Rita Levi-Montalchini and Stanley Cohen used DRG explants in an in vitro assay to isolate and purify the factor in the sarcoma that acted on the sensory neurons, which turned out to be NGF.

During the development of the nervous system, excess neurons are generated, and those that are superfluous to requirement are removed during a phase of naturally occurring cell death shortly after neurons start innervating their targets (Oppenheim, 1991). This phase of apoptotic cell death is thought to remove neurons with inappropriate connections and to match the number of surviving neurons to the size and functional requirements of their target fields. During this phase of naturally occurring cell death, neurons compete for a limited supply of neurotrophic factors. According to the neurotrophic hypothesis, neurons that acquire neurotrophic support survive, whereas those that are unsuccessful in the competition for neurotrophic factors die by apoptosis. The neurotrophic hypothesis was substantiated by the discovery and classic experiments on the first neurotrophic factor, nerve growth factor (NGF), by Hamburger, Levi-Montalcini and Cohen (Hamburger and Levi-Montalcini, 1949; Levi-Montalcini, 1987). The original experiments that hinted at the existence of NGF were performed to determine whether implantation of various tumour tissues into mice might support the survival of sensory neurons. Mouse sarcoma tissue evoked extensive growth of sensory fibres into the tumour. In addition, dorsal root ganglia (DRG) near the site of the tumour were significantly larger then the corresponding ganglia on the opposite side of the spinal cord. Further studies showed that the effect of the sarcoma was caused by a diffusible factor. After purification this diffusible factor was named nerve growth factor. Additional experiments on NGF revealed that injecting antibodies against NGF into newborn mice or rats resulted in virtually the complete disappearance of sympathetic ganglia (Levi-Montalcini and Booker, 1960) The administration of anti-NGF antibodies at earlier stages of development also reduced the number of neurons in rodent DRG. These data together with recent demonstration that postganglionic sympathetic neurons and the

majority of neural crest-derived sensory neurons are eliminated in mice lacking either NGF or its receptor tyrosine kinase TrkA clearly show that developing sympathetic and many sensory neurons require NGF for their survival (Yip et al., 1984).

NGF is the founder member of the neurotrophin family of structurally related proteins that comprises NGF, brain-derived neurotrophic factor (BDNF), neurotrophin (NT)-3 and NT-4/5 (now referred to as NT-4) in birds and mammals, together with two additional neurotrophins in fish, NT-6 and NT-7 (Barde, 1990). BDNF has been shown to promote the *in vitro* survival of placode-derived trigeminal, nodose, geniculate, petrosal and vestibular neurons during embryonic development (Davies et al., 1986; Lindsay et al., 1985a; Lindsay et al., 1985b) and the survival of the earliest differentiating neural crest-derived sensory neurons of the trigeminal ganglion and DRG. The neurons supported by these neurotrophic factors at early embryonic stages include many that will later become NGF dependent as they switch their neurotrophic factor requirements (Davies, 1997; Enokido et al., 1999; Farinas et al., 1996; Huang et al., 1999; Liebl et al., 1997; Pinon et al., 1996). Neurotrophins exert their effects by binding to and activating receptors that in turn initiate an array of intracellular signal transduction cascades (Hempstead, 2002; Miller and Kaplan, 2001). Neurotrophins signal through two classes of receptors. The first class of receptors are the Trk tyrosine kinases: TrkA, TrkB and TrkC. Trks bind neurotrophins with high affinity and specificity. TrkA is the cognate receptor for NGF, TrkB is the cognate receptor for BDNF and NT-4 and TrkC is the preferred receptor for NT-3. Under some circumstances NT-3 can also signal through TrkA and TrkB (Davies et al., 1995). The second class of neurotrophin receptor is p75, a member of the TNF receptor superfamily. p75 binds all neurotrophins with an equal affinity (Chao and Hempstead, 1995) (Figure 1.3).

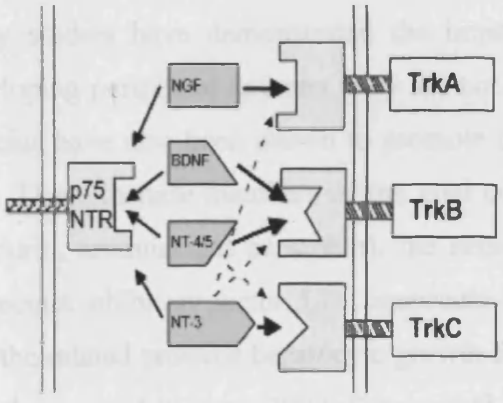

Figure 1.3: Schematic diagram illustrating the receptor specificity of neurotrophin family members.

Studies on transgenic mice mice lacking neurotrophins or their receptors have confirmed the importance of the neurotrophins in promoting the survival of developing neurons of the peripheral

nervous system. For example, BDNF-/- mice die perinatally and display defects in populations of sensory neurons that are dependent on BDNF for survival in culture (Ernfors et al., 1994; Jones et al., 1994). Trk B -/- mice also lose a substantial proportion of trigeminal, nodose and DRG neurons (Klein et al., 1993), while Trk C-/- mice have decreased numbers of myelinated axons emerging from the dorsal root of the spinal cord that correlates with the loss of a sub-population of DRG neurons (Klein, 1994). NT-3 deficient mice also display a significant loss of trigeminal and DRG neurons sensory neurons and sympathetic neurons (Farinas et al., 1996; Francis et al., 1999; Wilkinson et al., 1996). Mice lacking NGF, or its receptor, TrkA, show a dramatic loss of peripheral sympathetic neurons and nociceptive and thermoceptive sensory neurons of the DRG (Crowley et al., 1994; Henderson et al., 1994; Smeyne et al., 1994).

Transgenic mice over-expressing neurotrophins have also provided evidence to support the neurotrophic hypothesis. For example, mice that over-express NGF in skin have increased numbers of sympathetic and sensory neurons of the peripheral nervous system (Albers et al., 1994). Over-expression of NT-3 in the skin results in significantly increased numbers of neurons in trigeminal, dorsal root and sympathetic ganglia (Albers et al., 1996). Interestingly, peripheral over-expression of BDNF in epithelial cells does not alter the number of neurons in trigeminal or dorsal root ganglia, although it does significantly increase the number of neurons in the nodose ganglion (LeMaster et al., 1999).

Additional support for the neurotrophic factor hypothesis has been gained by studying the site, timing and level of expression of NGF. Initiation of NGF synthesis in the relevant peripheral target fields begins as invading axons start to enter the target field (Davies et al., 1987). Recent studies suggest that certain neurons may require neurotrophic support during the period their axons are growing to their targets in addition to requiring neurotrophic factors from their targets (Davies, 2003). Whilst many studies have demonstrated the importance of neurotrophins in regulating the survival of developing peripheral neurons, they are not alone in possessing this ability. Several other secreted proteins have also been shown to promote the survival of neurons of the PNS, both *in vitro* and *in vivo*. These include members of the glial cell-derived neurotrophic factor (GDNF) family (GDNF, neurturin, artemin and persephin), the neurotrophic cytokines (ciliary neurotrophic factor, CNTF; leukaemia inhibitory factor, LIF; oncostatin-M, OSM; cardiotrophin-1, CT-1 and interleukin-6, IL-6) and the related proteins hepatocyte growth factor (HGF) and macrophage-stimulating protein (MSP) (Airaksinen and Saarma, 2002; Forgie et al., 2003; Maina and Klein, 1999; Murphy et al., 1997). In addition to promoting the survival of developing PNS neurons, neurotrophins can also regulate certain aspects of target field innervation by developing PNS neurons (discussed in detail below) and

regulate the phenotype and plasticity of adult sensory neurons (Bibel and Barde, 2000; Davies, 2000; Petruska and Mendell, 2004; Pezet et al., 2002).

7.2 Neurotrophic factor independence and the acquistion of survival dependence

Several populations of neurons survive in culture independently of neurotrophic factors during the earliest stages of their development, shortly after differentiating from their precursor cells when their axons are starting to grow to their targets. These include placode-derived cranial sensory neurons of the chick embryo (Vogel and Davies, 1991), embryonic mouse trigeminal ganglion (Buchman and Davies, 1993), paravertebral sympathetic neurons (Coughlin and Collins, 1985; Ernsberger et al., 1989), retinal ganglion cells (Rodriguez-Tebar et al., 1989) and motoneurons (Mettling et al., 1995). The duration of neurotrophin independence and the onset of neurotrophin-dependent survival have been most thoroughly investigated in populations of placode-derived cranial sensory neurons of the chick embryo and in the sensory neurons of the embryonic mouse trigeminal ganglion. These experimental systems will be discussed in turn.

The placode-derived sensory neurons of the embryonic chick vestibular, geniculate, petrosal and nodose ganglia do not initially require neurotrophic factors to support in vitro survival following their differentiation from progenitor cells, and remain neurotrophic factor independent throughout the period of development when their axons are growing to their targets. Because the distances that the axons of these different populations of neurons have to grow to their targets and the lengths of time taken to reach these targets differ, the duration of neurotrophic factor independence differs between these neurons. When cultured at low density, in the absence of neurotrophins at a time when their earliest axons would be extending to their targets *in vivo*, these neurons die at different rates: vestibular neurons die rapidly, geniculate and petrosal neurons die at intermediate rates, and nodose neurons die slowly. Thus, neurons that have more distant targets and that are innervated later in development appear to have a more protracted period of neurotrophin independence. The majority of the neurons in these ganglia become dependent on BDNF for survival when their axons reach their targets (Davies, 1989; Vogel and Davies, 1991). Accordingly, vestibular neurons, which are the first to innervate their targets, are the first to express TrkB and the first to become dependent on BDNF for survival, whereas nodose neurons, which are the last to innervate their targets, are the last to express TrkB and the last to become dependent on BDNF for survival (Vogel and Davies, 1991). Robinson et al. 1996). The duration of neurotrophin independence, together with differences in axonal growth rate (described above), appear to coordinate the onset of neurotrophin dependence with the arrival of axons in the vicinity of their targets (Davies, 1994). These intrinsic differences in axonal growth rate

and duration of neurotrophin independence appeared to be specified in the placodal progenitor cells for vestibular and nodose neurons since neurons arising in otic vesicle cultures (presumptive vestibular neurons) have short neurites and die rapidly in the absence of neurotrophins, whereas neurons arising in third epibranchial placode cultures (presumptive nodose neurons) have long neurites and survive for several days and (Vogel and Davies, 1991). Heterotopic grafting experiments between the regions of presumptive placodal ectoderm that give rise to these neurons at E1.5 revealed that the presumptive placodal ectoderm is not determined to give rise to neurons of the vestibular or nodose phenotype at this stage (Vogel and Davies, 1993). Explantation of presumptive placodal ectoderm at E1.5 also showed that this ectoderm is not specified to differentiate into neurons at this stage. Moreover, non-neurogenic ectoderm from the trunk can give rise to nodose-type neurons when transplanted heterotopically to the nodose region at this stage. These results suggest that signals acting in the vicinity of presumptive placodal ectoderm specify the growth and survival characteristics of the neurons that differentiate from these ectodermal cells (Vogel and Davies, 1993). In the developing mouse trigeminal ganglion, early born trigeminal neurons (E9.5 to E11) initially survive in culture without neurotrophic factor support, and subsequently become dependent on BDNF and/or NT-3 between 24 and 48 hours in culture. Cultured neurons begin to respond robustly to NGF at E11.5, a time that corresponds to a significant increase in the differentiation of TrkA-positive neurons in the trigeminal ganglion and the arrival of the first TrkA-positive fibres in the peripheral target field epithelium where the highest levels of NGF are synthesized (Buchman and Davies, 1993; Davies and Lumsden, 1984; Enokido et al., 1999). The early response of developing trigeminal neurons to BDNF and NT-3 corresponds with both the onset of expression of the mRNAs encoding these neurotrophins in the mesenchyme that the neurons must grow through to reach peripheral target field epithelium and transient high level expression of the mRNA encoding full length, kinase competent TrkB receptors in the neurons themselves (Buchman and Davies, 1993; Ninkina et al., 1996). The levels of NGF mRNA in target field epithelium and TrkA mRNA in neurons are both up-regulated dramatically as trigeminal neurons begin to acquire NGF dependence *in vitro* and innervate target field epithelium *in vivo* (Davies et al., 1987; Enokido et al., 1999; Wyatt and Davies, 1993). The developmental expression of the mRNA encoding the common neurotrophin receptor, p75, in the mouse trigeminal ganglion also mirrors the acquisition of NGF responsiveness (Wyatt et al., 1990). Although NGF production in target fields is temporally correlated with the onset of target field innervation by NGF-responsive neurons, this appears to occur independently of target- field/axon interactions. Supportive evidence comes from the observation that NGF mRNA expression occurs on schedule in chick embryo hindlimb buds deprived of innervation (Rohrer et al., 1988). The detailed analysis of neurotrophin responsiveness in developing mouse trigeminal neurons demonstrates that

the expression of neurotrophic factors in the mesenchyme and epithelium of target fields and neurotrophin receptors by neurons are tightly temporally coordinated with the onset of target field innervation and the acquisition of neurotrophic factor dependence.

7.3 Neurotrophic factors regulate neurite growth

As the nervous system develops, functional connections are established between neurons and their targets. Whilst evidence suggests that initial neurite extension may be an intrinsic programme that does not require neurotrophic factor support, later stages of target field innervation require neurotrophic factors for successful completion. As part of my study was carried out on older axotomised neurons that depend on neurotrophic factor support for regenerative axonal growth and survival, I will give an overview of the evidence obtained from transgenic mouse studies that demonstrate the important role that neurotrophic factors play in regulating process outgrowth and establishing target field innervation. In addition, I will outline the intracellular signalling pathways that mediate axonal growth regulated by neurotrophic factors.

There are a number of mechanisms which regulate the length, branching, direction of extending neurites and the formation of functional synapses once neurites reach their targets. Many different extracellular signals, including soluble factors such as growth factors, cell surface and extracellular matrix proteins influence these processes.

Members of the neurotrophin family have been shown to be crucial regulators of axonal growth. *In vitro*, neurotrophins promote a significant increase in the density of axons extending from explanted embryonic peripheral ganglia, although these observations can be attributed in part to increased neuronal survival within explants in the presence of neurotrophins (Deckwerth et al., 1996; Markus et al., 2002). Analysis of target field innervation in neurotrophin and neurotrophin receptor null mice is complicated by the death of neurotrophin-dependent neurons during the period of target field innervation. Thus reduced target field innervation may be due to a reduction in growth promoting neurotrophin signalling or a reduction in the number of neurons projecting axons to target fields as a result of cell death, or a combination of both. Even so, the analysis of such transgenic mice suggests that BDNF and NT-3 are required for successful target field innervation by vestibular and cochlear ganglion neurons and that NGF/trkA signalling is required for successful target field innervation by sympathetic neurons of the SCG and sensory neurons of the DRG (Fagan et al., 1996; Postigo et al., 2002; Schimmang et al., 1995). In accordance with this, deletion of the common neurotrophin receptor, p75, results in significantly reduced axonal outgrowth from neural crest-derived sensory neurons at early embryonic ages before excessive neuronal death occurs due to p75 deletion (Bentley and Lee, 2000). More recent studies that have used transgenic mice to establish the roles of

neurotrophins in regulating target field innervation have made use of the fact that developmental neuronal death does not occur in transgenic mice lacking the pro-apoptotic protein, Bax (White et al., 1998). Double-transgenic mice lacking both Bax and neurotrophin or neurotrophin receptor expression are immune from neuronal death, thus allowing the effects of neurotrophic factor signalling deficits on target field innervation to be examined in isolation. Whilst both NGF and NT-3 support the elongation and branching of processes from sympathetic neurons *in vitro* (Orike et al., 2001), they appear to play distinct and complementary roles in regulating target field innervation *in vivo*. Bax/NGF double-null mutant mice have relatively normal axonal elongation of SCG neurons, but show defects in target-field terminal arborization. In contrast, Bax/NT-3 double-null mutant mice show decreased axonal extension long before the target field is reached (Glebova and Ginty, 2004; Kuruvilla et al., 2004). These data suggest that NT-3 is an intermediate factor, probably acting locally within the sympathetic ganglia and along the blood vessels sympathetic axons follow to reach their target organs, to promote initial axonal extension before neurons are exposed to NGF, whereas NGF is important for promoting terminal arborization and functional innervation of target fields. Interestingly, TrkA-positive nerve trunks and superficial terminal arbors of sensory neurons in the epidermis are absent in the hindlimbs of Bax -/- / NGF -/- double-transgenic mice, suggesting that NGF responsive DRG sensory neurons require NGF for both axonal extension and terminal arborization (Patel et al., 2000). An examination of Bax -/- / NT-3 -/- double-transgenic mice has also revealed that NT-3 is required for correct innervation of skeletal muscle by proprioceptive neurons and its mode of action involves both promoting axonal extension and target field terminal arborization (Patel et al., 2003). Analysis of Bax -/- / BDNF -/- double-transgenic mice has demonstrated that whilst cranial sensory neurons can navigate successfully to their various targets in the absence of BDNF, BDNF is required for afferents to arborize in the target fields and establish functional sensory connections (Hellard et al., 2004).

Several experiments designed in the late seventies showed that injection of NGF into cranial neurons caused excessive growth of sympathetic axons into the brain (Menesini Chen et al., 1978) Also, sensory neurons have been shown to turn towards a source of NGF in culture (Gundersen and Barrett, 1979). Even though this was widely interpreted that neurotrophins would act as a guidance molecule for neurons to grow towards their targets, the finding that NGF is not expressed in the target field until the first neurons are innervating it, showed that target derived NGF could not play a role in long-range axonal guidance (Davies, 1987). However, co-culture experiments of trigeminal neurons and their target tissue, maxillary epithelium and mesenchyme, showed that trigeminal neurons grow towards these targets. Application of function blocking antibodies against NGF did not disturb this process, indicating that NGF is not the source which attracts trigeminal neurons towards their targets. Anti-NT-

3 antibodies, and to a lesser extend anti-BDNF antibodies reduced neurite outgrowth and the application of both completely eliminated it (O'Connor and Tessier-Lavigne, 1999). In the ventral spinal cord, the expression of chemorepulsive signals act on DRG neurons to project towards the dorsolateral parts of the spinal cord. Netrin-1 has been shown to act as an early chemorepellent for DRG neurons and ectopically expressed netrin-1 in the dorsal and intermediate spinal cord prevents DRG neurons from being directed towards the dorsal spinal cord (Masuda et al., 2008). In the olfactory system, several guidance cues regulate axon guidance to innervate different layers within the olfactory epithelium. For example, axonal targeting within the dorso-ventral axis of the olfactory bulb is controlled by the graded expression of axon guidance cues and their receptors. The Slit receptor Robo2 is expressed in a high dorso-medial to low ventro-lateral gradient. Slit-1 expression in the ventral region of the olfactory epithelium prevents Robo-2 expressing axons to enter. Axonal targeting in the antero-posterior axis of the olfactory bulb is controlled through the differential expression of axon guidance molecules. Olfactory-receptors mediated signalling modulates the expression of molecules such as Npn-1 and Ephrin-A5 through a transcriptional mechanism. Olfactory sensory neurons containing high levels of cAMP express high levels of Npn-1 and low levels of Ephrin-A5 and as a result innervate specific glomerumi in a posterior region of the olfactory bulb (Cho et al., 2009).

7.4 Intracellular Signal Pathways Associated with Neuronal Survival and Growth: Trk- and $p75^{NTR}$ -mediated signalling pathways

The extracellular N-terminal domain of each Trk receptor consists of a cystein-rich cluster followed by three leucine- rich repeats, another cystein cluster and two immunoglobulin- like domains. Each receptor spans the membrane once and has a carboxy terminal cytoplasmic domain consisting of a tyrosine kinase domain surrounded by several tyrosine residues that serve as phosphorylation-dependent docking sites for cytoplasmic adaptors and enzymes. Truncated variants of TrkB and TrkC have been isolated that lack the cytoplasmic kinase domain and appear to sequester neurotrophins reducing the efficacy of signalling by full-length, kinase competent Trks (Reichardt, 2006; Zampieri and Chao, 2006). Upon binding neurotrophins, Trk receptors dimerize and specific tyrosine residues undergo phosphorylation in the Trk receptor cytoplasmic domain. Adaptor proteins, including Shc and FRS2 are recruited to these phosphorylated tyrosine residues, thereby coupling Trk receptors to three major intracellular signalling cascades which include the Ras-ERK (extracellular signal-regulated kinase) pathway, the PI3-Kinase (phosphatidylinositol-3-kinase)-Akt pathway and the phospholipase C (PLC)-γ-protein kinase C (PKC) pathway (Chao et al., 2006; Reichardt, 2006; Zampieri and Chao, 2006). Activation of the Ras-ERK pathway promotes neuronal differentiation,

including neurite growth, activation of PI3-Kinase promotes survival and growth of neurons, whereas activation of PLC-γ results in the activation of Ca^{2+}- and PKC-regulated pathways that affect synaptic plasticity.

NGF can be retrogradely transported from axon terminals by endocytosis of NGF-TrkA into signalling endosomes that are then transported back to neuronal cell bodies by microtubule driven mechanisms (Reichardt, 2006; Zweifel et al., 2005). Retrograde signalling is particularly important in relaying survival promoting signals back the cell body. Such signalling includes, increased activity of PI3-Kinase, which suppresses cell death by inhibiting the apoptotic activities of forkhead and Bcl 2-associated death protein (BAD), and ERK5, which indirectly activates the transcription factor CREB (cAMP responsive element- binding protein).

Axonal growth, terminal arborization and synaptic plasticity are likely to be predominantly the result of local intracellular signalling events that occur near to the growth cone/terminal arbors. These signalling events, involving Ras-ERK, PI3-kinase and PLC-γ activation, contribute to axonal outgrowth by regulating microtubule dynamics and actin stability (Gillespie, 2003; Reichardt, 2006). Retrograde transport of signalling endosomes to the cell soma is also likely to play a role in promoting axonal growth, since the transcription factors CREB and NFAT (nuclear factor of activated T-cells) have been shown to promote axonal growth (Graef et al., 2003; Lonze et al., 2002; Patel et al., 2003). The p75 NTR receptor is a member of the tumour necrosis factor superfamily with an extracellular domain that includes four cystein-rich motifs, a single transmembrane domain and a cytoplasmic domain that includes a "death" domain similar to those present in other members of this family (Liepinsh et al., 1997). p75 appears to modulate Trk receptor function in several ways. For example, p75 inhibits activation of Trk receptors by non-preferred neurotrophins both *in vitro* and *in vivo* (Bibel et al., 1999), and *in vitro* studies suggest that the presence of p75 NTR potentiates activation of TrkA by suboptimal concentrations of NGF (Davies et al., 1993). Before neurotrophins are secreted in their final form, they exist as proneurotrophins.

Proneurotrophins are precursor proteins of the neurotrophins which are about 240-260 amino acids long and are cleaved by various proteases to eventually become the much shorter, mature neurotrophins. It has been shown that proneurotrophins bind with high affinity to a complex of p75 with sortilin (Nykjaer et al., 2004) and usually this binding of proneurotrophins to p75 and sortilin initiates apoptosis (Lu et al., 2005; Reichardt, 2006). In the presence of high concentrations of neurotrophins and the absence of appropriate Trk expression, the binding of neurotrophins to p75 initiates a number of intracellular signalling pathways, many of which converge on Jun Kinase activation, that lead to apoptotic cell death (Lu et al., 2005) p75 also plays a direct role in modulating neuronal process outgrowth. In the absence of neurotrophin binding, the cytoplasmic

domain of p75 binds and sequesters the small cytoplasmic GTPase, RhoGDI, preventing it from forming a complex with RhoA. Free cytoplasmic RhoA inhibits axonal growth. The engagement of p75 by neurotrophins releases p75 bound RhoGDI into the cytoplasm, thus allowing it to sequester free cytoplasmic RhoA and thereby promote axonal growth (Reichardt, 2006).

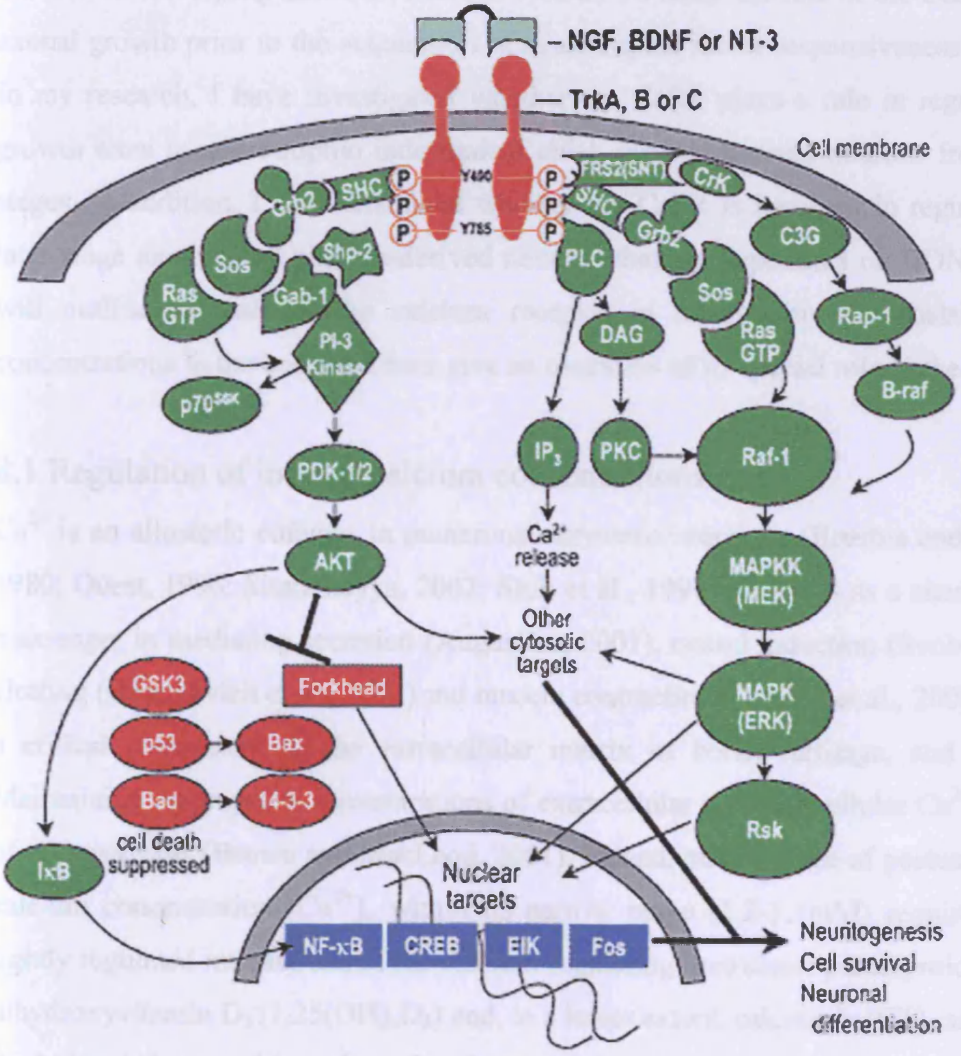

Figure1.4:

Illustration detailing some of the intracellular signalling pathways activated after ligand-mediated Trk activation which results in gene expression, increased neuronal survival and neurite outgrowth. Image adapted (Pollack and Harper, 2002)

8. The extracellular Ca^{2+}- sensing receptor (CaSR) and the regulation of extracellular ionised calcium concentration ($[Ca^{2+}]_o$)

The CaSR has recently been shown to regulate axonal outgrowth and branching from cultured neonatal mouse sympathetic neurons and modulate innervation of their target fields *in vivo* (Vizard et al., 2008). In addition, CaSR mRNA is expressed in many parts of the rat brain and PNS (Ferry et al., 2000; Yano et al., 2004). This raises the possibility that the CaSR plays an important role in the developing and adult nervous system. To date, the role of the CaSR in regulating *de novo* axonal growth prior to the acquisition of neurotrophic factor responsiveness has not been examined. In my research, I have investigated whether the CaSR plays a role in regulating intrinsic axonal growth rates in neurotrophin independent chick placode-derived neurons from early developmental stages. In addition, I have examined whether the CaSR is involved in regulating axonal growth in later stage axotomised placode-derived neurons that are dependent on BDNF for survival. Below I will outline the role of the calcium receptor in maintaining homeostasis of ionised calcium concentrations in the body and then give an overview of its special role in the nervous system.

8.1 Regulation of ionised calcium concentrations

Ca^{2+} is an allosteric cofactor in numerous enzymatic reactions (Brushia and Walsh, 1999; Cheung, 1980; Quest, 1996; Sitaramayya, 2002; Stull et al., 1997). It serves as a charge-carrier and a second messenger in mediating secretion (Augustine, 2001), neural induction (Svoboda et al., 1997), blood clotting (Ganitkevich et al., 2002) and muscle contraction (Gordon et al., 2000). Additionally, Ca^{2+} is a critical component of the extracellular matrix of bone, cartilage, and teeth (Boskey, 1992). Maintaining appropriate concentrations of extracellular and intracellular Ca^{2+} is vital to the survival of all organisms (Brown and MacLeod, 2001). Indeed, maintenance of postnatal extracellular ionised calcium concentration $[Ca^{2+}]_o$ within its narrow range (1.2-1.3mM) requires the coordinated and tightly regulated interactions of the calcium-regulating hormones; parathyroid hormone (PTH), 1,25-dihydroxyvitamin D_3 ($1,25(OH)_2D_3$) and, to a lesser extent, calcitonin (CT), and their effector organs; the kidneys, bone and intestine. Small but physiologically relevant changes in $[Ca^{2+}]_o$ are sensed by the cells of the parathyroid gland which subsequently regulate the secretion of PTH into the systemic circulation. A steep inverse sigmoidal relationship exists between $[Ca^{2+}]_o$ and PTH release, whereby slight decreases in systemic $[Ca^{2+}]_o$ promote the release of PTH into the systemic circulation, the targets of which then ensure normocalcaemia. It is now well established that the G-protein coupled, extracellular calcium-sensing receptor (CaSR) allows parathyroid cells to sense changes in $[Ca^{2+}]_o$ and regulate the secretion of PTH, thereby allowing $[Ca^{2+}]_o$ to act as a first messenger. Furthermore, the CaSR is expressed by thyroidal C-cells and its high $[Ca^{2+}]_o$-evoked activation promotes the

secretion of calcitonin, an anti-hypercalcaemic hormone. In addition, the CaSR is also expressed in tissues that serve as targets for these hormones, where it regulates local processes that contribute to maintaining systemic $[Ca^{2+}]_o$ homeostasis. During development, elevated levels of $[Ca^{2+}]_o$ (1.69mM) are maintained in the foetus by the CaSR independently of maternal $[Ca^{2+}]_o$ (Brown and MacLeod, 2001).

8.2 Structure of the CaSR

The extracellular Ca^{2+} sensing receptor is a class III, G-protein coupled, heptahelical receptor (GPCR). The human CaSR is 1078 amino acids residues long and has 3 predicted structural domains: a large hydrophilic N-terminal extracellular domain (ECD) of 612 residues which confers specificity to its low affinity physiological ligand, $[Ca^{2+}]_o$; the seven α-helical transmembrane domain (TMD) of about 250 amino acids; and a hydrophilic C-terminal intracellular domain (ICD) 216 amino acids long, which couples to various G-proteins. The functional, cell surface form of the CaSR is a homodimer linked by disulphide bond within the ECD and a non-covalent, hydrophobic interaction between the transmembrane domains of each CaSR monomer (Bai, 2004).

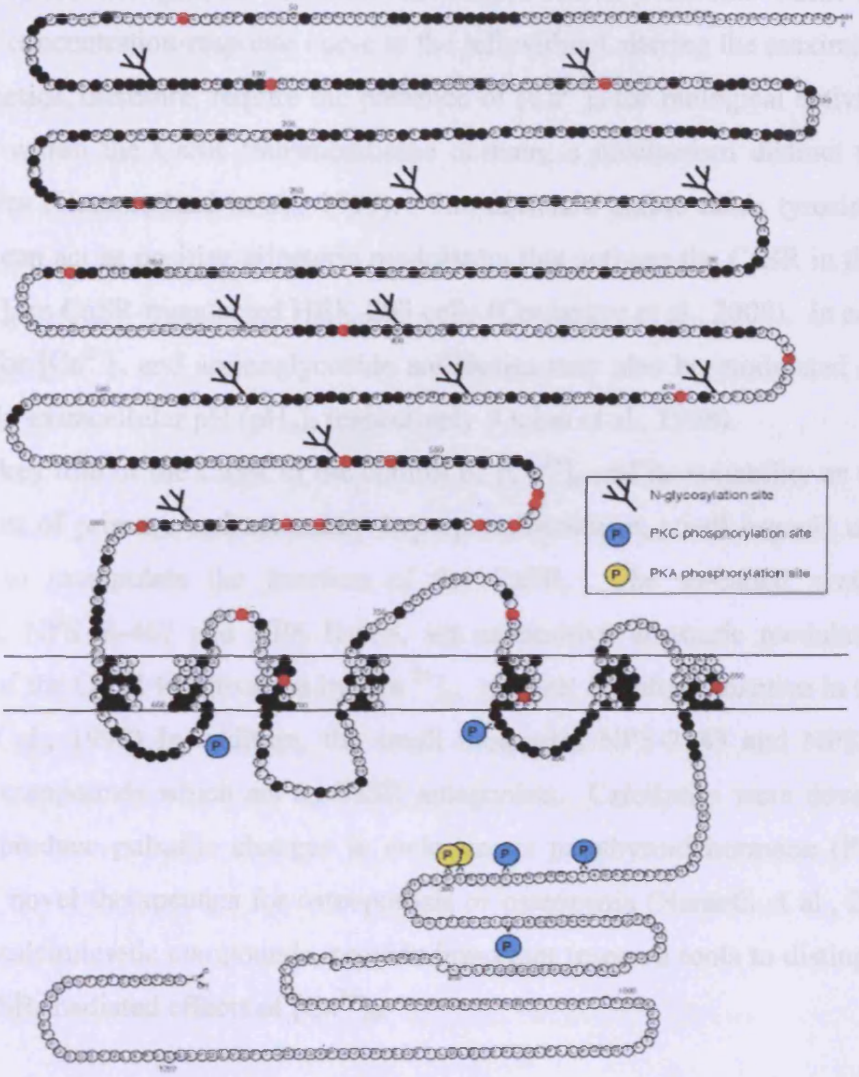

Figure 1.5: The predicted structure of the Calcium Sensing Receptor: Image adapted from (Bai, 2004)

8.3 Pharmacological Characterisation of the CaSR

While extracellular Ca^{2+} is the primary physiological ligand of the CaSR *in vivo*, however, other ligands may activate the CaSR directly (class I calcimimetics) or potentiate the receptors sensitivity to other physiological agonists (class II calcimimetics). Class I calcimimetics, including $[Ca^{2+}]_o$ itself, are orthosteric CaSR agonists. These are organic or inorganic polycations that do not require the presence of $[Ca^{2+}]_o$ to activate the CaSR. Class I calcimimetics include a number of di- and trivalent cations, polyamines, aminoglycosides and polybasic amino acids (Fig. 1.6) and are believed

to act predominantly within the CaSR ECD (Chang and Shoback, 2004; Hu et al., 2005). Class II calcimimetics are endogenous allosteric modulators which potentiate CaSR sensitivity to $[Ca^{2+}]_o$, shifting the concentration-response curve to the left without altering the maximal response. The class II calcimimetics, therefore, require the presence of $[Ca^{2+}]_o$ for biological activity and are thought to act largely within the CaSR transmembrane domain, a mechanism distinct to that of the class I calcimimetics (Hammerland et al., 1999). The aromatic amino acids tyrosine, phenylalanine and tryptophan can act as positive allosteric modulators that activate the CaSR in the presence of at least 1mM $[Ca^{2+}]_o$ in CaSR-transfected HEK-293 cells (Conigrave et al., 2000). In addition, the affinity of the CaSR for $[Ca^{2+}]_o$ and aminoglycoside antibiotics may also be modulated by ionic strength and alterations in extracellular pH (pH_o), respectively (Quinn et al., 1998).

Due to the key role of the CaSR in the control of $[Ca^{2+}]_o$ and its suitability as a molecular target for the treatment of primary and secondary hyperparathyroidism, small organic compounds have been developed to manipulate the function of the CaSR. The so-called synthetic "calcimimetic" compounds, NPS R-467 and NPS R-568, act as positive allosteric modulators and increase the sensitivity of the CaSR to activation by $[Ca^{2+}]_o$, and are, therefore, inactive in the absence of $[Ca^{2+}]_o$ (Nemeth et al., 1998) In addition, the small molecules NPS-2143 and NPS-89636 are so-called 'calcilytic' compounds which act as CaSR antagonists. Calcilytics were developed as compounds that could produce pulsatile changes in endogenous parathyroid hormone (PTH) which could be suitable as novel therapeutics for osteoporosis or osteopenia (Nemeth et al., 2001). However they, along with calcimimetic compounds, provide important research tools to distinguish between CaSR- and non CaSR-mediated effects of $[Ca^{2+}]_o$.

Class I	Inorganic cations (e.g. La^{3+}, Gd^{3+}, Ca^{2+}, Ba^{2+}, Mg^{2+})
	Polyamines (e.g. spermine, spermidine)
	Aminoglycoside antibiotics (e.g. streptomycin, gentamycin, neomycin)
	Polybasic amino acids (e.g. polylysine, polyarginine)
Class II	Aromatic L-amino acids (e.g. tyrosine, phenylalanine, tryptophan)
	Ionic strength
	pH
	Synthetic calcimimetics (e.g. NPS R-467, NPS R-568)

Figure 1.6: List of class I and class II CaSR agonists

8.4 CaSR Expression and Function in the Nervous System

In addition to its expression in tissues responsible for controlling $[Ca^{2+}]_o$, the CaSR is also widely expressed in both the developing and adult PNS and CNS. Indeed, within the adult rodent PNS the CaSR is expressed in neurons of DRG (Wang et al., 2003) trigeminal ganglion (Heyeraas et al., 2008) and the superior cervical ganglion (SCG) (Vizard et al., 2008).Within the rat CNS, the CaSR is expressed in multiple sites including the olfactory bulb, piriform cortex, cerebral cortex, hippocampus, amygdala, basal ganglia, diencephalon thalamus, hypothalamus, zona incerta, mesencephalon and cerebellum (Yano et al., 2004). Until recently, however, a functional role for the CaSR in the nervous system has only been speculated. For example, it has been proposed that a general role for the CaSR at the post-synaptic membrane, the CaSR may sense activity-dependent changes in $[Ca^{2+}]_o$ in and around the synaptic cleft (Rusakov and Fine, 2003; Vassilev et al., 1997). Recent evidence has revealed a role for the CaSR in neuronal development. The CaSR has been shown to be expressed in the superior cervical ganglion (SCG), a population of sympathetic neurons which innervates targets in the head, including the iris. SCG neurons exposed to maximally activating concentrations of $[Ca^{2+}]_o$ show an increase in axonal growth and branching *in vitro*. The growth- promoting effects of high $[Ca^{2+}]_o$ are confined to a narrow developmental window between E18-P0, a stage of development when axons from these neurons are innervating and branching extensively in their target fields *in vivo*. Manipulating CaSR function using CaSR agonists or antagonists, or expressing a dominant negative CaSR during this stage of development also has marked effects on axonal growth *in vitro*. Furthermore, E18 SCG CaSR-deficient neurons grow with smaller and less complex neurite arbors *in vitro* and the iris of CaSR-deficient animals has decreased sympathetic innervation density *in vivo* compared to wild-type and heterozygous littermates. Neurons of the SCG would be exposed to the elevated level of foetal $[Ca^{2+}]_o$ (~1.7mM) during this period of development in utero, thereby providing a tonic signal for CaSR activation *in vivo* (Vizard et al., 2008). Furthermore, the over-expression of a dominant-negative CaSR in early postnatal hippocampal pyramidal neurons maintained in slice culture results in a decrease in the size and complexity of the dendritic arbors emerging from these neurons. In vivo, the activity of the CaSR may be affected by activity-dependent changes in $[Ca^{2+}]_o$ during post-natal life to modulate hippocampal neuron dendritic arborization, thereby linking changes in neural activity with changes in dendritic architecture (Vizard et al., 2008).

8.5 Signal Transduction Pathways Downstream of CaSR Activation

Although the mechanism by which the CaSR regulates the growth of neural processes is yet to be elucidated, the downstream signalling effectors in many other cell types are known (Ward, 2004). Stimulated CaSR's can activate phospholipases C, A2 and D. CaSR mediated activation of PLC appears to entail a direct, G- protein mediated process, probably involving $G_{q/11}$. Activation of PLC leads to the generation of inositol triphosphate (IP_3) and diacylglycerol (DAG). The former mobilises intracellular calcium stores, whereas the latter leads to the activation of protein kinase C (PKC). Activation of phospholipase D by high extracellular calcium appears to involve activation of the receptor associated G-protein, $G_{12/13}$ which then activates the small GTPase, Rho. Rho in turn stimulates phospholipase D, resulting in the production of the second messenger molecule, phosphatidic acid. Activation of the cytostolic form of PLA_2 ($cPLA_2$) by high extracellular calcium and other CaSR agonists might be indirect, utilizing CaSR-mediated, PLC-dependent stimulation of PKC. $cPLA_2$ generates the second messenger arachidonic acid. CaSR ligands also decrease intracellular cAMP production by stimulating the CaSR associated G-protein, G_i. In addition, CaSR activation in some cell types can lead to the phosphorylation and activation of numerous kinases that are central components of important signalling cascades. A summary of the intracellular signalling that arises from CaSR activation in non-neuronal cells is shown in figure 1.7.

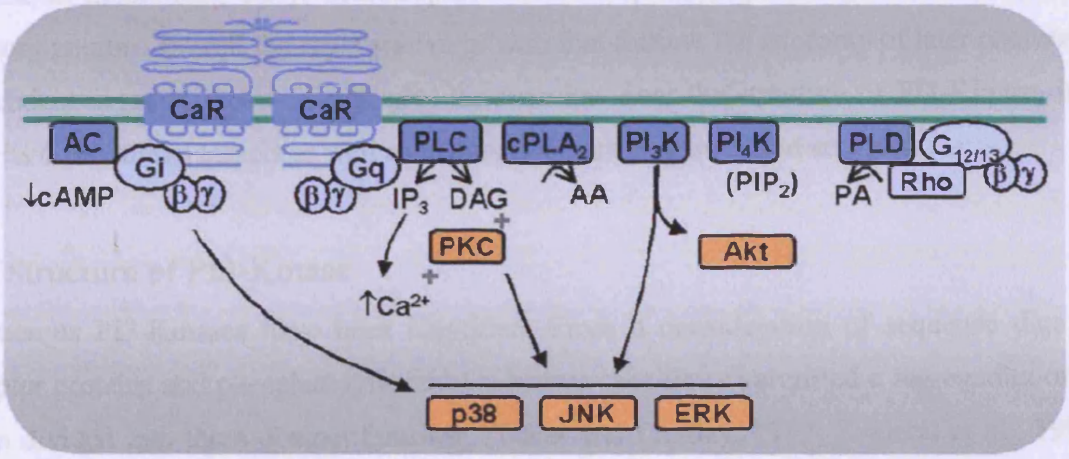

Figure 1.7: Image adapted from (Ward, 2004)

9. PI3-Kinase, Glycogen Synthase Kinase 3 and MAP- Kinase signalling

Because of their central roles in transducing extracellular signals during neuronal development and their importance in the context of this study, this section will focus on a description of PI3-Kinase, Glycogen Synthase Kinase 3 and MAP-Kinase signalling in the context of their roles in regulating neuronal survival and process outgrowth.

Membrane phosphoinositides were recognized many years ago as precursors for second messengers in cell surface receptor–coupled signal transduction pathways. In the first pathway involving phosphoinositides to be elucidated, membrane phosphatidylinositol 4,5 diphosphate ($PI(4,5)P_2$) is hydrolyzed to inositol (1,4,5) triphosphate (IP3) and diacylglycerol (DAG) by various isoforms of phospholipase C (Bootman et al., 1995; Nishizuka, 1992). Subsequently, IP3 releases calcium from intracellular stores (Bootman et al., 1995), whereas DAG activates protein kinases C. PI3-Kinase is a central player in a more recently characterised signalling pathway that revolves around dynamic changes in membrane phosphoinositide composition. PI3-Kinase catalyses the generation of phosphatidylinositol 3,4,5 triphosphate ($PI(3,4,5)P_3$) from ($PI(4,5)P_2$) at the plasma membrane by phosphorylation of the D-3 position of the inositol ring. A number of proteins that are important in intracellular signalling pathways that promote cell differentiation, growth and survival translocate to the plasma membrane and are subsequently activated by binding directly to ($PI(3,4,5)P_3$) via their pleckstrin homology (PH) domains (Cantley, 2002). In this study, I investigated the role of PI3-Kinase in modulating early, neurotrophic factor-independent axonal growth from placode-derived sensory neurons as well the regenerative growth that follows the axotomy of later neurotrophic factor dependent neurons. Below, I will give an overview over the structure of PI3-Kinase, its activation and its downstream targets as well as the involvement in growth and survival.

9.2 Structure of PI3-Kinase

Numerous PI3-Kinases have been identified. From a consideration of sequence data, binding of adaptor proteins and phosphatidylinositol substrate specificity permitted a segregation of PI3Ks have been divided into three distinct families (Toker and Cantley, 1997; Zvelebil et al., 1996). Class I PI3-Kinases are heterodimers of approximately 200 kDa, composed of a 110-120 kDa catalytic subunit and a 50-100 kDa adaptor/regulatory subunit, that are capable of phosphorylating PI 4-P and $PI(4,5)P_2$ in vitro. Adaptor subunits keep the catalytic subunit quiescent in non-stimulated cells. The preferred *in vivo* substrate for class I PI3-Kinases, seems to be $PI(4,5)P_2$ (Hawkins et al., 1992; Stephens et al., 1991). Activation of class I PI3-Kinases is controlled by extracellular signalling via receptors with intrinsic protein tyrosine kinase activity, receptors coupled to src-like protein tyrosine

kinases or G protein-linked receptors. Class I PI3-Kinases are the predominant generators of membrane ($PI(3,4,5)P_3$) and are the focus of the research on PI3-Kinase in this thesis. Class II PI3-Kinases, with an *in vitro* substrate specificity restricted to PI and PI 4-P, are 170-210 kDa proteins with a characteristic C-terminal C2 homology domain. This class is subdivided into three class 2 enzymes that are thought to act as monomeric enzymes. Class III PI3-Kinases are homologous to *S. cerevisiae* Vps34p (vascular protein sorting mutant,) and phosphorylate only PtdIns (Hawkins et al., 1992). The activity of Vps34p depends on a functional Vps15p protein Ser/Thr kinase, which recruits the phosphatidylinositol kinase to late Golgi compartments (De Camilli et al., 1996).

9.3 Signal Transduction Pathways involving Class I PI3-Kinases

Activation of PI3-Kinases by extracellular agonists is associated with their translocation to the plasma membrane where they get access to lipid substrates. Class I PI3-Kinases are subdivided into two groups depending on the adaptor proteins involved in regulating PI3-kinase catalytic subunit activity. PI3-kinases that utilise the p85 adaptor subunit are directed to phosphorylated tyrosine motifs on the intracellular domains of activated receptor tyrosine kinases or phosphorylated adaptor proteins associated these receptors (class IA). The GTP-binding protein, Ras, is activated by ligand-induced tyrosine phosphorylation of certain receptor tyrosine kinases via recruitment and phosphorylation of the adaptor proteins Grb2 and SOS to the receptor. Activated Ras can directly phosphorylate and activate PI3-Kinase (Rodriguez-Viciana et al., 1994). The Class 1B PI3-Kinase, PI3-Kinase Q interacts with adaptor protein p101 that in turn interacts with trimeric G proteins associated with G-protein-coupled receptors (Cantley, 2002).

One important PI3-Kinase downstream target is the protein serine/threonine (Ser/Thr) kinase Akt/PKB (formerly called RAC), which is activated through membrane localization (Andjelkovic et al., 1997) and Ser/Thr phosphorylation (Alessi et al., 1996; Andjelkovic et al., 1996). Both of these events are dependent on the generation of $PI(3,4,5)P_3$ by PI3-Kinase. The PH domain of Akt/PKB promotes translocation to the plasma membrane by binding to $PI(3,4,5)P_3$ (Klippel et al., 1997), and phosphorylation of Akt at Thr308 and Ser473 (Alessi et al., 1996) requires phosphoinositide-dependent kinases (PDKs), which are also activated by translocating to the plasma membrane and binding $PI(3,4,5)P_3$. Interestingly, one phosphoinositide-dependent kinase, PDK1, has been recently shown to phosphorylate and activate protein kinases C (PKC) directly (Chou et al., 1998; Le Good et al., 1998). Integrin-linked kinase (ILK, interacting with the cytoplasmic domain of L1, L2, and L3 integrin subunits (Hannigan et al., 1996) has been shown to be activated by $PI(3,4,5)P_3$ and to phosphorylate Akt/PKB on Ser473. Moreover, catalytically inactive, dominant-negative ILK inhibits

endogenous phosphorylation of Akt/PKB on Ser473. ILK might thus qualify as the first member of the PDK2 family.

The actions of catalytically active Akt/PKB include phosphorylation and inactivation of GSK3 (Cross et al., 1995) and the pro-apoptotic factor BAD (Borasio et al., 1993; Datta et al., 1997). Furthermore, PI3-Kinase activity leads to multiple phosphorylations of p70 S6-kinase, which is involved in G1 cell cycle transition (Chung et al., 1994)PI3-Kinase also mediates Jun amino-terminal kinase (JNK) activation through a Rac/PAK/MEKK/MKK4/JNK pathway.

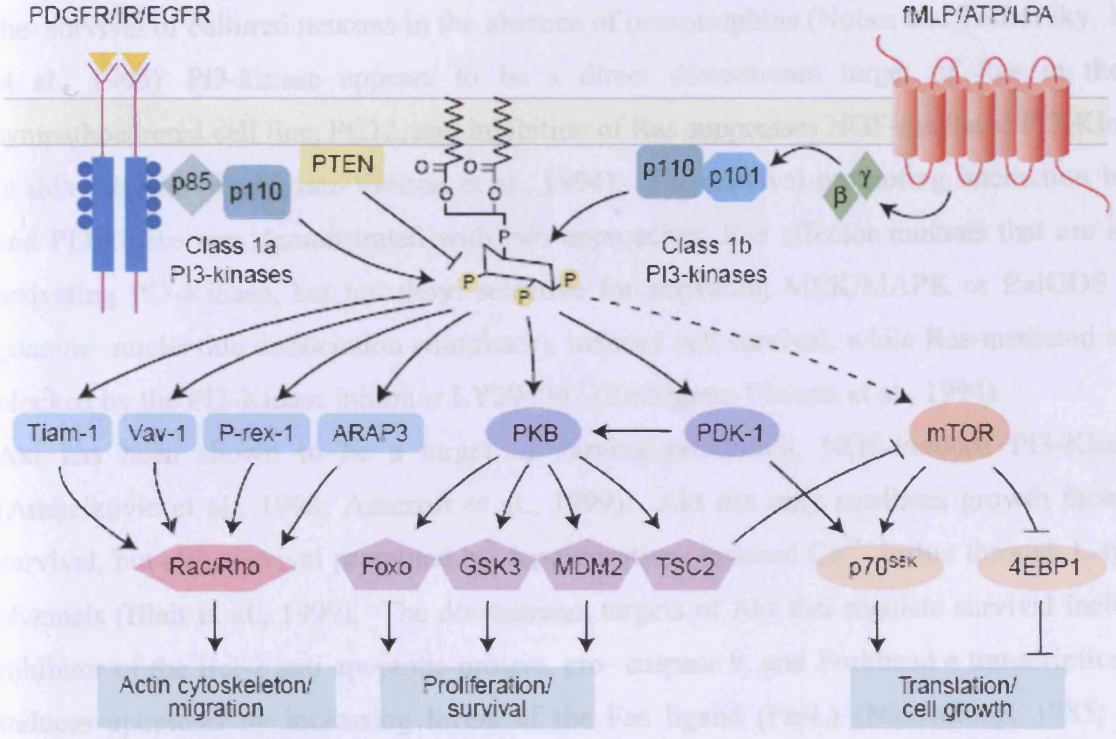

Figure 1.8: PI3 kinase signalling pathway. Signalling pathway adapted from: Expert reviews in molecular medicine (Stokoe, 2005)

9.4 PI3-Kinase regulates neuronal survival

PI3-Kinase has been shown to be responsible for neurotrophin regulated cell survival in peripheral sympathetic and sensory neurons (Huang and Reichardt, 2001; Reichardt, 2006). However, one study has claimed that PI3-Kinase inhibition does not decrease NGF-mediated survival in rat sympathetic neurons (Borasio et al., 1993). The first neurotrophin-activated signalling protein shown to mediate the survival of neurons was the GTP-binding protein Ras. Inhibition of Ras decreases the survival of most populations of sympathetic neurons. In accordance with this, promoting Ras activity increases the survival of cultured neurons in the absence of neurotrophins (Nobes and Tolkovsky, 1995; Vogel et al., 1995). PI3-kinase appears to be a direct downstream target of Ras in the PC12 rat sympathoadrenal cell line, PC12, and inhibition of Ras suppresses NGF-mediated PI3-Kinase activity in this cell line (Rodriguez-Viciana et al., 1994). The survival-promoting interaction between Ras and PI3-kinase was demonstrated with two approaches. Ras effector mutants that are selective for activating PI3-Kinase, but not those selective for activating MEK/MAPK or RalGDS (ras-related guanine- nucleotide dissociation stimulator), induced cell survival, while Ras-mediated survival was blocked by the PI3-Kinase inhibitor LY294002 (Rodriguez-Viciana et al., 1994).

Akt has been shown to be a target of survival-promoting, NGF-induced PI3-Kinase activity (Andjelkovic et al., 1998; Ashcroft et al., 1999). Akt not only mediates growth factor regulated survival, but also survival promoted by depolarisation- induced Ca^{2+} influx through L-type calcium channels (Blair et al., 1999). The downstream targets of Akt that regulate survival include Bad, an inhibitor of the Bcl-2 anti apoptotic protein, pro- caspase 9, and Forkhead a transcription factor that induces apoptosis by increasing levels of the Fas ligand (FasL) (Nieuwkoop, 1985; Rosenquist, 1981). Akt also promotes the activation of the transcription factor STAT3, leading to increased expression of antiapoptotic members of the Bcl-2 family, including Bcl-2 in pro-B lymphocyte lines and Bcl-xL in myeloid and fibroblast cell lines (Catlett-Falcone et al., 1999; Fukada et al., 1996; Karni et al., 1999)STAT3 activation by PI3-kinase/Akt appears to play an important role in the cytokine mediated survival of embryonic mouse nodose neurons (Alonzi et al., 2001).

9.5 Glycogen synthase kinase 3 (GSK3)

GSK3 was initially characterised because of the key role it plays in insulin signalling. In the absence of insulin-insulin receptor interaction, GSK3 inhibits glycogen synthase activity by phosphorylating it. However, the binding of insulin to its receptor activates Akt (via PI3-kinase) which subsequently phosphorylates a serine residue in the amino terminus of GSK3, thereby causing its inactivation (Figure 1.8). This suppression of GSK3 activity allows the dephosphorylation of glycogen synthase which promotes glycogen synthesis (Parker et al., 1983).

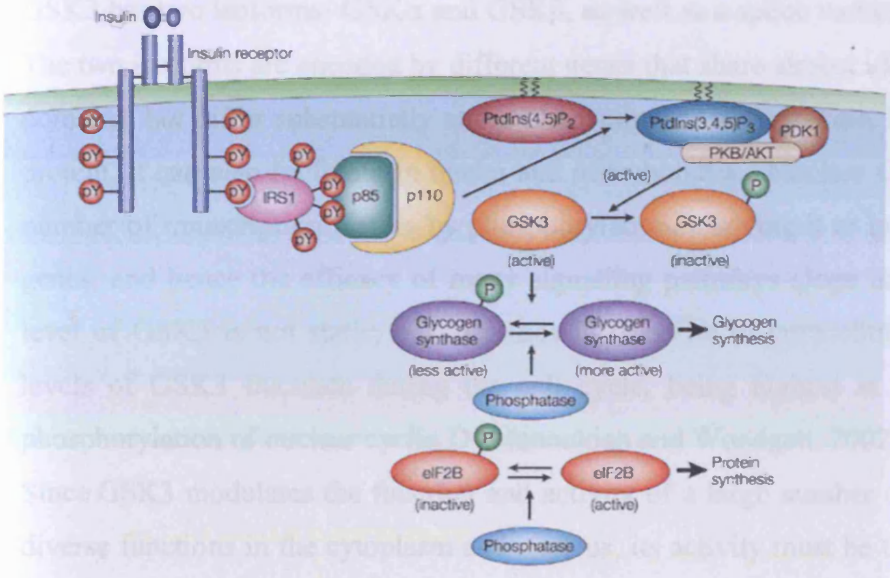

Figure1.9: The insulin signalling pathway
Adapted from (Cohen and Frame, 2001)

9.6 Structure of GSK3 and the regulation of its activity

The structure of GSK3 is similar to that of mitogen-activated protein kinase (MAPK) family members. GSK3 is phosphorylated at a tyrosine residue that is in an equivalent position to the phosphotyrosine residue in MAPKs (Hughes et al., 1993).

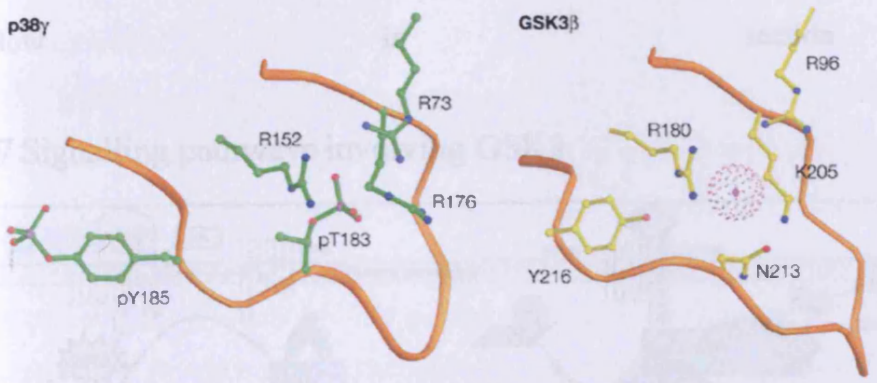

Figure 1.10: Schematic structure of GSK3β Adapted from (Cohen and Frame, 2001)

GSK3 has two isoforms- GSKα and GSKβ, as well as a splice variant of GSKβ (Mukai et al., 2002). The two isoforms are encoded by different genes that share almost identical sequences in their kinase domains, but differ substantially at the N-terminal. Although GSK3 is considered to be a cytosolic protein, it can also be found in nuclei and mitochondria. Nuclear GSK3 regulates the activity of a number of transcription factors by phosphorylation, enabling it to influence the expression of many genes, and hence the efficacy of many signalling pathways (Jope and Johnson, 2004). The nuclear level of GSK3 is not static, but increases in response to intracellular cues. For example, nuclear levels of GSK3 fluctuate during the cell cycle, being highest at the S-phase which targets the phosphorylation of nuclear cyclin D (Manoukian and Woodgett, 2002).

Since GSK3 modulates the function and activity of a large number of substrate proteins with many diverse functions in the cytoplasm and nucleus, its activity must be tightly regulated within the cell. The activity of GSK3 is regulated by a number of mechanisms. The first of these is phosphorylation of GSK3. Phosphorylation of the serine 9 residue of GSK3β or serine 21 residue of GSK3α by Akt and a number of other kinases results in significant inhibition of GSK3 activity. Other signalling pathways that can lead to GSK3 inactivation by serine phosphorylation include the MAPK cascade, cyclic AMP (cAMP) dependent protein kinase A and other $PI(3,4,5)P_3$ dependent pathways not involving Akt (Armstrong et al., 2001; Fang et al., 2000; Hughes et al., 1993; Stambolic and Woodgett, 1994). In contrast to serine phosphorylation, tyrosine phosphorylation of residue 216 of GSKβ or residue 279 of GSK3α by a group of at present poorly defined kinases promotes GSK3 activity. (Jope and Johnson, 2004). A second parameter that regulates GSK3 activity is the phosphorylation state of its substrates, since many substrates need "priming" for phosphorylation by GSK3 by prior phosphorylation events. Other factors regulating GSK3 activity are cellular localization and interaction with GSK3 binding proteins (Jope and Johnson, 2004). Figure 1.11 illustrates three of the main signalling pathways involving GSK3. These pathways will be briefly explained in the following section. In addition, figure 1.11 illustrates how GSK3 can regulate microtubule dynamics and growth cone motility. This aspect of GSK3 function will be discussed

below in section 1.10.

9.7 Signalling pathways involving GSK3

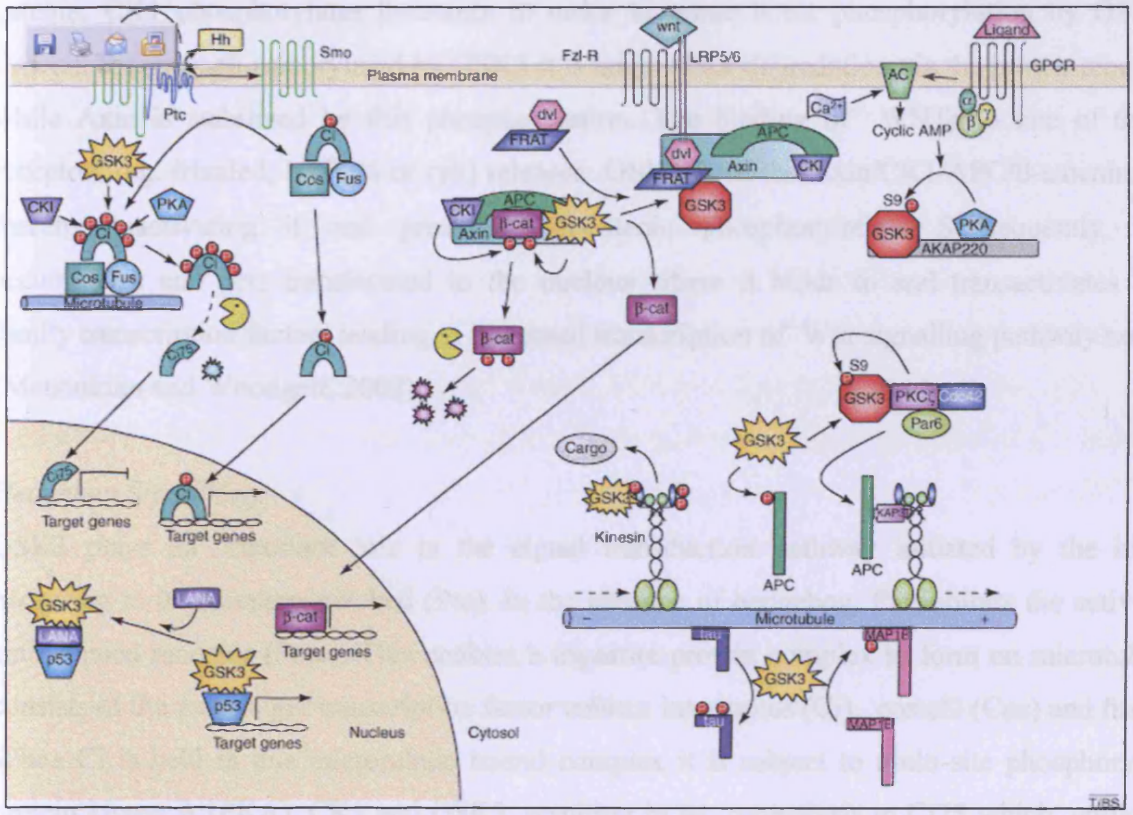

Figure 1.11: Hedgehog, Wnt and G-protein signalling Adapted (Jope and Johnson, 2004)

WNT signalling pathway:

In the absence of WNT ligands, cytoplasmic GSK3 is bound to a protein complex containing the scaffold protein, axin, CK1 (casein kinase 1), APC (Adenomatous polyposis coli protein) and β-catenin. CK1 phosphorylates β-catenin in order to prime it for phosphorylation by GSK3. If β-Catenin becomes phosphorylated by GSK3 it is targeted for degradation via the proteasome pathway, while Axin is stabilized by this phosphorylation. The binding of WNTs to one of their many receptors (eg. frizzled, LRP5/6 or ryk) releases GSK3 from the Axin/CK1/APC/β-catenin complex, thereby inactivating it and preventing β-catenin phosphorylation. Subsequently, β-catenin accumulates and gets translocated to the nucleus where it binds to and transactivates TCF/LEF family transcription factors leading to increased transcription of Wnt signalling pathway target genes (Manoukian and Woodgett, 2002).

Hedgehog Signalling:

GSK3 plays an important role in the signal transduction pathway initiated by the binding of hedgehog to its receptor, patched (Ptc). In the absence of hedgehog, Ptc inhibits the activity of the smoothened receptor (Smo). This enables a tripartite protein complex to form on microtubules that consists of the zinc finger transcription factor cubitus interruptus (Ci), costal2 (Cos) and fused (Fus). When Ci is held in this microtubule bound complex it is subject to multi-site phosphorylation by protein kinase A (PKA), CK1 and GSK3, resulting in its proteolysis to Ci75 which, unlike Ci, is a transcriptional repressor. Stimulation of Ptc by Hedgehog activates Smo, resulting in the dissociation of the microtuble bound Cos/Fus/Ci complex, decreased phosphorylation of Ci and hence decreased proteolysis to Ci75. Released Ci translocates to the nucleus to function as a transcriptional activator (Jope and Johnson, 2004).

Signalling pathway via cyclic AMP second messenger:

In the presence of appropriate G-proteins, ligand engagement of G-Protein coupled receptors (GPCR's) can result in the stimulation of adenylyl cyclase (AC) activity and increased cAMP production. Increased cAMP production in turn leads to increased protein kinase A activity. The PKA anchoring protein 220 binds both PKA and GSK3 keeping them in close proximity, thereby allowing activated PKA to serine phosphorylate and inhibit GSK3 in a localised manner (Jope and Johnson, 2004).

9.8 Role of GSK3 in cell survival

As discussed above, phosphorylation and inactivation of GSK3 is a downstream event in PI3-kinase mediated survival signalling. In accordance with this, over-expression of GSK3 induces apoptosis in PC12 cells, whereas expression of a dominant-negative, kinase inactive isoform of GSK3 into the same cells prevents cell death induced by inhibiting PI3-kinase (Pap and Cooper, 1998). Similarly, over-expression of GSK3 in the human neuroblastoma cell line SH-SY5Y, potentiates staurosporine and heat-shock induced apoptosis and ectopic expression of dominant-negative GSK3 protects cells from apoptosis in a cell line model of Huntington's disease. In addition, lithium, which is an inhibitor of GSK3, provides protection from apoptosis in both of these cell line based apoptosis models (Bijur et al., 2000; Carmichael et al., 2002). Nuclear levels of GSK3 increase rapidly during apoptosis (Bijur and Jope, 2001). One target of nuclear GSK3 is the transcription factor, p53. The direct binding of GSK3 to p53 activates GSK3 and activated GSK3 subsequently promotes the transcriptional and apoptotic activities of p53 (Watcharasit et al., 2002). Nuclear GSK3 is also capable of inhibiting the activity of survival-promoting transcription factors, such as heat-shock factor 1 (Li et al., 2002).GSK3β knockout mice develop normally until mid-gestation, but die around embryonic day 14 due to massive tumour necrosis factor-α (TNFα) induced hepatocyte apoptosis (Hoeflich et al., 2000; Schotte et al., 2001). This finding demonstrates the isoform specific functions of GSK3, since GSK3α is unable to compensate for the loss of GSK3β.

9.9 MAP-Kinase signalling

Mitogen activated protein kinases (MAP kinases) are a group of related proteins that are crucially involved in a wide range of signalling pathways that play important roles in proliferation, differentiation, regulation of gene expression, survival/apoptosis and responses to stress. In general, MAP kinase signalling pathways consist of a signalling cascade involving four distinct steps. The initial step is plasma membrane receptor mediated activation of MAP kinase kinase kinases (MAPKKK's or MP3K's) via a number of proteins including Ras, PKC and PKA. In the second step, MAP3K's phosphorylate and activate MAP kinase kinases (MAPKK's or MAP2K's), which in turn phosphorylate and activate MAP kinases (MAPK's) by dual phosphorylation of threonine and tyrosine residues in the motif T-X-Y. In the fourth step of the cascade, MAP kinases can either phosphorylate non-kinase proteins, such as transcription factors, or activate further kinases that are often referred to as MAP kinase-activating protein kinases (MAPKAP kinases or MK's) (Qi and Elion, 2005).

The classical MAP kinase pathway, and the first to be fully elucidated, involves the MAP kinases ERK1 and ERK2. This pathway can be initiated in a number of ways including; ligands binding to cytokine and growth factor associated receptor tyrosine kinases, G-protein-coupled receptor activation, integrin activation by extracellular matrix components and certain cell stressors. The MAP3K's in the classical pathway are A-Raf, B-Raf and c-Raf-1 and these activate the MAP2K's, MEK1 and MEK2. ERK1 and ERK2 phosphorylate and modulate the activity of numerous proteins including the transcription factors STAT3, Ets, CREB, CBP, NFκB and Myc and the cytoplasmic isoform of phospholipase A_2 (Qi and Elion 2005 J Cell Science; Yoon and Seger 2006 Growth factors). Kinase targets of ERK1 and ERK2 include the ribosomal S6 kinases, rsk 1 and rsk 2 (Howe et al., 1992), and MAPKAP kinase-2, a protein that phosphorylates glycogen synthase kinase 3 at Ser-7 (Stokoe et al., 1992)

Four other MAPK families have been identified and characterised, in addition to the ERK1/ ERK2 family. These are; the Jun N-terminal kinases (JNK1, JNK2 and JNK3), p38 MAP kinases (p38α, p38β and p38γ), ERK3 and ERK4, ERK5 (Qi and Elion, 2005). Each of these four MAPK families utilise different MAP3K's, MAP2K's and downstream substrates. JNK's play important roles in neuronal development and apoptosis, whereas p38's are key regulators of cell migration, proliferation and differentiation, particularly in the immune system. In the nervous system, p38's appear to be implicated in regulating the myelination of axons, in both the PNS and CNS, and in the aetiology of neuropathic pain (Ji and Suter, 2007). The roles of ERK3/4 and ERK5 are less well characterised than ERK1/2, JNK and p38 MAP kinases. Each of the five MAPK familes, and the corresponding upstream and downstream kinases of their signalling modules, are associated with numerous intracellular scaffolding proteins. These scaffolding proteins appear to act both to segregate different modules and to modulate their activity by binding phosphatases and cytoskeletal proteins. Recent research has identified a large family of dual specificity phosphatases that dephosphorylate threonine and tyrosine residues of MAP kinases, thereby regulating their kinase activity. Evidence is accumulating to suggest that many of these phosphatases are cell type and MAP-kinase type specific (Jeffrey et al., 2007). In addition, several single specificity threonine or tyrosine phosphatases also modulate MAP kinase function (Qi and Elion, 2005).

9.10 ERK1/ERK2 activation is involved in neurotrophin-promoted neurite growth bur not in neurotrophin mediated-neuronal survival in vitro

Most studies investigating the role of ERK1/2 in neurotrophin mediated survival have used either PC12 cells or sympathetic neurons and have focused on NGF. Although NGF induces a strong activation of ERK1/2 in sympathetic neurons and PC12 cells, inhibition of MEK1, the principle upstream activator of ERK1/2, has minimal effects on NGF dependent neuronal survival (Creedon et al., 1996; Virdee and Tolkovsky, 1996). In accordance with this, adenovirus mediated expression of dominant-negative isoforms of several kinases within the ERK signalling casacade does not reduce the survival of NGF stimulated PC12 cells or embryonic mouse sensory neurons in serum free culture (Klesse et al., 1999). Interestingly, inhibition of MEK1 or the expression of dominant-negative ERK dramatically reduces the ability of NGF to promote neurite outgrowth from PC12 cells and sympathetic neurons, strongly suggesting that the ERK1/2 MAP kinase pathway mediates NGF-induced process outgrowth (Creedon et al., 1996; Klesse et al., 1999; Virdee and Tolkovsky, 1996).

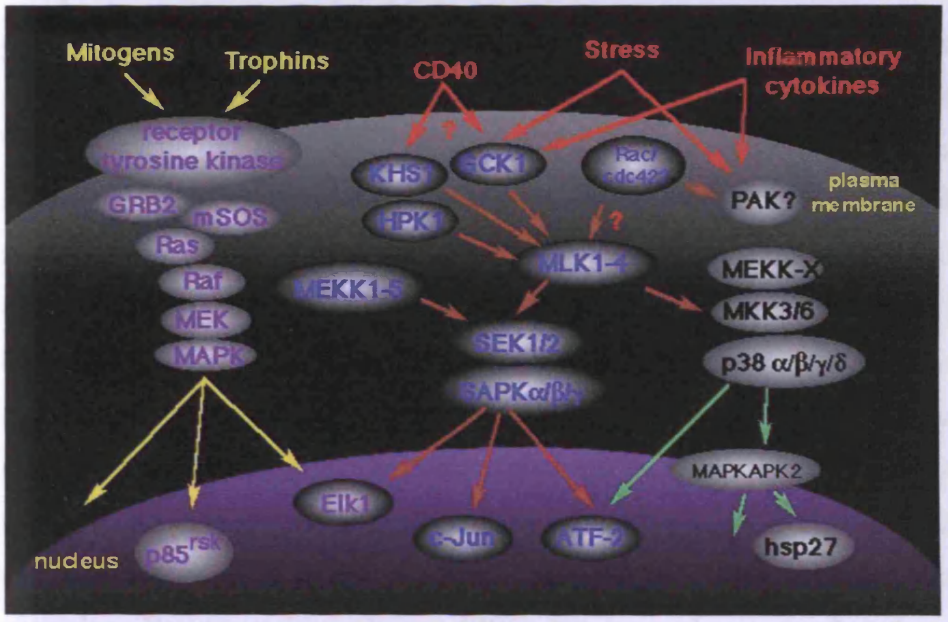

Figure 1.12: MAP Kinase signalling pathway. Signalling pathway adapted from: kinase.uhnres.utoronto.ca/signallingmap.html

10. The roles of GSK3β, PI-3 Kinase and MAP-Kinase signalling in regulating neuronal process outgrowth

GSK3β has been found on the leading edge of the growth cone where it is maintained in its inactive form (Eickholt et al., 2002). Experimental inactivation of GSK3β in cerebellar granule cells results in growth cone expansion, axonal spreading and increased branching of neuritic processes (Lucas et al., 1998), whereas semaphorin 3A and lysophosphatic acid, both of which activate GSK3β, cause growth cone collapse and neurite retraction (Sayas et al., 2002). These observations raise the possibility that inactivation and activation of GSK3β promote growth cone extension and collapse, respectively, implicating GSK3β in the regulation of neuronal process outgrowth and synaptic remodelling.

Several mechanisms have been proposed to account for the inhibitory effects of activated GSK3β on growth cone extension. The protein APC, which as described above forms a complex with β-catenin, CK1, axin and GSK3β as part of the Wnt signalling pathway, is also associated with microtubules. The positioning of functional APC at the plus-end of microtubules is essential for maintaining the appropriate direction of microtubule assembly and hence growth cone extension. Activated GSK3β appears to phosphorylate APC and disrupt its function in both astrocytes and neurons. Indeed it has been shown that inactivation of GSK3β locally within growth cones by Cdc42-Par6-aPKC mediated serine phosphorylation increases the association of APC with the plus-ends of microtubules and is necessary for normal astrocyte motility (Etienne-Manneville and Hall, 2003; Jimbo et al., 2002). Similarly, local NGF-induced activation of PI3-Kinase at the distal tips of embryonic DRG axons has been shown to lead to local inactivation of GSK3β in growth cones (via the PI3-kinase substrate ILK) which in turn increases the association of APC with the tips of microtubules, leading to growth cone extension (Zhou et al., 2004). A similar mechanism appears to be involved in regulating axon specification and elongation in hippocampal neurons (Jiang et al., 2005). APC is not the only substrate of activated GSK3β that plays a role in regulating microtubule assembly and hence axonal extension. For example, activated GSK3 has been shown to phosphorylate Collapsin Response Mediator Protein-2 (CRMP-2) thereby reducing its ability to bind to tubulin dimers and promote microtubule polymerization (Yoshimura et al., 2005). CRMP-2 appears to play an important role in determining neuronal polarity by promoting the elongation of one dendrite to become an axon. In accordance with this, over-expression of CRMP-2 in cultures of embryonic rat hippocampal neurons results in the formation of multiple axons. Non-phosphorylated, CRMP-2 is predominantly localised in the tips of axonal growth cones in cultured hippocampal neurons, together with serine phosporylated, inactive, GSK3β. In the same neurons, activation of the PI3-kinase/Akt pathway by either NT-3 or BDNF promotes the serine phosphorylation and inactivation of GSK3β which in turn

leads to reduced CRMP-2 phosphorylation and enhanced axonal extension (figure 1.12). In addition to APC and CRMP-2, GSK3β has been shown to phosphorylate the microtubule-associated proteins tau and MAP1B (Lucas et al., 1998; Sperber et al., 1995; Trivedi et al., 2005). In contrast to its effects on other microtubule associated proteins, GSK3β activates MAP1B by phosphorylation, thereby promoting its ability to destabilise microtubules, increase the rate of axon elongation and reduce the size of growth cones (Owen and Gordon-Weeks, 2003; Trivedi et al., 2005).

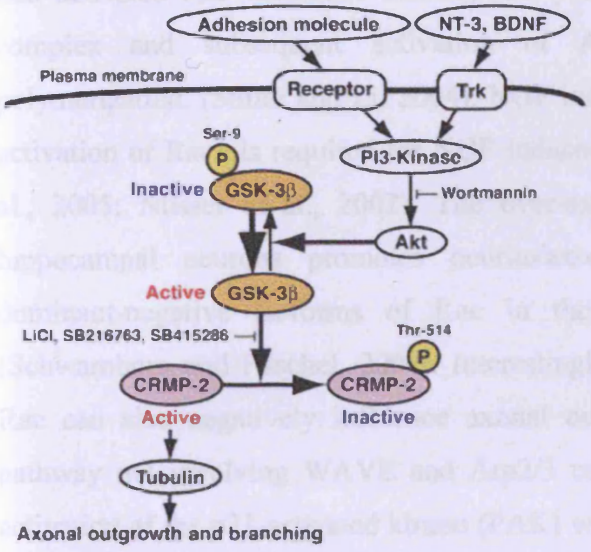

Figure 1.13: Signalling via PI3-Kinase
Model to Regulate the phosphorylation of CRMP-2 by GSK-3βNT-3, BDNF, and adhesion molecules, which are thought to activate PI3-kinase, thereby producing PIP_3. PIP_3 activates Akt via PDK. Activated Akt phosphorylates and inactivates GSK-3β. The binding activity of CRMP-2 to tubulin is decreased by the phosphorylation by GSK-3β. Nonphosphorylated CRMP-2 binds to tubulin heterodimers to promote microtubule assembly, thereby enhancing axon elongation and branching.

Adapted from
(Yoshimura et al., 2005)

GSK3β can also regulate axonal outgrowth from neurons by a mechanism that does not involve phosphorylation of microtubule associated proteins. It has recently been shown that transcription factors of the nuclear factor of activated T-cells (NFATc) family play a role in regulating axonal outgrowth during vertebrate development. NFATc family members are activated by the cytoplasmic phosphatase, calcineurin, leading to their nuclear import and the transcription of several genes that promote axonal extension. GSK3β is one of several kinases that can inactivate NFATc family transcription factors, thereby inhibiting axonal extension (Nguyen and Di Giovanni, 2008). GSK3β can also phosphorylate the cyclic AMP response element binding protein (CREB) transcription factor, thereby inhibiting its DNA binding activity (Grimes and Jope, 2001). As discussed below, CREB appears to play an important role in neurotrophin mediated axon extension.

In addition to influencing microtubule polymerisation via modulation of Akt, ILK, Cdc42 and GSK3 activity, PI3-kinase can also promote neuronal process outgrowth by modulating actin dynamics (figure 1.13) Indeed, PI3-Kinase has been shown to be activated at the leading edge

of axonal growth cones where it co-localises with polymerizing actin filaments (Shi et al., 2003; Zhou et al., 2004). A series of studies in non-neuronal cells has provided clues as to how activated PI3-Kinase in the growth cone may regulate actin dynamics in extending axons. In non-neuronal cells, PI3-Kinase regulates actin filament assembly mainly via the activation of Rac and Cdc42 (Hall and Nobes, 2000; Raftopoulou and Hall, 2004). Over-expression of constitutively active Rac in cultured 3T3 cells enhances membrane ruffling, lamellipodia protrusion and cell motility (Nobes and Hall, 1995). More recent studies suggest that activated Rac facilitates lamellipodia protrusion via activation of the WAVE protein complex and subsequent activation of Arp2/3. Activated Arp2/3 promotes actin polymerization. (Smith and Li, 2004). NGF induced activation of PI3-kinase and subsequent activation of Rac1 is required for NGF induced neurite outgrowth from PC12 cells (Aoki et al., 2005; Nusser et al., 2002). The over-expression of constitutively active Rac in rat hippocampal neurons promotes neurite/axon elongation, whereas over-expression of dominant-negative isoforms of Rac in the same neurons inhibits neurite outgrowth (Schwamborn and Puschel, 2004). Interestingly, the modulation of actin polymerisation by Rac can also negatively influence axonal outgrowth in drosophila neurons by a second pathway not involving WAVE and Arp2/3 complexes. In this pathway, Rac induces the activation of the p21-activated kinase (PAK) which in turn phosphorylates and activates LIM domain-containing kinases (LIMK) leading to the phosphorylation of the actin depolymerisation factor, cofilin. Thus in *Drosophila* neurons at least, Rac can modulate actin polymerisation dynamics by activating two pathways that have opposing effects on axon extension. (Ng and Luo, 2004).

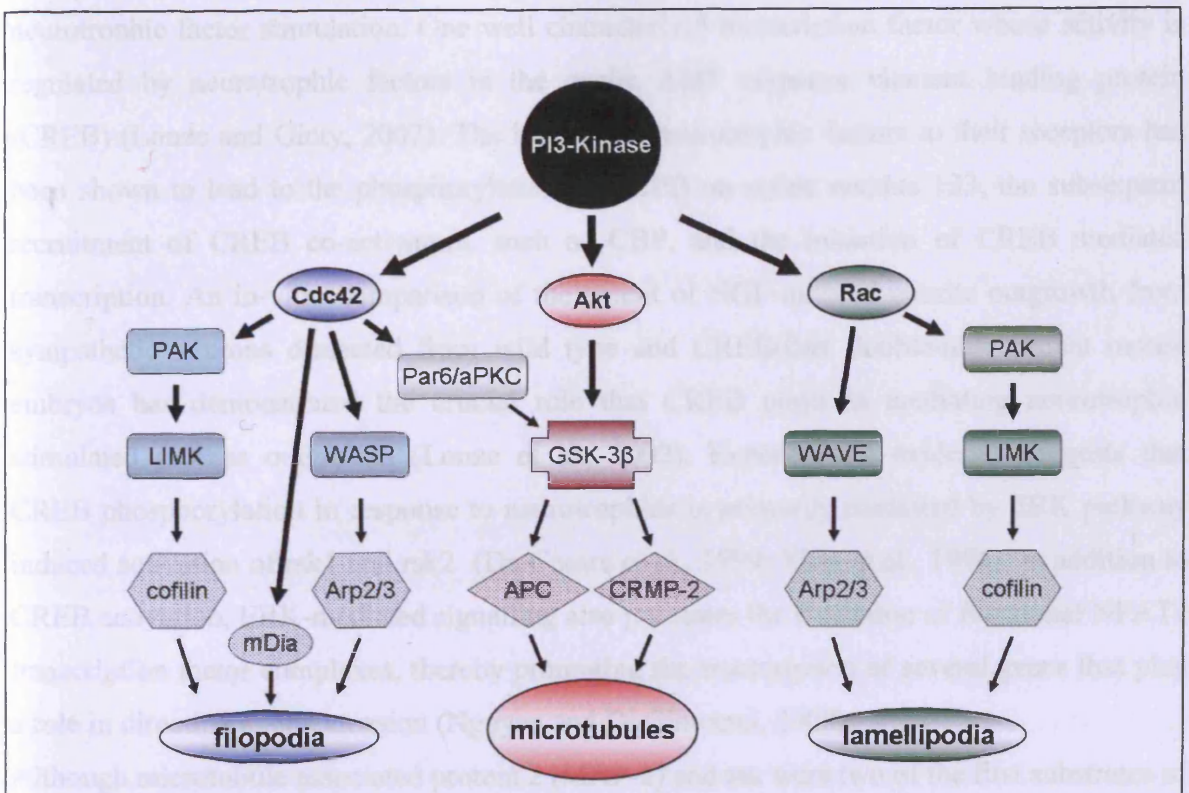

Figure 1.14 Local PI3-kinase signalling activates signalling pathways that modulate both microtubule and actin polymerization to regulate growth cone extension (Zhou and Snider, 2006)

In non-neuronal cells, Cdc42 appears to modulate actin rearrangements that are involved in filopodia formation. It achieves this either by sequential activation of WASP family proteins and the Arp2/3 complex, or by direct activation of the actin binding protein, mDia (Higgs and Pollard, 2000). Activated Cdc42, like Rac, can also activate the PAK, LIMK, cofilin pathway (Govek et al, 2005). PI3-Kinase mediated activation of Cdc42 has been shown to be an important event in the process of NGF-induced neurite outgrowth from PC12 cells (Aoki et al., 2005). Cdc42 also appears to play a role in regulating neurite outgrowth from cultured neurons. For example, over-expression of active Cdc42 in chick spinal cord neurons promotes filopodia formation and neurite/axon elongation (Brown et al., 2000) and BDNF induced activation of Cdc42 in filopodia of Xenopus spinal cord neurons is associated with filopodia extension (Robles et al., 2005).

Long-range axon extension requires elevated gene transcription, to provide the raw materials for axon assembly, not just local signalling events in the vicinity of the growth cone. MAP-kinase signalling appears to play a major role in regulating the activity of transcription factors

that direct the transcription of genes associated with axon extension in response to neurotrophic factor stimulation. One well characterised transcription factor whose activity is regulated by neurotrophic factors is the cyclic AMP response element binding protein (CREB) (Lonze and Ginty, 2002). The binding of neurotrophic factors to their receptors has been shown to lead to the phosphorylation of CREB on serine residue 133, the subsequent recruitment of CREB co-activators, such as CBP, and the initiation of CREB mediated transcription. An in-vitro comparison of the extent of NGF-induced neurite outgrowth from sympathetic neurons dissected from wild type and CREB/Bax double-null mutant mouse embryos has demonstrated the crucial role that CREB plays in mediating neurotrophin stimulated process outgrowth (Lonze et al., 2002). Experimental evidence suggests that CREB phosphorylation in response to neurotrophins is primarily mediated by ERK pathway induced activation of rsk1 and rsk2 (De Cesare et al., 1999; Xing et al., 1996). In addition to CREB activation, ERK-mediated signalling also promotes the formation of functional NFATc transcription factor complexes, thereby promoting the transcription of several genes that play a role in directing axon extension (Nguyen and Di Giovanni, 2008).

Although microtubule associated protein 2 (MAP-2) and tau were two of the first substrates of MAP-kinases to be identified (Ray and Sturgill, 1987) relatively little is known about the role of MAP-kinase signalling in the local modulation of microtubule / actin polymerisation dynamics and hence growth cone extension. An elegant study using compartmentalised chambers and exogenous expression of wild type and mutated trkB isoforms in cultured rat SCG neurons has demonstrated that localised axonal ERK signalling is required to induce local axon assembly in response to BDNF (Atwal et al., 2000). A more recent study has shown that the phosphorylation and activation of the microtubule associated protein, MAP1B, by GSK3 is positively regulated by ERK activity during neurotrophin-induced axon growth, creating a possible link between ERK signalling and axonal microtubule dynamics (Goold and Gordon-Weeks, 2005). ERK signalling has also been implicated in regulating actin filament dynamics, since pharmacological inhibition of ERK in growing axons results in growth cone collapse associated with rapid actin depolymerization (Atwal et al., 2003). There is increasing evidence that some mRNAs encoding actin related cytoskeletal proteins are translated in the local vicinity of extending growth cones. Examples include β-actin, cofilin and GAP43 mRNAs (Bassell et al., 1998; Smith et al., 2004; Willis et al., 2005). Interestingly, ERK signalling can regulate local protein translation in axonal growth cones in response to extracellular cues that either promote growth cone extension or collapse (Campbell and Holt, 2003; Wu et al., 2005).

11. Aims and Objectives

The aim of my research was to ascertain whether the CaSR plays any role in the development of sensory neurons, and if so, to determine the intracellular molecular mechanisms that mediate the effects of the CaSR on these neurons. The specific objectives at the outset were as follows:

(i). To determine if activation of the CaSR by physiological levels of $[Ca^{2+}]_o$ affects either the survival of or growth of axons from embryonic sensory neurons at the stage when their axons are growing to their targets in vivo and the neurons are not dependent on neurotrophic factors for survival.

(ii). If the CaSR did affect early de novo axonal growth, to investigate if it plays any role in governing intrinsic differences in growth rate related to target distance.

(iii). To determine if activation of the CaSR by physiological levels of $[Ca^{2+}]_o$ affects either the survival of or the regeneration of axons from embryonic sensory neurons in culture at stages in development after their axons have reached their targets in vivo and the neurons have become dependent on neurotrophic factors for survival.

(iv). To investigate the intracellular signalling pathways that mediate the effects of the CaSR in developing sensory neurons, with a particular focus on several key signalling pathways that have been implicated in regulating axonal growth and/or neuronal survival, namely, MAP-Kinase, PI3-Kinase and GSK3 signalling.

Chapter 2

Material and Methods

2.1 Introduction

Because the peripheral and central axons of different cranial sensory ganglia have markedly different distances to grow to reach their targets during development, cultures of cranial sensory neurons at the stage when their axons would reach their targets *in vivo* have been useful for studying differences in *de novo* axonal growth rate and the onset of neurotrophic factor dependence in relation to differences in the timing of the target field innervation. Naturally occurring cell death occurs in cranial sensory ganglia during target-innervating stages where each population of cranial sensory neurons become dependent on a particular neurotrophic factor or combination of factors. Studying these neurons at this stage of development has been useful for analysing the function and co-operation of neurotrophic factors.

The research described in this thesis uses a variety of *in vitro* and *in vivo* protocols to analyse neuronal survival and process outgrowth. The *in vitro* protocols developed in this lab are well established, widely used and serve as a powerful tool for investigating the mechanisms of neuronal survival and neurite outgrowth.

2.1.1 Making Tungsten Needles

Tungsten needles were used to complete dissections and to remove adherent connective tissue from the dissected neuronal tissue. To make tungsten needles, two 3-5 cm pieces of 0.5 mm diameter tungsten wire (Goodfellow, Cambridge) were cut and at the end 1cm of each bent by an angle between 60°-90°. This end was immersed in 1M KOH and a 3-12V AC current was passed through the wire and a second electrode immersed in the solution. The tungsten is etched away, forming a taper from the bend to the tip of the needle. The needles were then held in chuck- grip platinum wire holders and sterilised using either a Bunsen flame or 70 % ethanol.

2.1.2 Preparation of culture substratum

Neurons were grown on a laminin/ polyornithine substratum. Dishes were prepared by transferring either 1ml Poly-DL-ornithine (Sigma) / borate solution to 35mm tissue culture dishes (Greiner), or 250 µl to each well of a 4- well- dish (Greiner), and left overnight at room temperature. The poly- ornithine solution was aspirated the following morning and the dishes were washed twice with sterile distilled water before being allowed to air dry in the laminar flow hood. Two or three hours prior to the use, 100 µl of a 20 $mg.ml^{-1}$ solution of laminin (Sigma) in Hank's Balance Salt Solution (HBSS, Gibco, Invitrogen) was transferred to the

centre of each dish and subsequently spread over the dish surface. The dishes were then placed in a tissue culture incubator for 2-3 hrs. The dishes were then removed from the incubator and washed twice with sterile distilled water, taking care not to let the dishes to dry out, and then 1 ml of medium added immediately after washing.

2.1.3 Preparation of culture medium

Ham's modified F-14 (JRH Biosciences) was obtained in powdered form where a 10X concentrate would be made, including the antibiotics penicillin G (Sigma) and streptomycin sulphate (Sigma, final concentrations in 1X F-14: 179 μM and 68.8 μM, respectively) and stored at 25ml aliquots at –20 °C. To make F-14, 500 mg sodium hydrogen carbonate (BDH) was dissolved in 250 ml tissue culture- grade distilled water (Gibco, Invitrogen), 25 ml of this was replaced with the 10X F-14 concentrate. The 1x F-14 solution was then supplemented with 2.5 ml 200 mM glutamine (Gibco, Invitrogen, 2 mM final) and 25 ml of 10% HIHS.

2.2 Dissection techniques

2.2.1 Dissection of early cranial sensory ganglia

All dissections and subsequent preparations of neuronal cultures were carried out in a laminar flow hood using standard sterile technique. Fertile chicken eggs were incubated in a forced-draft, humidified incubator at 38 °C for the required time. To remove the embryos from the eggs, the egg was held with he blunt end uppermost where the air space is located. This end was disinfected with 70 % ethanol and allowed to dry. The shell was cracked in a line around the air space with scissors. This portion of the shell was removed and the embryo was carefully removed together with the adherent membranes with a pair of curved forceps. The embryo was washed in a petri dish containing L-15 medium and all membranes were removed with a pair of watchmaker's forceps. The embryos where then transferred into a 60mm Petri dish containing L-15 medium. Here the embryos were then carefully staged according to criteria set out by Hamburger-Hamilton (see Fig. 2.1).

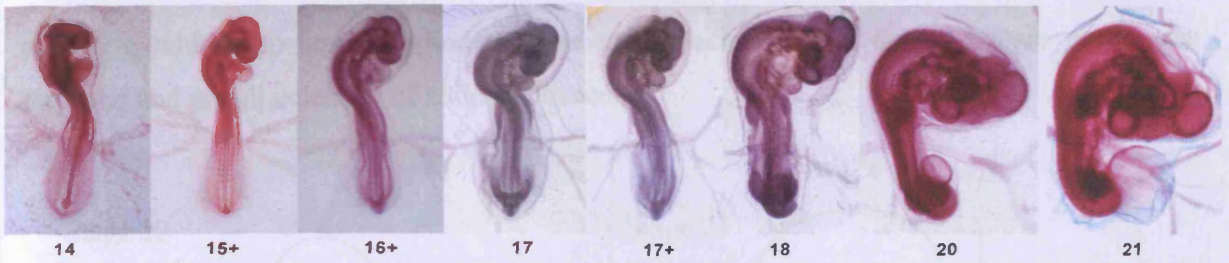

Figure 2.1: Staging diagrams for chicken embryos. Adapted from the Hamburger- Hamilton staging diagrams.

Tungsten needles were used to make the transverse cuts to isolate the part of the developing head that contains the trigeminal, geniculate, vestibular and nodose ganglia. The head was bisected along the sagittal plane. This was done by inserting the tungsten needle into the cavity of the developing fourth ventricle. The tissue was orientated so that the dorsal aspect lay next to the bottom of the petri dish. Then it was cut through the roof of the fourth ventricle. The tissue then was orientated so that the ventral aspect was facing the bottom of the petri dish. Tungsten needles were used to remove the hindbrain from the medial aspect of each half of the bisected tissue. With the tissue lying on its side, the ganglia could be observed.

The ganglia were dissected from the surrounding tissue by bringing two tungsten needles down on either side of each ganglion and remove any adherent connective tissue with these needles. Ganglia were collected into a separate dish, transferred there using a siliconized Pasteur pipette.

2.2.2 Isolation of nodose ganglia in mid- embryonic development

The embryos were extracted from the eggs by using a pair of curved forceps placed beneath the neck. The embryos were decapitated close to the base of the skull. Skin was removed from the front of the neck and the upper thorax by using a pair of watchmaker's forceps and the great vessels emerging from the heart where exposed by separating the overlying muscular and skeletal tissues at the upper part of the thorax. One blade of the watchmaker's forceps was inserted deep to the root of the great vessel. The great vessels were grasped and their attachment to the heart was severed by using a pair of watchmaker's forceps. The great vessels were and the attached tissues lying in front of the neck pulled out gently away from the underlying vertebral column, by using a second pair of forceps to loosen the tissue so that they peal away from the vertebral column without tearing. Tissue containing the nodose ganglia was harvested in a fresh 60mm Petri dish containing L-15 medium. Tissue was subdissected using tungsten needles. Nodose ganglia can easily be recognized by their

glistering white appearance, spindle shape and attached vagus nerve. Vagus nerve was removed and ganglia cleaned of adherent tissue.

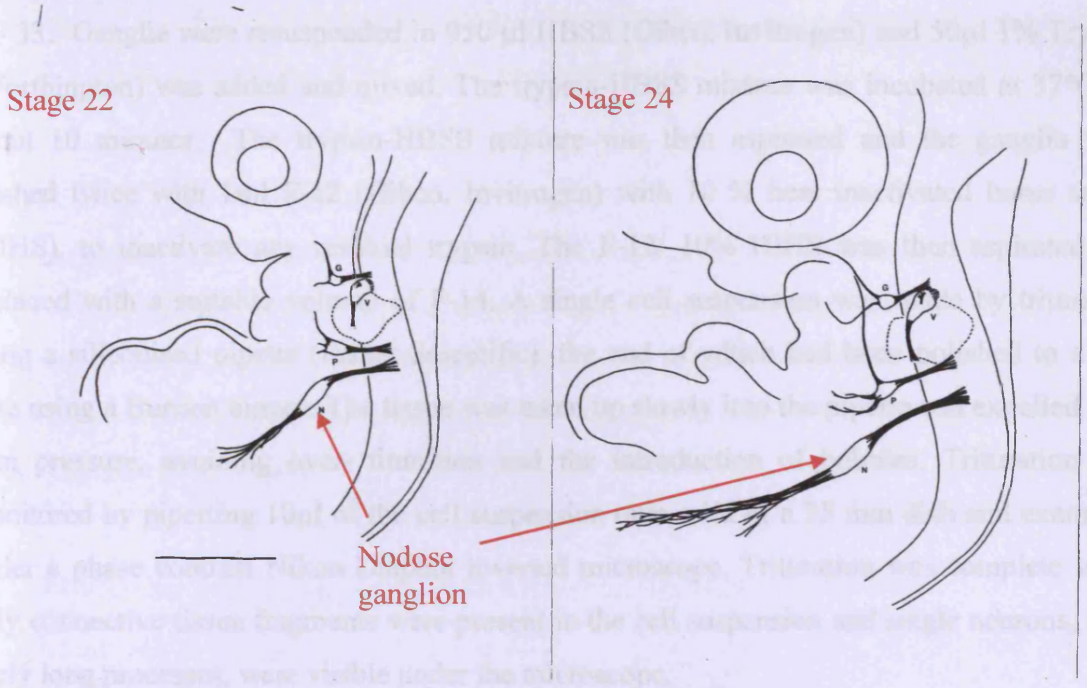

Figure2.2: Location of the nodose Ganglion in early development. Scalebar = 1mm

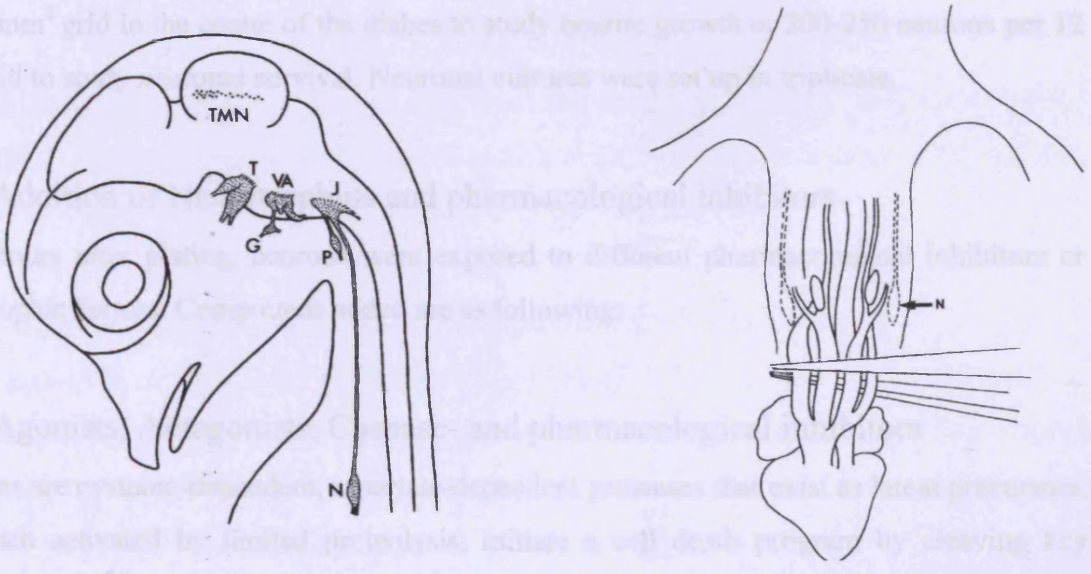

Figure 2.3: dissection of mid- embryonic chick nodose ganglia. The ganglia are located in the neck and can be obtained after removing the heart

2.2.3 Dissociated neuronal cultures

Dissociated cultures of chick nodose ganglion neurons were set up from embryos from stages 18- 33. Ganglia were resuspended in 950 µl HBSS (Gibco, Invitrogen) and 50µl 1% Trypsin (Worthington) was added and mixed. The trypsin-HBSS mixture was incubated at 37°C for about 10 minutes. The trypsin-HBSS mixture was then aspirated and the ganglia were washed twice with 1ml F-12 (Gibco, Invitrogen) with 10 % heat inactivated horse serum (HIHS), to inactivate any residual trypsin. The F-12/ 10% HIHS was then aspirated and replaced with a suitable volume of F-14. A single cell suspension was made by trituration using a siliconised pipette (Fisher Scientific), the end of which had been polished to a fine bore using a Bunsen burner. The tissue was taken up slowly into the pipette and expelled with firm pressure, avoiding over- tituration and the introduction of bubbles. Trituration was monitored by pipetting 10µl of the cell suspension onto a lid of a 35 mm dish and examined under a phase contrast Nikon Diaphot inverted microscope. Trituration was complete when only connective tissue fragments were present in the cell suspension and single neurons, with fairly long processes, were visible under the microscope.

2.2.4 Seeding neurons

Neurons were seeded in laminin-coated 35 mm dishes at a density of either 100-150 neurons per 12 mm^2 grid in the centre of the dishes to study neurite growth or 200-250 neurons per 12 mm^2 grid to study neuronal survival. Neuronal cultures were set up in triplicate.

2.2.5 Addition of Neurotrophins and pharmacological inhibitors

Three hours after plating, neurons were exposed to different pharmacological inhibitors or neurotrophic factors. Compounds added are as following:

2.2.6 Agonists, Antagonists, Caspase- and pharmacological inhibitors

Caspases are cysteine-dependent, aspartate-dependent proteases that exist as latent precursors, and when activated by limited proteolysis, initiate a cell death program by cleaving key components of the cell infrastructure and activate additional apoptotic mechanisms. Caspase activation can occur by either the receptor mediated (Fas ligand/ TNF α- mediated, for example) apoptotic pathway, leading to the activation of pro- caspase 8, or the mitochondrial apoptotic pathway, resulting in the association of Bcl-2 family members with the mitochondria, release of cytochrome c and activation of pro- caspase 9. The broad spectrum

caspase inhibitor III (Boc-D-FMK, Calbiochem), used in this study, acts by binding irreversibly to the caspase active site, directed by a peptide recognition sequence bound to a functional group (fluromethylketone, FMK). In experiments performed in the presence of caspase inhibitors, 8 µl were added into 2 ml of culture medium.

Bio: (2'Z, 3'E)-6-Bromoindirubin-3'-oxime

GSK3 inhibitor/ Calbiochem: Bio is a cell- permeable, selective and reversible ATP-competitive inhibitor of GSK3 α/β. After applying the inhibitor GSK3 α/β is not able to phosphorylate its substrates. In experiments done in the presence of bio, we used a final concentration of 100 nM of the inhibitor as we found this an adequate concentration in our dose- response experiments.

Ly 294002: 2-(4-Morpholinyl)-8-phenyl-4H-1-benzopyran-4-one

PI3 kinase inhibitor/Calbiochem: LY294002 is a cell permeable, potent and specific phosphatidylinositol 3-kinase inhibitor that acts on the ATP- binding site of the enzyme, on the catalytic subunit of DNA- activated protein kinase. In our experiments we used a concentration of 50 µl in each dish.

U0126: 1,4-Diamino-2,3-dicyano-1,4-bis(2-minophenylthio)butadiene

Mek inhibitor/Calbiochem The U0126 compound is a potent and specific inhibitor of MEK1 and MEK2. The inhibition is non-competitive with respect to MEK substrates, ATP and Erk. We used a concentration of 10 µM in each dish for our experiments.

U0124: 1,4-Diamino-2,3-dicyano-1,4-bis(methylthio)butadiene

U0124 is used as negative control to the MEK inhibitor U0126 and provided by Calbiochem. This compound does not inhibit MEK even at concentrations of 100 µM.We used a concentration of 10 µM in each dish for our experiments.

PD98059: 2'-Amino-3'-methoxyflavone

The PD98059 compound is a Mek inhibitor, provided by Invitrogen. A selective and cell-permeable inhibitor of MAP kinase kinase (MEK) that acts by inhibiting the activation of MAP kinase and subsequent phosphorylation of MAP kinase substrates. PD98059 does not

block NGF-dependent activation of PI 3-kinase. We used a final concentration of 10 μM for our experiments.

Calhex 231

Calhex 231 is a potent CaSR agonist (calcilytic) that activates the receptor at nM levels. The compound was provided by TRC

Calindol Hydrochloride

This compound is a specific CaSR antagonist (calcimimetic) that inactivates the receptor at nM levels. Calindol Hydrochloride was provided by TRC.

BDNF: Brain derived neurotrophic factor

In experiments where neurons would go apoptosis in the absence of BDNF, we added a final concentration of 10ng/ml of BDNF into each dish. BDNF is provided by R&D Systems.

2.1.7 Expression constructs

The p110α of PI3K expression constructs were gifts from Dr. Julian Downward (Cancer Research UK, London, United Kingdom). The p110 subunit was constructed as described (Volinia et al., 1994), in brief, DNA fragments, encoding the carboxy terminus of bovine p110α with an extension corresponding to the farnesylation-palmitylation signal from H-Ras, were amplified by PCR with the sense primer 5'CACACACTCCATCAGTGGCTCAAAGACAAGAAC3' and the antisense primer 5'CGCGGATCCTCAAGAGAGCACACACTTACAGTTCAAAGCATGCTGC3'. The PCR products were digested with *Cla*I and *Bam*HI, ligated into the p110 sequence, and subcloned into the mammalian expression vector pSG5 (Stratagene) to generate p110-CAAX. The construct was confirmed by DNA sequencing (Volinia et al., 1994).

The p85 Mutant of PI3-Kinase was a generous gift from Cathrine Mounier, Département des Sciences Biologiques, Centre de recherche BioMed, Université du Québec, Montréal, Canada. Previous work has shown that the p85 deletion mutant lacking the p110 binding site works as a dominant negative regulator for wild-type p85 in competing for upstream docking proteins (Dhand, R. EMBO J. 1994). The mutant p85(Δ478-513) was constructed as described (Dhand et al., 1994). Briefly, the 478-513 coding region, corresponding to the p110 binding domain, was deleted from the wild-type p85 using PCR. Two PCR fragments (P1 and P2) were

generated. P1 encompassed nucleotides 1-1431 and had a *Bgl*II site introduced at the 5'-end. P2 encompassed nucleotides 1542-2172 and had 30 bases complementary to the 3'-end of P1 product introduced at the 5'-end. After purification, the two PCR fragments were mixed, denaturated, and reannealed. Using primers at each end, the mutated p85 was then reamplified by PCR and subcloned into pShuttle-CMV vector digested by *Bgl*II and *Eco*RV. The pShuttle-CMV-Δp85 plasmid was then mixed with pAdEasy-1 vector to prepare recombinant adenovirus as described previously (He et al., 1998). Chick CaSR was cloned by Thomas Vizard using PCR from chicken brain Poly A(+) RNA (Clontech) using a LongRange 2 step RT-PCR kit (Qiagen) and the forward primer 5'-ACA GAG GGA CAA ATA CCA GCA CTG-3' and reverse primer 5'-CTG GAG GTA AAG CTA CAT CTG CTG-3'. The 4kb PCR product was then ligated into pGEM-T Easy (Promega) and the correct sequence confirmed by restriction analysis and nucleotide sequencing before cloning into pcDNA3.1. The R185Q dominant negative mutation was introduced to the second and third positions of codon 185 of the chicken CaSR sequence using a QuikChange Multi Site-Directed Mutagenesis kit (Stratagene) and the mutagenic primers 5'-GTT CAA GTC CTT CCT CCA CAC AAT CCC CAA TGA CG-3' and 5'-AGT TCA AGT CCT TCC TCC AAA CAA TCC CCA ATG AC-3' (Vizard, T.N. personal communication)

The HA-GSK3β R96E construct was a gift from Trevor Dale. Mutant GSK-3 constructs were generated using site-directed mutagenesis according to the manufacturer's instructions (QuikChange; Stratagene).
Surface scanning mutagenesis was performed on HA-tagged GSK-3 cDNAs within the pcDNA3.1_ expression vector. The R96E mutation, a exchange of Arginine into Glutamic acid is directed to the basic pocket in the gsk3 catalytic cleft. Two other residues make up this pocket, R180 and K205. This mutation removes the catalytic activity and therefore reduces the activity of GSK3.

2.1.8 Quantification of neuronal survival

To determine neuronal survival, a standard graticule for examining each culture dish was made from the base of a 900mm plastic Petri dish, where a scalpel blade was used to inscribe a 12 x 12 mm^2 grid consisting of 2 mm squares. Cells were counted 3-4 hours after plating by mounting the graticule on an inverted phase- contrast Nikon Diaphot microscope. Each dish was then placed over the graticule and the number of neurons present in the 12 mm^2 grid was

then counted. Neurons which had not been attached to the substratum were ignored. The number of phase- bright neurons in all dishes was counted after 24 hrs intervals until necessary. The number of 24 hrs or 48 hrs was then expressed as a percentage of the initial cell count. For each survival experiment, the mean percentage survival from three dishes per condition was determined.

2.1.9 Measuring total neurite length

Neurons were fluorescently labelled using calcein- acetoxymethyl ester (AM) fluorogenic esterase substrate (Molecular Probes, Invitrogen). 4µl of Calcein-AM (1mg.ml $^{-1}$ in DMSO) was added to 2 ml of cell culture medium and incubated for 10-30 mins. The dye is retained in cells that have intact membranes but does not label dead cells. For every condition studied, 40 to 70 neurons were digitally captured using either a Zeiss laser scanning microscope LSM 510 or Zeiss Axiovert 200 inverted fluorescent microscope using Simple PCI software. Total neurite length was measured using Zeiss examiner software. Neurons were traced over using a 1 pixel line that automatically measured neurite length.

2.1.10 Transfection of neurons by electroporation

Electroporations were carried out using the Microporator MP100 (Digital Bio). Electroporation, or electropermeabilization, is a significant increase in the electrical conductivity and permeability of the cell plasma membrane caused by an externally applied electrical field. Pores are formed when the voltage across a plasma membrane exceeds its dielectric strength. If the strength of the applied electrical field and/or duration of exposure to it are properly chosen, the pores formed by the electrical pulse reseal after a short period of time, during which extracellular compounds have a chance to enter into the cell.

Ganglia were trypsinised, washed twice with F-12/10% horse serum and washed a further two times with PBS. The ganglia were then pelleted by centrifugation for 2 min at 2000 x g, the PBS was then aspirated and replaced with Resuspension Buffer (12 µl per transfection). The ganglia were then mechanically dissociated by passing through a sterile pipette tip several times. For each transfection, 12 µl of cell suspension was then transferred to 0.5ml microfuge tubes containing 1µg target plasmid and 0.5 µg pYFP. The cell-DNA mixture was then drawn into a MicroPorator Pipette, making sure not to introduce air bubbles. The MicroPorator Pipette was then transferred to the pipette station were it was inserted into the Microporation tube, containing 3ml Electrolytic Buffer E. Each transfection was carried out using the following settings:

Voltage	1400 V
Pulse Width	10 ms
Pulse Number	3

After transfection, the cells were immediately transferred to F-14 medium and plated in 4-well dishes. The number of neurons transfected compared to non-transfected cells was between 30 and 40 % in all experiments.

2.1.11 Quantification of neuronal survival and neurite outgrowth in transfected cultures

YFP- labelled neurons were counted 24 hrs after plating using a Zeiss Axiovert 200 inverted microscope and again at 48 hrs. the number of neurons surviving at 48hrs was then expressed as a percentage of the initial number of neurons counted at 24 hrs

Fluorescent images of the neurons counted were taken after 24Hrs in culture using a Zeiss Axiovert 200 invered fluorescent microscope and neurite ougrowth quantified according to methods described above.

2.1.12 Immunocolocalisation of the CaSR in Dissociated Neurons

Neurons were grown in 4-well 35 mm dishes (Greiner) and fixed after 24 hrs using ice-cold methanol. Cells were then washed twice with PBS before blocking with 5 % bovine serum albumin (BSA), 0.02 % Triton-X100 in phosphate buffered saline (PBS, Sigma) for 1 hour. The primary antibody, the anti- CaSR polyclonal antibody (Imgenex), was added in 1% BSA, 0.02 % Triton-X in PBS, together with a monoclonal β-III tubulin antibody (R&D Systems, used at 1:1000) as a neuronal marker and incubated overnight at 4 °C. The cells were then washed three times with PBS before applying the secondary antibodies, Alexa 488-conjugated anti- rabbit IgG (Molecular Probes) and Alexa 594-conjugated anti-mouse IgG (Molecular Probes) diluted 1:500 in 1 % BSA, 0.02 % Triton-X in PBS for 90 mins at room temperature, protected form light. The secondary antibodies were removed and the cells washed a further three times with PBS. Immunofluorescence as visualised using a Zeiss laser scanning microscope LSM 510 and images were acquired and processed using LSM 510 software.

2.1.13 Western Blotting

The Biorad system was used for running polyacrylamide gels in size of 72 x 83 x 75 mm^3. After pouring the separating gel with an acrylamide concentration of 10 %, the acrylamide solution was covered with isopropanol to ensure a level surface and to avoid an inhibitory effect of O_2. After the gel was polymerized, the isopropanol was removed and the stacking gel solution was added. Combs of 10 wells were used with a breadth of 7.5mm. Before running the gel, samples were boiled shortly for 3 minutes to destroy any remaining secondary or tertiary structure in the samples which could bind to the SDS. 10 µl of Rainbow marker (Bio-Rad) was loaded as reference. After transferring into the electrophoresis chamber with electrophoresis buffer, gels were run first at a voltage of 80 V (EPS, Amersham) and then, when the samples reached the separating gel, the voltage was increased to 150V.

2.1.14 Transferring to nitrocellulose membrane

Proteins separated during gel electrophoresis were transferred to Hybond™-P PVDF membrane (Amersham) by assembling a blot sandwich under transfer buffer which comprised; sponge, gel-sized Whatman paper, gel, PVDF membrane (activated by a prior rinse in methanol), gel-sized Whatman paper, sponge. The sandwich was sealed in a within a blotting cassette, transferred to the electrophoresis chamber and immersed in transfer buffer. Transfer was carried out in the electrophoresis chamber at 80V for 1 hour with ice to keep it cool. Successful transfer of proteins was determined by the transfer of molecular weight markers to the nitrocellulose membrane and by immersion of the membrane in Ponceau S (0.2 % in 3 % TCA, Serva) for 3-5mins. The membrane was then rinsed with water until the proteins were visible.

2.1.15 Immuno-detection

Ponceau stained membranes were again rinsed with water and then blocked by incubating with 10 ml PBS-0.1 % Tween (PBS-T) containing 5% dried milk for 1 hour, to prevent non-specific binding of the antibodies. After blocking, the membrane was incubated with the primary antibody (dilutions listed in Table 2.4) overnight at 4 °C. The following day the membrane was washed 3 x 10 min with PBS-T. After washing, the membrane was incubated with a horseradish peroxidase (HRP)-conjugated secondary antibody diluted in PBS-T containing 5% dried milk (specific dilutions in Table 2.4) for 1 hour. The antibody/PBS-T-

milk solution was removed and the membrane was washed for a further three times with PBS-T. ECL Plus detection system (Amersham) was used to detect immobilised proteins conjugated to HRP-labelled antibodies. HRP and peroxide catalyse the oxidation of a PS-3 Acridan substrate, generating thousands of acridinium ester intermediates per minute. These intermediates react with peroxide under alkaline conditions providing high intensity chemiluminescence which can be detected by autoradiography film. Briefly, 50 µl ECL plus solution B is added to 2 ml solution A, mixed, pipetted onto the membrane and incubated for 5min at room temperature. The excess detection reagent was poured off and the membrane transferred to an ECL Hyperfilm cassette. Hyperfilm ECL (Amersham) was placed over the membrane and exposed for 1 min before developing using a Xograph developing machine.

2.1.16 Stripping

To re-probe the PVDF membrane with another antibody, the membrane was stripped to remove both primary and secondary antibodies, this was carried out by incubating membranes in stripping buffer (see Appendix) for 15 min at 55 °C with a further 10 min rocking at room temperature. Membranes were then washed with 3 x 10min PBS-T to remove remaining traces of stripping solution. The membrane was blocked again by incubating with PBS-T containing 5 % milk for 60 minutes and then incubated with the next primary antibody as described above.

2.1.17 Antibodies and Proteins

Dilution of antibodies:

Antibody	Source and Company	Dilution
Anti-phospho Akt	Polyclonal Antibody specific to pS473 (Acris), Rabbit	1:1000
Anti-phospho GSK3	Rabbit polyclonal p-GSK3 alpha and beta (abcam)	1:1000
Anti-Akt	Rabbit polyclonal to pan-Akt (abcam)	1:1000
Anti-GSK3	Rabbit polyclonal GSK3 (alpha and beta) (abcam)	1:1000
Anti Rabbit	Promega	1:2000
Anti Mouse	Promega	1:2000

Figure 2.4: Dilutions of antibodies

All Antibodies were diluted in 1 % BSA + 0.02 % Azide

2.1.18 Quantitative PCR

2.1.19 RNA Isolation

10-12 ganglia from chicken embryos at early developmental stages were collected for each RNA isolation, pelleted and stored at –80 °C until required. Total RNA from the unprocessed

ganglia was extracted using RNeasy ® Kit (Qiagen) according to the manufacturer's protocol and stored in RNAse- free dH_2O at –70 °C until required.

2.1.20 cDNA Synthesis using STRATASCRIPT® RT

cDNA synthesis reactions were assembled on ice and contained; 4 µl 10X StrataScript ® buffer, 2µl $pd(N)_6$ Random Hexamers ($0.005U.\mu l^{-1}$; Amersham Biosciences), 2 µl deoxynucleoside triphosphate (dNTP) mixture (100 mM), 0.38µl StataScript® Reverse Transcriptase ($50U.\mu l^{-1}$), 3µl RNA and Rnase free dH_2O to 40 µl and were incubated at 42°C for 90minutes. The subsequent cDNA was then stored at –20 °C for long periods or 4 °C if to be used immediately.

2.1.21 Quantitative PCR using Stratagene MX3000P

In real-time PCR using SYBR green binding to amplified cDNA, we are simply measuring the fluorescence increase as the dye binds to the increasing amount of DNA in the reaction tube. We hope that this increase in fluorescence is coming from the DNA that we wish to measure but some of the signal could come from DNA other than that which we are trying to amplify. The way to make sure that the correct fragments were amplified is checking the products' melting curve.

Each real-time PCR reaction was prepared using 2.5 µL of cDNA, 2.5 µL of Brilliant QPCR core buffer (Stratagene), 1.5 µL of 3 mM $MgCl_2$ (Stratagene), 0.5µL of primers, 0.4 µL of (1/500) reference dye (Stratagene), 0.25 µL (1/4000) Sybr Green® (Invitrogen), 1 µL of 20 mM dNTP's (Stratagene), 15.8µL of distilled water and 0.33 µL of Hot Taq® enzyme (Stratagene).

The following table shows the primer set for each gene and the respective annealing temperature.

Gene	Sense Locus	Sequence	Annealing Temperature	Melting temperature
Ck_CaSR	F XM_416491	5'- ACA ATA CCC ATA GAC TC -3'	**Ta:** 48.3°C	**Tm:** 87.2°C
	R	5'- ATT ACA GCA ACA CTT -3'		

2.1.22 Standard curve

The most accurate quantitative result from real time PCR is to compare the experimental sample with the reference gene. The reference gene is to be used as a loading control (or internal standard) and should have various features, such as: having the same copy number in all cells; be expressed in all cells, and have a medium copy number, to permit more accurate comparison. The reference gene we used was glyceraldehyde-3-phosphate dehydrogenase (GAPDH). The standard curve for the real time PCR was prepared with Stage 28 whole - embryo cDNA synthesized using the same method of the samples. This standard curve was prepared by serially diluting Stage 28 whole -embryo cDNA from 1 to 1/64 using the cDNA blank mixture (cDNA synthesis reaction mixture without template RNA) 2.5µl of each dilution and a no template control (NTC- cDNA blank mix only) was transferred to 0.2ml optical PCR tubes (Stratagene) containing the PCR reaction mixture. Following amplification of the standard dilutions, a standard curve was generated by plotting the log of the initial template copy number against the ct value for each dilution. The ct value (threshold cycle) is the first cycle at which the PCR instrument can distinguish amplification- generated fluorescence from background signal. The Ct values of the unknown samples were then compared with the standard curve and the initial quantities determined.

2.1.23 Statistical Analyses

The sample number (n) shown for each experiment describes either the total number of neurons sampled (for neurite growth experiments) or the total number of separate cultures carried out (for neuronal growth and survival experiments). Where data is shown from more than one experiment, the number of separate cultures is indicated. Data are presented as means ± SEM, and statistical significance was determined by the unpaired T-test or, if there were more than two sets of data compared, then one-way analysis of variance (ANOVA) with Tukey post hoc test was used. The significance was accepted for $P< 0.05$.

Chapter 3

Regulation of *de novo* axonal growth from cranial sensory neurons by the extracellular calcium-sensing receptor (CaSR)

3.1 Introduction

The great majority of studies of the molecular mechanisms that control axonal growth rate have been undertaken either on neuronal cell lines or on axotomised neurons that regenerate axons in culture. Virtually nothing is known about the molecular control of axonal growth rate at the developmentally significant stage when neurons are initiating and extending axons to their targets. There are two main reasons for this. First, because of the very small size of neuronal populations at the relevant stage of embryonic development, it is technically challenging to harvest neurons for *in vitro* studies of *de novo* axonal growth. Second, the very limited numbers of neurons that can be harvested from embryos at the appropriate early stages of development imposes severe restrictions of the biochemical studies that can be undertaken to investigate the molecular mechanisms regulating axonal growth rate.

Despite these technical difficulties, *de novo* axonal growth exhibits several features that distinguish it from axon regeneration, and thus make it an intriguing, important and especially relevant topic for study in the field of developmental neuroscience. First, neuronal survival and axon extension are independent of neurotrophic factors for many populations of neurons at this early stage of their development (Davies and Lumsden, 1984; Davies, 1987; Vogel and Davies, 1991). In contrast, neurons that have already innervated their targets and regenerate axons in culture, not only depend on particular neurotrophic factors for survival, but also extend axons in response to these factors (Deckwerth et al., 1996; Markus et al., 2002). Second, neurons extending axons in culture at the stage of development when their axons are normally growing to their targets *in vivo* replicate key features of their appropriate *in vivo* morphology. For example, sensory neurons cultured at this early stage of development exhibit the characteristic bipolar morphology, with two unbranched axons growing from opposite poles of the cell body, as observed *in vivo* (Davies, 1989). In marked contrast, neurotrophin-dependent sensory neurons that have already innervated their targets regenerate an abnormal morphology in culture. Typically, these regenerating neurotrophin-dependent sensory neurons are multipolar, with excessively branched axons (Scott and Davies, 1993). Third, and most intriguingly, certain populations of neurons exhibit distinctive rates of axonal growth both *in vivo* and *in vitro* at the stage when their axons are growing to their targets that are lost when they are cultured during the later stage of neurotrophin dependence (Davies, 1989).

The most striking and thoroughly characterized example of distinctive differences in *de novo* axonal growth rates is provided by four populations of placode-derived cranial sensory neurons of the chicken embryo. The neurons of the vestibular, geniculate, petrosal and nodose ganglia are born during the same period of development and start extending axons to their peripheral and central targets at approximately the same time, but have different distances to grow to reach their targets. Vestibular neurons have the closest targets, nodose neurons have the most distant targets, and geniculate and petrosal neurons have targets of intermediate distance. The rate at which the axons of these neurons grow to their targets *in vivo* is correlated with target distance: vestibular neurons have the slowest axon growth rates, and nodose neurons the fastest. Importantly, these distinctive differences in axonal growth rate appear to be intrinsic property of the neurons. When they are cultured at very low density or as isolated single cells at the stage of development when their axons are normally growing to their targets, they extend axons at different rates: the axons of nodose neurons growing faster than those of petrosal neurons, which grow faster than those of geniculate neurons, which grow faster than those of vestibular neurons. At this stage of development, the neurons survive independently of neurotrophins and axonal growth rate is unaffected by BDNF, the neurotrophin that the majority of the neurons in each ganglion become dependent on when their axons reach their targets (Davies, 1989). In addition to axonal growth rate, the duration of neurotrophin independence and the expression of TrkB in these early neurons is also correlated with target distance. Vestibular neurons are the first to express TrkB and the first to become dependent on BDNF for survival, whereas nodose neurons are last (Robinson et al., 1996; Vogel and Davies, 1991). The duration of neurotrophin independence, together with intrinsic differences in axonal growth rate, appear to coordinate the onset of neurotrophin dependence with the arrival of axons in the vicinity of their targets (Davies, 1994).

The aim of the research reported in this chapter was to identify a molecular mechanism that plays a role in effecting differences in axonal growth rate at the stage of development when axons are growing to their targets. For this work, I focused on the populations of placode-derived cranial sensory neurons that have the greatest differences in axonal growth rate, namely, those of the vestibular and nodose ganglia of Hamilton-Hamburger Stage 20 chicken embryos, the stage when many of their axons are growing to their peripheral and central targets *in vivo*. Because neurotrophins play no role in regulating axonal growth from these neurons at this early stage of development, I focused on alternative possible mechanisms of axon growth regulation. One recently identified regulator of axonal growth in the developing

nervous system is the CaSR. This is expressed at relatively high levels in embryonic mouse superior cervical ganglia (SCG) just before birth, a stage in development when the axons of these neurons are innervating and branching extensively in their distal targets (Vizard et al., 2008). Manipulating CaSR function in these neurons by varying $[Ca^{2+}]_o$, by using CaSR agonists and antagonists or by expressing a dominant-negative CaSR markedly affects neurite growth *in vitro* during a narrow developmental window during the immediate perinatal period when CaSR expression is highest. SCG neurons lacking the CaSR have smaller neurite arbors *in vitro*, and sympathetic innervation density is reduced in CaSR-deficient mice *in vivo*. These findings suggest that under the hypercalcaemic conditions of the embryo, the activated CaSR in SCG neurons promotes, by an intracellular mechanism yet to be elucidated, axonal growth and branching that is physiologically relevant for the establishment of normal sympathetic innervation density *in vivo* (Vizard et al., 2008).

In this chapter I report that CaSR is expressed in placode-derived cranial sensory neurons of the chicken embryo, with higher levels of CaSR mRNA in nodose compared with vestibular neurons, and that manipulating CaSR function in nodose, but not vestibular neurons, affects axonal growth rate. These findings provide the first evidence for a mechanism involved in regulating intrinsic differences in early axonal growth rate.

3.2 Results

3.2.1 CaSR mRNA and protein is expressed in early placode-derived cranial sensory neurons

I began investigating the potential involvement of the CaSR in regulating axonal growth from early placode-derived neurons by using RT-QPCR to determine if CaSR mRNA is expressed in vestibular and nodose ganglia at the stage of development when axons are growing to their targets and ascertain the relative levels of expression in these ganglia. Total RNA was extracted from pooled nodose and vestibular ganglia harvested from stage 20 chicken embryos, and after reverse transcription, primers based on the published chicken CaSR sequence were used to amplify CaSR cDNA. To compare the relative levels of CaSR mRNA in these ganglia and correct for differences in ganglion size, I also used real-time PCR to measure the level of mRNA encoding the ubiquitous, constitutively expressed, housekeeping protein glyceraldehyde phosphate dehydrogenase (GAPDH). CaSR mRNA was detected in both nodose and vestibular ganglia, with significantly higher levels in the nodose ganglion (approximately 3-fold higher in the nodose ganglion compared to the vestibular ganglion) (Fig. 3.1). While the great majority of cells in these early ganglia are

neurons and neuroblasts, I nonetheless carried out immunocytochemistry using a specific affinity-purified anti-CaSR polyclonal antibody to identify which cells express the CaSR in dissociated cultures established from stage 20 nodose and vestibular ganglia. In double-labelled preparations, in which neurons were positively identified with anti-β-III tubulin antibodies, the CaSR antibody stained the cell bodies, entire axons and growth cones of all nodose (Fig. 3.2) and all vestibular neurons (Fig. 3.3). None of the very few non-neuronal cells were immunoreactive for CaSR, and staining was not evident with the secondary antibody alone when the primary antibody was omitted (data not shown).

3.2.2 Varying $[Ca^{2+}]_o$ over the CaSR sensitivity range influences the extent of axonal growth from stage 20 nodose neurons but not vestibular neurons

To begin investigating the potential role of the CaSR in regulating axonal growth from early nodose and vestibular neurons, I cultured these neurons at low density in medium containing several different concentrations of extracellular Ca^{2+}, spanning the CaSR response range. The sensitivity of CaSR to changes in $[Ca^{2+}]_o$ varies within the range of 0.5 to 3 mM according to cell type and the signalling events or physiological responses being quantified. The EC_{50} or IC_{50} ranges between ~1 mM and ~1.7 mM (Ferry et al., 2000; Nemeth et al., 1998). In the case of E18 mouse SCG neurons, comparison of the extent of neurite growth from wild type and CaSR-deficient neurons has demonstrated that 0.7mM $[Ca^{2+}]_o$ has a minimal effect on CaSR-promoted neurite growth, and detailed dose response analysis has demonstrated that 2.3 mM $[Ca^{2+}]_o$ exerts the maximal effect on CaSR-promoted neurite growth (Vizard et al., 2008). For this reason, these same concentrations were used in the experiments described here together with two intermediate concentrations, 1.1 mM and 1.3 mM, the latter being the standard $[Ca^{2+}]_o$ in media generally used to culture embryonic neurons.

Nodose and vestibular neurons were plated at low density in laminin-coated tissue culture dishes containing medium with different levels of $[Ca^{2+}]_o$. The number of neurons within a standard grid in the centre of each dish was counted three hours after plating, and again after 24 hours in order to estimate the number of neurons surviving under each experimental condition. The neurons were stained with the fluorescent vital dye calcein-AM at 24 hours, and photomicrographs of randomly selected neurons were taken for quantification of neurite length. Because the great majority of stage 20 nodose neurons survive independently of neurotrophins for 24 hours following plating, these neurons were grown without neurotrophins. Cell counts confirmed that the majority of nodose neurons had

survived without neurotrophins for 24 hours, as expected, and revealed no significant differences in survival over the $[Ca^{2+}]_o$ range studied (Fig. 3.4 A). Measurements of total axon length revealed a dose-dependent increase with $[Ca^{2+}]_o$, with a highly significant, two-fold difference between 0.7 mM and 1.1 mM, and smaller increases in axonal length between the higher concentrations (Fig. 3.4 B). These findings show that varying $[Ca^{2+}]_o$ over the CaSR sensitivity range influences the magnitude of axonal growth from embryonic nodose ganglion neurons at the stage when these axons are normally growing to their targets.

Because a significant proportion of stage 20 vestibular neurons start becoming dependent on BDNF for survival within 24 hours after plating, all cultures received the irreversible caspase inhibitor Boc-D-FMK to prevent excessive loss of neurons during this period. A caspase inhibitor, rather than BDNF, was used to sustain the survival of those neurons that acquire BDNF dependence during the 24 hour culture period because the aim of these experiments was to investigate neurotrophin-independent axon growth. Neuron counts revealed that over 80% of the neurons survived in these cultures for 24 hours and there was no significant difference in survival between cultures containing 0.7 mM and 2.3 mM $[Ca^{2+}]_o$ (Fig. 3.5 A). In marked contrast to nodose neurons, the shorter axons of vestibular neurons were not stimulated to grow by 2.3 mM $[Ca^{2+}]_o$ at stage 20 in development (Fig 3.5 B). This suggests that the CaSR does not regulate *de novo* axonal growth from vestibular neurons at this early stage in their development. However, because a caspase inhibitor was used in the vestibular neuron experiments, the nodose neuron experiments were repeated under identical conditions with the same caspase inhibitor to control for any unexpected effect of this reagent that could account for the different responses of the two kinds of neurons to changes in $[Ca^{2+}]_o$. In these experiments, nodose neurons were grown in parallel in 0.7 mM and 2.3 mM $[Ca^{2+}]_o$ in presence and in the absence of Boc-D-FMK. Quantification of neuronal survival and axonal length after 24 hours revealed almost identical results in the presence and absence of Boc-D-FMK. There was no significant difference in survival under all experimental conditions, and there were highly significant, ~3-fold differences in axonal length between the 0.7 mM and 2.3 mM $[Ca^{2+}]_o$ conditions in both the presence and in the absence of Boc-D-FMK (Fig. 3.6). Taken together, the above results show that changes in $[Ca^{2+}]_o$ over the response range of the CaSR affect neurotrophin-independent axon growth from nodose neurons but not vestibular neurons of stage 20 chicken embryos.

3.2.3 The CaSR agonist Gd^{3+} enhances axonal growth from stage 20 nodose neurons incubated with 0.7 mM $[Ca^{2+}]_o$, but does not affect the growth of vestibular neurons

The above findings implicate the CaSR in mediating the effects of $[Ca^{2+}]_o$ on neurotrophin-independent axonal growth from cultured stage 20 nodose neurons. To provide further support for the involvement of the CaSR, I carried out experiments with a potent CaSR agonist, the trivalent ion of the rare-earth metal, gadolinium. Gd^{3+}, which activates the CaSR in the absence of Ca^{2+} (Hofer and Brown, 2003).

Nodose and vestibular neurons were cultured for 24 hours in medium containing 0.7 mM $[Ca^{2+}]_o$ alone or 0.7 mM $[Ca^{2+}]_o$ with Gd^{3+} at a concentration of 1 pM. Neuron counts revealed that Gd^{3+} did not affect the survival of either nodose neurons or vestibular neurons (Fig 3.7 A). Whereas Gd^{3+} had no significant effect on axon growth from vestibular neurons, it caused a three-fold increase in the length of nodose neuron axons (Fig. 3.7 B). In further dose response studies, Gd^{3+} at concentrations down to 0.1 pM enhanced axon growth from nodose neurons incubated with 0.7 mM $[Ca^{2+}]_o$ to a similar extent to that observed in medium containing 2.3 mM $[Ca^{2+}]_o$ without affecting survival (Fig.3.8) These results provide further support for a role for the CaSR in promoting axon growth from nodose neurons but not vestibular neurons at a stage in development when the axons of these neurons are growing to their targets *in vivo*.

3.2.4 The CaSR agonist, Calhex, and the CaSR antagonist, Calindol, modulate axonal growth from stage 20 nodose neurons.

The specific CaSR agonist, Calhex, and CaSR antagonist, Calindol, have recently become commercially available. I therefore decided to confirm the involvement of the CaSR in regulating *de novo* axon growth by using them in experiments with stage 20 nodose neurons. Nodose neurons were cultured with 0.7 mM $[Ca^{2+}]_o$ with and without 10 nM of Calhex. Whilst Calhex did not alter the survival of stage 20 nodose neurons, it greatly increased the length of their axons (Fig. 3.9). In further experiments, stage 20 nodose neurons were cultured with and without 10 nM Calindol in medium containing 2.3 mM Ca^{2+}, a calcium concentration that activates the CaSR to promote axon elongation. Calindol did not affect the survival of stage 20 nodose neurons cultured with 2.3 mM $[Ca^{2+}]_o$ (Fig. 3.10 A). However, Calindol was able to significantly reduce axonal length under the same culture conditions (Fig. 3.10 B, $p< 0.0001$, ANOVA with Fisher's ad hoc). These findings provide further evidence that the CaSR plays a role in promoting *de novo* axon growth

3.2.5 Inhibiting G_i proteins with Pertussis toxin prevents Gd^{3+}–induced axonal growth stage 20 nodose neurons Gd^{3+}

To obtain further, though indirect, support for the involvement of the CaSR in enhancing *de novo* axonal growth in from stage 20 nodose neurons, I examined the effects of pharmacologically inhibiting G proteins with Pertussis toxin (PTX). PTX catalyzes the ADP-ribosylation of the α subunits of the heterotrimeric G proteins G_i, G_o, and G_t which prevents these G proteins from interacting with G protein-coupled receptors like the CaSR on the cell membrane (Katada and Ui, 1982). Nodose neurons were cultured for 24 hours at low density in medium containing 0.7 mM $[Ca^{2+}]_o$ with and without 1pM Gd^{3+} alone or with 1pM Gd^{3+} plus 1mg/ml PTX. Neuron counts revealed that PTX did not affect the survival of nodose neurons (Fig. 3.11 A), but completely inhibited the ability of Gd^{3+} to enhance axon growth (Fig. 3.11 B). This finding is consistent with the involvement of CaSR in regulating *de novo* axon growth rate from early nodose neurons.

3.2.6 Effects of over-expressing wild type and dominant-negative CaSRs on axonal growth from stage 20 nodose neurons

To provide an additional test of the role of the CaSR in promoting early axonal growth, I transfected stage 20 nodose and vestibular neurons with pcDNA3.1 expression plasmids containing the cDNAs encoding either the wild-type chicken CaSR or a mutated chicken CaSR with an arginine-to-glutamine substitution (R185Q) that exerts a dominant-negative effect on CaSR function (Vizard T.N. personal correspondence) Expression plasmids were electroporated into freshly dissociated stage 20 nodose and vestibular neurons, using the high-efficiency microporator, and neurons were cultured in media containing 2.3 mM Ca^{2+}. To control for the transfection procedure, control cultures were transfected with an empty pcDNA3.1 vector. A yellow fluorescent protein (YFP) expression plasmid was included in all transfection procedures to identify the transfected neurons. The YFP expression plasmid was assumed to be taken up and expressed by the same neurons as the CaSR expression plasmids because co-transfection experiments with mixtures of two expression plasmids encoding different coloured fluorescent proteins demonstrated that both fluorescent proteins are invariably expressed in the same neurons (data not shown). The typical transfection efficiency of early chicken sensory neurons with the microporator ranged from 30% to 40% (data not shown). Fluorescent neurons were counted 24 hrs after plating and after 48 hrs in culture, allowing the percentage neuronal survival of fluorescent neurons at 48 hrs compared

to 24 hrs to be determined. Fluorescent images for analysis of axonal growth were captured 24 hr after transfection.

The axons of nodose neurons transfected with the wild type CaSR expression plasmid and cultured in medium containing 2.3 mM $[Ca^{2+}]_o$ for 24 hours after transfection were significantly longer than those of control plasmid transfected neurons (Fig. 3.12 B). Nodose neurons transfected with the dominant-negative CaSR expression plasmid and cultured under the same conditions had significantly shorter axons than control plasmid transfected neurons (Fig. 3.12 B). Estimates of neuronal survival showed no significant differences between all three experimental groups (Fig. 3.12 A). These results not only provide additional support for a role for the CaSR in promoting axonal growth from early nodose neurons, but suggest that the level of endogenous CaSR expression is limiting for the response of the neurons to maximally activating levels of $[Ca^{2+}]_o$. It should be pointed out that transfected nodose neurons extend axons more slowly than non-transfected neurons. This is not a peculiar feature of nodose neurons, but is a consistent finding in transfection studies of many other kinds of sensory and autonomic neurons cultured from embryonic and postnatal mice (Vizard et al., 2008). In contrast to nodose neurons, axonal growth from vestibular neurons was unaffected by over-expression of the wild type CaSR. Transfection of vestibular neurons with the dominant-negative CaSR were not carried out because any potential effect on axon growth would be difficult to ascertain since the length of axons was already very short in control-transfected vestibular neurons. There were no significant differences in axon length between control and wild type CaSR transfected neurons after 24 hours incubation in medium containing 2.3 mM $[Ca^{2+}]_o$ (Fig. 3.12 B) and no significant differences in neuronal survival (Fig. 3.12 A). These results demonstrate that over-expression of the CaSR is not in itself sufficient to confer increased axon growth in response to maximally activating levels of $[Ca^{2+}]_o$. This raises the possibility that mere expression of sufficient levels of the CaSR in early neurotrophin-independent nodose neurons is not the only difference between nodose and vestibular neurons that facilitates rapid axon growth from the former.

3.2.7 The role of the CaSR in regulating axon growth from older, BDNF-dependent nodose and vestibular neurons

Previous work has shown that the CaSR plays a role in promoting axonal growth and branching from late fetal mouse sympathetic neurons during a developmental window when the axons of these neurons are innervating their targets and are dependent on target-derived

NGF for survival. To investigate if the CaSR plays any role in regulating regenerative axon growth from nodose and vestibular neurons at later developmental stages when these neurons are innervating their targets and are dependent on BDNF for survival, I assayed the levels of CaSR mRNA expression and investigated the effects of manipulating CaSR function between stages 25 and 30.

3.2.8 Developmental changes in CaSR mRNA expression in nodose and vestibular ganglia

The level of CaSR mRNA relative to GAPDH mRNA was measured by RT-QPCR in total RNA extracted from nodose and vestibular ganglia harvested from stage 20, stage 25 and stage 30 chicken embryos as outlined in section 3.2.1. Figure 3.13 shows that the levels of CaSR mRNA expressed in nodose ganglia were similar at stages 20 and 25, but there was a marked, almost 4-fold, increase in expression between stages 25 and 30. In contrast, the levels of CaSR mRNA expressed in vestibular ganglia were not significantly different between the three stages studied. Nodose ganglia expressed significantly higher levels of CaSR mRNA compared to vestibular ganglia at all stages analysed. Since the CaSR is clearly expressed at functional levels in stage 20 nodose ganglia, these findings suggest that functional levels of the CaSR protein are also expressed in nodose neurons after they reach their targets and become dependent on BDNF for survival, thus raising the possibility that the CaSR may modulate the extent of BDNF-promoted, regenerative axon outgrowth at stages 25 and 30. This hypothesis was tested in section 3.2.9, below. In contrast, although vestibular neurons express CaSR mRNA throughout the earliest period of BDNF dependency, the levels expressed at stages 25 and 30 are of a similar order of magnitude as those expressed at stage 20.

3.2.9 Extracellular calcium modulates the extent of BDNF-promoted axonal growth in older, BDNF-responsive nodose neurons

To investigate the potential role of the CaSR in modulating BDNF-promoted axonal growth, I cultured stage 27 and stage 30 nodose neurons at low density in the presence and absence of BDNF in medium containing either 0.7 mM or 2.3 mM $[Ca^{2+}]_o$. The number of neurons within a standard grid in the centre of each dish was counted three hours after plating, and again after 24 hours in order to estimate the number of neurons surviving under each experimental condition. Neurons were stained with the fluorescent vital dye calcein-AM at 24 hours, and photomicrographs of randomly selected neurons were taken for quantification of

neurite length. Although nodose neurons start to express TrkB, from stage 25 in development (Robinson et al., 1996), the survival of stage 27 nodose neurons was not significantly greater in the presence of BDNF in media containing either 0.7mM or 2.3mM $[Ca^{2+}]_o$ after 24 hours in culture (Fig. 3.14 A). However, BDNF greatly increased the extent of axonal outgrowth from stage 27 nodose neurons after this time in culture in media containing 0.7 mM and 2.3 mM $[Ca^{2+}]_o$ (Fig. 3.14 B). In the absence of BDNF, the extent of axonal outgrowth was not significantly different between cultures containing 2.3 mM $[Ca^{2+}]_o$ and 0.7 mM $[Ca^{2+}]_o$. In contrast, in the presence of BDNF, the extent of axonal outgrowth was significantly greater in cultures containing 2.3 mM $[Ca^{2+}]_o$ compared to 0.7 mM $[Ca^{2+}]_o$. In cultures established from stage 30 embryos, BDNF significantly enhanced neuronal survival in media containing 0.7 mM and 2.3 mM $[Ca^{2+}]_o$, and there was no significant difference in survival between cultures containing 0.7 mM and 2.3 mM $[Ca^{2+}]_o$ in the presence and absence of BDNF (Fig. 3.15 A). Since stage 30 nodose neurons require BDNF for maximal survival in culture, image analysis of axonal outgrowth was only performed on neurons cultured with BDNF. Increasing $[Ca^{2+}]_o$ to 2.3mM enhanced BDNF-promoted axonal outgrowth from stage 30 nodose neurons by 2.5-fold compared to 0.7mM $[Ca^{2+}]_o$ (Fig. 3.15 B).

3.2.10 CaSR agonists enhance axonal growth from stage 30 nodose neurons incubated with 0.7 mM $[Ca^{2+}]_o$, whereas the CaSR antagonist, Calindol, inhibits axonal growth in 2.3 mM $[Ca^{2+}]_o$

To obtain further support for a role for the CaSR in modulating axon growth in BDNF-dependent stage 30 nodose neurons, I cultured these neurons for 24 hours in medium containing BDNF and 0.7 mM Ca^{2+} with and without either 10 nM Calhex or 1 pM Gd^{3+}. Neuron counts revealed that neither Calhex nor Gd^{3+} significantly affected neuronal survival (Figs 3.16 A and 3.18 A, respectively). However, Calhex promoted a 3.5-fold increase in axon length after 24 hours in culture (Fig. 3.16 B) and Gd^{3+} increased axon length by 5-fold over the same period (Fig. 3.18 B). Significantly, the axon growth-promoting effect of Gd^{3+} was completely prevented by treatment with 1mg/ml of the Gi protein inhibitor, PTX (Fig. 3.18 B). In further experiments, stage 30 nodose neurons were cultured with and without 10 nM Calindol in medium containing BDNF and 2.3 mM Ca^{2+}, a calcium concentration that activates the CaSR to promote axon elongation. Calindol did not affect the survival of stage 30 nodose neurons cultured with BDNF in 2.3 mM $[Ca^{2+}]_o$ (Fig. 3.17 A). However, Calindol was able to significantly reduce axonal length under the same culture conditions (Fig. 3.17 B,

$p < 0.0001$, ANOVA with Fisher's ad hoc). These results provide further support for an involvement of the CaSR in enhancing BDNF-promoted axon growth from nodose neurons that have begun to innervate their targets *in vivo*.

3.2.11 Extracellular calcium modulates the extent of BDNF-promoted axonal growth in older, BDNF-responsive vestibular neurons

Neither increased $[Ca^{2+}]_o$ nor Gd^{3+} promoted *de novo* axonal outgrowth from cultured stage 20 vestibular neurons. Whilst this may reflect the low level of CaSR mRNA expressed by vestibular neurons, the inability of exogenously expressed wild type CaSR protein to enhance *de novo*, BDNF-independent axon growth from stage 20 vestibular neurons in media containing a high calcium concentration suggests that crucial signalling pathways that transduce CaSR activation into increased axonal growth are absent at this stage. To ascertain whether activation of the CaSR could influence later, BDNF-dependent, regenerative axon outgrowth from vestibular neurons, I cultured stage 25 vestibular neurons for 24 hrs in medium containing 10 ng/ml BDNF and calcium ion concentrations ranging from 0.7 mM to 2.3 mM. Figure 3.19 A shows that although increasing $[Ca^{2+}]_o$ in increments from 0.7 mM to 2.3 mM appears to promote slightly increased survival of stage 25 vestibular neurons cultured with BDNF, the increases in survival are not statistically significant. In contrast, 1.3 mM and 2.3 mM $[Ca^{2+}]_o$ increase the mean total axon length of stage 25 vestibular neurons cultured with BDNF to the extent of BDNF-promoted axon outgrowth from stage 25 vestibular neurons by around 60% compared with neurons cultured with 0.7 mM $[Ca^{2+}]_o$. These increases are highly statistically significant ($p < 0.001$) (Fig. 3.19).

To further investigate the role of the CaSR in modulating BDNF-promoted axonal outgrowth from stage 25 vestibular neurons, I used electroporation to co-transfect pcDNA3.1 based expression constructs encoding YFP and the wild type CaSR into vestibular neurons at this developmental stage and cultured them in medium containing 2.3mM calcium and 10 ng/ml BDNF. Control neurons were co-transfected with empty pcDNA3.1 together with pcDNA3.1 encoding YFP. Whilst over-expression of the wild type CaSR did not alter neuronal survival compared to control-transfected neurons, it increased the extent of axon outgrowth by 2.5-fold compared to control cultures (Fig 3.20 A and B). Together, the data in Figures 3.19 and 3.20 demonstrate that by stage 25, vestibular neurons express the signal transduction machinery that links CaSR activation to axon growth and that CaSR activation can enhance BDNF-promoted axon growth.

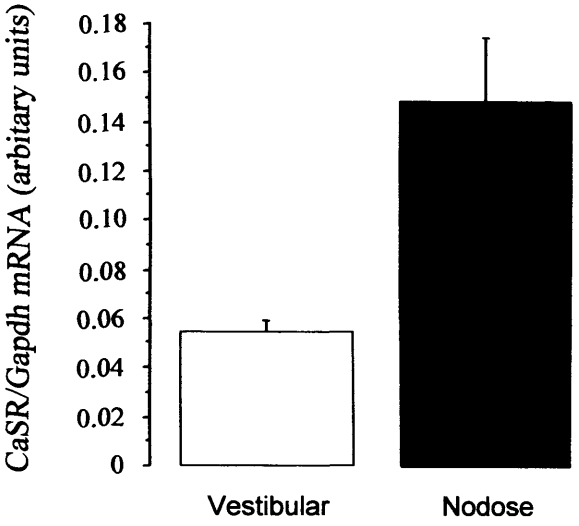

Figure 3.1: Expression levels of CaSR mRNA in stage 20 nodose and vestibular ganglia
The graph shows the levels of CaSR mRNA relative to Gapdh mRNA expressed in stage 20 nodose and vestibular ganglia.
Stage 20 nodose neurons expressed a level of CaSR mRNA relative to Gapdh mRNA that is approximately 3-fold higher than that expressed by stage 20 vestibular neurons. The difference in relative CaSR mRNA expression between the two ganglia is staisitically significant (P= 0.024 ANOVA with Fisher's ad hoc). n = 3 separate dissections for both ganglia.

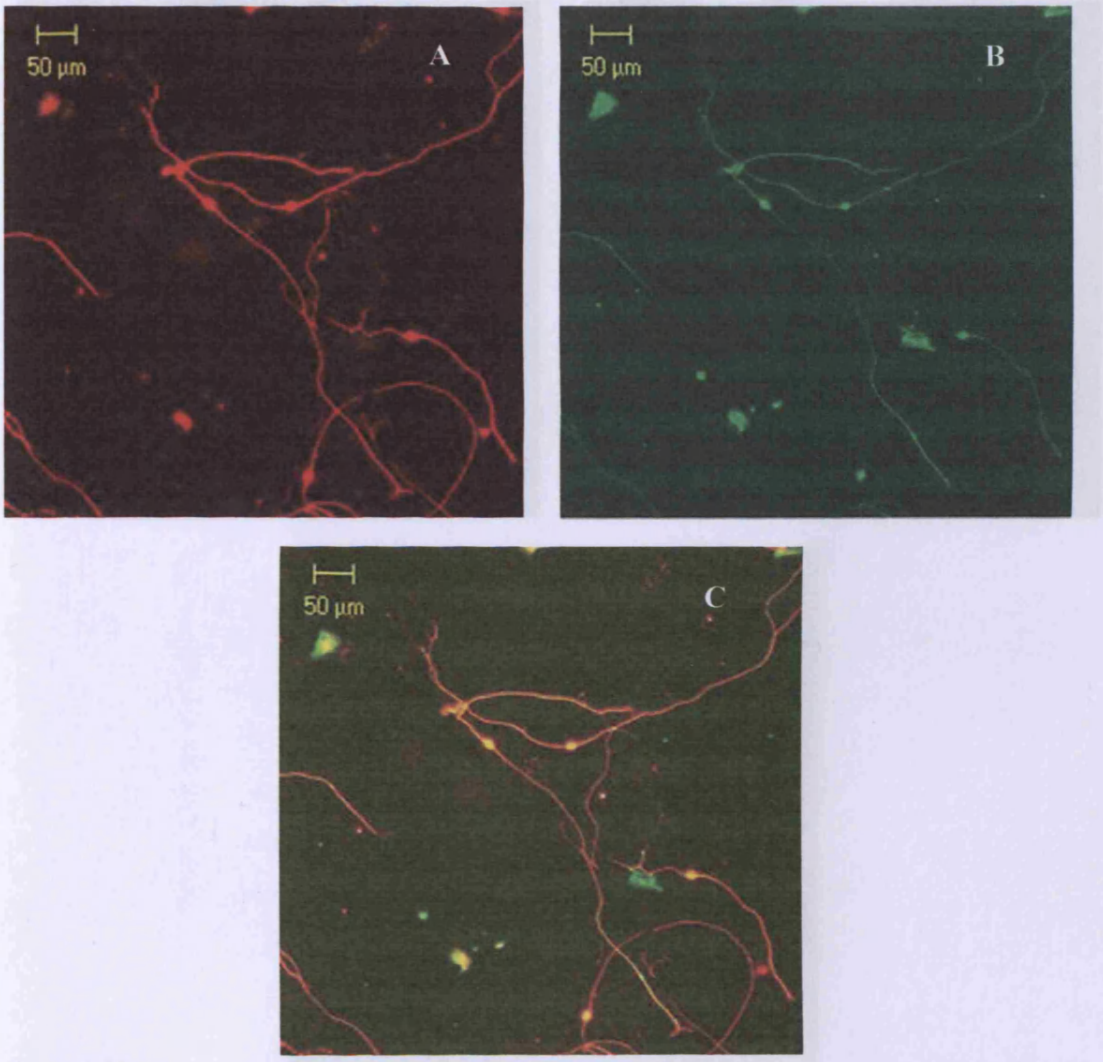

Figure 3.2: The CaSR is expressed in stage 20 nodose neurons.
Stage 20 nodose neurons were cultured in the absence of neurotrophins for 24 hours before being fixed and double-labelled with antibodies against the CaSR and β-III Tubulin.
A-C are representative confocal microscope images showing double-labelling of the same field with an antibody against β-III Tubulin combined with an FITC conjugated secondary antibody **(A)** and an antibody against the CaSR combined with a rhodamine conjugated secondary antibody **(B)**. The merged image **(C)** demonstrates that the CasR was expressed in the cell soma and processes of all stage 20 nodose neurons.

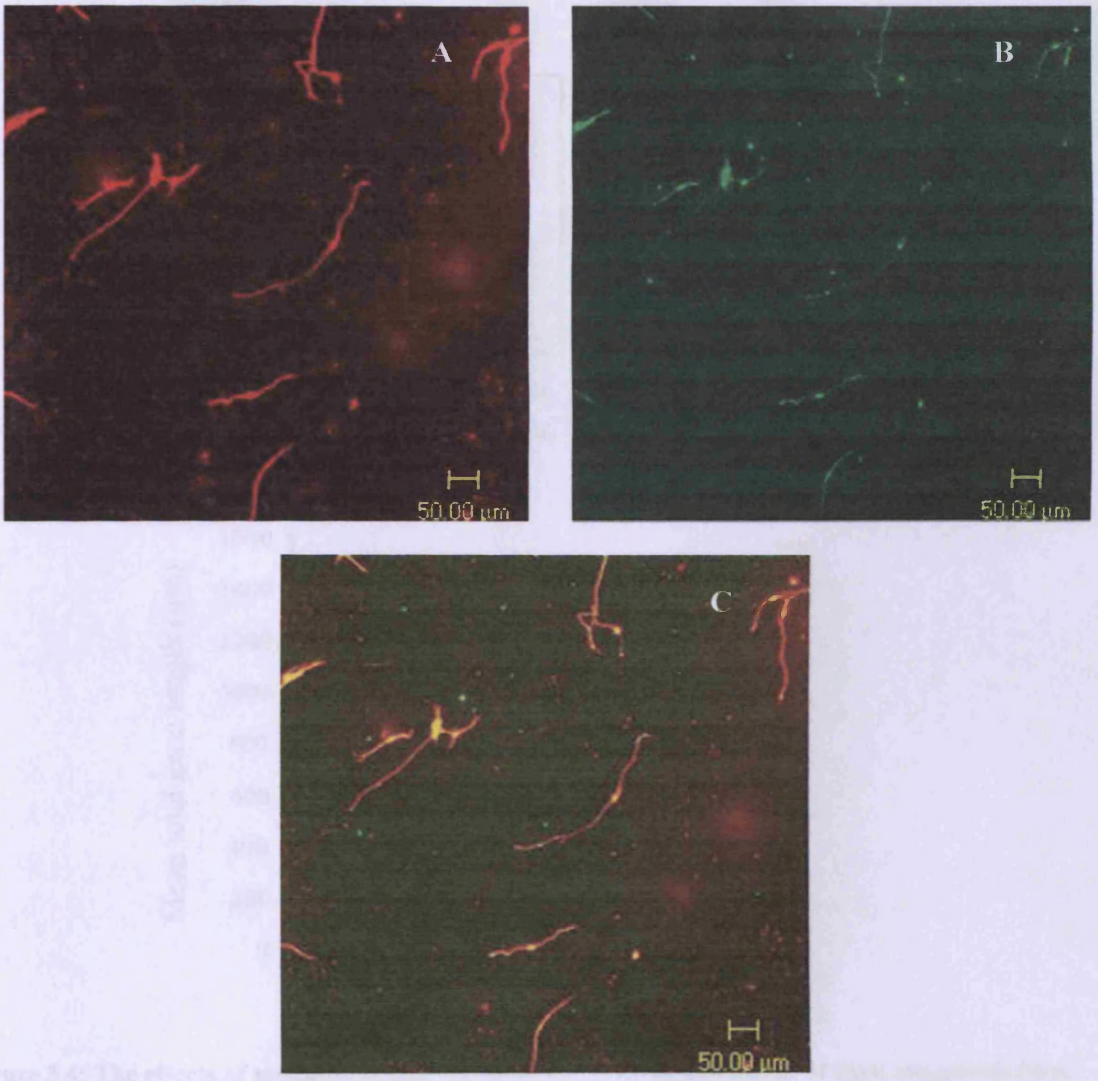

Figure 3.3: The CaSR is expressed in stage 20 vestibular neurons.
Stage 20 vestibular neurons were cultured in the absence of neurotrophins for 24 hours before being fixed and double-labelled with antibodies against the CaSR and β-III Tubulin.
A-C are representative confocal microscope images showing double-labelling of the same field with an antibody against β-III Tubulin combined with an FITC conjugated secondary antibody **(A)** and an antibody against the CaSR combined with a rhodamine conjugated secondary antibody **(B)**. The merged image **(C)** demonstrates that the CasR was expressed in the cell soma and processes of all stage 20 vestibular neurons.

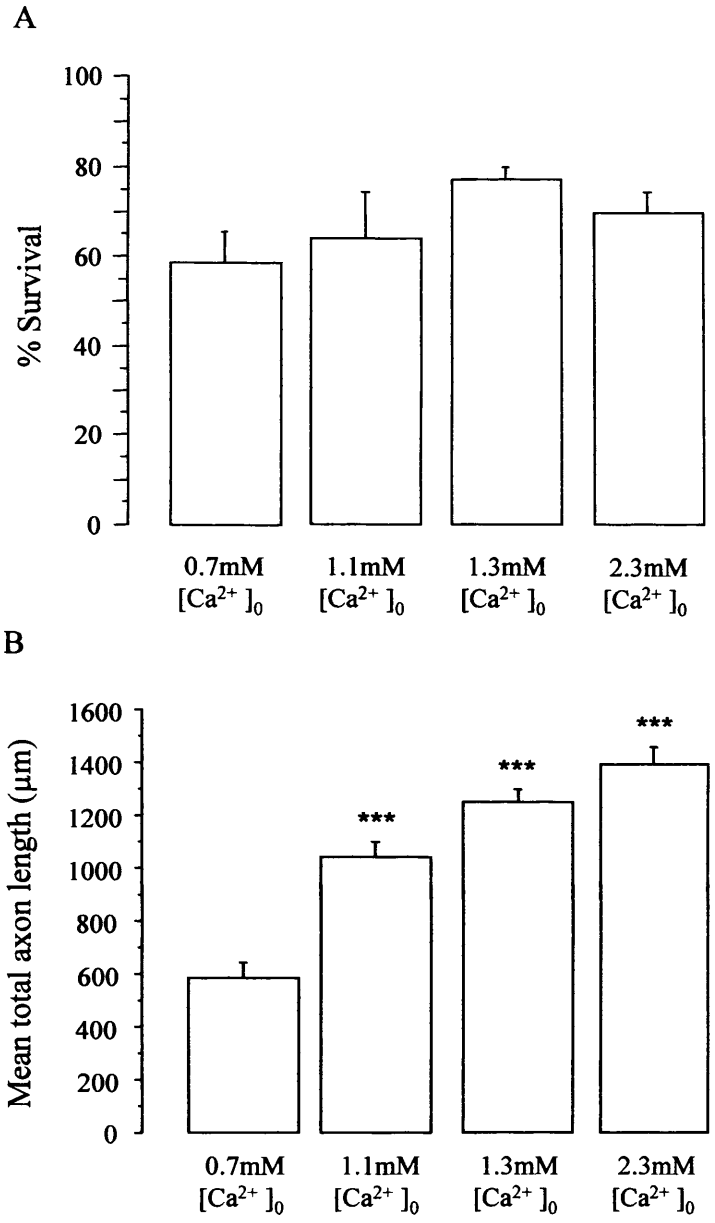

Figure 3.4: The effects of modulating $[Ca^{2+}]_0$ on the survival of and extent of axon outgrowth from cultured stage 20 nodose neurons.

Stage 20 nodose neurons were cultured without BDNF for 24 hours in media containing either 0.7mM, 1.1mM, 1.3mM or 2.3mM Ca^{2+}. Neurons were counted 3 hrs after plating and after 24 hrs in culture, allowing percentage neuronal survival at 24 hrs to be determined. Fluorescent images of surviving neurons were also captured after 24hrs in culture. These images were analysed to calculate the extent of axon outgrowth in each culture condition.

A: Percentage neuronal survival at 24 hours. Altering $[Ca^{2+}]_0$ in a range between 0.7mM and 2.3mM did not affect the survival of cultured stage 20 nodose neurons. Data are the mean +/- SEM from three separate cultures each containing triplicate dishes for each condition.

B: Increasing $[Ca^{2+}]_0$ from 0.7mM to 2.3mM significantly increased axon outgrowth in a dose dependent manner. n= 150 neurons per condition from 3 different experiments. Data are presented as the mean ± SEM. ***denotes a p value of less than 0.0001 after statistical comparisons with control (ANOVA with Fisher's ad hoc).

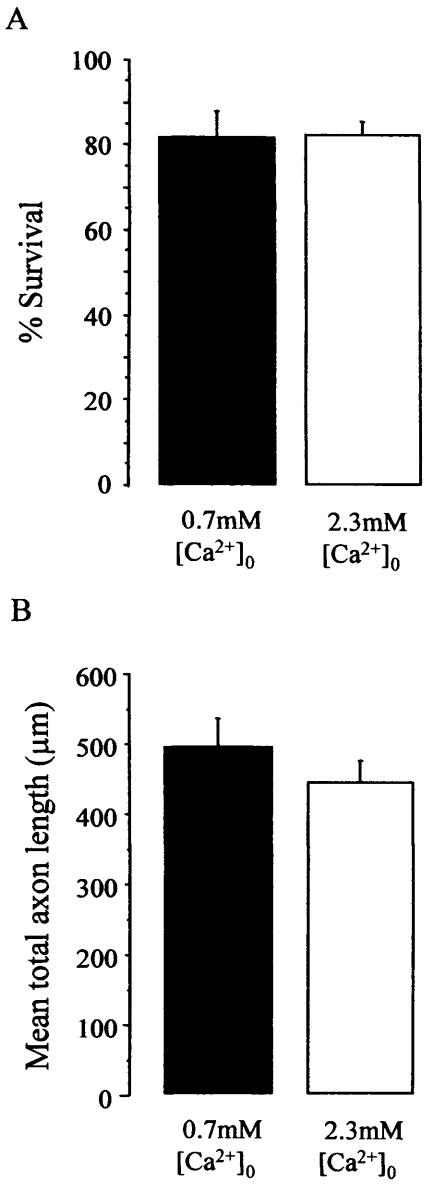

Figure 3.5: The effects of modulating $[Ca^{2+}]_0$ on the survival of and extent of axon outgrowth from cultured stage 20 vestibular neurons.

Stage 20 vestibular neurons were cultured in media containing either 0.7mM or 2.3mM Ca^{2+} for 24 hours. Because cultures did not contain BDNF, they were supplemented with the pan caspase inhibitor Boc-D-FMK to sustain neuronal survival. Neurons were counted 3 hrs after plating and after 24 hrs in culture, allowing percentage neuronal survival at 24 hrs to be determined. Fluorescent images of surviving neurons were also captured after 24hrs in culture. These images were analysed to calculate the extent of axon outgrowth in each culture condition.

A: Percentage neuronal survival at 24 hours. There was no significant difference in survival between stage 20 vestibular neurons cultured in media containing either 0.7mM or 2.3mM Ca^{2+} Data are the mean +/- SEM from three separate cultures each containing triplicate dishes for each condition.

B: Mean total axon length of neurons. There was no significant difference in the extent of axon outgrowth between stage 20 vestibular neurons cultured in media containing either 0.7mM or 2.3 mM Ca^{2+}. n= 150 neurons per condition from 3 different experiments. Data are presented as the mean ± SEM.

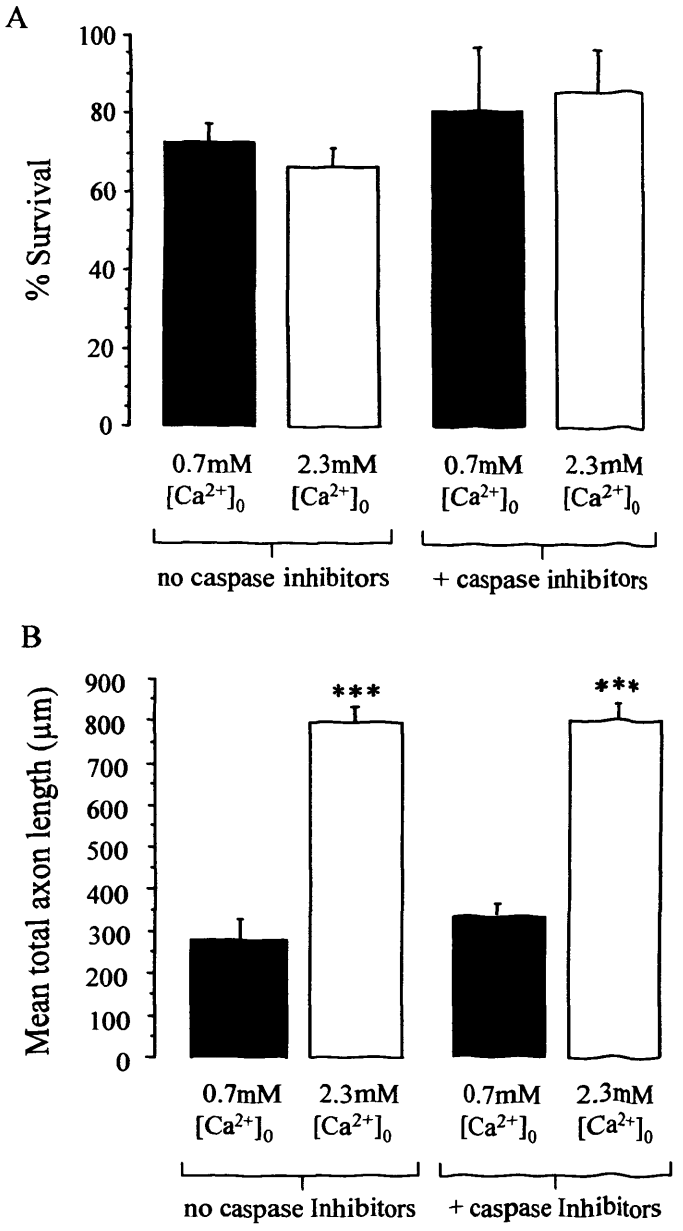

Figure 3.6: The effects of modulating$[Ca^{2+}]_0$ on survival of and axon outgrowth from stage 20 nodose neurons in the presence and absence of caspase inhibitor.

Stage 20 nodose neurons were cultured for 24 hours without BDNF. Half of the cultures contained media without caspase inhibitors and either 0.7mM Ca^{2+} or 2.3mM Ca^{2+}. The other half of the cultures contained media supplemented with the pan caspase inhibitor Boc-D-FMK and either 0.7mM Ca^{2+} or 2.3mM Ca^{2+}. Neurons were counted 3 hrs after plating and after 24 hrs in culture, allowing percentage neuronal survival at 24 hrs to be determined. Fluorescent images of surviving neurons were also captured after 24hrs in culture. These images were analysed to calculate the extent of axon outgrowth in each culture condition.

A: Percentage neuronal survival at 24 hours. In accordance with figure 3.4, there was no significant difference in survival between stage 20 nodose neurons cultured in media containing either 0.7mM Ca^{2+} or 2.3mM Ca^{2+} in the absence of caspase inhibitors. In addition, the caspase inhibitor Boc-D-FMK did not affect the survival of stage 20 nodose in media containing either concentration of Ca^{2+}. Data are the mean +/- SEM from three separate cultures each containing triplicate dishes for each condition.

B: Mean total axon length of neurons. 2.3mM $[Ca^{2+}]_0$ increased axonal growth to the same extent, compared to 0.7mM $[Ca^{2+}]_0$, in both the presence and absence of the caspase inhibitor Boc-D-FMK. n= 150 neurons per condition from 3 different experiments. Data are presented as the mean ± SEM. *** denotes a p value of less than 0.0001 after statistical comparisons with cultures containing 0.7mM Ca^{2+} (ANOVA with Fisher's ad hoc).

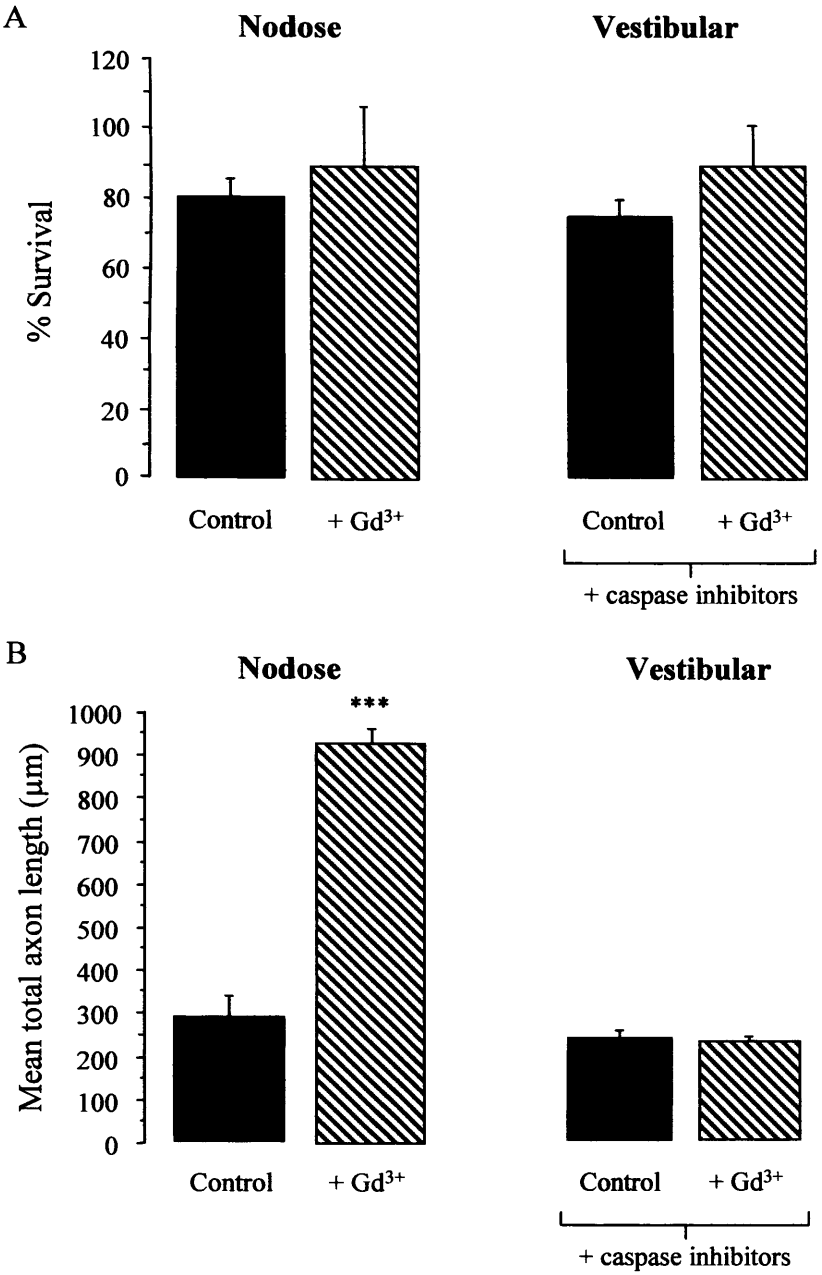

Figure 3.7:The effects of Gd^{3+} on the survival of and the extent of axon outgrowth from stage 20 nodose and vestibular neurons cultured in media containing a low calcium concentration.

Stage 20 nodose and vestibular neurons were cultured for 24 hrs, without BDNF, in media containing 0.7mM Ca^{2+}. Vestibular neuron cultures were supplemented with the caspase inhibitor Boc-D-FMK to prevent apoptosis in the absence of BDNF or without with 1pM Gd^{3+}. Neurons were counted 3 hrs after plating and after 24 hrs in culture, allowing percentage neuronal survival at 24 hrs to be determined. Fluorescent images of surviving neurons were also captured after 24hrs in culture. These images were analysed to calculate the extent of axon outgrowth in each culture condition.

A: Percentage neuronal survival at 24 hours. 1pM Gd^{3+} did not modulate the survival of stage 20 nodose neurons in media containing a low concentration of Ca^{2+}. Similarly, 1pM Gd^{3+} did not modulate the survival of stage 20 vestibular neurons cultured in media containing a low concentration of Ca^{2+} together with caspase inhibitors. Data are the mean +/- SEM from three separate cultures containing triplicate dishes for each condition.

B: Mean total axon length of neurons. The addition of 1pM Gd^{3+} to cultures of stage 20 nodose neurons containing media with a low concentration of calcium significantly increased the extent of axon outgrowth. In contrast, 1pM Gd^{3+} did not increase axon outgrowth from stage 20 vestibular neurons cultured in media containing a low concentration of calcium together with caspase inhibitors. n = 150 neurons per condition from 3 different experiments. Data are presented as the mean ± SEM. *** denotes a p value of less than 0.0001 after statistical comparisons with control (ANOVA with Fisher's ad hoc).

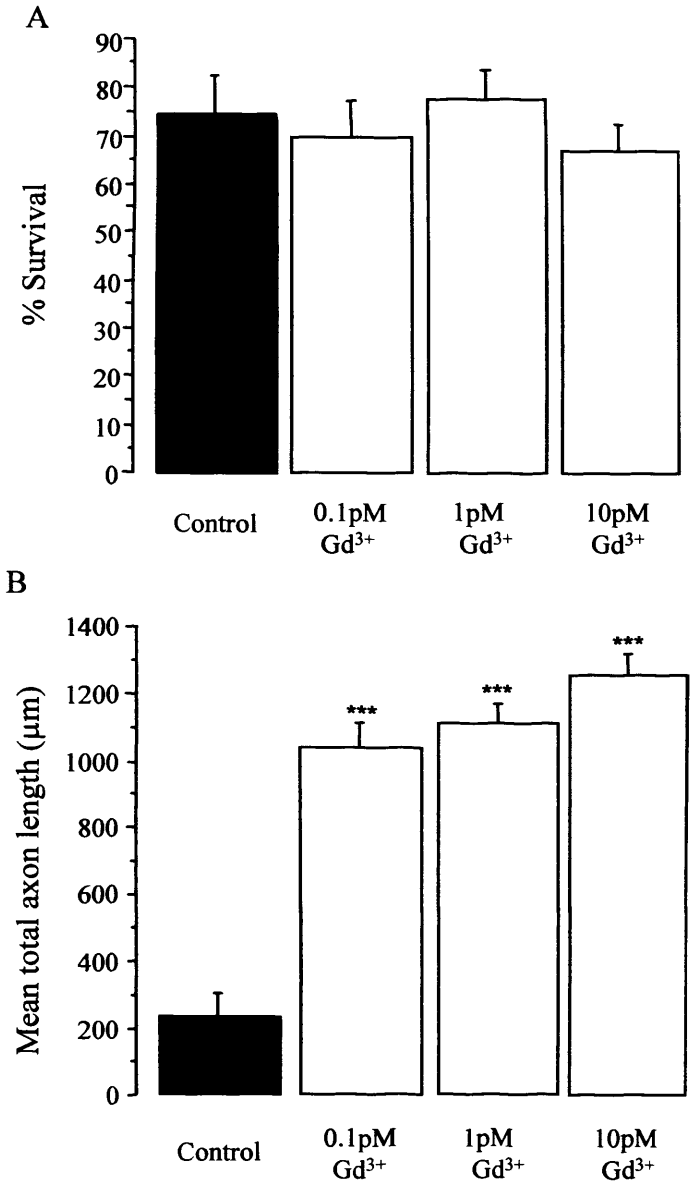

Figure 3.8: The effects of Gd^{3+} on the survival of and the extent of axon outgrowth from stage 20 nodose neurons cultured in media containing a low calcium concentration.

Stage 20 nodose neurons were cultured for 24 hours, in the absence of neurotrophins, in media containing 0.7mM Ca^{2+}. With the exception of control cultures, cultures were supplemented with a range of 0.1pM to 10pM of Gd^{3+}. Neurons were counted 3 hrs after plating and after 24 hrs in culture, allowing percentage neuronal survival at 24 hrs to be determined. Fluorescent images of surviving neurons were also captured after 24hrs in culture, so that the extent of axon outgrowth could be determined in each culture condition.

A: Percentage neuronal survival at 24 hours. There were no significant differences in survival between cultures containing 0.7mM Ca^{2+} alone and 0.7mM Ca^{2+} supplemented with either 0.1pM, 1pM or 10pM Gd^{3+}. Data are the mean +/- SEM from three separate cultures each containing triplicate dishes for each condition.

B: Mean total axon length of neurons. 0.1pM, 1pM and 10pM of Gd^{3+} significantly increased axonal growth compared to 0.7mM Ca^{2+} alone. n= 150 neurons per condition from 3 different experiments. Data are presented as the mean ± SEM. *** denotes a p value of less than 0.0001 after statistical comparisons with control (ANOVA with Fisher's ad hoc).

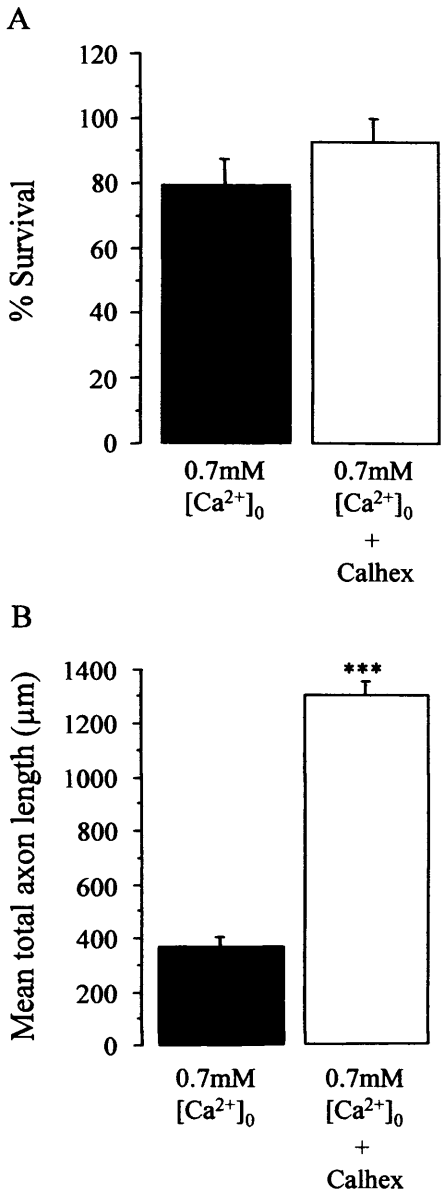

Figure 3.9: The effects of the CaSR agonist, Calhex on the survival of and the extent of axon outgrowth from stage 20 nodose neurons cultured in media containing 0.7mM $[Ca^{2+}]_0$

Stage 20 nodose neurons were cultured for 24 hours, in the absence of neurotrophins, in media containing 0.7mM Ca^{2+}. With the exception of control cultures, cultures were supplemented with 10nM of Calhex. Neurons were counted 3 hrs after plating and after 24 hrs in culture, allowing percentage neuronal survival at 24 hrs to be determined. Fluorescent images of surviving neurons were also captured after 24hrs in culture, so that the extent of axon outgrowth could be determined in each culture condition.

A: Percentage neuronal survival at 24 hours. There was no significant differences in survival between cultures containing 0.7mM Ca^{2+} alone and 0.7mM Ca^{2+} supplemented with Calhex. Data are the mean +/- SEM from three separate cultures each containing triplicate dishes for each condition.

B: Mean total axon length of neurons. Calhex significantly increased axonal growth compared to 0.7mM Ca^{2+} alone. n= 150 neurons per condition from 3 different experiments.

Data are presented as the mean ± SEM. *** denotes a p value of less than 0.0001 after statistical comparisons with control (ANOVA with Fisher's ad hoc).

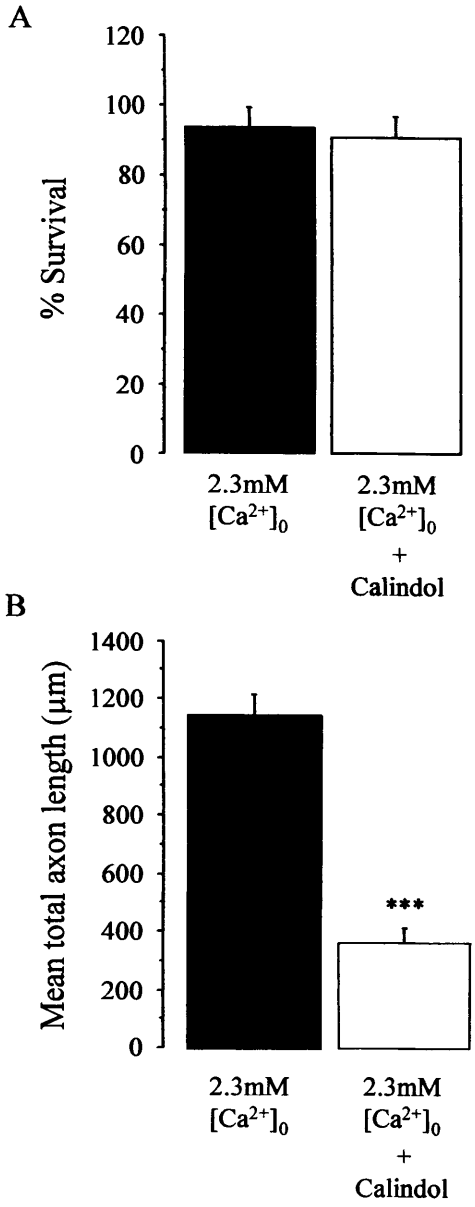

Figure 3.10: The effects of the CaSR antagonist, Calindol on the survival of and the extent of axon outgrowth from stage 20 nodose neurons cultured in media containing 2.3mM $[Ca^{2+}]_0$.

Stage 20 nodose neurons were cultured for 24 hours, in the absence of neurotrophins, in media containing 2.3mM Ca^{2+}. With the exception of control cultures, cultures were supplemented with 10nM of Calindol. Neurons were counted 3 hrs after plating and after 24 hrs in culture, allowing percentage neuronal survival at 24 hrs to be determined. Fluorescent images of surviving neurons were also captured after 24hrs in culture, so that the extent of axon outgrowth could be determined in each culture condition.

A: Percentage neuronal survival at 24 hours. There was no significant difference in survival between cultures containing 2.3mM Ca^{2+} alone and 2.3mM Ca^{2+} supplemented with Calindol. Data are the mean +/- SEM from three separate cultures each containing triplicate dishes for each condition.

B: Mean total axon length of neurons. Calindol significantly decreased axonal growth compared to 2.3mM Ca^{2+} alone. n= 150 neurons per condition from 3 different experiments.

Data are presented as the mean ± SEM. *** denotes a p value of less than 0.0001 after statistical comparisons with control (ANOVA with Fisher's ad hoc).

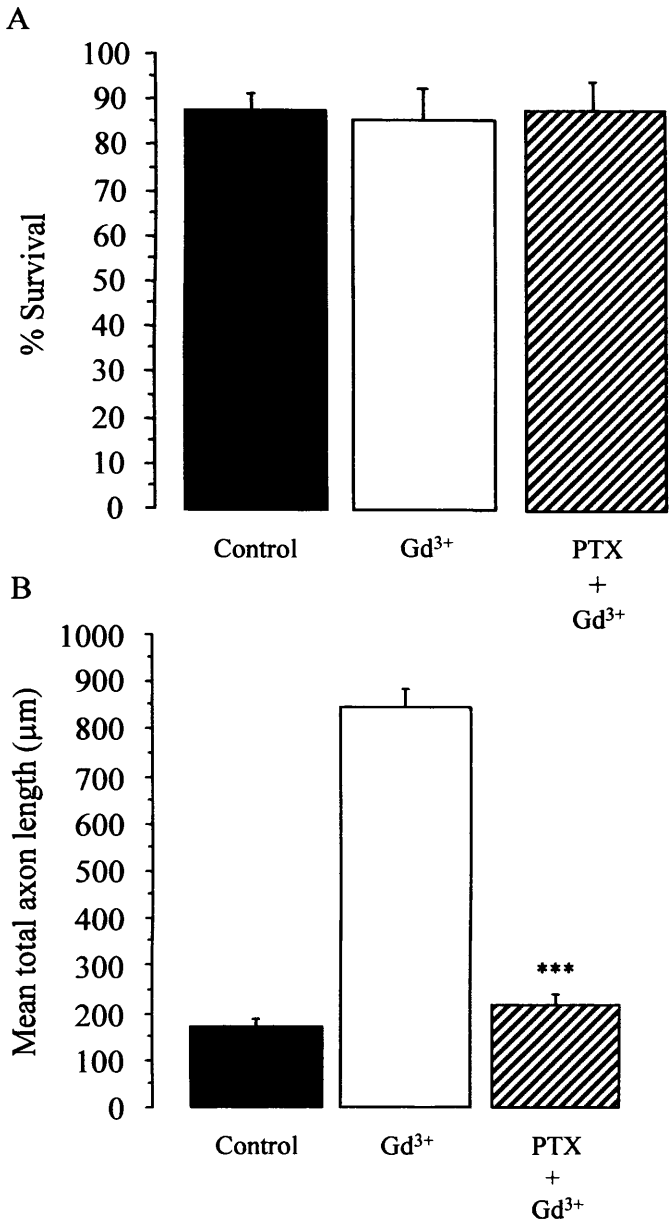

Figure 3.11: The effects of PTX on the survival of and extent of axonal outgrowth from stage 20 nodose neurons cultured in media containing 0.7mM $[Ca^{2+}]_0$ plus 1pM Gd^{3+}.

Stage 20 nodose neurons were cultured for 24 hours, in the absence of neurotrophins, in media containing 0.7mM Ca^{2+}. With the exception of control cultures, cultures were supplemented with 1pM of Gd^{3+} alone or 1pM of Gd^{3+} together with 1mg/ml PTX. Neurons were counted 3 hrs after plating and after 24 hrs in culture, allowing percentage neuronal survival at 24 hrs to be determined. Fluorescent images of surviving neurons were also captured after 24hrs in culture, so that the extent of axon growth could be determined in each culture condition.

A: Percentage neuronal survival at 24 hours. There were no significant differences in neuronal survival between control cultures and cultures containing either 1pM Gd $^{3+}$ alone or 1pM of Gd^{3+} plus 1mg/ml PTX. Data are the mean +/- SEM from three separate cultures each containing triplicate dishes for each condition.

B: Mean total axon length of neurons. 1pM of Gd^{3+} significantly increasd axonal growth compared to control cultures. The Gd^{3+} induced increase in axon length was dramatically reduced in the presence of 1mg/ml PTX.

n= 150 neurons per condition from 3 different experiments. Data are presented as the mean ± SEM. *** denotes a p value of less than 0.0001 after statistical comparisons with Gd^{3+} alone (ANOVA with Fisher's ad hoc).

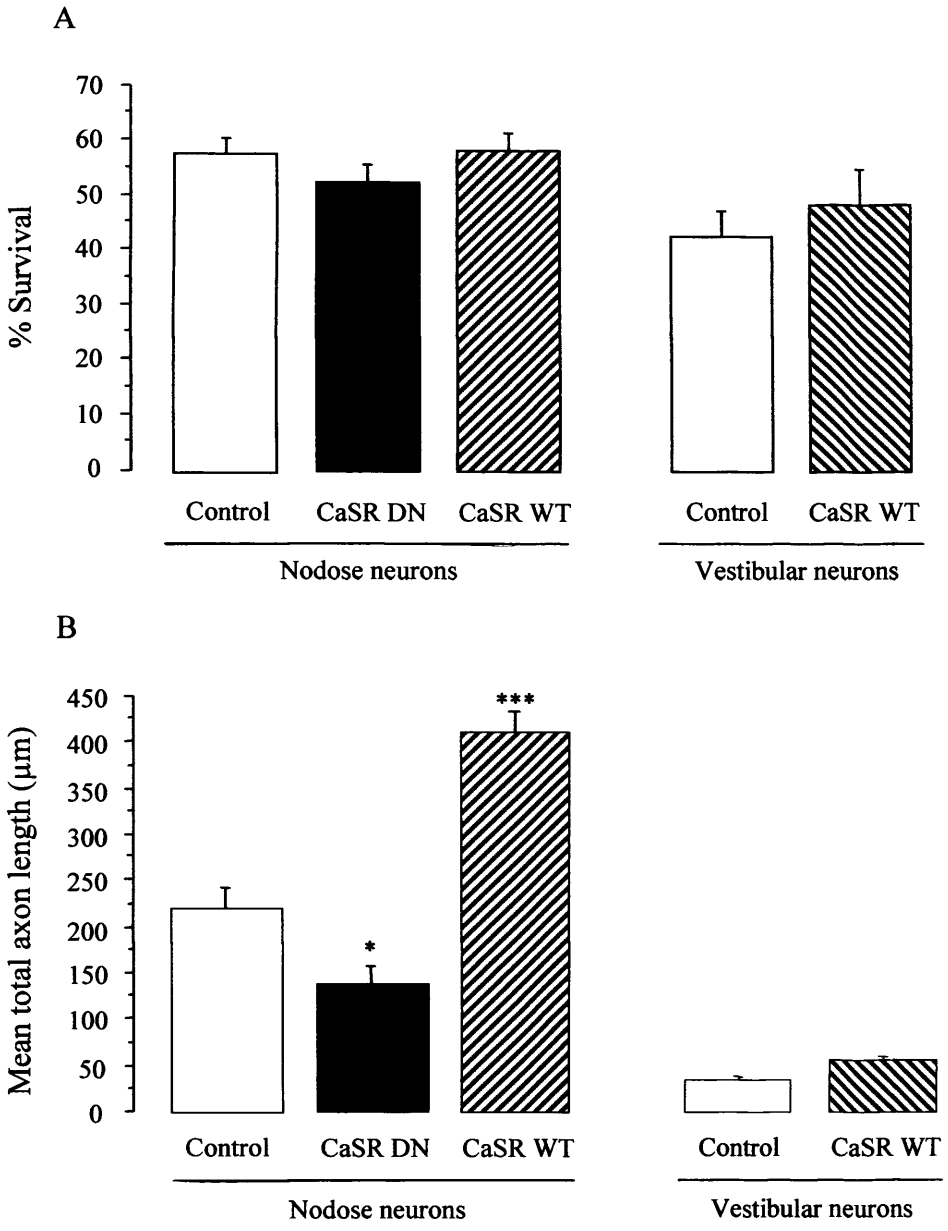

Figure 3.12: Transfection of cDNA expression constructs encoding either wild type or dominant-negative CaSRs into stage 20 nodose and vestibular neurons cultured in medium containing 2.3mM $[Ca^{2+}]_0$

Stage 20 nodose and vestibular were cultured in the absence (nodose neurons) or presence of BDNF (vestibular neurons), in medium containing 2.3mMCa^{2+}. Neurons were co-transfected, by electroporation, with pYFP together with either the empty expression vector pcDNA3.1 (control), pcDNA3.1 containing the cDNA encoding the wild type CaSR (CaSR WT), or pcDNA3.1 containing the cDNA encoding a dominant-negative isoform of the CaSR (CaSR DN). Fluorescent neurons were counted 24 hrs after plating and after 48 hrs in culture, allowing the percentage neuronal survival of fluorescent neurons at 48 hrs compared to 24 hrs to be determined. Fluorescent images for subsequent analysis of process growth were captured after a 24 hr culture period.

A: Percentage neuronal survival after 48 hrs. Over-expression of either the wild type or dominant-negative CaSR in stage 20 nodose or vestibular neurons did not modulate their survival in media containing 2.3mM Ca^{2+}.

B: Mean total axon length of neurons. In media containing 2.3mM Ca^{2+}, over-expression of the dominant-negative CaSR decreased axon outgrowth from stage 20 nodose neurons compared to control tranfected neurons. In contrast, over-expression of the wild type CaSR significantly increased axon growth compared to control transfected neurons. Over-expression of either the dominant-negative or wild type CaSR did not effect axon outgrowth from stage 20 vestibular neurons compared to controls. n = 90 neurons per condition from 3 different experiments). Data presented are the mean ± SEM. *** denotes $p < 0.0001$ and * denotes $p < 0.01$after statistical comparisons with controls (ANOVA with Fisher's ad hoc).

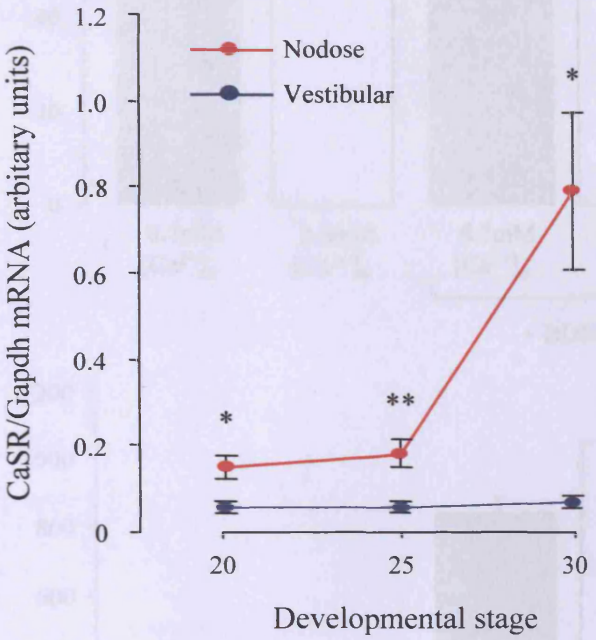

Figure 3.13: The relative levels of CaSR mRNA expressed in stage 20, 25 and 30 nodose and vestibular ganglia.
RT-QPCR was used to assay the levels of CaSR mRNA expressed in stage 20, 25 and 30 nodose and vestibular ganglia. CaSR mRNA levels are normalised to the expression of the mRNA for the housekeeping protein Gapdh. CaSR mRNA was expressed at similar low levels in vestibular ganglia at stage 20, 25 and 30. CaSR mRNA was expressed at significantly higher levels in nodose ganglia compared to vestibular ganglia at all three developmental stages studied. The levels of CaSR mRNA expression increased more than three-fold in nodose ganglia between stage 25 and stage 30. n = 3 separate dissections for both ganglia at each developmental stage. * denotes a p value of less than 0.05 and ** denotes a p value of less than 0.01 after statistical comparisons between the levels of CaSR mRNA expressed within nodose and vestibular ganglia at each developmental stage (students paired t-test).

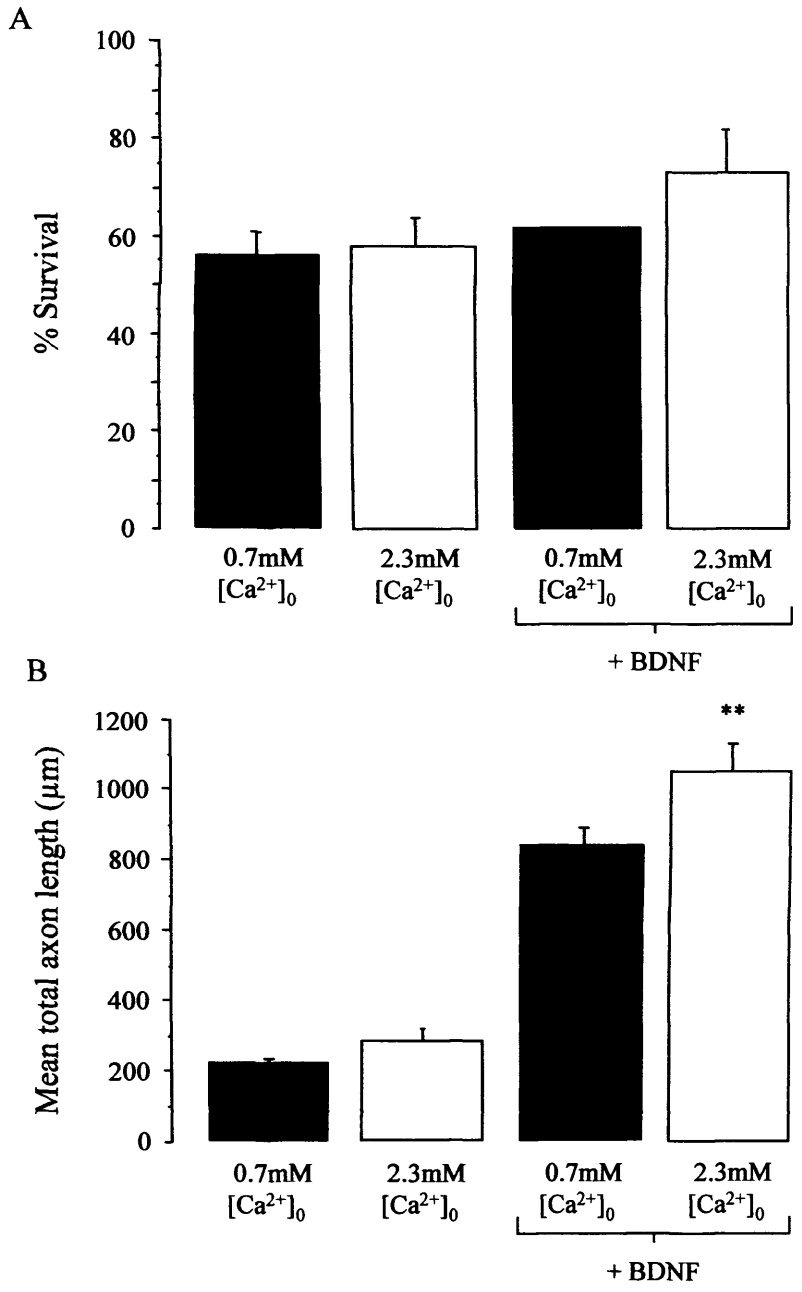

Figure 3.14:The effects of modulating $[Ca^{2+}]_0$ on the survival of and extent of axon outgrowth from stage 27 nodose neurons cultured either with or without BDNF.

Stage 27 nodose neurons were cultured for 24 hours, either in the presence or absence of 10 ng/ml BDNF, in media containing either 0.7mM Ca^{2+} or 2.3mM Ca^{2+}. Neurons were counted 3 hrs after plating and after 24 hrs in culture, allowing percentage neuronal survival at 24 hrs to be determined. Fluorescent images of surviving neurons were also captured after 24hrs in culture. These images were analysed to calculate the extent of axon outgrowth in each culture condition.

A: Percentage neuronal survival at 24 hours. There were no significant differences in neuronal survival between cultures containing either 0.7mM $[Ca^{2+}]_0$ or 2.3mM $[Ca^{2+}]_0$ either with or without BDNF. Data are the mean +/- SEM from three separate cultures each containing triplicate dishes for each condition.

B: Mean total axon length of neurons. Although BDNF did not significantly promote the survival of stage 27 nodose neurons, it greatly increased the extent of axon outgrowth from them. In the absence of BDNF, 2.3mM $[Ca^{2+}]_0$ did not significantly promote axon outgrowth compared to 0.7mM $[Ca^{2+}]_0$. However, in BDNF supplemented cultures 2.3mM $[Ca^{2+}]_0$ significantly increased axon outgrowth compared to 0.7mM $[Ca^{2+}]_0$. n= 150 neurons per condition from 3 different experiments. Data are presented as the mean ± SEM. ** denotes a p value of less than 0.001 after statistical comparison with BDNF supplemented cultures in media containing 0.7 mM Ca^{2+} (ANOVA with Fisher's ad hoc).

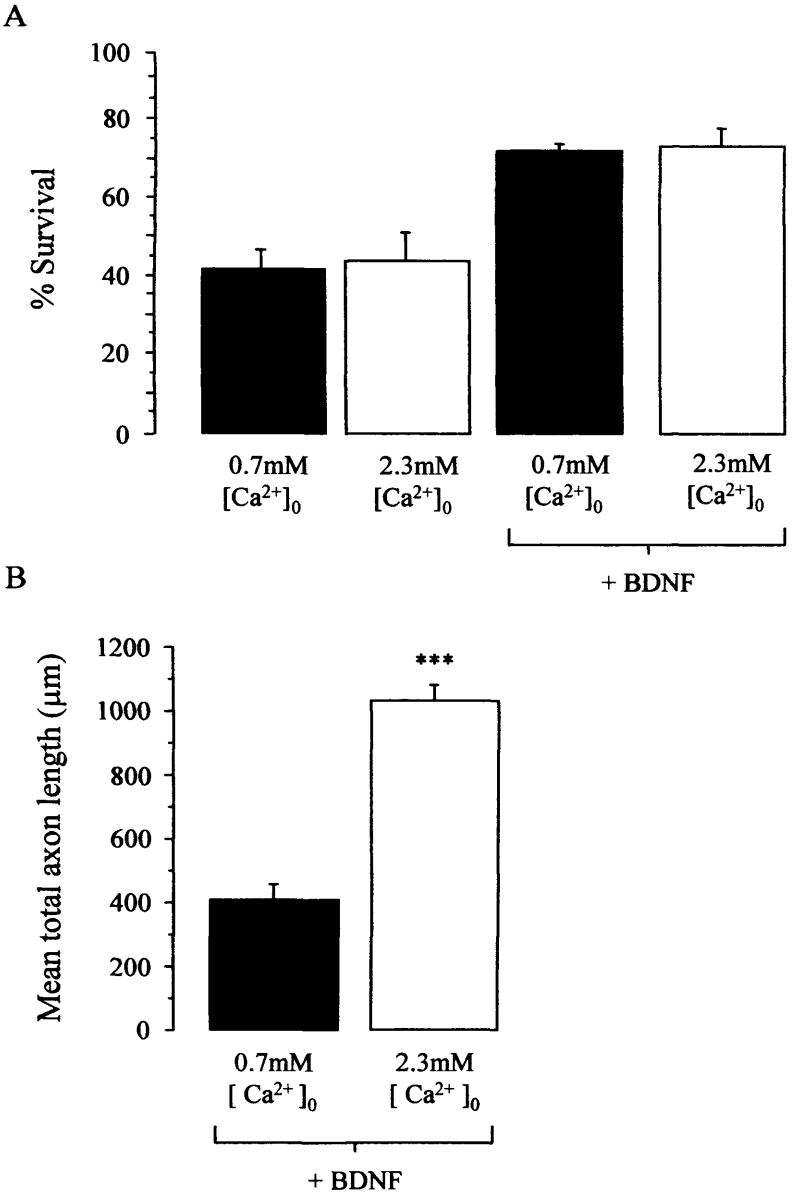

Figure 3.15: The effects of modulating $[Ca^{2+}]_0$ on the survival of and extent of axon outgrowth from stage 30 nodose neurons cultured in media containing BDNF.

Stage 30 nodose neurons were cultured for 24 hours, with or without 10 ng/ml BDNF, in media containing either 0.7mM Ca^{2+} or 2.3mM Ca^{2+}. Neurons were counted 3 hrs after plating and after 24 hrs in culture, allowing percentage neuronal survival at 24 hrs to be determined. Fluorescent images of surviving neurons were also captured after 24hrs in culture. These images were analysed to calculate the extent of axon outgrowth in each culture condition.

A: Percentage neuronal survival at 24 hours. Although BDNF promoted increased survival of cultured stage 30 nodose neurons, there were no significant differences in survival between cultures containing either 0.7mM $[Ca^{2+}]_0$ or 2.3mM $[Ca^{2+}]_0$ either with or without BDNF. Data are the mean +/- SEM from three separate cultures each containing triplicate dishes for each condition.

B: Mean total axon length of neurons cultured with BDNF. 2.3mM $[Ca^{2+}]_0$ significantly increased axonal growth compared to 0.7mM $[Ca^{2+}]_0$ in the presence of BDNF. n= 150 neurons per condition from 3 different experiments. Data are presented as the mean ± SEM. *** denotes a p value of less than 0.0001 after statistical comparison with neurons cultured in media containing 0.7 mM Ca^{2+} (ANOVA with Fisher's ad hoc).

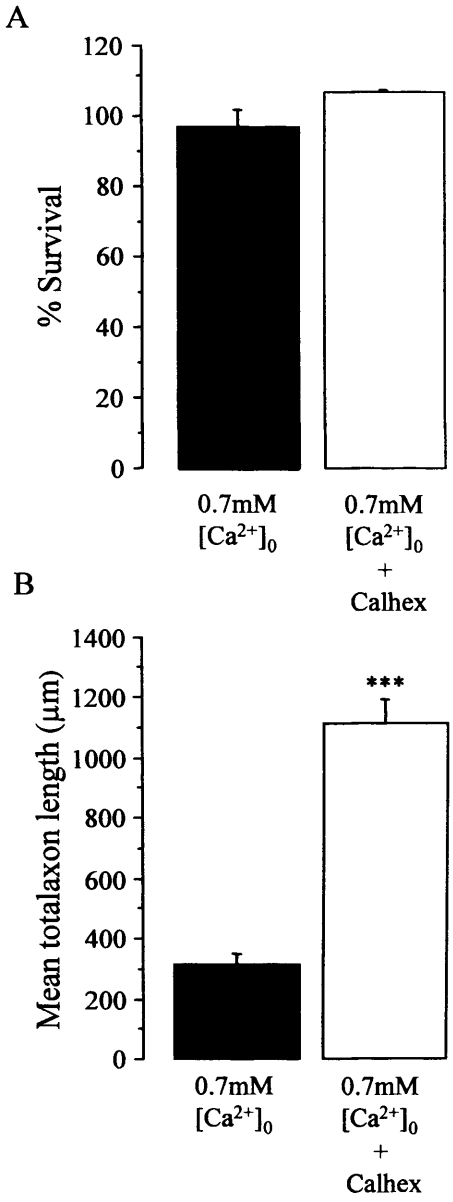

Figure 3.16: The effects of theCaSR agonist, Calhex on the survival of and the extent of axon outgrowth from stage 30 nodose neurons cultured in media containing 0.7mM $[Ca^{2+}]_0$

Stage 30 nodose neurons were cultured for 24 hours, in the absence of neurotrophins, in media containing 0.7mM Ca^{2+}. With the exception of control cultures, cultures were supplemented with 10nM of Calhex. Neurons were counted 3 hrs after plating and after 24 hrs in culture, allowing percentage neuronal survival at 24 hrs to be determined. Fluorescent images of surviving neurons were also captured after 24hrs in culture, so that the extent of axon outgrowth could be determined in each culture condition.

A: Percentage neuronal survival at 24 hours. There was no significant difference in survival between cultures containing 0.7mM Ca^{2+} alone and 0.7mM Ca^{2+} supplemented with Calhex. Data are the mean +/- SEM from three separate cultures each containing triplicate dishes for each condition.

B: Mean total axon length of neurons. Calhex significantly increased axonal length compared to 0.7mM Ca^{2+} alone. n= 150 neurons per condition from 3 different experiments.
Data are presented as the mean ± SEM. *** denotes a p value of less than 0.0001 after statistical comparison with 0.7mM Ca^{2+} alone (ANOVA with Fisher's ad hoc).

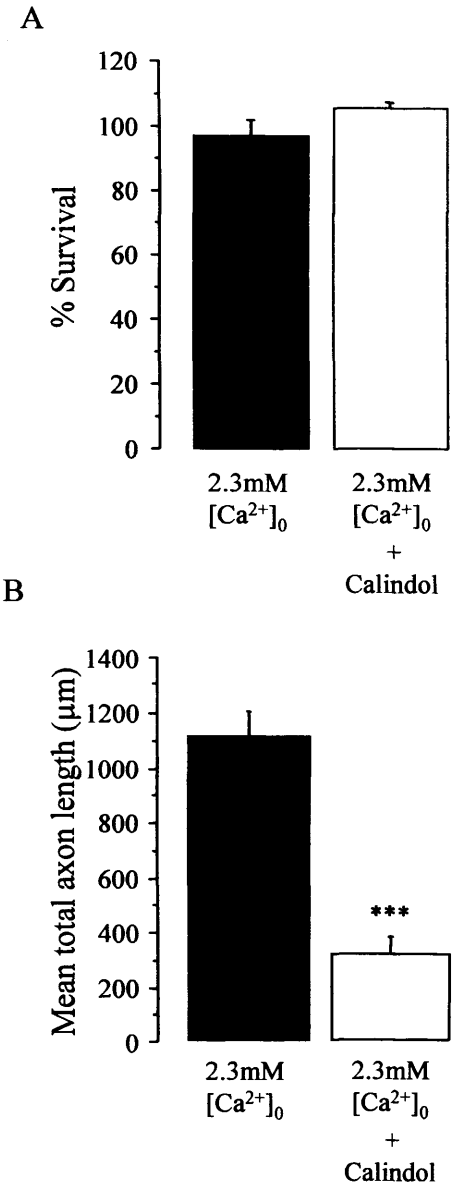

Figure 3.17: The effects of the CaSR antagonist, Calindol on the survival of and the extent of axon outgrowth from stage 30 nodose neurons cultured in media containing 2.3mM $[Ca^{2+}]_0$.

Stage 30 nodose neurons were cultured for 24 hours, in the absence of neurotrophins, in media containing 2.3mM Ca^{2+}. With the exception of control cultures, cultures were supplemented with 10nM of Calindol. Neurons were counted 3 hrs after plating and after 24 hrs in culture, allowing percentage neuronal survival at 24 hrs to be determined. Fluorescent images of surviving neurons were also captured after 24hrs in culture, so that the extent of axon outgrowth could be determined in each culture condition.

A: Percentage neuronal survival at 24 hours. There was no significant difference in survival between cultures containing 2.3mM Ca^{2+} alone or 2.3mM Ca^{2+} supplemented with Calindol. Data are the mean +/- SEM from three separate cultures each containing triplicate dishes for each condition.

B: Mean total axon length of neurons. Calindol significantly increased axonal growth compared to 2.3mM Ca^{2+} alone. n= 150 neurons per condition from 3 different experiments.

Data are presented as the mean ± SEM. *** denotes a p value of less than 0.0001 after statistical comparison with 2.3 mM Ca^{2+} alone (ANOVA with Fisher's ad hoc).

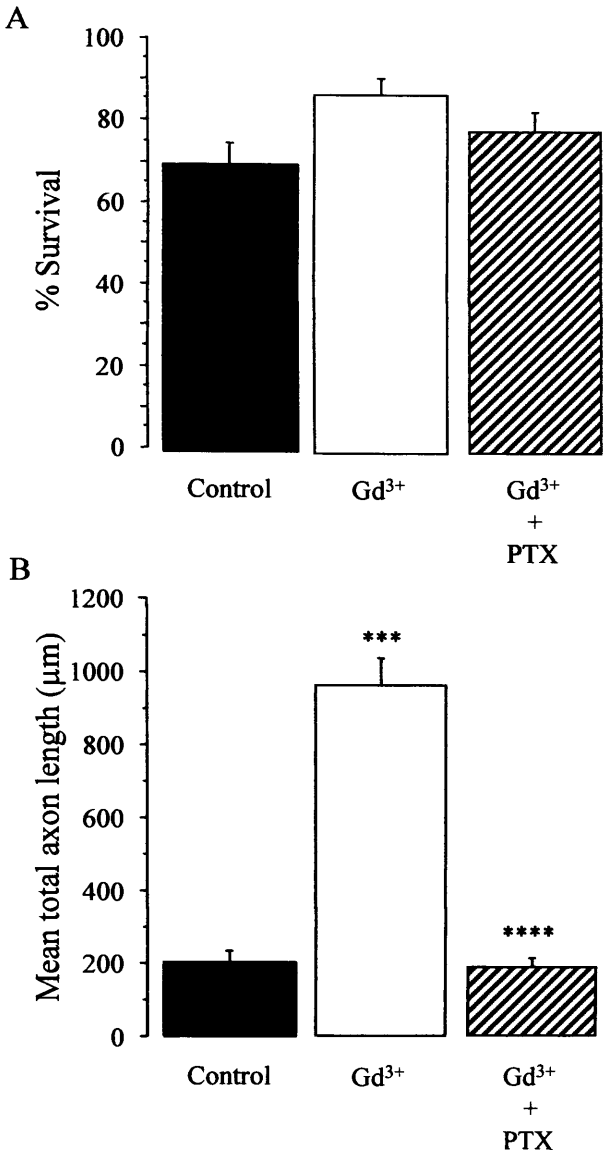

Figure 3.18: The effects of PTX on the survival of and extent of axon outgrowth from stage 30 nodose neurons cultured Gd^{3+} and medium containing BDNF and 0.7mM $[Ca^{2+}]_0$.

Stage 30 nodose neurons were cultured for 24 hours in media containing 10ng/ml BDNF. With the exception of control cultures, cultures were supplemented with either 1pM of Gd^{3+} alone or 1pM of Gd^{3+} together with 1mg/ml PTX. Neurons were counted 3 hrs after plating and after 24 hrs in culture, allowing percentage neuronal survival at 24 hrs to be determined. Fluorescent images of surviving neurons were also captured after 24hrs in culture, so that the extent of axon outgrowth could be determined in each culture condition.

A: Percentage neuronal survival at 24 hours. There were no significant differences in survival between control cultures and cultures supplemented with either 1pM Gd^{3+} alone or 1pM of Gd^{3+} together with 1mg/ml PTX. Data are the mean +/- SEM from three separate cultures each containing triplicate dishes for each condition.

B: Mean total axon length of neurons. 1pM of Gd^{3+} significantly increased axonal growth compared to control cultures and this increase can be prevented by 1mg/ml PTX. n= 150 neurons per condition from 3 seperate experiments. Data are presented as the mean ± SEM. *** denotes a p value of less than 0.0001 after statistical comparisons with control and **** denotes a p value of less than 0.0001 after statistical comparison with Gd^{3+} (ANOVA with Fisher's ad hoc).

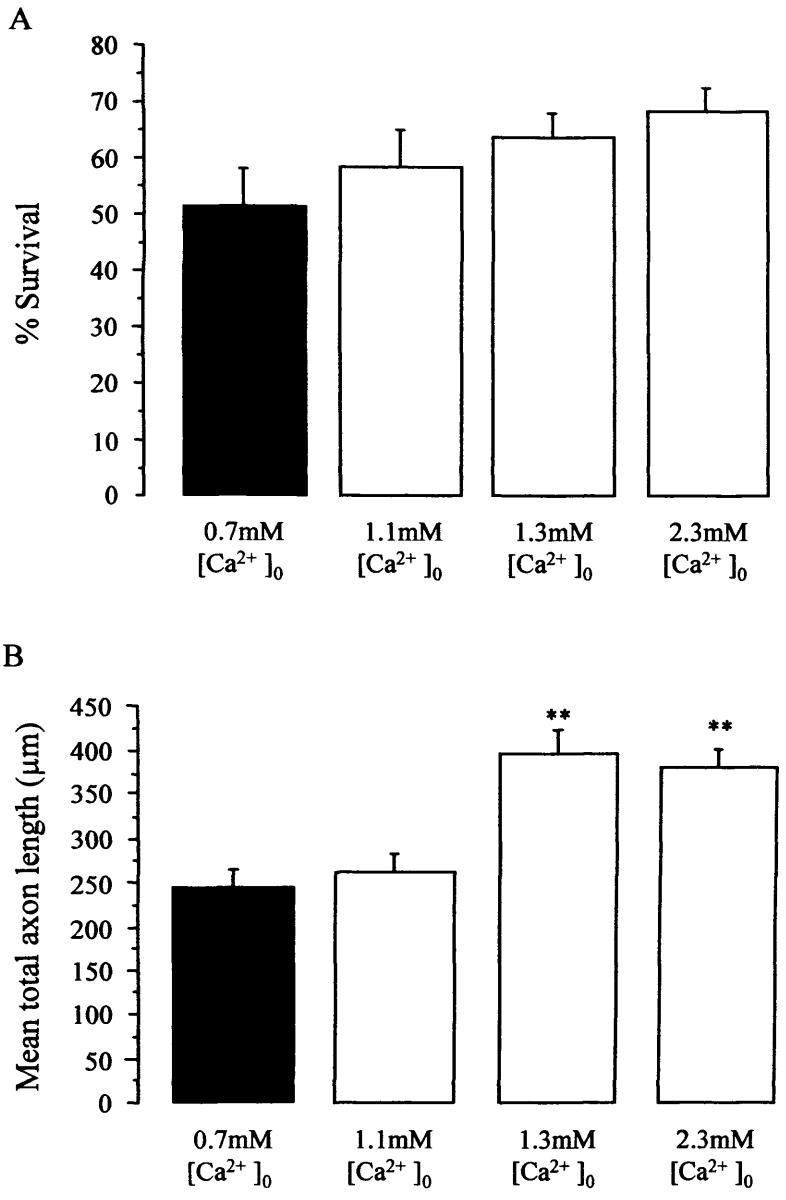

Fig 3.19: The effect of modulating $[Ca^{2+}]_0$ on the survival of and extent of axon outgrowth from stage 25 vesibular neurons cultured in medium containing BDNF.

Stage 25 vestibular neurons were cultured for 24 hours, in the presence of 10 ng/ml BDNF, in media containing either 0.7mM, 1.1mM, 1.3mM or 2.3mM Ca^{2+}. Neurons were counted 3 hrs after plating and after 24 hrs in culture, allowing percentage neuronal survival at 24 hrs to be determined. Fluorescent images of surviving neurons were also captured after 24hrs in culture. These images were analysed to calculate the extent of axon outgrowth in each culture condition.

A: Percentage neuronal survival at 24 hours. There were no significant differences in survival between BDNF supplemented cultures containing either 0.7mM, 1.1mM, 1.3mM or 2.3mM Ca^{2+}. Data are the mean +/- SEM from three separate cultures each containing triplicate dishes for each condition.

B: Mean total axon length of neurons. 1.3mM and 2.3mM $[Ca^{2+}]_0$ significantly increased axon outgrowth from stage 25 cultured vestibular neurons compared to 0.7mM $[Ca^{2+}]_0$. However, 1.1mM $[Ca^{2+}]_0$ did not promote axon outgrowth compared to neurons cultured in media containing 0.7mM Ca^{2+}. n = 150 neurons per condition from 3 different experiments. Data are presented as the mean ± SEM. ** denotes a p value of less than 0.001after statistical comparisons with neurons cultured in media containing 0.7 mM Ca^{2+} (ANOVA with Fisher's ad hoc).

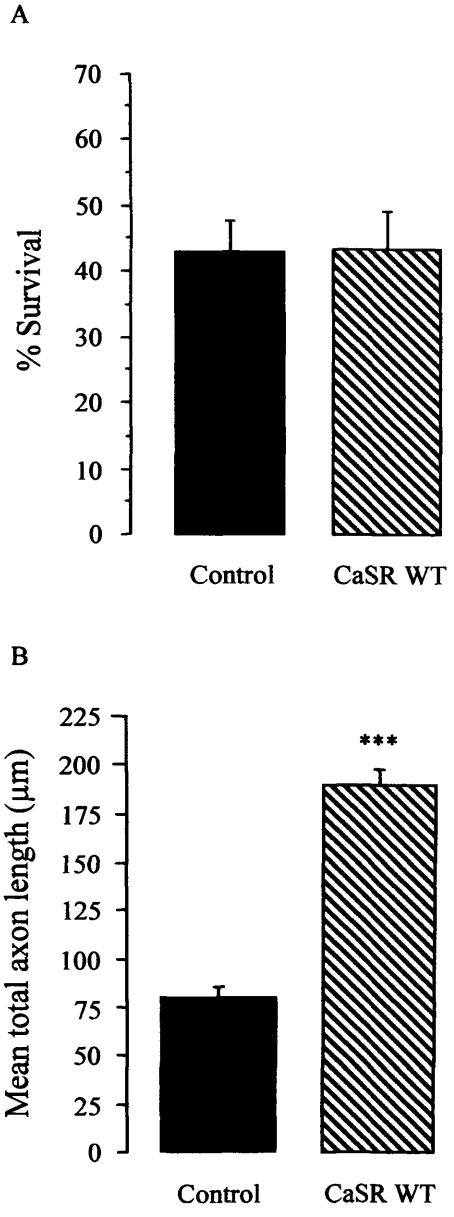

Figure 3.20: Transfection of a cDNA expression construct encoding the wild type CaSR into stage 26 vestibular neurons cultured in media containing 2.3 mM $[Ca^{2+}]_0$.

Stage 26 vestibular were cultured in medium containing 2.3mMCa $^{2+}$ plus 10 ng/ml BDNF. Electroporation was used to co-transfect neurons with pYFP together with either the empty expression vector pcDNA3.1 (control) or pcDNA3.1 containing the cDNA encoding the wild type CaSR (CaSR WT). Neurons were counted 24 hrs after plating and after 48 hrs in culture, allowing percentage neuronal survival at 48 hrs to be determined. Fluorescent images for subsequent analysis of process outgrowth were captured after a 24 hr after transfection.

A: Percentage neuronal survival after 48 hrs. Overexpression of the wild type CaSR in stage 26 vestibular neurons did not effect their survival compared to control transfect neurons.

B: Mean total axon length of neurons. Overexpression of the wild type CaSR in stage 26 vestibular neurons significantly increased the extent of axon outgrowth compared to control transfected neurons. n = 90 neurons per condition from 3 different experiments.
Data presented are the mean ± SEM. *** denotes $p < 0.0001$ after statistical comparison with control (ANOVA with Fisher's ad hoc).

3.3 Discussion

It has recently been reported that the CaSR plays a crucial, physiologically relevant, role in promoting axonal growth and branching from mouse sympathetic neurons during a window of development in the immediate perinatal period when the axons of these neurons are ramifying extensively in their targets under the influence of target-derived NGF. Neonatal mice lacking CaSR have reduced sympathetic innervation density, but normal numbers of sympathetic neurons (Vizard et al., 2008). The research presented in this chapter not only extends the role of the CaSR in regulating axonal growth to developing sensory neurons of chick embryos at a stage in development when they are responsive to target-derived BDNF but also to the earliest stages of neuronal development when sensory axons are growing to their targets before the neurons have become dependent on neurotrophins for survival. As with developing sympathetic neurons, the CaSR affects axonal growth from embryonic sensory neurons but has no effect on their survival.

One of the most interesting aspects of my data is that they suggest a mechanism that may account for the marked intrinsic differences in axon growth rates displayed by different populations of neurotrophic factor-independent cranial sensory neurons at the stage in development when their axons are growing to their targets (Davies, 1989). Among populations of placode-derived cranial sensory neurons in the chick embryo, nodose neurons, which have the most distant targets, extend axons towards their targets at the fastest rate, whereas vestibular neurons, which have the closest targets, have the slowest growing axons. At stage 20, when many nodose and vestibular axons are growing to their targets *in vivo*, nodose ganglia express 3-fold higher levels of CaSR mRNA relative to GAPDH mRNA than vestibular ganglia. Whilst, immunocytochemistry demonstrates that stage 20 nodose and vestibular neurons both express CaSR protein, the non-quantitative nature of this techniques precludes a comparison of relative levels of CaSR protein expressed by both types of neurons. Also, the small number of neurons present in chick stage 20 cranial sensory ganglia makes a semi-quantative assessment of relative CaSR levels between the two ganglia by Western Blotting technically very challenging. For these reasons, it has been difficult to ascertain if the highly significant differences in the relative levels of CaSR mRNA between nodose and vestibular ganglia are translated into significant differences in the levels of CaSR proteins in nodose and vestibular neurons. Both elevated $[Ca^{2+}]_o$ and the potent CaSR agonists Gd^{3+} and Calhex greatly increase the mean length of axons growing from stage 20 nodose neurons after 24 hrs in cultures. I have demonstrated that the increase in axon length induced by elevated $[Ca^{2+}]_o$ can be inhibited by the CaSR antagonist, Calindol, and that Gd^{3+} -promoted axon

growth can be inhibited by the G-protein inhibitor, PTX, strongly suggesting that the CaSR receptor mediates the axon growth promoting effects of these molecules. In accordance with this, over-expression of a dominant-negative CaSR protein in stage 20 nodose neurons cultured for 24 hours in media containing 2.3mM calcium significantly reduces the mean length of axons compared to control transfected neurons. In marked contrast to nodose neurons, neither increased $[Ca^{2+}]_o$ nor Gd^{3+} enhance *de novo* axonal growth from cultured stage 20 vestibular neurons. Whilst the lack of effect of these molecules may reflect a lower level of CaSR expression by vestibular neurons, the ability of exogenously expressed wild type CaSR protein to promote BDNF-independent axon growth from stage 20 nodose neurons, but not stage 20 vestibular neurons, in media containing a high (2.3 mM) $[Ca^{2+}]_o$ suggests that crucial signalling pathways that transduce CaSR activation into increased axon growth are absent in vestibular neurons at this stage of development.

The level of $[Ca^{2+}]_o$ in developing vertebrate embryos is 1.69 mM (Brown and MacLeod, 2001), a level that is high enough to significantly activate the chick CaSR and enhance axon growth from stage 20 nodose neurons as shown in figure 3.4. It is therefore tempting to speculate that the faster *in vivo* growth of nodose neurons compared to vestibular neurons (Davies, 1989). is due to CaSR activation and signalling in the former. Verification of this hypothesis will require further experimental studies, particularly *in ovo*. For example, I will use whole mount staining with neurafilament antibodies to determine whether *in ovo* application of Calindol specifically reduces the growth rate of axons emerging from newly differentiated nodose neurons, but not vestibular neurons. Similarly, I will use *in ovo* electroporation to transfect a dominant-negative CaSR expression plasmid containing a neuron specific promotor into very early chicken embryos to see if the dominant-negative CaSR specifically reduces the growth rate of nodose neurons *in ovo*.

Interestingly, the ability of CaSR activation to promote BDNF-independent axonal growth from newly differentiated nodose neurons appears to be short lived, since elevated $[Ca^{2+}]_o$ does not increase axon extension from stage 27 nodose neurons cultured without BDNF. Whilst the survival of cultured stage 27 nodose neurons is not dependent on BDNF, I have shown that BDNF greatly increases the length of axons projecting from nodose neurons at this age, an effect that is enhanced by elevated $[Ca^{2+}]_o$ and therefore presumably CaSR activation. This finding, together with the fact that the levels of CaSR mRNA expressed by stage 27 nodose neurons is higher than that expressed by stage 20 nodose neurons, suggests that developmental changes in the repertoire of growth-related signalling pathways may be

responsible for the loss in the ability of the CaSR to promote BDNF-independent axon outgrowth at stage 27. This possibility will be explored in Chapter 4, below.

I have shown that either elevated $[Ca^{2+}]_o$, 1 pM Gd^{3+} or 10 nM Calhex are capable of enhancing BDNF-promoted axon outgrowth from stage 30 nodose neurons. The fact that Gd^{3+}-enhanced axon growth can be inhibited by PTX and elevated $[Ca^{2+}]_o$ –promoted axon growth can be inhibited by Calindol strongly suggests that the CaSR mediates the growth promoting effects of these molecules. CaSR activation by elevated $[Ca^{2+}]_o$ increases the extent of BDNF-promoted axon outgrowth by some 2.5-fold at stage 30 compared to 20% at stage 27. It is tempting to speculate that the greater efficacy of CaSR activation in enhancing BDNF-promoted axonal outgrowth at stage 30 compared to stage 27 is linked to the higher expression of CaSR mRNA at stage 30. This hypothesis needs to be tested by comparing the extent of BDNF-promoted axon outgrowth from stage 27 and stage 30 nodose neurons that have been transfected with the wild type CaSR cDNA expression construct and cultured in media containing either high $[Ca^{2+}]_o$, 1pM Gd^{3+} or 10nM Calhex.

The data presented in this chapter clearly demonstrates that CaSR activation does not enhance the rate of *de novo*, BDNF-independent axon outgrowth from newly differentiated stage 20 vestibular neurons. However, 1.3 mM and 2.3mM $[Ca^{2+}]_o$ increases the length of axons projecting from stage 25 vestibular neurons cultured with BDNF by some 60% compared to vestibular neurons cultured with BDNF in media containing 0.7mM Ca^{2+}. If CaSR mRNA expression reflects CaSR protein expression, the relatively small effect that CaSR activation has on axon outgrowth from stage 25 vestibular neurons may be due to the low level of CaSR expressed by vestibular neurons at this stage. In accordance with this, over-expression of the wild type CaSR in stage 25 vestibular neurons increases the extent of BDNF-promoted axon outgrowth by 2.5-fold.

Although the data presented in this chapter suggest that activation of the CaSR can enhance BDNF-promoted axon outgrowth from nodose neurons, and to a lesser extent vestibular neurons, more detailed experimental work is required to confirm this interpretation of the data. In particular, the physiological relevance of my *in vitro* data also needs to be tested by both *in ovo* electroporation of an expression construct encoding the dominant-negative chick CaSR under the control of a neuron-specific promotor and *in ovo* application of the specific CaSR antagonist, Calindol.

Summary

I have shown that CaSR activation can promote *de novo* axon growth from newly differentiated nodose neurons, but not vestibular neurons. Since the level of $[Ca^{2+}]_0$ in the developing chick is high enough to significantly activate the CaSR, my data suggests that selective CaSR activation in nodose neurons may at least partly account for the differences in the intrinsic rates of *de novo*, neurotrophic factor-independent, axonal growth between nodose and vestibular neurons. This hypothesis needs to be tested and validated by further *in vitro* and *in ovo* experimental studies

Later in development, CaSR activation enhances BDNF-promoted, regenerative axonal growth from cultured nodose neurons, and to a lesser extent vestibular neurons. Once again, the physiological relevevance of this finding needs to be investigated further with additional *in vitro* and *in ovo* experimental studies.

Chapter 4

Developmental switch in the signal transduction pathways required for axonal growth

4.1 Introduction

The data presented in Chapter 3 clearly demonstrates that activation of the CaSR by either elevated $[Ca^{2+}]_o$ or 1pM Gd^{3+} enhances BDNF-independent, *de novo* axon growth from cultured stage 20 and 23 nodose neurons. CaSR activation also enhances BDNF-promoted axon growth from later stage nodose neurons. As outlined in Chapter 1, several studies have identified the intracellular signalling proteins GSK3, PI3-Kinase and ERK1/2 as key players in modulating neurotrophic factor-promoted axon growth. For example, GSK3 regulates the binding of several proteins to microtubules, thereby enhancing microtubule polymerization (Etienne-Manneville and Hall, 2003; Jimbo et al., 2002; Yoshimura et al., 2005). In addition to influencing microtubule polymerization dynamics by regulating GSK3 activity (Yoshimura et al., 2005), PI3-kinase also promotes neuronal process extension by modulating actin polymerization dynamics (Aoki et al., 2005; Nusser et al., 2002). The binding of neurotrophins to their receptor tyrosine kinases initiates a series of signalling events that leads to the activation of ERK1/2 that can in turn promote the phosphorylation and activation of the transcription factors CREB and NFATc. Activated CREB and NFATc lead to increased transcription of several genes that promote axon extension (De Cesare et al., 1999; Lonze and Ginty, 2002; Nguyen and Di Giovanni, 2008). Whilst the signal transduction pathways that regulate neurotrophic factor-promoted, regenerative axon growth have been well characterised, no information exists on the signal transduction pathways that modulate *de novo* axon growth, in part because, until now, no extracellular signals have been identified that are capable of regulating the rate of *de novo* axon growth.

Activation of the CaSR initiates a number of intracellular signal transduction pathways downstream of initial G-protein coupling, the nature of which depends on both cell type and the physiological outcome of CaSR activation (Ward, 2004). One signalling pathway that is activated by CaSR agonists is the ERK1/2 MAP-kinase pathway. ERK activation by CaSR agonists has been demonstrated in numerous cell types, including fibroblasts, osteoclasts, parathyroid cells and kidney proximal tubule cells. In many cases PD98059, an inhibitor of MEK1/2, the upstream activators of ERK1/2 in the classical MAP-Kinase pathway, has been shown to prevent ERK1/2 activation by CaSR agonists (Ward, 2004). The PI3-kinase inhibitors wortmannin and LY2942004 prevent CaSR agonist-induced activation of ERK in the HEK cell line, primate ovarian surface epithelial cells (OSE cells) and human parathyroid cells, suggesting that CaSR activation can also lead to activation of PI3-kinase upstream of ERK activation. In addition, treatment of human OSE cells with CaSR agonists has been

shown to activate PI3-kinase, leading to phosphorylation of its downstream target, Akt. PI3-kinase mediated phosphorylation and activation of Akt and ILK in neurons has been shown to result in the phosphorylation of GSK3 which modulates its activity (Jiang et al., 2005; Yoshimura et al., 2005; Zhou et al., 2004). Since CaSR activation can result in PI3-kinase and Akt activation (Ward, 2004)it is also possible that activation of the CaSR may also be able modulate the activity of GSK3 in certain cell types.

The aim of the research presented in this chapter was to begin to characterise the intracellular signalling pathways that transduce activation of the CaSR into enhanced neurotrophin-independent axon growth from early nodose neurons and BDNF-dependent axon elongation from these neurons at later stages of development. Because of their involvement in mediating neurotrophic factor-promoted axon growth in several kinds of neurons and because they have been shown to be downstream targets of the activated CaSR in certain cell types, I decided to examine the potential roles of PI3-Kinase, ERK and GSK3 in transducing CaSR activation into enhanced axon growth. The role of PI3-kinase was investigated primarily by determining the effects of the specific pharmacological PI3-Kinase inhibitor LY294002 on axon growth. Similarly, the specific GSK3 inhibitor, Bio ((2'Z,3'E)-6-Bromoindirubin-3'oxime (Sato et al., 2004), was used to examine the role of GSK3 signalling in axon growth. Because no effective selective ERK1/2 inhibitors are currently available, the role of ERK in transducing activation of the CaSR into enhanced axon growth was investigated by inhibiting the function of MEK1/2, the upstream kinases in the ERK1/2 MAP-Kinase signalling cascade, by PD98059.

My findings suggest that PI3-kinase signalling plays a pivotal role in transducing CaSR-enhanced, neurotrophin-independent axon growth from early nodose neurons and that GSK3 signalling plays a major role in transducing the growth-enhancing effects of CaSR activation on BDNF-promoted axonal growth from older BDNF-dependent nodose neurons.

4.2 Results

4.2.1 Effects of PI3-kinase, GSK3 and MEK1/2 inhibitors on CaSR-promoted BDNF-independent axon growth from stage 20 nodose neurons

To begin to investigate the signalling pathways that transduce activation of the CaSR into enhanced neurotrophic factor-independent axon growth, I cultured stage 20 nodose neurons at low density on laminin-coated tissue culture dishes, in BDNF-free medium containing 0.7 mM $Ca^{2+}$and 1pM of the potent CaSR agonist Gd^{3+} in the presence and

absence of pharmacological inhibitors of PI3-kinase, GSK3 and MEK1/2. Measurement of axon lengths 24 hours after plating confirmed the experimental results presented in Chapter 3 that 1pM Gd^{3+} substantially increased axon growth from early nodose neurons incubated in medium containing 0.7 mM Ca^{2+} (Fig. 4.1A). This Gd^{3+}-enhanced axon growth was significantly decreased by all three inhibitors ($p< 0.0001$ in all cases, ANOVA with Fisher's ad hoc), with the greatest decrease being brought about by the PI3-kinase inhibitor LY294002, where the axons were 70% shorter (Fig. 4.1C). the MEK1/2 inhibitor PD98059 caused a 50% reduction in axon length (Fig. 1C), and the GSK3 inhibitor Bio caused a 30% reduction in axon length (Figs. 4.1B and C). Neurons counts carried out 24 hours after plating revealed there were no significant differences in survival under all experimental conditions at this time (Fig. 4.2). These results suggest that PI3-kinase signalling plays a major role in CaSR-enhanced, neurotrophin-independent axon growth from stage 20 nodose neurons, with lesser roles played by MEK1/2-ERK1/2 signalling and GSK3 signalling. These results also demonstrate that neither PI3-kinase, GSK3 nor MEK1/2 are required for neurotrophin-independent survival at this early stage of development.

I carried out additional experiments to ascertain whether inhibition of PI3-kinase, GSK3 and MEK1/2 had any effect on the low level of axonal growth from stage 20 nodose neurons grown in BDNF-free medium containing 0.7 mM Ca^{2+} without the CaSR agonist Gd^{3+}. Measurement of axon lengths 24 hours after plating revealed no significant differences in axon lengths between control cultures (no pharmacological inhibitors) and cultures containing either LY294002, PD98059 or Bio (Fig. 4.3B), and no significant differences in survival under these different experimental conditions (Fig. 4.3A). While these results suggest that neither PI3-kinase, GSK3 nor MEK1/2 signalling are required for the very limited axonal growth that occurs at minimal levels of CaSR activation, this conclusion is subject to the caveat that is more difficult to clearly observe an effect on axon growth when the axons are so short. However, these results further confirm that activated PI3-kinase, GSK3 and MEK1/2 are not required for neurotrophin-independent survival.

4.2.2 Effects of expressing PI3-kinase mutant proteins on CaSR-promoted, BDNF-independent axon growth from stage 20 nodose neurons

Because of the clear and pronounced effects of the PI3-kinase inhibitor LY294002 on early CaSR-promoted, neurotrophin independent axon growth, I carried out experiments to confirm the role of PI3-kinase by an alternative approach. I co-transfected stage 20 nodose neurons with a YFP expression plasmid together with a plasmid expressing either a

constitutively active PI3-Kinase or a dominant-negative PI3-Kinase. Control cultures were co-transfected with the YFP plasmid and an empty pcDNA3.1 expression plasmid. The neurons were incubated in medium containing 1.3mM Ca^{2+}, a $[Ca^{2+}]_o$ that leads to significant activation of the chick CaSR and enhanced axon growth (Fig. 3.4 B). YFP expressing co-transfected neurons were counted after 24 hours and 48 hours in culture, and the percentage survival of YFP expressing neurons at 48 hours was calculated relative to the number of YFP-positive neurons counted at 24 hours. This protocol for assessing the survival of co-transfected neurons was adopted because YFP is not robustly expressed in transfected cultures until 24 hrs. YFP expressing neurons were imaged 24 hours after plating for measurements of axonal length.

Expression of constitutively active PI3-Kinase did not significantly alter the survival of stage 20 nodose neurons compared to control transfected cultures (Fig. 4.4A) but significantly increased mean total axon length by approximately 30% (Fig. 4.4B, $p< 0.01$, ANOVA with Fisher's ad hoc). Surprisingly, expression of dominant-negative PI3-Kinase significantly enhanced the survival of stage 20 nodose neurons by 25% compared to control transfected cultures ($p< 0.001$, ANOVA with Fisher's ad hoc). However, in accordance with the data obtained with LY294002, expression of dominant negative PI3-kinase reduced mean total axon length compared to control transfected cultures by approximately 60% (Fig. 4.4B), a reduction that was highly statistically significant ($p< 0.0001$, ANOVA with Fisher's ad hoc). Although the length of transfected neurons is less than non-transfected neurons, as noted in Chapter 3, these data nonetheless support the conclusion of the pharmacological inhibitor experiments that PI3-Kinase plays an important role in transducing the effects of activated CaSR into enhanced neurotrophin-independent axon growth from early nodose neurons, but is not required for neurotrophin-independent neuronal survival.

As in the pharmacological inhibitor experiments reported above, I carried out additional experiments to ascertain if expression of mutant PI3-kinase proteins affects axonal growth from stage 20 nodose neurons grown in BDNF-free medium containing 0.7 mM Ca^{2+}. Measurement of axon lengths 24 hours after plating revealed no significant differences in survival or axon lengths between control-transfected neurons and neurons transfected with plasmids expressing either constitutively active PI3-Kinase or a dominant-negative PI3-Kinase (Fig. 4.5). These results suggest that PI3-kinase activity does not affect CaSR-independent axon growth from early, stage 20 nodose neurons.

4.2.3 CaSR activation in stage 20 nodose neuron results in Akt phosphorylation

Akt is a major downstream target of activated PI3-Kinase, and has previously been shown to play a role in mediating both neurotrophic factor-promoted neuronal survival (Alonzi et al., 2001; Andjelkovic et al., 1998; Ashcroft et al., 1999) and axon elongation (Yoshimura et al., 2005). To provide further evidence for the participation of PI3-kinase in CaSR-promoted axon growth from early neurotrophin-independent axon growth, I investigated whether activation of the CaSR in stage 20 nodose neurons leads to Akt phosphorylation. Stage 20 nodose neurons were cultured in the absence of BDNF in medium containing 0.7mM Ca^{2+} for 4 hours prior to stimulation with 1pM Gd^{3+}. The cells were lysed 5, 10, 30 and 60 minutes after stimulation by Gd^{3+}, and extracted proteins were run on denaturing gels and Western blotted to membranes. Control (non-stimulated) and BDNF-treated cultures were lysed alongside Gd^{3+}-stimulated neurons at the 5 minute time point. The upper panel of figure 4.6A shows a representative Western Blot of cell lysates probed with an antibody against phospho-Akt, and the lower panel shows the same filter after stripping and reprobing with an antibody against tubulin to allow normalisation of the phospho-Akt signal to protein concentration within the lysate. Addition of 1pM Gd^{3+} resulted in a rapid, transient increase in the levels of phospho-Akt that returned to basal levels within 30 minutes after the addition of Gd^{3+}. Scanning and quantitative analysis of ECL films, followed by normalization of phospho-Akt levels to tubulin, revealed that the addition of 1pM Gd^{3+} to cultures increased the levels of phospho-Akt by some 30% compared to control cultures 10 mins after Gd^{3+} treatment (Fig. 4.6B). BDNF had no apparent effect on phospho-Akt levels. These findings suggest that Gd^{3+}-induced CaSR activation leads to Akt phosphorylation, which is consistent with PI3-Kinase activation as a result of CaSR activation.

4.2.4 Effects of PI3-kinase, GSK3 and MEK1/2 inhibitors on CaSR-promoted, BDNF-independent axon growth from stage 23 nodose neurons

In addition to studying the effects of pharmacological inhibitors on CaSR-promoted neurite growth from nodose neurons during the earliest stages of neurotrophin-independent axon growth at stage 20, I also studied the effects of these reagents at stage 23, a later time point in the period of neurotrophin independence. These neurons were cultured in BDNF-free medium containing 0.7 mM $Ca^{2+}$and 1pM of the potent CaSR agonist Gd^{3+} in the presence and absence of pharmacological inhibitors of PI3-kinase, GSK3 and MEK1/2. Measurement of axon lengths after 24 hours showed that, as in the case of stage 20 neurons, 1pM Gd^{3+} caused a greater than five-fold increase in axon length compared with non-stimulated control

neurons (Fig. 4.7A), and all three inhibitors caused highly significant reductions in the length of Gd^{3+}-stimulated neurons ($p< 0.0001$ in all cases, ANOVA with Fisher's ad hoc). As for stage 20 neurons, the greatest decrease in Gd^{3+}-stimulated axon growth was brought about by the PI3-kinase inhibitor LY294002, although the reduction was even greater than at stage 20 (90% shorter and less than control cultures containing BDNF alone, Fig. 4.7C). The MEK1/2 inhibitor PD98059 caused a similar reduction in axon length to that observed in stage 20 neurons (Fig. 4.7C). However, in marked contrast to stage 20 neurons where the GSK3 inhibitor Bio caused a 30% reduction in axon length, Bio caused an 80% reduction in axon length at stage 23 (Fig. 4.7B). As in stage 20 cultures, neuron counts carried out 24 hours after plating revealed there were no significant differences in survival under all experimental conditions at stage 23 (Fig. 4.8). These results suggest that both PI3-kinase signalling and GSK3 signalling play major roles in CaSR-enhanced, neurotrophin-independent axon growth from stage 23 nodose neurons, with a lesser role played by MEK1/2-ERK1/2 signalling. These results also demonstrate that neither PI3-kinase, GSK3 nor MEK1/2 are required for neurotrophin-independent survival at this stage of development.

4.2.5 Effects of PI3-kinase, GSK3 and MEK1/2 inhibitors on CaSR-promoted, BDNF-dependent axon growth from stage 27 nodose neurons

The data in chapter 3 clearly demonstrates that both BDNF and elevated $[Ca^{2+}]_o$ promote axon extension from stage 27 and older nodose neurons, although CaSR activation by its physiological ligand does not appear to promote significant axon elongation in the absence of BDNF (Figs. 3.12 and 3.13). The identity of the intracellular signalling pathways that transduce CaSR and trkB activation into enhanced axon outgrowth from nodose neurons at these later developmental stages were investigated using a similar experimental approach to that used to investigate BDNF-independent CaSR signalling in relation to enhanced *de novo* axon growth in sections 4.2.1 and 4.2.4. At stage 27, nodose neurons were cultured for 24 hours in BDNF-supplemented medium containing 0.7 mM $Ca^{2+}$and 1pM of the potent CaSR agonist Gd^{3+} in the presence and absence of pharmacological inhibitors of PI3-kinase, GSK3 and MEK1/2. Measurement of axon lengths after 24 hours showed that 1pM Gd^{3+} caused an almost five-fold increase in axon length compared with neurons grown with BDNF alone (Fig. 4.9A). In marked contrast to CaSR-promoted, BDNF-independent axon growth from stage 23 neurons, CaSR-promoted, BDNF-dependent axon growth from stage 27 neurons was not significantly reduced by either the PI3-kinase inhibitor LY294002 or MEK1/2 inhibitor PD98059 (Fig. 4.9C). However, the inhibition of GSK3 by Bio was able to reduce the extent

of BDNF- and Gd^{3+}- enhanced axon growth from stage 27 nodose neurons to less than that seen in cultures without Gd^{3+} (Fig 4.9B). Neuron counts carried out 24 hours after plating revealed there were no significant differences in survival under all experimental conditions at this time (Fig 4.10). These results suggest that at stage 27, when maximal axonal growth is dependent on both BDNF and activation of the CaSR, GSK3 plays a critical role in axonal extension, but that neither PI3-kinase nor MEK1/2 are required.

4.2.6 Effects of PI3-kinase, GSK3 and MEK1/2 inhibitors on CaSR-promoted, BDNF-dependent axon growth from stage 33 nodose neurons

By stage 33, BDNF is required to promote the survival of the majority of nodose neurons over a 24 hour culture period (Fig. 4.11). Since most neurons die in the absence of BDNF, cultures for assessing the extent of axon growth in the absence of BDNF were supplemented with the pan-caspase inhibitor, Boc-D-FMK. At a concentration of 10μM, this caspase inhibitor was as effective as BDNF in supporting the survival of stage 33 nodose neurons over a 24 hour culture period in medium containing 1.3 mM Ca^{2+} (Fig. 10). Neither LY294002, Bio nor PD98059 affected the survival of stage 33 nodose neurons incubated for 24 hours in BDNF-supplemented medium (Figs. 4.11A, B and C, respectively). There was negligible axon growth from stage 33 neurons cultured in the absence of BDNF, and BDNF-promoted axon growth in medium containing 1.3 mM Ca^{2+} was completely unaffected by either LY294002 or PD98059 (Figs. 4.12A and C). However, as in stage 27 cultures, the GSK3 inhibitor Bio totally abrogated BDNF-promoted axon growth when neurons were cultured in medium that activated the CaSR (Fig. 4.12B). These results suggest that BDNF-promoted axon growth from neurons grown in medium containing sufficient Ca^{2+} to activate the CaSR is critically dependent on GSK3 signalling.

Essentially similar results were obtained when stage 33 neurons were cultured in BDNF-supplemented medium containing 0.7 mM $Ca^{2+}$and 1pM Gd^{3+}. In these cultures, Bio virtually eliminated BDNF- and activated CaSR-promoted axon growth and neither LY294002 nor PD98059 reduced BDNF- and activated CaSR-promoted axon growth (Fig. 4.13B and C). Paradoxically, LY294002 promoted a consistent and significant increase in axon length in cultures supplemented with BDNF and 1pM Gd^{3+} ($p< 0.0001$, ANOVA with Fisher's ad hoc). Whereas neither Bio, LY294002 nor PD98059 affected the survival of stage 33 neurons cultured for 24 hours in BDNF-supplemented medium containing 0.7 mM $Ca^{2+}$and 1pM Gd^{3+}, the percent survival in BDNF-supplemented medium containing 0.7 mM $Ca^{2+}$and 1pM Gd^{3+} was significantly greater than in BDNF-supplemented medium containing

0.7 mM Ca^{2+} without Gd^{3+} (Fig. 4.14, $p< 0.01$, ANOVA with Fisher's ad hoc). This latter observation raises the possibility that activation of the CaSR might contribute to the survival of nodose neurons at this stage of development.

To further examine the role of GSK3 signalling in BDNF-promoted axon outgrowth from older nodose neurons cultured in medium containing 1.3 mM $[Ca^{2+}]_o$, I co-transfected stage 30 nodose neurons with a YFP expression plasmid together with a plasmid expressing either wild type GSK3 or dominant-negative GSK3. Control cultures were co-transfected with the YFP plasmid and an empty pcDNA3.1 expression plasmid. All cultures were supplemented with 10 ng/ml BDNF. YFP expressing co-transfected neurons were counted after 24 hours and 48 hours in culture, and the percentage survival of YFP expressing neurons at 48 hours was calculated relative to the number of YFP-positive neurons counted at 24 hours.

Neither over-expression of wild type GSK3 nor expression of dominant-negative GSK3 significantly affected the survival of stage 30 nodose neurons after 48 hours in culture compared to control transfected neurons (Fig. 4.15A). Measurements of axon length 24 hours after transfection revealed no significant differences between neurons over-expressing wild type GSK3 and control transfected neurons. However, expression of dominant-negative GSK3 significantly decreased mean total axon length by approximately 60% compared to control transfected neurons (Fig. 4.15B, $p< 0.0001$, ANOVA with Fisher's ad hoc). These results support the importance of GSK in BDNF-promoted axon growth from BDNF-dependent nodose neurons grown in medium containing physiological levels of extracellular calcium.

To further prove a role for GSK3 in transducing CaSR activation in the presence of BDNF into enhanced axon growth, I briefly exposed stage 30 nodose neurons, that had been cultured for 4 hrs in medium containing 0.7mM Ca^{2+}, to the specific and potent CaSR agonist, Calhex, that has only recently become commercially available. After 5, 15 and 30 minute time points, I lysed the neurons and prepared the lysate for Western blotting. As discussed in chapter1, the activity of GSK3 is regulated either by serine phosphorylation on residue 9 of GSK3β or residue 21 of GSK3α, or by tyrosine phosphorylation of residue 216 of GSK3β or residue 279 of GSK3α.. Serine phosphorylation leads to inactivation of GSK3 proteins, whereas tyrosine phosphorylation promotes GSK3α and β activity (Jope and Johnson, 2004). I therefore probed Western blot filters with antibodies against either serine phosphorylated GSK3α/β or tyrosine phosphorylated GSK3α/β. Filters were also stripped and re-probed for tubulin to ensure lysates contained equal quantities of protein. Figure 4.16A demonstrates that

Calhex induced tyrosine phosphorylation of GSK3α/β within 5 minutes and this enhanced tyrosine phosphorylation persisted for at least 30 minutes. In contrast, Calhex did not induce serine phosphorylation of GSK3α/β (Fig. 4.16B). This data suggests that tyrosine phosphorylation of GSK3 is an important step in the signal transduction pathway that connects CaSR activation to enhanced axon growth.

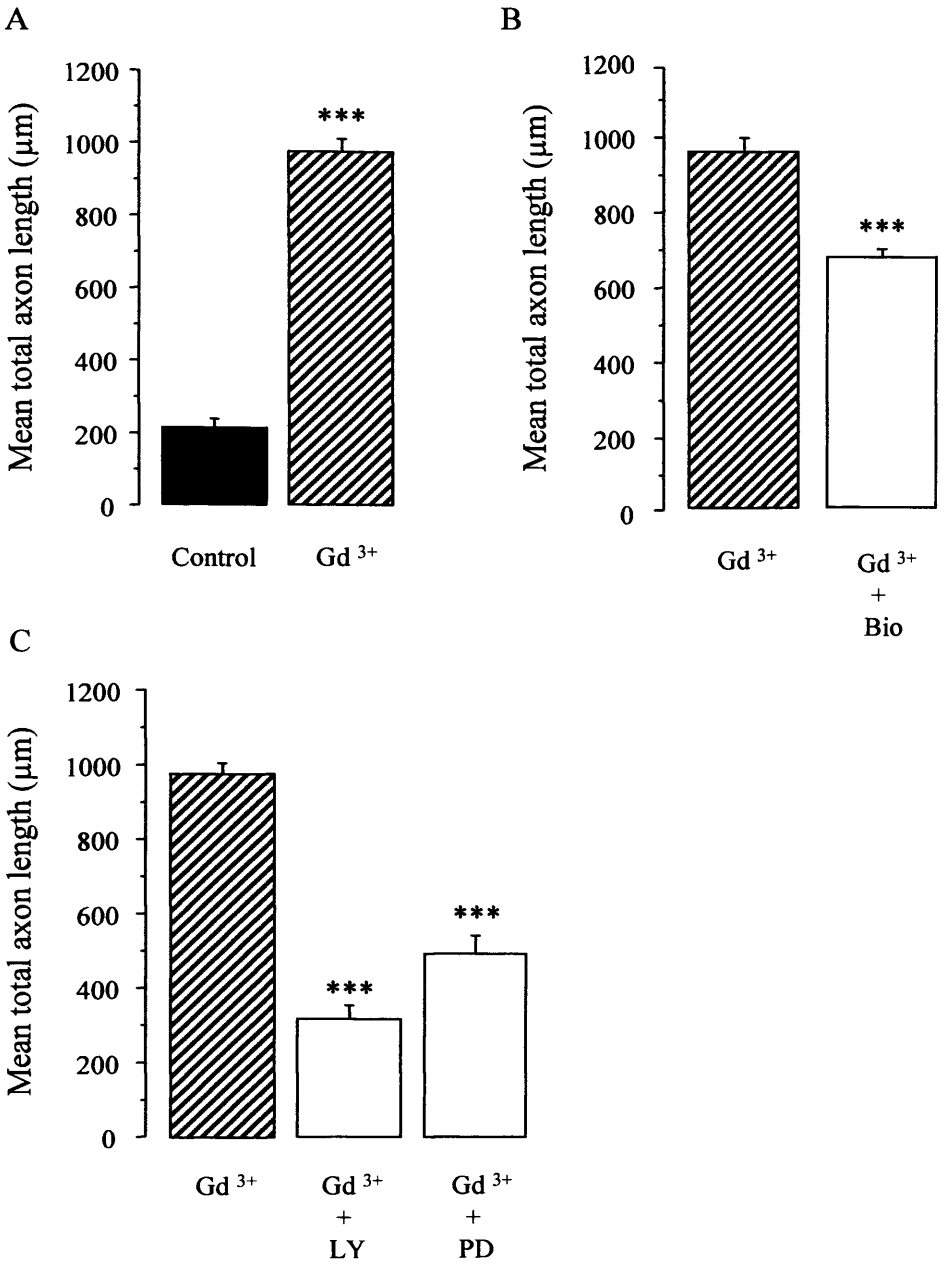

Figure 4.1: The effects of GSK3, PI3-Kinase and MEK1/2 inhibitors on axon outgrowth from stage 20 nodose neurons cultured in media containing a low calcium concentration plus 1pM Gd^{3+}.

Stage 20 nodose neurons were cultured without BDNF, in media containing 0.7mMCa^{2+}. With the exception of control cultures, culture media was supplemented with either 1pM Gd^{3+} alone or 1pM Gd^{3+} plus either 10µM of the GSK inhibitor, Bio, 50µM of the PI3-Kinase inhibitor, LY294002 or 10 µM of the MEK1/2 inhibitor, PD98059. Fluorescent images for analysis of process growth were captured after a 24 hr culture period.

A: 1pM Gd^{3+} increased mean total axon length in media containing a low calcium concentration.

B: Bio reduced mean total axon length in the presence of 1pM Gd^{3+}.

C: In the presence of 1pM Gd^{3+}, LY294002 and PD98059 decreased mean total axon length compared to neurons cultured with Gd^{3+} alone.

n = 150 neurons per condition from 3 different experiments. Data presented are the mean ± SEM. *** denotes $p < 0.0001$ after statistical comparisons with control (A) or Gd $^{3+}$ (B and C) (ANOVA with Fisher's ad hoc).

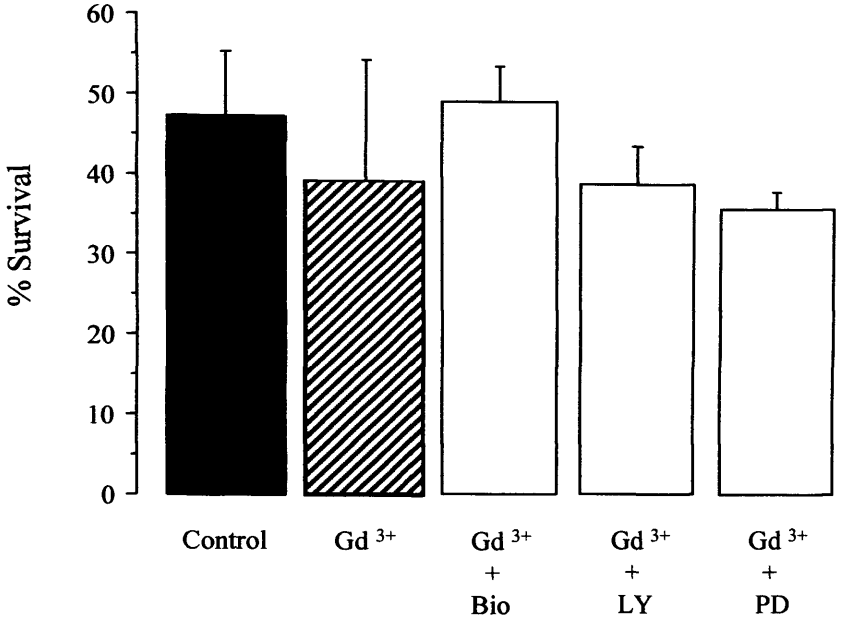

Figure 4.2: The effects of GSK3, PI3-Kinase and MEK1/2 inhibitors on the survival of stage 20 nodose neurons cultured in media containing a low calcium concentration plus 1pM Gd^{3+}.
Stage 20 nodose neurons were cultured for 24 hours, in the absence of BDNF, in media containing 0.7mMCa^{2+}. With the exception of control cultures, culture media was supplemented with either 1pM Gd^{3+} alone or 1pM Gd^{3+} plus either 10μM of the GSK inhibitor, Bio, 50μM of the PI3-Kinase inhibitor, LY204002 or 10 μM of the MEK1/2 inhibitor, PD98059. Neurons were counted 3 hrs after plating and after 24 hrs in culture, allowing percentage neuronal survival at 24 hrs to be determined. There were no significant differences in survival between control cultures and cultures supplemented with Gd^{3+} alone or Gd^{3+} plus either Bio, LY or PD. Data are the mean +/- SEM from three separate cultures containing triplicate dishes for each condition.

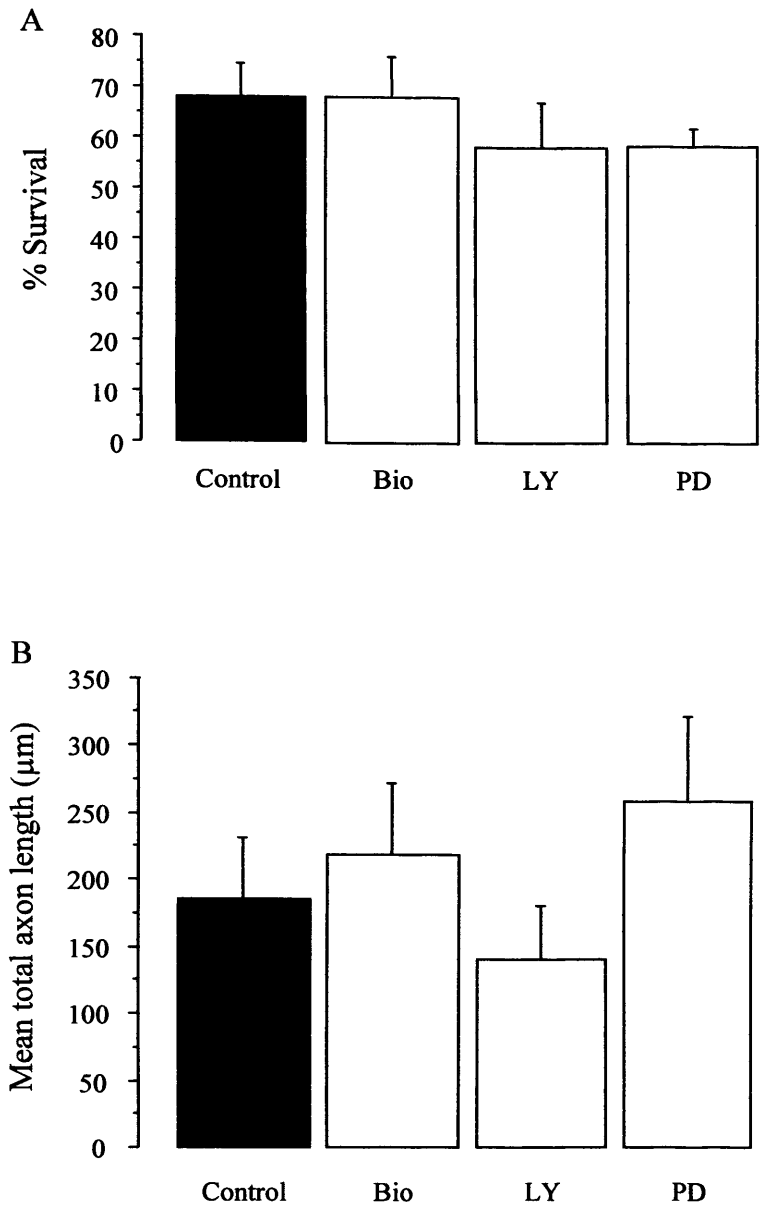

Figure 4.3: The effects of GSK3, PI3-Kinase and MEK1/2 inhibitors on the survival of and axon outgrowth from stage 20 nodose neurons cultured in media containing 0.7mM $[Ca^{2+}]_0$.
Stage 20 nodose neurons were cultured for 24 hours, in the absence of BDNF, in media containing 0.7mM $[Ca^{2+}]_0$. With the exception of control cultures, culture media was supplemented with either 10µM of the GSK inhibitor, Bio, 50µM of the PI3-Kinase inhibitor, LY294002 or 10 µM of the MEK1/2 inhibitor, PD98059. Neurons were counted 3 hrs after plating and after 24 hrs in culture, allowing percentage neuronal survival at 24 hrs to be determined. Fluorescent images of surviving neurons were also captured after 24hrs in culture, so that the extent of axon elongation could be determined.

A: Percentage neuronal survival at 24 hours. There were no significant differences in survival between any of the culture conditions. Data are the mean +/- SEM from three separate cultures containing triplicate dishes for each condition.

B: Average total axon length of neurons cultured in each condition. Bio, LY or PD did not effect neuritic process outgrowth in the absence of Gd^{3+}. n= 150 neurons per condition from 3 different experiments. Data are presented as the mean ± SEM.

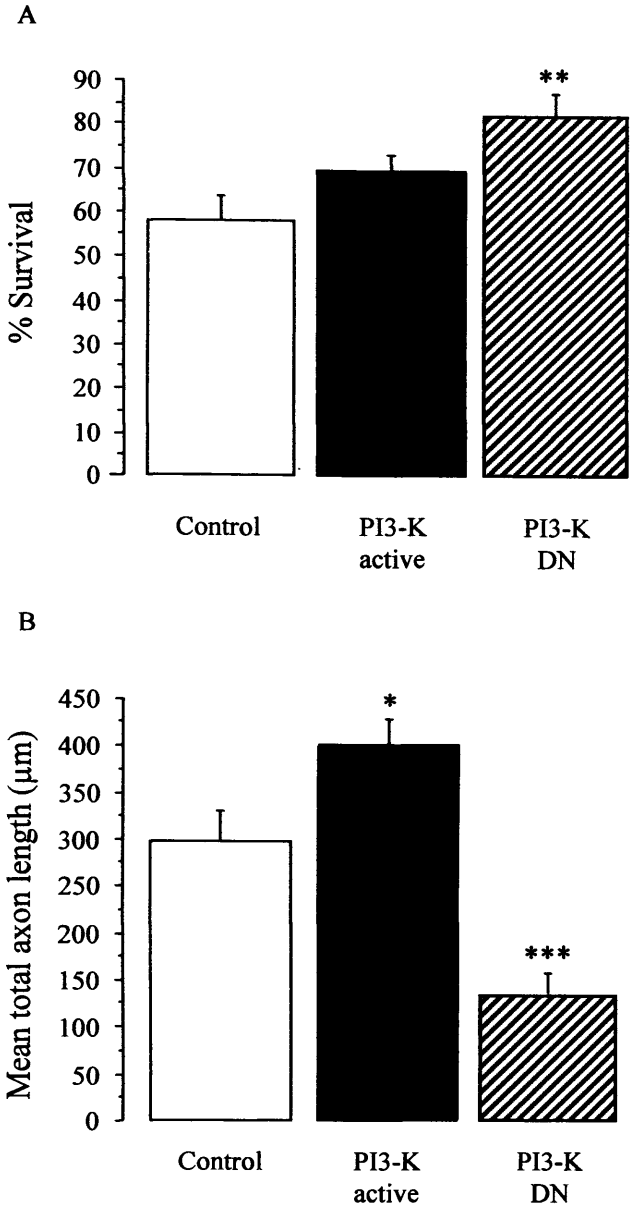

Figure 4.4: The effects of modulating PI3-Kinase signalling on the survival of and extent of axon outgrowth from cultured stage 20 nodose neurons cultured in media containing 1.3mM $[Ca^{2+}]_0$.

Stage 20 nodose neurons were cultured in the absence of neurotrophins, in media containing 1.3mM $[Ca^{2+}]_0$. Electroporation was used to co-transfect neurons with the expression vector pcDNA3.1 containing cDNA encoding YFP together with either empty pcDNA3.1 (control), pcDNA3.1 containing the cDNA encoding constitutively active PI3-Kinase (active) or pcDNA3.1 containing the cDNA encoding a dominant negative PI3-Kinase (DN). Co-transfected YFP expressing neurons were counted 24 hrs after plating and after 48 hrs in culture, allowing percentage neuronal survival at 48 hrs to be determined. Fluorescent images of YFP expressing neurons for subsequent analysis of process growth were captured after a 24 hr culture period.

A: Over-expression of constitutively active PI3-Kinase did not significantly effect the survival of stage 20 nodose neurons. In contrast, over-expression of dominant-negative PI3-Kinase signficantly increased the survival of cultured stage 20 nodose neurons compared to control cultures .

B: Over-expression of dominant-negative PI3-Kinase significantly decreased mean total axon length of stage 20 nodose neurons compared to control cultures, whereas over-expression of constitutively active PI3-Kinase increased the extent of axon outgrowth.

n = 90 neurons per condition from 3 different experiments. Data presented are the mean ± SEM. *** denotes $p < 0.0001$, ** denotes $p < 0.001$ and * denotes $p < 0.01$ after statistical comparisons with control (ANOVA with Fisher's ad hoc).

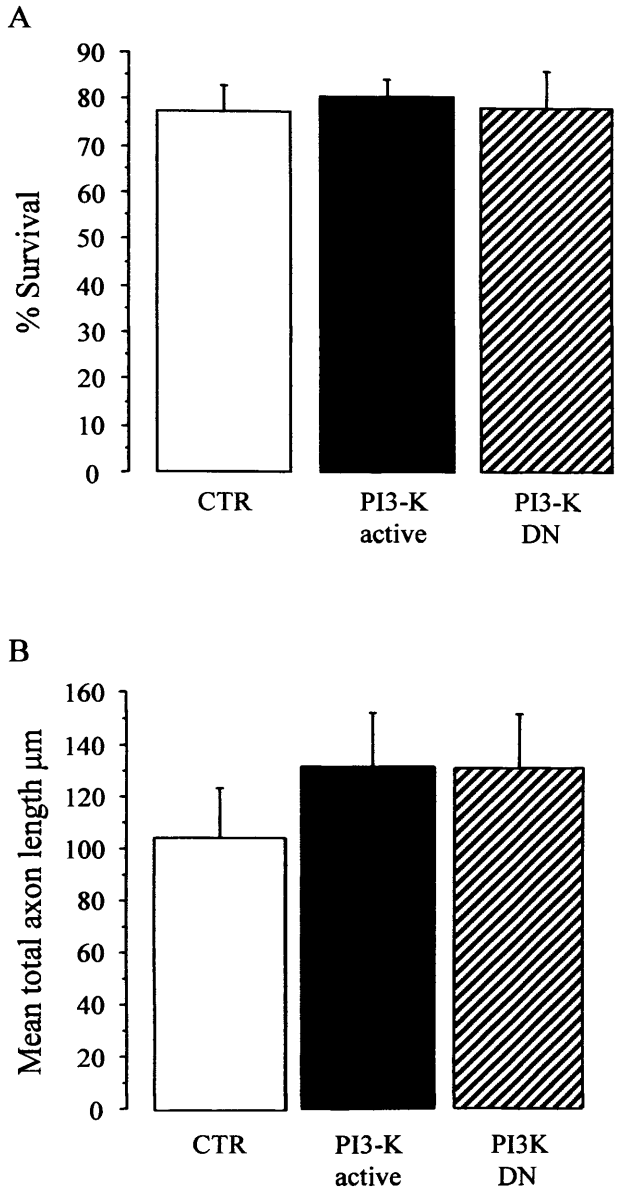

Figure 4.5: The effects of modulating PI3-Kinase signalling on the survival of and extent of axon outgrowth from stage 20 nodose neurons cultured in conditions that minimally activate the CaSR.
Stage 20 nodose neurons were cultured in the absence of neurotrophins, in media containing 0.7mM $[Ca^{2+}]_0$. Electroporation was used to co-transfect neurons with the expression vector pcDNA3.1 containing cDNA encoding YFP together with either empty pcDNA3.1 (control), pcDNA3.1 containing the cDNA encoding constitutively active PI3-Kinase (active) or pcDNA3.1 containing the cDNA encoding a dominant negative PI3-Kinase (DN). Co-transfected YFP expressing neurons were counted 24 hrs after plating and after 48 hrs in culture, allowing percentage neuronal survival at 48 hrs to be determined. Fluorescent images of YFP expressing neurons for subsequent analysis of process growth were captured after a 24 hr culture period.

A: Over-expression of constitutively active PI3-Kinase or dominant-negative PI3-Kinase did not alter the survival of stage 20 nodose neurons compared to control cultures .

B: Over-expression of constitutively active PI3-Kinase or dominant-negative PI3-Kinase did not alter the mean total length of axons projecting from stage 20 nodose neurons compared to control cultures.

n = 90 neurons per condition from 3 different experiments. Data presented are the mean ± SEM.

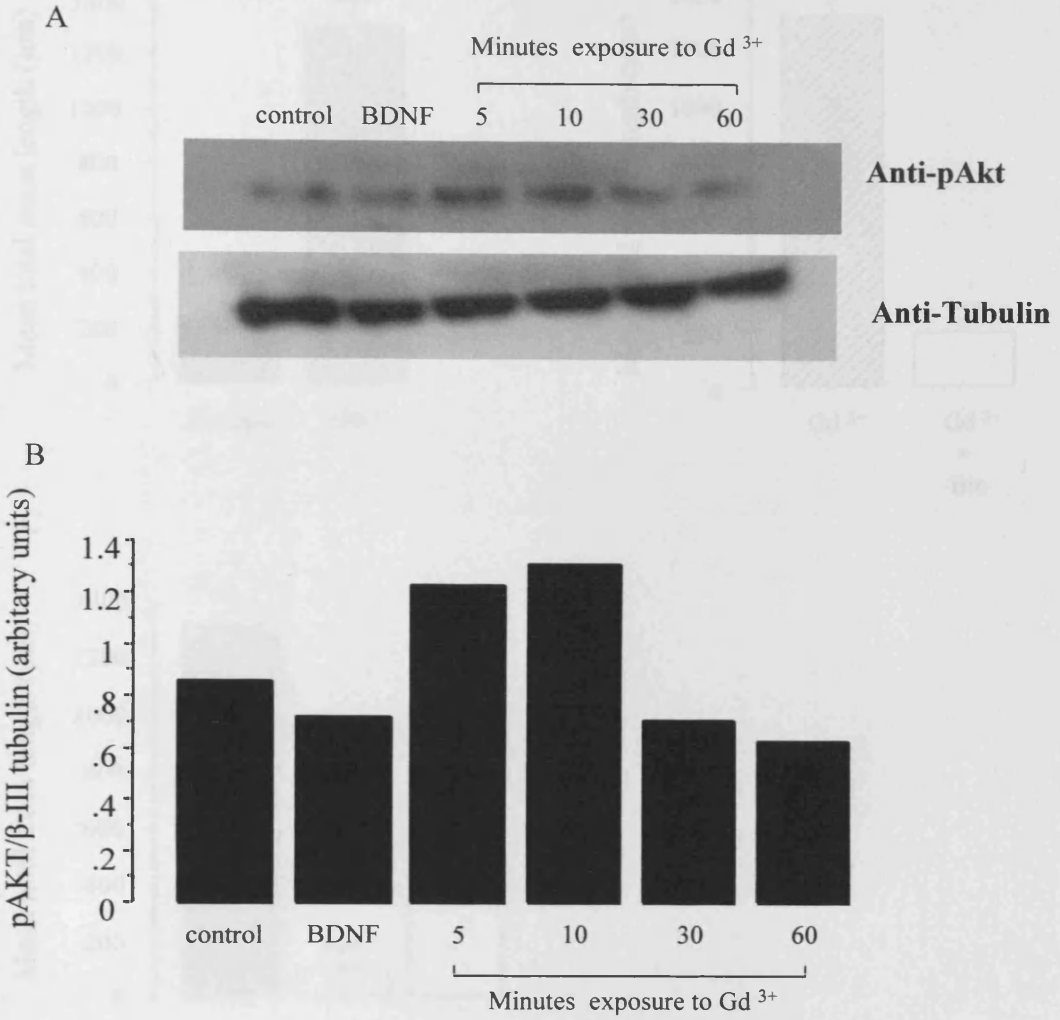

Figure 4.6: Gd^{3+} rapidly and transiently phosphorylates Akt in stage 20 nodose neurons cultured in media containing a low concentration of calcium.

Stage 20 nodose neurons were cultured in media containing 0.7mM $[Ca^{2+}]_0$ for 4 hrs. With the exception of control and BDNF only cultures, neurons were stimulated by the addition of 1pM Gd^{3+}. Cells treated with Gd^{3+} were lysed, and the lysate prepared for western blotting, either 5, 10, 30 or 60 minutes after stimulation. Control and BDNF only cultures were lysed alongside the cultures for the 5 minute Gd^{3+} stimulation time point.

A: Western blots demonstrating that increased levels of phosporylated Akt were present in stage 20 nodose neurons following 5 and 10 minute exposure to Gd^{3+}. Phosphorylated Akt appeared to return to basal levels within 30 minutes of Gd^{3+} treatment. Filters were re-probed with an antibody against β-III tubulin to allow normalization and quantification of the phospho-Akt signal.

B: Graphical representation of the normalised levels of phospo-Akt following densitometric analysis of the western blots shown in A. Increased levels of phosp-Akt, a known target for activated PI3-Kinase, after Gd^{3+} stimulation raises the possibility that PI3-Kinase may exert neuritic outgrowth promoting activity at least partially via activation of Akt.

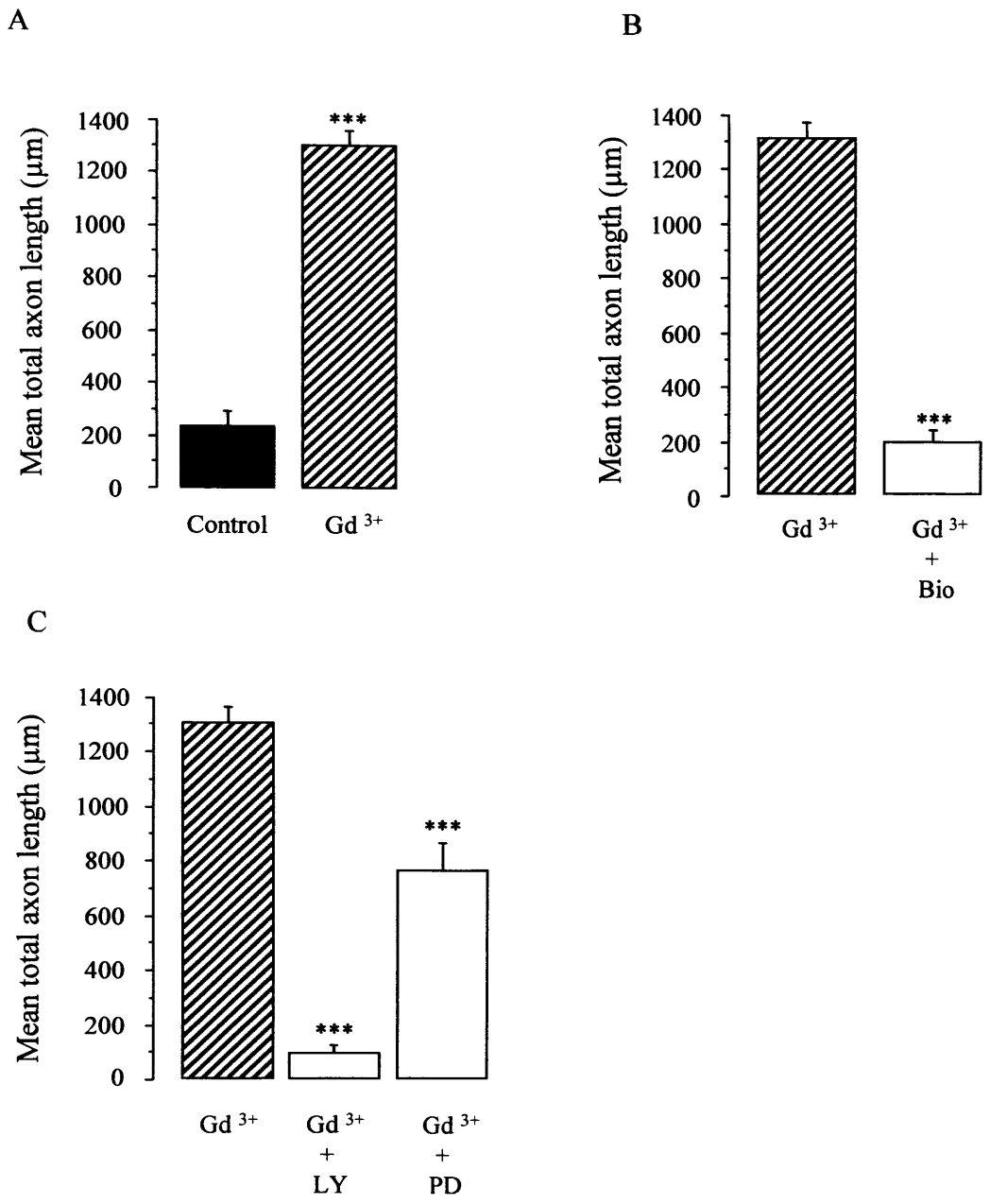

Figure 4.7: The effects of GSK3, PI3-Kinase and MEK1/2 inhibitors on the extent of axon outgrowth from stage 23 nodose neurons cultured in media containing a low calcium concentration in the presence of 1pM Gd^{3+}.

Stage 23 nodose neurons were cultured without BDNF in media containing 0.7mM $[Ca^{2+}]_0$With the exception of control cultures, culture media was supplemented with either 1pM Gd^{3+} alone or 1pM Gd^{3+} plus either 10µM of the GSK inhibitor, Bio, 50µM of the PI3-Kinase inhibitor, LY294002 or 10 µM of the MEK1/2 inhibitor, PD98059. Fluorescent images for analysis of process growth were captured after a 24 hr culture period.

A: 1pM Gd^{3+} increased mean total neurite length in media containing a low calcium concentration.

B: Bio reduced mean total neurite growth in the presence of 1pM Gd^{3+}.

C: In the presence of Gd^{3+}, LY294002 and PD98059 decreased mean total neurite length compared to neurons cultured with Gd^{+} alone.

n = 150 neurons per condition from 3 different experiments. Data presented are the mean ± SEM. *** denotes $p < 0.0001$ after statistical comparisons with control (A) or Gd^{3+} (B and C) (ANOVA with Fisher's ad hoc).

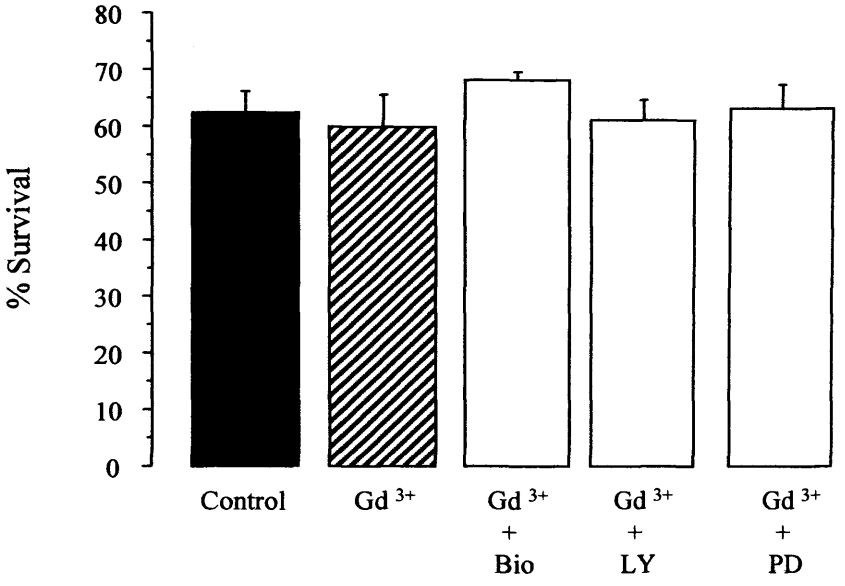

Figure 4.8: The effects of GSK3, PI3-Kinase and MEK1/2 inhibitors on the survival of stage 23 nodose neurons cultured in media containing a low calcium concentration in the presence of 1pM Gd^{3+}.

Stage 23 nodose neurons were cultured for 24 hours, in the absence of BDNF, in media containing 0.7mM $[Ca^{2+}]_0$. With the exception of control cultures, culture media was supplemented with either 1pM Gd^{3+} alone or 1pM Gd^{3+} plus either 10μM of the GSK inhibitor, Bio, 50μM of the PI3-Kinase inhibitor, LY294002 or 10 μM of the MEK1/2 inhibitor, PD98059. Neurons were counted 3 hrs after plating and after 24 hrs in culture, allowing percentage neuronal survival at 24 hrs to be determined. There were no significant differences in survival between control cultures and cultures supplemented with Gd^{3+} alone or Gd^{3+} plus either Bio, LY or PD. Data are the mean +/- SEM from three separate cultures containing triplicate dishes for each condition.

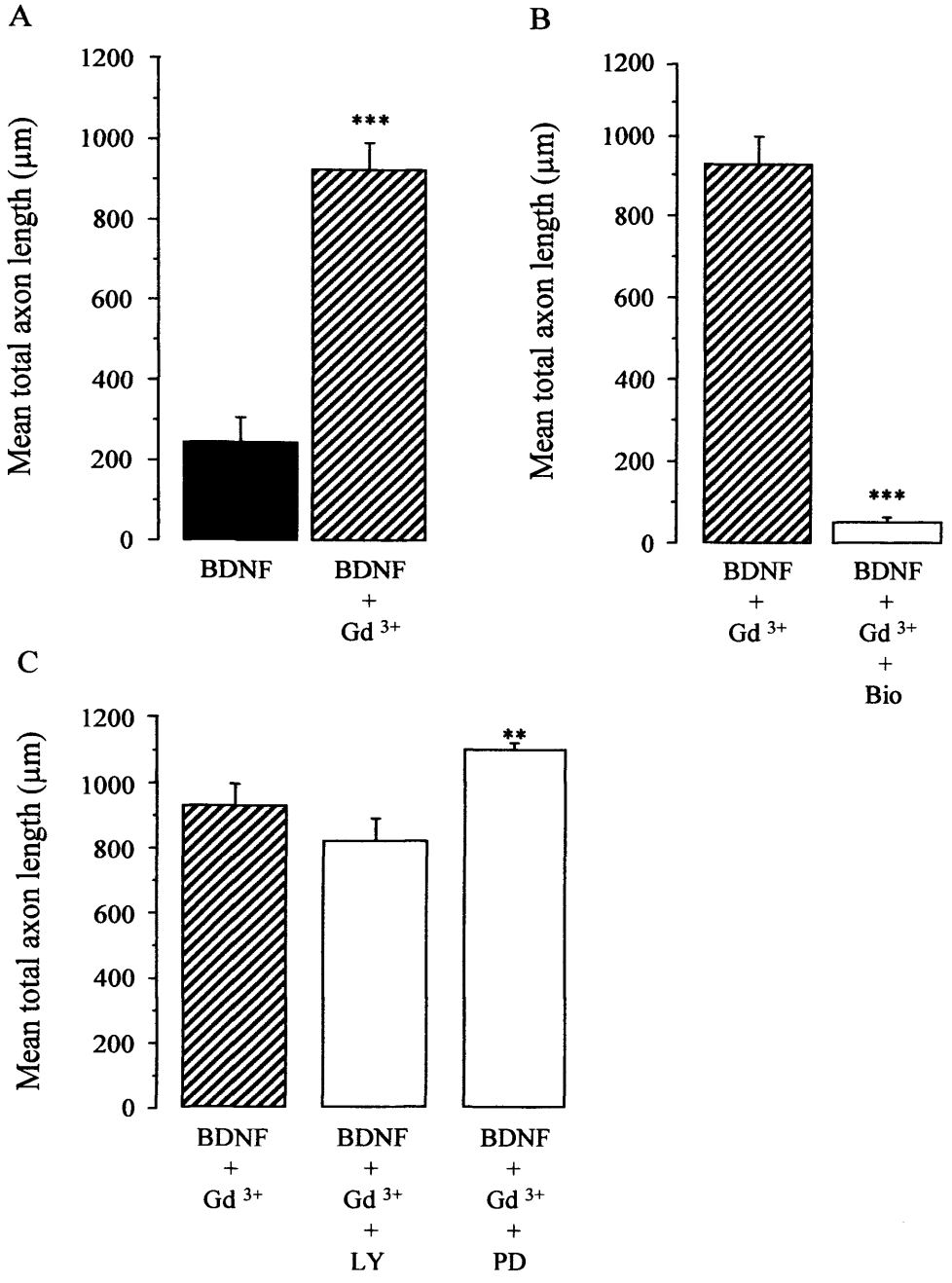

Figure 4.9: The effects of GSK3, PI3-Kinase and MEK1/2 inhibitors on the extent of axon outgrowth from stage 27 nodose neurons cultured in media containing a low calcium concentration in the presence of BDNF and Gd^{3+}.

Stage 27 nodose neurons were cultured with 10 ng/ml BDNF in media containing 0.7mM $[Ca^{2+}]_0$. With the exception of BDNF only cultures, culture media was supplemented with either 1pM Gd^{3+} alone or 1pM Gd^{3+} plus either 10µM of the GSK inhibitor, Bio, 50µM of the PI3-Kinase inhibitor, LY294002 or 10 µM of the MEK1/2 inhibitor, PD98059. Fluorescent images for subsequent analysis of process growth were captured after a 24 hr culture period.

A: 1pM Gd^{3+} increased mean total axon length in media containing a low calcium concentration and BDNF

B: Bio dramatically reduced mean total axon length in the presence of BDNF plus Gd^{3+}.

C: In the presence of BDNF plus Gd^{3+}, LY204002 did not effect axon outgrowth whereas PD98059 increased mean total axon length compared to neurons cultured with BDNF plus Gd^{3+} alone.

n = 150 neurons per condition from 3 different experiments. Data presented are the mean ± SEM. *** denotes $p < 0.0001$ after statistical comparisons with BDNF alone (A) or BDNF plus Gd^{3+} (B), whereas ** denotes $p < 0.001$ compared to BDNF plus Gd^{3+} (ANOVA with Fisher's ad hoc).

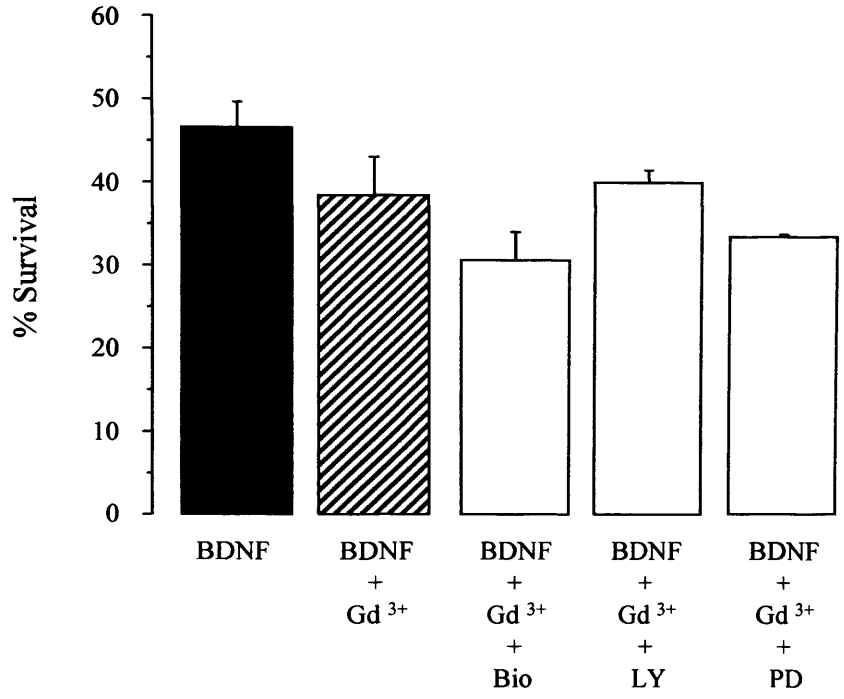

Figure 4.10: The effects of GSK3, PI3-Kinase and MEK1/2 inhibitors on the survival of stage 27 nodose neurons cultured in media containing a low calcium concentration in the presence of BDNF and 1pM Gd^{3+}.

Stage 27 nodose neurons were cultured for 24 hours, in the presence of 10 ng/ml BDNF, in media containing 0.7mM $[Ca^{2+}]_0$. With the exception of BDNF only cultures, culture media was supplemented with either 1pM Gd^{3+} alone or 1pM Gd^{3+} plus either 10μM of the GSK inhibitor, Bio, 50μM of the PI3-Kinase inhibitor, LY294002 or 10 μM of the MEK1/2 inhibitor, PD98059. Neurons were counted 3 hrs after plating and after 24 hrs in culture, allowing percentage neuronal survival at 24 hrs to be determined. There were no significant differences in survival between BDNF containing cultures and BDNF containing cultures supplemented with 1pM Gd^{3+} alone or 1pM
Gd^{3+} plus Bio, LY or PD. Data are the mean +/- SEM from three separate cultures containing triplicate dishes for each condition.

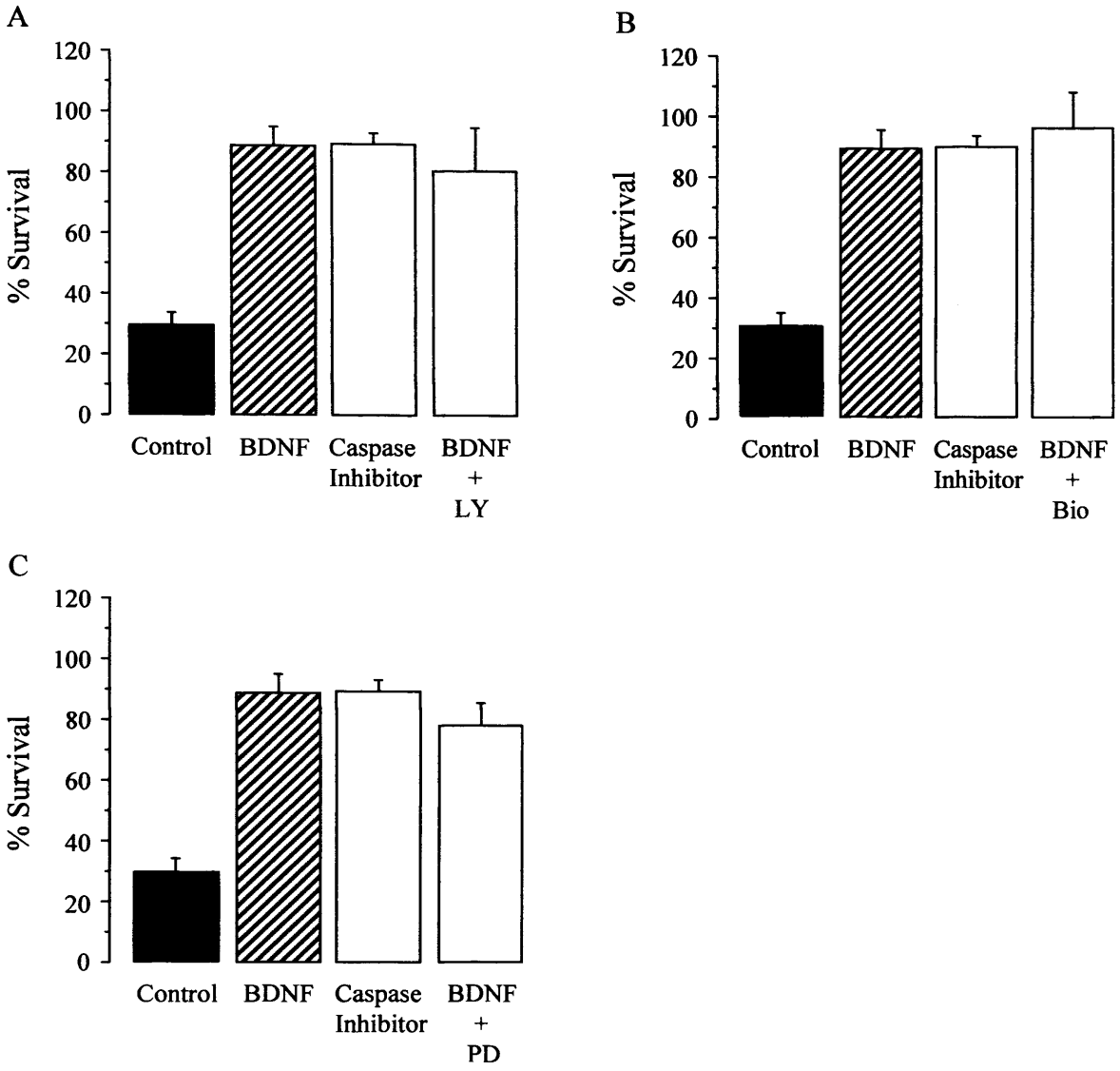

Figure 4.11: The effects of BDNF, caspase inhibitors and GSK3, PI3-Kinase and MEK1/2 inhibitors on the survival of stage 33 nodose neurons cultured in media containing 1.3mM $[Ca^{2+}]_0$.
Stage 33 nodose neurons were cultured in media containing 1.3mM$[Ca^{2+}]_0$. With the exception of control cultures, culture media was supplemented with either 10 ng/ml BDNF alone, 10μM caspase inhibitors alone, or 10 ng/ml BDNF plus either 10μM of the GSK inhibitor, Bio, 50μM of the PI3-Kinase inhibitor, LY294002 or 10 μM of the MEK1/2 inhibitor, PD98059. Neurons were counted 3 hrs after plating and after 24 hrs in culture, allowing percentage neuronal survival at 24 hrs to be determined.
A, B and C: Stage 33 nodose neurons required BDNF to support in vitro survival. In the absence of BDNF, caspase inhibitors also supported the survival of stage 33 nodose neurons over a 24 hour culture period. Neither Bio **(A)** , LY **(B)** or PD **(C)** affected the survival of stage 33 nodose neurons cultured with 10 ng/ml BDNF.
Data are the mean +/- SEM from three separate cultures containing triplicate dishes for each condition.

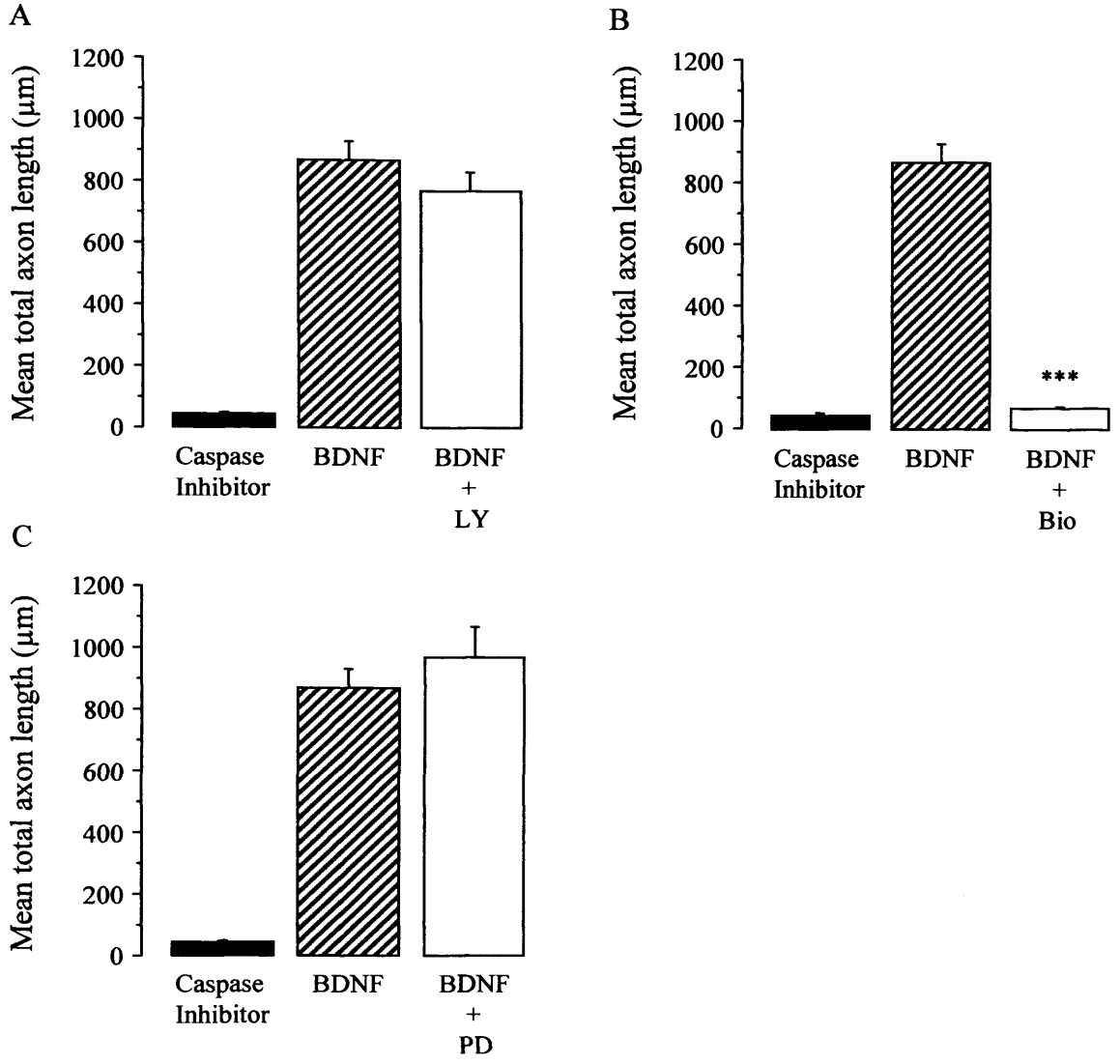

Figure 4.12: The effects of BDNF and GSK3, PI3-Kinase and MEK1/2 inhibitors on the extent of axon outgrowth from stage 33 nodose neurons cultured in media containing 1.3mM $[Ca^{2+}]_0$.

Stage 33 nodose neurons were cultured either in the presence of 10µM caspase inhibitors, or with 10 ng/ml BDNF, in media containing 1.3mM$[Ca^{2+}]_0$. Some BDNF containing cultures were supplemented with either 10µM of the GSK inhibitor, Bio, 50µM of the PI3-Kinase inhibitor, LY294002 or 10 µM of the MEK1/2 inhibitors, PD98059. Fluorescent images for subsequent analysis of axon growth were captured after a 24 hr culture period.

A, B and C: Stage 33 nodose neurons required BDNF to promote significant axon outgrowth in media containing 1.3mM Ca^{2+}

A: The GSK3 inhibitor, Bio, dramatically reduced BDNF promoted axon outgrowth.

B: The PI3-Kinase inhibitor, LY294002, and **(C)** the MEK inhibitor, PD 98059, did not significantly modulate BDNF promoted axon outgrowth from stage 33 nodose neurons cultured in media containing 1.3mM Ca^{2+}.

n = 150 neurons per condition from 3 different experiments. Data presented are the mean ± SEM. *** denotes $p < 0.0001$ after statistical comparisons with BDNF (ANOVA with Fisher's ad hoc).

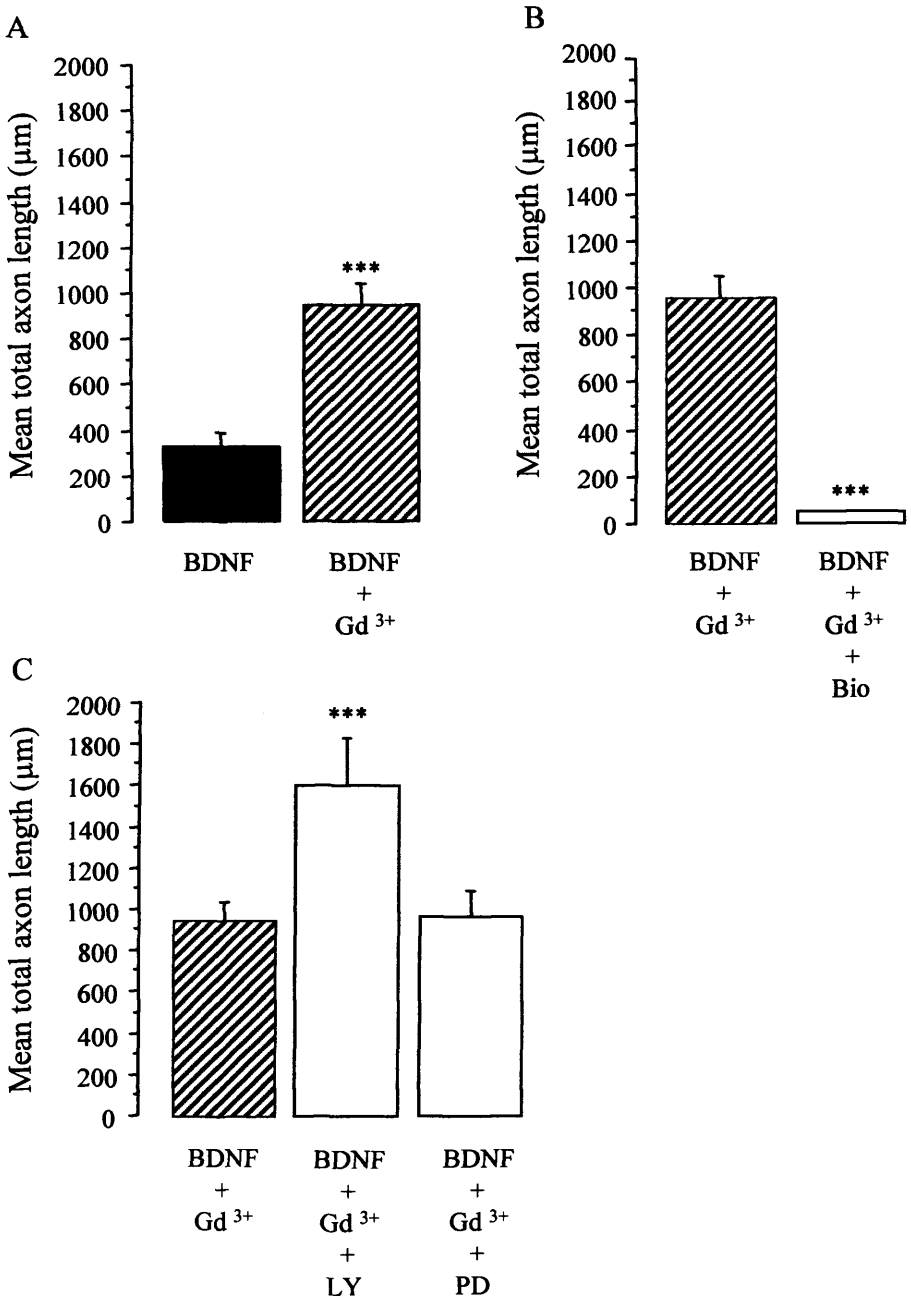

Figure 4.13: The effects of GSK3, PI3-Kinase and MEK1/2 inhibitors on the extent of axon outgrowth from stage 33 nodose neurons cultured in media containing a low calcium concentration in the presence of BDNF and 1pM Gd^{3+}.

Stage 33 nodose neurons were cultured with 10 ng/ml BDNF in media containing 0.7mM $[Ca^{2+}]_0$. With the exception of BDNF only cultures, culture media was supplemented with either 1pM Gd^{3+} alone or 1pM Gd^{3+} plus either 10µM of the GSK inhibitor, Bio, 50µM of the PI3-Kinase inhibitor, LY294002 or 10 µM of the MEK1/2 inhibitor, PD98059. Fluorescent images for subsequent analysis of process growth were captured after a 24 hr culture period.

A: 1pM Gd^{3+} increased mean total axon length in media containing a low calcium concentration plus BDNF.

B: Bio dramatically reduced mean total axon length in the presence of BDNF plus Gd^{3+}.

C: In the presence of BDNF plus Gd^{3+}, LY294002 promoted axon growth. In contrast PD98059 had no affect on the extent of axon outgrowth compared to neurons cultured in the presence of BDNF plus Gd^{3+} alone.

n = 150 neurons per condition from 3 different experiments. Data presented are the mean ± SEM. *** denotes $p < 0.0001$ after statistical comparisons with BDNF alone (A) or BDNF plus Gd^{3+} (B and C) (ANOVA with Fisher's ad hoc).

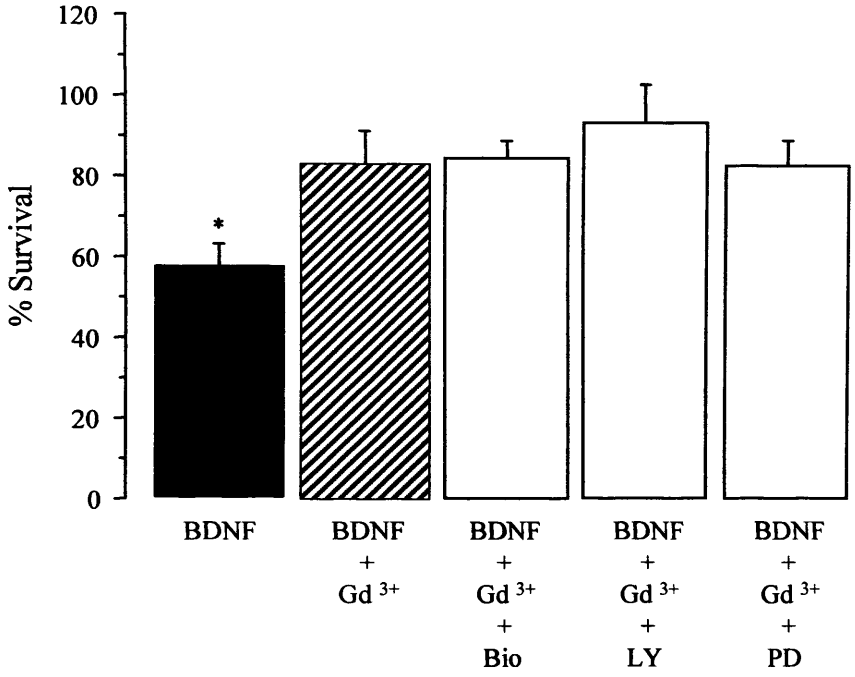

Figure 4.14: The effects of GSK3, PI3-Kinase and MEK1/2 inhibitors on the survival of stage 33 nodose neurons cultured in media containing a low calcium concentration in the presence of BDNF and 1pM Gd^{3+}.

Stage 33 nodose neurons were cultured for 24 hours, in the presence of 10 ng/ml BDNF, in media containing 0.7mM $[Ca^{2+}]_0$. With the exception of BDNF only cultures, culture media was supplemented with either 1pM Gd^{3+} alone or 1pM Gd^{3+} plus either 10μM of the GSK inhibitor, Bio, 50μM of the PI3-Kinase inhibitor, LY294002 or 10 μM of the MEK1/2 inhibitor, PD98059. Neurons were counted 3 hrs after plating and after 24 hrs in culture, allowing percentage neuronal survival at 24 hrs to be determined. There were no significant differences in survival between BDNF containing cultures supplemented with Gd^{3+} alone or Gd^{3+} plus Bio, LY or PD, although Gd^{3+} plus BDNF appeared to enhance survival compared to BDNF alone. Data are the mean +/- SEM from three separate cultures containing triplicate dishes for each condition. * denotes $p < 0.01$ after statistical comparisons between BDNF and BDNF plus Gd^{3+} (ANOVA with Fisher's ad hoc).

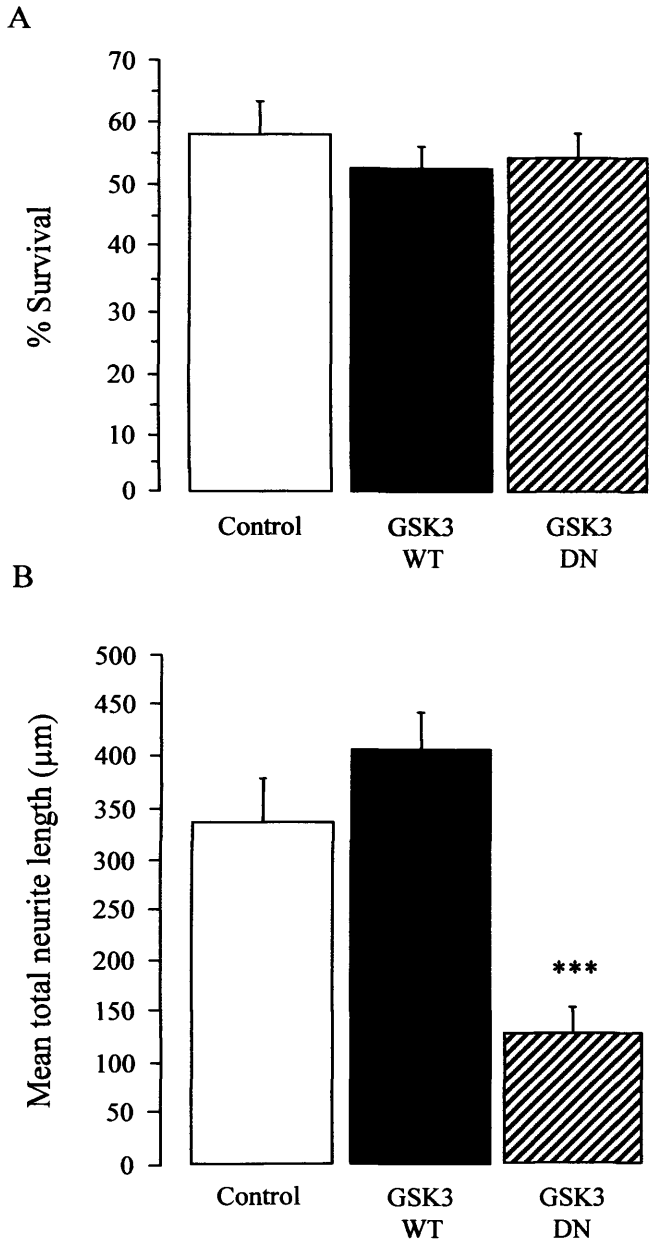

Figure 4.15: The effects of modulating GSK3 signalling on the survival of and process outgrowth from stage 30 nodose neurons cultured in media containing 1.3mM Ca^{2+}.

Stage 30 nodose neurons were cultured with 10 ng/ml BDNF in media containing 1.3mM $[Ca^{2+}]_0$. Electroporation was used to co-transfect neurons with the expression vector pcDNA3.1 containing cDNA encoding YFP together with either empty pcDNA3.1 (control), pcDNA3.1 containing the cDNA encoding wild type GSK3 (GSK3 WT) or pcDNA3.1 containing the cDNA encoding a dominant negative GSK3 (GSK3 DN). Co-transfected YFP expressing neurons were counted 24 hrs after plating and after 48 hrs in culture, allowing percentage neuronal survival at 48 hrs to be determined. Fluorescent images of YFP expressing neurons for subsequent analysis of process growth were captured after a 24 hr culture period.

A: Over-expression of either wild type GSK3 or dominant-negative GSK3 did not significantly alter the survival of cultured stage 30 nodose neurons compared to control cultures .

B: Over-expression of dominant-negative GSK3 significantly decreased mean total neurite length of stage 30 nodose neurons compared to control cultures, whereas over-expression of wild type GSK3 did not significantly effect the extent of neurite outgrowth compared to control cultures.

n = 90 neurons per condition from 3 different experiments. Data presented are the mean ± SEM. *** denotes $p < 0.0001$ after statistical comparison with control (ANOVA with Fisher's ad hoc).

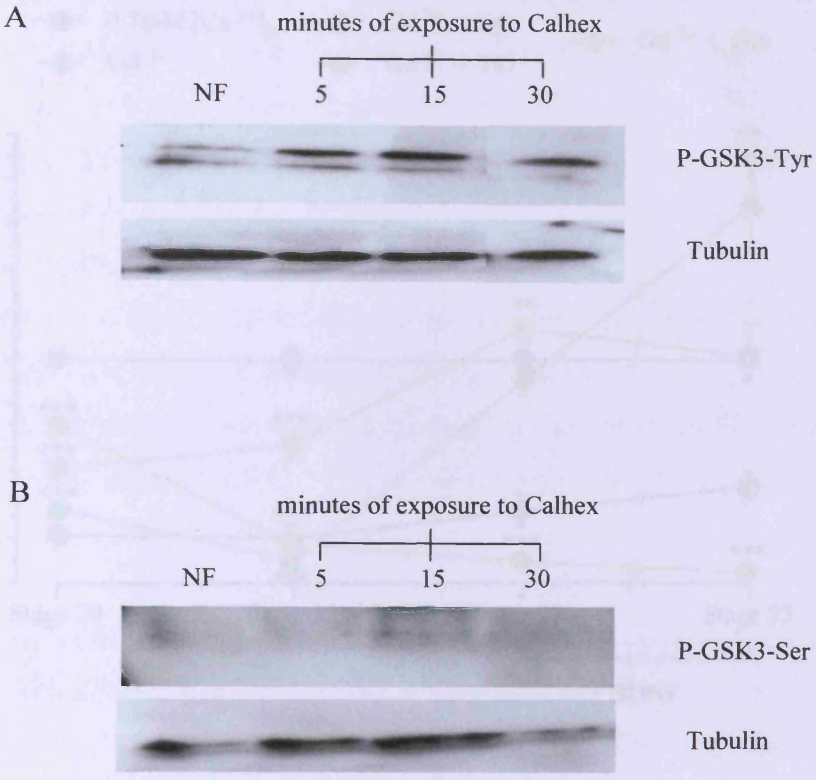

Figure 4.16: The specific CaSR agonist Calhex rapidly phosphorylates GSK3 on its regulatory tyrosine residue, but not its regulatory serine residue, in stage 30 nodose neurons cultured in media containing a low concentration of calcium.

Stage 30 nodose neurons were cultured in media containing 0.7mM $[Ca^{2+}]_0$ for 4 hrs. With the exception of control cultures, neurons were stimulated by the addition of 25nM Calhex. Cells were lysed, and the lysate prepared for western blotting, either 5, 10, 30 or 60 minutes after stimulation. Control cultures (NF) were lysed alongside the cultures for the 5 minute Gd^{3+} stimulation time point.

A: Western blots demonstrating that increased levels of tyrosine phosporylated GSK3 were present in stage 30 nodose neurons following 5, 15 and 30 minute exposure to Calhex. Filters were re-probed with an antibody against β-III tubulin.

B: Western blots demonstrating no increased phosporylation of GSK3 on its serine residue when stage 30 nodose neurons are exposed to the CaSR agonist Calhex. Filters were re-probed with an antibody against β-III tubulin.

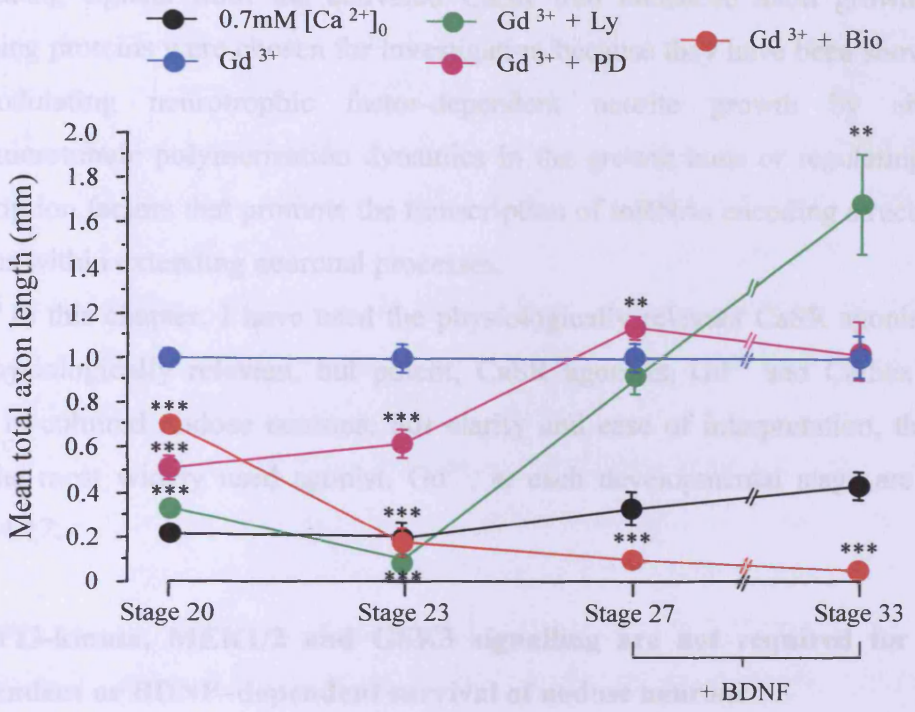

Figure 4.17: Summary of the effects of GSK3, PI-3 Kinase and MEK1/2 inhibitors on the extent of axon outgrowth from stage 20, 23, 27 and 33 nodose neurons cultured in media containing a low calcium concentration in the presence of 1pM Gd^{3+}

Mean total axon length data from figures 4.12, 4.14, 4.16 and 4.18 is shown. For clarity, data has been normalised to mean total axon length of neurons cultured with 1pM Gd^{3+} at each stage.

The GSK3 inhibitor, Bio, significantly reduced the ability of Gd^{3+} to promote axon outgrowth at all stages. The inhibitory effects of Bio on Gd^{3+} promoted axon elongation increases between stage 20 and stage 33.

The PI3-kinase inhibitor, LY294002, significantly reduced the ability of Gd^{3+} to promote axon outgrowth at stages 20 and 23. However, LY294002 does not interfere with the ability of Gd^{3+} to increase axon length at stage 27 and potentiated the effects of Gd^{3+} at stage 33.

The MEK1/2 inhibitor, PD98059, significantly reduced the ability of Gd^{3+} to enhance axon length at stages 20 and 23, but not stages 27 or 33.

n = 150 neurons per condition from 3 different experiments for each developmental stage. Data presented are the mean ± SEM. *** denotes $p < 0.0001$ after statistical comparisons with Gd^{3+} alone (stages 20 and 23) or BDNF plus Gd^{3+} (stage 27 and 33), whereas ** denotes $p < 0.001$compared to BDNF plus Gd^{3+} (ANOVA with Fisher´s ad hoc).

4.3 Discussion

The aim of this chapter was to use pharmacological inhibitors of PI3-kinase, GSK3 and MEK1/2 to determine whether any of these signalling proteins are involved in transducing signals from the activated CaSR into enhanced axon growth. These three signalling proteins were chosen for investigation because they have been shown to play a role in modulating neurotrophic factor-dependent neurite growth by either regulating actin/microtubule polymerization dynamics in the growth cone or regulating the activity of transcription factors that promote the transcription of mRNAs encoding structurally important proteins within extending neuronal processes.

In this chapter, I have used the physiologically relevant CaSR agonist, Ca^{2+}, and the non-physiologically relevant, but potent, CaSR agonists, Gd^{3+} and Calhex to activate the CaSR in cultured nodose neurons. For clarity and ease of interpretation, the data obtained with the most widely used agonist, Gd^{3+}, at each developmental stage are summarised in figure 4.17.

4.3.1 PI3-kinase, MEK1/2 and GSK3 signalling are not required for either BDNF-independent or BDNF–dependent survival of nodose neurons

PI3-kinase- and GSK3-mediated signalling have previously been shown to play a role in regulating the survival of both neurotrophic factor dependent neurons and neuronal cell lines under conditions that trigger apoptosis (Andjelkovic et al., 1998; Ashcroft et al., 1999; Bijur and Jope, 2001; Klesse et al., 1999; Pap and Cooper, 1998; Rodriguez-Viciana et al., 1994). It was, therefore, surprising that inhibiting these signalling proteins did not effect the survival of either newly differentiated, neurotrophic factor-independent or later stage, BDNF-dependent, placode-derived cranial sensory neurons of the chicken embryo. The great majority of studies on the roles of PI3-Kinase and GSK3 in mediating neuronal survival have utilised neuronal cell lines and rodent sympathetic neurons, neural-crest-derived sensory neurons and motoneurons. It is possible, therefore, that placode-derived cranial sensory neurons of the chicken embryo utilise different signalling pathways to promote survival compared to the rodent neurons and cell lines hitherto studied. However, in accordance with previously published data (Creedon et al., 1996; Klesse et al., 1999), inhibition of MEK1/2 by PD98059 did not effect the survival of cultured chick nodose neurons, either in the presence or absence of BDNF. The fact that the signalling protein inhibitors used in this study did not significantly effect neuronal survival makes the effects of PI3-kinase, MEK1/2 and GSK3 inhibitors on activated CaSR-promoted axon growth far easier to interpret.

4.3.2 Signalling pathways that mediate CaSR-promoted *de novo* axon growth

In accordance with the data in chapter 3, 1pM Gd^{3+} was able to promote robust *de novo* axon growth from neurotrophic factor-independent stage 20 and 23 nodose neurons. Blocking the function of PI3-Kinase by LY294002 had a profound inhibitory effect on activated CaSR-promoted axon outgrowth at both stages. In contrast, LY294002 did not reduce the length of axons projecting from stage 20 nodose neurons cultured in medium containing 0.7mM Ca^{2+}, culture conditions that do not significantly activate the CaSR. Interestingly, LY294002 was able to reduce the length of axons projecting from stage 23 nodose neurons stimulated with 1 pM Gd^{3+} to below those of neurons cultured in 0.7mM Ca^{2+} alone. This may reflect an ability of 0.7mM $[Ca^{2+}]_o$ to activate the CaSR sufficiently to promote limited axon elongation.

Further confirmation that PI3-Kinase plays an important role in activated CaSR-promoted axon growth in the absence of BDNF was obtained by transfecting stage 20 neurons with plasmids expressing either constitutively active or dominant-negative PI3-Kinase and culturing the neurons in medium containing either 0.7mM or 1.3mM Ca^{2+}. Over-expression of constitutively active PI3-Kinase significantly increased axon length in medium containing 1.3mM Ca^{2+}, whereas over-expression of dominant-negative PI3-Kinase reduced axon length in the same medium. The over-expression of either protein did not alter the length of axons extending from nodose neurons cultured in medium containing 0.7mM Ca^{2+}. Additional evidence that PI3-kinase is involved in activated CaSR-promoted axon growth is provided by the demonstration that Akt, a major downstream target of activated PI3-Kinase, is rapidly phosphorylated after the addition of 1pM Gd^{3+} to cultures of stage 20 nodose neurons. Taken together the data presented in this chapter demonstrate that PI3-Kinase plays an important role in transducing activation of the CaSR into enhanced BDNF-independent axon growth. Whilst this finding is in accordance with the observations that PI3-Kinase can be activated downstream of G protein-coupled receptor stimulation in non-neuronal cells (De Camilli et al., 1996) and PI3-kinase signalling promotes neurotrophic factor-dependent axon growth (Aoki et al., 2005; Jiang et al., 2005; Shi et al., 2003; Yoshimura et al., 2005; Zhou et al., 2004) this is the first demonstration that PI3-Kinase signalling promotes *de novo* axon growth.

Inhibiting either MEK1/2 or GSK3 also significantly decreased the extent of Gd^{3+}-promoted axon elongation from stage 20 and 23 nodose neurons. MEK1/2 inhibition reduced Gd^{3+}-promoted axon growth by around 50% at both stage 20 and 23. Inhibiting GSK3 with

Bio reduced Gd^{3+}-promoted axon growth by 30% at stage 20 and eliminated it at stage 23. At both stages, LY294002 was a more potent inhibitor of Gd^{3+}-enhanced axon growth than either PD98059 or Bio, indicating that, of the three signalling proteins investigated, PI3-kinase plays the most important role in transducing activation of the CaSR into enhanced *de novo* axon growth.

Although, ERK signalling in response to neurotrophic factors has previously been shown to induce local axon assembly and to promote the transcription of mRNAs involved in axon growth by activating the transcription factors CREB and NFATc (Atwal et al., 2000; Lonze and Ginty, 2002; Nguyen and Di Giovanni, 2008; Xing et al., 1996; Xing et al., 1998), I have demonstrated for the first time that ERK activation also promotes *de novo* axon growth. The activation of Akt and ILK by PI3-kinase has previously been shown to lead to the phosphorylation of GSK3 and subsequent growth cone extension and axon elongation (Zhou et al., 2004; Jiang et al., 2005; Zhou and Snider, 2006). In addition, the ERK1/2 MAPK pathway has also been shown to phosphorylate GSK3 via MAPKAP Kinase-2 (Jope and Johnson, 2004; Stambolic and Woodgett, 1994; Stokoe et al., 1992). Together with my data, these previous findings may suggest that PI3-kinase and ERK are upstream of GSK3 phosphorylation in the signal transduction pathway that leads to enhanced axon growth following CaSR activation. However, in these previous studies, activated PI3-Kinase and ERK1/2 lead to the phosphorylation of GSK3 on its regulatory serine residue and resulted in the inactivation of GSK3. Inactivation of GSK3 by serine phosphorylation has previously been implicated in promoting axon growth (Jiang et al., 2005; Zhou and Snider, 2006; Zhou et al., 2004). In contrast, my data clearly shows that inhibition of GSK3 by Bio, an inhibitor that blocks ATP binding to GSK3 and prevents phosphorylation of downstream substrates, has a detrimental effect on activated CaSR-promoted axon growth in the absence of BDNF. This suggests that stimulation of GSK3 activity rather than its inactivation is an important step in coupling CaSR stimulation to *de novo* axon growth. This novel finding and the nature of GSK3 activation is discussed further in section 4.3.3, below.

My data raise the possibility that the serine threonine kinase, Akt is a downstream target of PI3-kinase following CaSR activation. As mentioned above, previously published literature has suggested that GSK3 is a major target of Akt in pathways that regulate axon growth and that Akt phosphorylates GSK3 on its regulatory serine residue to inhibit its activity and promote microtubule polymerization. In light of the data obtained by using Bio in my experiments it seems unlikely that GSK3 is the target of activated CaSR stimulated Akt. Further experiments are therefore needed to identify the substrates of Akt following CaSR

activation and to determine whether these substrates are linked to signalling pathways that can promote axon growth. In addition to regulating microtubule dynamics via Akt, PI3-kinase can also promote filopodial and lamellipodial extension by modulating actin polymerization kinetics by pathways that include activation of either Cdc42 or Rac (Zhou and Snider, 2006). Future Western blot experiments are needed to determine whether either Cdc42 or Rac activation occurs following CaSR activation. If this is the case, further culture experiments need to be performed to find out whether activation of these small GTPases is necessary for CaSR-promoted axon growth.

4.3.3 Signalling pathways that mediate CaSR-promoted BDNF-dependent axon growth

Surprisingly, PI3-kinase did not appear to play a role in transducing CaSR and trkB activation into enhanced axon elongation from stage 27 chick nodose neurons. Moreover, LY294002 enhanced axon growth from stage 33 nodose neurons cultured with 1pM Gd^{3+} in the presence of BDNF, raising the possibility that PI3-Kinase activation at this stage inhibits axon growth. This finding is at odds with the well characterised role of PI3-Kinase in mediating neurotrophic factor-promoted neuronal process outgrowth from various types of rodent neurons and cell lines (Aoki et al., 2005; Jiang et al., 2005; Nusser et al., 2002; Yoshimura et al., 2005; Zhou et al., 2004). Curiously, inhibiting PI3-kinase in stage 33 nodose neurons cultured in medium containing 1.3mM Ca^{2+} plus BDNF did not affect axon length. This anomaly may be due to the fact that Gd^{3+} is a more potent activator of the CaSR, and hence promotes greater axon growth, than its main physiological ligand, Ca^{2+}. Alternatively, it is possible that activation of the CaSR by both agonists is qualitatively different, resulting in the recruitment of different G proteins and the activation of different intracellular signalling cascades. Limited evidence already exists to suggest that different agonists may activate the CaSR in qualitatively different ways (Ward, 2004). Whilst the lack of involvement of PI3-Kinase signalling in BDNF-promoted axon growth from later stage nodose neurons is surprising, it may indicate that signalling pathways that mediate neurotrophin-promoted process outgrowth from chick placode-derived cranial sensory neurons differ from those in rodent neurons and cell lines.

In contrast to its role in mediating CaSR-enhanced axon growth at early developmental stages, MEK1/2-ERK signalling did not appear to be involved in BDNF and activated CaSR-promoted axon growth at stages 27 and 33. This finding is also surprising, since ERK signalling has previously been shown to be involved in regulating neuronal process outgrowth in response to neurotrophic factors (Atwal et al., 2000; Lonze and Ginty,

2002; Nguyen and Di Giovanni, 2008; Xing et al., 1996; Xing et al., 1998). Once again, previously published data has been taken from studies involving rodent neurons and cell lines, and it may be that signalling pathways differ in the chick or the particular placode-derived sensory neurons studied.

My data clearly show that GSK3 is an extremely important component of the signalling cascades that convert CaSR activation in the presence of BDNF into enhanced axon elongation. Bio was able to reduce the mean length of axons projecting from stage 27 and 33 nodose neurons cultured with BDNF and 1pM Gd^{3+} to below that of neurons cultured in BDNF alone. Although this suggests that Bio can completely block axon growth promoted by CaSR activation as well as inhibiting growth promoted by trkB activation, the experimental design used in my studies precludes a definitive determination of whether GSK3 transduces signals downstream of either the activated CaSR or activated trkB, or both. Bio was also able to completely abolish BDNF-promoted growth from stage 33 neurons cultured in medium containing 1.3mM Ca^{2+}. Once again, although this strongly suggests that GSK3 is involved in transducing trkB activation into enhanced axon growth, the experimental design cannot determine to what extent GSK3 also signals downstream of the activated CaSR to promote axon elongation, since 1.3mM Ca^{2+} significantly activates the CaSR. The pivotal role of activated GSK3 in transducing CaSR stimulation in the presence of BDNF into enhanced axon growth was further established by transfection experiments at stage 30 using either wild type GSK3 or dominant-negative GSK3 expression plasmids. Whilst over-expression of wild type GSK3 did not increase the length of axon growing from stage 30 nodose neurons cultured in medium containing 1.3mM Ca^{2+}, the expression of dominant-negative GSK3 greatly reduced the length of axons in the same culture medium.

As discussed above, inhibition of GSK3 activity by serine phosphorylation is normally associated with neurotrophic factor-promoted neurite growth. My novel data clearly demonstrate that in chick nodose neurons it is GSK3 activation that promotes axon growth. GSK3 activity is normally tightly controlled by a balance of inhibitory serine phosphorylation and stimulatory tyrosine phosphorylation (Jope and Johnson, 2004). To determine whether CaSR activation did indeed lead to tyrosine phosphorylation of GSK3, I carried out Western blots of cell lysates extracted from stage 30 nodose neurons that had been stimulated by 25mM of the potent and specific, commercially available CaSR agonist, Calhex, in medium containing 0.7mM Ca^{2+} and lacking BDNF. Western blots clearly demonstrated that Calhex induced a rapid phosphorylation of GSK3 on its regulatory tyrosine residue without affecting the phosphorylation status of the regulatory serine residue.

Whilst my data suggest that CaSR activation promotes neurite growth from later stage, BDNF-dependent nodose neurons by a signalling pathway that involves GSK3 activation by tyrosine phosphorylation, several pertinent questions need addressing to further characterise this signalling pathway. For example, experiments need to be performed with Bio using an experimental design that will allow a clear distinction between the roles of CaSR activation and trkB activation in promoting neurite growth from later stage nodose neurons. It will also be important to determine whether trkB activation in absence of CaSR stimulation also leads to tyrosine phosphorylation and activation of GSK3 in the absence of serine phosphorylation. In addition, the recently available potent and specific CaSR antagonist, Calindol, will be useful to specifically isolate axon growth-promoting signalling pathways initiated by either trkB activation or CaSR activation.

The novel observation that tyrosine phosphorylation and stimulation of GSK3 activity is a key step in transducing CaSR and/or trkB activation into enhanced axon growth from BDNF dependent chick cranial sensory neurons, begs the question of what is the identity of the tyrosine kinase that is responsible for activation of GSK3. One candidate is the soluble intracellular tyrosine kinase, src. Although src has previously been shown to be activated following neurotrophin receptor stimulation (Reichardt, 2006) there are no reports that CaSR activation can modulate its activity. Further Western blot experiments are needed to determine if activation of either the CaSR or trkB can promote src phosphorylation in BDNF dependent chick cranial sensory neurons. If this proves to be the case, experiments with specific src inhibitors could be used to investigate whether src activation downstream of either CaSR or trkB activation is necessary for enhanced axon elongation.

Summary

The data in this chapter demonstrate a clear switch in the signalling pathways that are involved in promoting axon elongation from chick nodose neurons from early BDNF-independent stages of *de novo* axon growth to later BDNF-dependent stages of axon growth. PI3-Kinase is the key signalling protein that links CaSR activation to enhanced axon growth at the earliest developmental stages, whereas GSK3 is the major signalling protein associated with later CaSR- and trkB-promoted axon elongation. Importantly, my data demonstrates that activation of GSK3 by tyrosine phosphorylation is a crucial step leading to enhanced axon growth in later stage chick nodose neurons. Further experiments are warranted to fully characterise this novel developmental switch the intracellular signalling network that governs axonal growth.

General Discussion

Until recently, the CaSR has been studied in the context of systemic $[Ca^{2+}]_0$ homeostatis. Although the widespread expression of the CaSR in the nervous system has been known for many years, the first role for the CaSR in the nervous system was only recently established by the demonstration that activation of the CaSR in SCG neurons during a narrow developmental window in the immediate perinatal periods enhances NGF-promoted axonal growth and branching in vitro and the finding that sympathetic innervation is defective in newborn mice lacking the CaSR gene (Vizard et al., 2008).

My work has extended the role of the CaSR in regulating axonal growth to the earliest stages of neuronal development. I have demonstrated that activation of the CaSR is required for the neurotrophin-independent extension of axons from the placode-derived neurons of the nodose ganglion at the time in development when these neurons are extending axons towards their targets. Nodose neurons have distant targets and exhibit an especially fast rate of axonal growth at this stage of development. In contrast, the placode-derived neurons of the vestibular ganglion, which have nearby targets and extend axons at a much slower rate to these targets, express lower levels of the CaSR than nodose neurons, and activity of the CaSR in these neurons has no affect on axon growth rate. Because of the hypercalcaemic milieu of the embryo, these findings imply that differences in the level of CaSR expression in early placode-derived neurons plays a role in governing intrinsic differences in the rates at which axons grow from these neurons to their targets. However, high levels of CaSR expression are not sufficient to confer fast axonal growth since overexpression of CaSR in neurotrophin-independent vestibular neurons did not enhance axonal growth rate. One reason for this might be because the signalling mechanisms downstream of the receptor are not active at this stage of development in these neurons, since overexpression the CaSR at later stages in development significantly increased axon growth from BDNF-dependent vestibular neurons. The fact that we found CaSR upregulated mRNA expression in nodose neurons during development while it stayed at the same levels thoughout development in vestibular neurons also points at a missing signalling mechanism in early stages. One further experiment to confirm different levels of CaSR expression in nodose and vestibular neurons are semi-quantitative western blots, where there should be a visible upregulation in CaSR protein in nodose neurons but not in vestibular neurons during development.

The technical difficulty using electroporation, is that placode-derived chicken neurons at these early stages in development are very sensitive to electroporation. The overall growth

rate decreased significantly compared to non-electroporated neurons. I can exclude that the reporter we used for transfection -YFP- to have a toxic effect on the neurons, since I also carried out transfections without the reporter and stained the neurons with a CaSR antibody. Even though transfected neurons could not be identified visually, the overall count and analysis of these neurons showed an increase or decrease in growth, respectively, but still an overall decrease in neurite length compared to non-transfected neurons.

To confirm that the CaSR dominant negative is effective, since it had to be cloned into the chicken construct, we could use two different approaches. Either by electroporation of nodose neurons and then running a western blot afterwards, looking for the CaSR downstream signalling. This approach is technically impossible, as by using this method there will not be enough protein to detect any downstream signalling. Another approach could be to look at a stable cell line expressing the CaSR wild type or dominant-negative constructs. I should find enhanced activated signalling downstream the wild type expressing cell line, while I should find reduced signalling in the dominant-negative expressing cell line. Overexpressing both constructs at the same time should bring signalling back to control levels.

An important issue will be to determine the physiological relevance of these *in vitro* observations. To this end, experiments are currently in progress to pharmacologically manipulate CaSR function *in ovo*, to see if such manipulations affect axonal growth rate and target innervation by nodose and vestibular neurons. These experiments involve administering the CaSR antagonist to stage 15 embryos, a time in development when neuroblasts have differentiated into neurons and axons start to extend towards their targets. Embryos are subsequently fixed at later stages and whole-mount neurofilament antibody staining carried out to visualize the respective nerves and measure their lengths. If my *in vitro* findings are relevant for *in vivo* development, I would predict that the CaSR antagonist would affect the growth of nodose but not vestibular axons. *In ovo* electroporation of DN CaSR has been also been attempted to address the physiological relevance of my *in vitro* observations, but electroporation of the respective placodes was either not successful or the very few cases in which placodes transfected, the embryos did not survive long enough to carry out the analysis.

After nodose ganglion axons reach their targets, the neurons become dependent on BDNF for survival, and BDNF promotes the growth and branching of the axons in vitro, which may reflect a role of BDNF in facilitating the terminal branching and ramification of these axons in their targets. Manipulation of CaSR in cultured nodose neurons at this stage of development has also demonstrated that activation of the CaSR is crucial for BDNF-promoted axonal growth and branching. Studies to investigate the signalling pathways that mediate CaSR

dependent axonal growth in developing nodose neurons has not only provided the first evidence for the intracellular molecular mechanisms by which CaSR affects axonal growth, but have revealed a completely unexpected switch in the signalling pathways that are required for axonal growth at neurotrophin-independent and BDNF-dependent stages of development. To investigate axon growth after target innervation and to examine the possibility of a cross-talk in CaSR and Trk signalling, I carried out initial experiments to see if the CaSR is signalling together with or independently of the Trk receptor. Culturing neurons in the presence of high and low $[Ca^{2+}]_0$, but in the absence of BDNF (but in the presence of caspase inhibitor Boc-D-FMK), did not show differences in axon growth in stage 30 nodose neurons. Neurons cultured in low $[Ca^{2+}]_0$ but in the presence and absence of BDNF increased axon growth in the cultures containing BDNF, but only up to half the length as I found the high and low $[Ca^{2+}]_0$ in the presence of BDNF.

This experiment suggests that the CaSR and Trk receptor need to be activated simultaneously, but whether the signalling pathways are linked can not be answered through this approach.

Experiments using selective pharmacological inhibitors have revealed that PI3-kinase signalling is required for neurotrophin-independent axon growth and GSK3 signalling is required for BDNF-dependent growth. One of the greatest technical obstacles in the further analysis of CaSR signalling at these neurons during these early stages of development is the extremely limited availability of nodose neurons for biochemical studies. Indeed, because of the very small size of this ganglion, Western blot analysis was technically impossible up until the very end of the phase of neurotrophin-independence. Nonetheless, I was able to provide confirmatory evidence for CaSR-dependent PI3-kinase signalling at this stage of development, and was able to demonstrate that CaSR activates GSK3 by a non-canonical mechanism that involves tyrosine phosphoryation of the enzyme during the stage of BDNF dependence. While I provided additional supportive evidence for these two signalling pathways in regulating axonal growth at these respective stages of development by transfecting the neurons with plasmids expressing mutated signalling proteins, nodose neurons turned out to be very sensitive to electroporation, in that the overall growth rate dropped significantly compared to non-electroporated neurons.

GSK3 has previously been reported to be constitutively active within the cell, and increases axon growth through its inactivation following signalling events that lead to phosphorylation on serine 9 (Armstrong et al., 2001; Fang et al., 2000; Hughes et al., 1993; Li et al., 2000; Stambolic and Woodgett, 1994). In marked contrast, my work shows in

embryonic chicken nodose neurons that inactivation of GSK3 with the pharmacological inhibitor Bio, leads to decreased axon growth. Furthermore, GSK3 activation has been shown to be further enhanced by phosphorylation on tyrosine 216 (Jope and Johnson, 2004), and my data clearly indicate that CaSR-dependent phosphorylation of GSK3-α on tyrosine 216 results in embryonic nodose neurons enhances axonal growth. How GSK3 is phosphorylated on this tyrosine residue in nodose neurons is not clear. I did experiments to see if the src tyrosine kinase is involved in CaSR signalling, and found that while src phosphorylation is increased by CaSR activation, either by elevated $[Ca^{2+}]_0$ or by the CaSR agonist Calhex, the src inhibitor PP2 did not decrease the level of phospho-tyrosine GSK3, suggesting that activation of src is not required for CaSR-dependent phosphorylation of GSK3 in nodose neurons.

While activation of the CaSR enhances the growth rate of nodose ganglion axons during the stages of neurotrophin independence and BDNF dependence, it is unlikely that the extracellular calcium and the CaSR play any direct role in axon guidance. This is because there is no evidence for and no reason to expect the presence of Ca2+ gradients in the extracellular fluid in the embryo that could differentially activate the CaSR across the growth cone. Rather, the relative hypercalcaemia of the embryo would likely granule cell growth cones to BDNF has been shown to be due to TrkB-dependent Ca2+-permeant TRPC channel opening (Li et al., 2005). Although BDNF is unlikely to be a long-range cue for early nodose neurons, since TrkB is not expressed by these neurons at the stage when their axons are growing to their targets (Robinson et al., 1996), it may play a role in local guidance of growth lead to constitutive activation of the CaSR in all locations on the surface of cells that express it. It is possible, however, that constitutive activation of the CaSR could indirectly affect the molecular mechanisms involved in axon guidance by affecting the sensitivity of such mechanisms to extracellular signals that govern growth cone direction. For example, since gradients of intracellular Ca2+ within the growth cone can influence growth cone turning, if CaSR affects the mean [Ca2+]i in the growth cone as a result of stimulating release of Ca2+ from intracellular stores, for example, this might affect the sensitivity of the molecular mechanisms that transduce [Ca2+]i gradients into directional responses of the growth cone to extracellular signals that bring about [Ca2+]i gradients in the growth cone. In future work it will be interesting to test the possibility that activation of the CaSR affects the sensitivity of growth cones to chemoattractants and chemorepellents. For example, BDNF-induced chemo-attractive turning of cerebellar cones in their target fields later in development. If so, it would be interesting to investigate if turning responses of growth cones to BDNF gradients is affected by the level of CaSR activation.

Appendix

Appendix

SDS polyacrylamide gel electrophoresis

Sample buffer	100mM Tris pH 6.8 (Sigma) 2% SDS (Serva) 10% Glycerol 0.5% Bromphenol 5% β- Mercaptoethanlol (Sigma)
Electrophoresis buffer	250mM Tris (Sigma) 1.9M glycine (Merck) 0.1% SDS (Serva)
10% separating gel(10ml)	4.05ml H_2O 2.6 ml 1.5M Tris pH 8.8, 0.4% SDS 0.65ml 30% Acrylamide (Biorad) 5µl TEMED (Biorad) 50µl 10%APS (Biorad)
4% stacking gel(5ml)	3.05 H_2O 1.3ml 0.5 M Tris pH 6.8, 0.4% SDS 0.65 ml 30% Acrylamide (Biorad) 5µl TEMED (Biorad) 50µl 10% APS (Biorad)
Transfer buffer	20mM Tris (Sigma) 150mM Glycine (Merck) 0.1% SDS (Serva) 10% Methanol (Merck)
PBS Tween	PBS 0.1% Polyoxyethylene sorbitan monolaurate (Sigma)

Blocking solution	PBS Tween 5% Milk Powder
4% stacking gel (5ml)	3.05 ml H_2O 1.3ml 0.5M Tris pH 6.8, 0.4% SDS 0.65ml 30% Acrylamide/Bis solution (Biorad) 5µl TEMED 50µl 10% APS (Biorad)
Transfer buffer	20mM Tris (Sigma) 150mM Glycine (Merck) 0.1% SDS (Serva) 10% Methanol (Merck)
PBS Tween	PBS 0.1% Polyoxyethylene sorbitan monolaurate (Sigma)
Blocking solution	PBS Tween 5% milk powder
Stripping buffer	5mM Na_2HP_4 2% SDS (Serva) and freshly added: 0.02% β-Mercaptoethanol (Sigma)

Poly-ornithine Solution

9.2g boric acid (Sigma) was dissolved in 1L dH_2O and adjusted to PH 8.4 with NaOH.
500mg poly-DL-ornithine hydrobromide (Sigma) was dissolved in the borate solution and filter serilized using a 0.2μm Acrocap filter unit (Pall Corporation). The poly- ornithine solution was stored in two 500 ml bottles at 4°C for up to 2 weeks.

Trypsin

50mg Trypsin (Worthington) was dissolved in 5ml Ca^{2+} / Mg^{2+} free PBS (Gibco, Invitrogen) , filter sterilized and stored at 50μl aliquots at –20°C

Siliconised pipettes

Glass Pasteur pipettes (Fisher Scientific) were placed in a large beaker which was filled with dH_2O up to ¾ length of the pipettes and left for 2 mins. The dH_2O was removed and replaced with dichlorodimethylsaline (BDH) and left for 30 mins. The pipettes where then washed 5 times with dH_2O, a further 2 times with sterile PBS then placed in pipette boxes and autoclaved.

References

Airaksinen, M. S., and Saarma, M. (2002). The GDNF family: signalling, biological functions and therapeutic value. Nat Rev Neurosci *3*, 383-394.

Albers, K. M., Perrone, T. N., Goodness, T. P., Jones, M. E., Green, M. A., and Davis, B. M. (1996). Cutaneous overexpression of NT-3 increases sensory and sympathetic neuron number and enhances touch dome and hair follicle innervation. J Cell Biol *134*, 487-497.

Albers, K. M., Wright, D. E., and Davis, B. M. (1994). Overexpression of nerve growth factor in epidermis of transgenic mice causes hypertrophy of the peripheral nervous system. J Neurosci *14*, 1422-1432.

Alessi, D. R., Andjelkovic, M., Caudwell, B., Cron, P., Morrice, N., Cohen, P., and Hemmings, B. A. (1996). Mechanism of activation of protein kinase B by insulin and IGF-1. Embo J *15*, 6541-6551.

Alonzi, T., Middleton, G., Wyatt, S., Buchman, V., Betz, U. A., Muller, W., Musiani, P., Poli, V., and Davies, A. M. (2001). Role of STAT3 and PI 3-kinase/Akt in mediating the survival actions of cytokines on sensory neurons. Mol Cell Neurosci *18*, 270-282.

Alvarez, I. S., and Navascues, J. (1990). Shaping, invagination, and closure of the chick embryo otic vesicle: scanning electron microscopic and quantitative study. Anat Rec *228*, 315-326.

Andjelkovic, M., Alessi, D. R., Meier, R., Fernandez, A., Lamb, N. J., Frech, M., Cron, P., Cohen, P., Lucocq, J. M., and Hemmings, B. A. (1997). Role of translocation in the activation and function of protein kinase B. J Biol Chem *272*, 31515-31524.

Andjelkovic, M., Jakubowicz, T., Cron, P., Ming, X. F., Han, J. W., and Hemmings, B. A. (1996). Activation and phosphorylation of a pleckstrin homology domain containing protein kinase (RAC-PK/PKB) promoted by serum and protein phosphatase inhibitors. Proc Natl Acad Sci U S A *93*, 5699-5704.

Andjelkovic, M., Suidan, H. S., Meier, R., Frech, M., Alessi, D. R., and Hemmings, B. A. (1998). Nerve growth factor promotes activation of the alpha, beta and gamma isoforms of protein kinase B in PC12 pheochromocytoma cells. Eur J Biochem *251*, 195-200.

Andrianantoandro, E., and Pollard, T. D. (2006). Mechanism of actin filament turnover by severing and nucleation at different concentrations of ADF/cofilin. Mol Cell *24*, 13-23.

Aoki, K., Nakamura, T., Fujikawa, K., and Matsuda, M. (2005). Local phosphatidylinositol 3,4,5-trisphosphate accumulation recruits Vav2 and Vav3 to activate Rac1/Cdc42 and initiate neurite outgrowth in nerve growth factor-stimulated PC12 cells. Mol Biol Cell *16*, 2207-2217.

Armstrong, J. L., Bonavaud, S. M., Toole, B. J., and Yeaman, S. J. (2001). Regulation of glycogen synthesis by amino acids in cultured human muscle cells. J Biol Chem *276*, 952-956.

Ashcroft, M., Stephens, R. M., Hallberg, B., Downward, J., and Kaplan, D. R. (1999). The selective and inducible activation of endogenous PI 3-kinase in PC12 cells results in efficient NGF-mediated survival but defective neurite outgrowth. Oncogene *18*, 4586-4597.

Atwal, J. K., Massie, B., Miller, F. D., and Kaplan, D. R. (2000). The TrkB-Shc site signals neuronal survival and local axon growth via MEK and P13-kinase. Neuron *27*, 265-277.

Atwal, J. K., Singh, K. K., Tessier-Lavigne, M., Miller, F. D., and Kaplan, D. R. (2003). Semaphorin 3F antagonizes neurotrophin-induced phosphatidylinositol 3-kinase and mitogen-activated protein kinase kinase signaling: a mechanism for growth cone collapse. J Neurosci *23*, 7602-7609.

Augustine, G. J. (2001). How does calcium trigger neurotransmitter release? Curr Opin Neurobiol *11*, 320-326.

Bai, M. (2004). Structure-function relationship of the extracellular calcium-sensing receptor. Cell Calcium *35*, 197-207.

Baker, C. V., and Bronner-Fraser, M. (2000). Establishing neuronal identity in vertebrate neurogenic placodes. Development *127*, 3045-3056.

Barde, Y. A. (1990). The nerve growth factor family. Prog Growth Factor Res *2*, 237-248.

Bassell, G. J., Zhang, H., Byrd, A. L., Femino, A. M., Singer, R. H., Taneja, K. L., Lifshitz, L. M., Herman, I. M., and Kosik, K. S. (1998). Sorting of beta-actin mRNA and protein to neurites and growth cones in culture. J Neurosci *18*, 251-265.

Bentley, C. A., and Lee, K. F. (2000). p75 is important for axon growth and schwann cell migration during development. J Neurosci *20*, 7706-7715.

Bibel, M., and Barde, Y. A. (2000). Neurotrophins: key regulators of cell fate and cell shape in the vertebrate nervous system. Genes Dev *14*, 2919-2937.

Bibel, M., Hoppe, E., and Barde, Y. A. (1999). Biochemical and functional interactions between the neurotrophin receptors trk and p75NTR. Embo J *18*, 616-622.

Bicker, G. (2005). STOP and GO with NO: nitric oxide as a regulator of cell motility in simple brains. Bioessays *27*, 495-505.

Bijur, G. N., De Sarno, P., and Jope, R. S. (2000). Glycogen synthase kinase-3beta facilitates staurosporine- and heat shock-induced apoptosis. Protection by lithium. J Biol Chem *275*, 7583-7590.

Bijur, G. N., and Jope, R. S. (2001). Proapoptotic stimuli induce nuclear accumulation of glycogen synthase kinase-3 beta. J Biol Chem *276*, 37436-37442.

Blair, L. A., Bence-Hanulec, K. K., Mehta, S., Franke, T., Kaplan, D., and Marshall, J. (1999). Akt-dependent potentiation of L channels by insulin-like growth factor-1 is required for neuronal survival. J Neurosci *19*, 1940-1951.

Bootman, M. D., Missiaen, L., Parys, J. B., De Smedt, H., and Casteels, R. (1995). Control of inositol 1,4,5-trisphosphate-induced Ca2+ release by cytosolic Ca2+. Biochem J *306 (Pt 2)*, 445-451.

Borasio, G. D., Markus, A., Wittinghofer, A., Barde, Y. A., and Heumann, R. (1993). Involvement of ras p21 in neurotrophin-induced response of sensory, but not sympathetic neurons. J Cell Biol *121*, 665-672.

Boskey, A. L. (1992). Mineral-matrix interactions in bone and cartilage. Clin Orthop Relat Res, 244-274.

Bradke, F., and Dotti, C. G. (1999). The role of local actin instability in axon formation. Science *283*, 1931-1934.

Brault, V., Moore, R., Kutsch, S., Ishibashi, M., Rowitch, D. H., McMahon, A. P., Sommer, L., Boussadia, O., and Kemler, R. (2001). Inactivation of the beta-catenin gene by Wnt1-Cre-mediated deletion results in dramatic brain malformation and failure of craniofacial development. Development *128*, 1253-1264.

Brown, E. M., and MacLeod, R. J. (2001). Extracellular calcium sensing and extracellular calcium signaling. Physiol Rev *81*, 239-297.

Brown, M. D., Cornejo, B. J., Kuhn, T. B., and Bamburg, J. R. (2000). Cdc42 stimulates neurite outgrowth and formation of growth cone filopodia and lamellipodia. J Neurobiol *43*, 352-364.

Brunjes, P. C., and Frazier, L. L. (1986). Maturation and plasticity in the olfactory system of vertebrates. Brain Res *396*, 1-45.

Brushia, R. J., and Walsh, D. A. (1999). Phosphorylase kinase: the complexity of its regulation is reflected in the complexity of its structure. Front Biosci *4*, D618-641.

Buchman, V. L., and Davies, A. M. (1993). Different neurotrophins are expressed and act in a developmental sequence to promote the survival of embryonic sensory neurons. Development *118*, 989-1001.

Cameron, L. A., Footer, M. J., van Oudenaarden, A., and Theriot, J. A. (1999). Motility of ActA protein-coated microspheres driven by actin polymerization. Proc Natl Acad Sci U S A *96*, 4908-4913.

Campbell, D. S., and Holt, C. E. (2003). Apoptotic pathway and MAPKs differentially regulate chemotropic responses of retinal growth cones. Neuron *37*, 939-952.

Cantley, L. C. (2002). The phosphoinositide 3-kinase pathway. Science *296*, 1655-1657.

Carmichael, J., Sugars, K. L., Bao, Y. P., and Rubinsztein, D. C. (2002). Glycogen synthase kinase-3beta inhibitors prevent cellular polyglutamine toxicity caused by the Huntington's disease mutation. J Biol Chem *277*, 33791-33798.

Catlett-Falcone, R., Landowski, T. H., Oshiro, M. M., Turkson, J., Levitzki, A., Savino, R., Ciliberto, G., Moscinski, L., Fernandez-Luna, J. L., Nunez, G., *et al.* (1999). Constitutive

activation of Stat3 signaling confers resistance to apoptosis in human U266 myeloma cells. Immunity *10*, 105-115.

Chang, W., and Shoback, D. (2004). Extracellular Ca2+-sensing receptors--an overview. Cell Calcium *35*, 183-196.

Chao, M. V., and Hempstead, B. L. (1995). p75 and Trk: a two-receptor system. Trends Neurosci *18*, 321-326.

Chao, M. V., Rajagopal, R., and Lee, F. S. (2006). Neurotrophin signalling in health and disease. Clin Sci (Lond) *110*, 167-173.

Charron, F., and Tessier-Lavigne, M. (2005). Novel brain wiring functions for classical morphogens: a role as graded positional cues in axon guidance. Development *132*, 2251-2262.

Cheung, W. Y. (1980). Calmodulin plays a pivotal role in cellular regulation. Science *207*, 19-27.

Cho, J. H., Prince, J. E., and Cloutier, J. F. (2009). Axon guidance events in the wiring of the mammalian olfactory system. Mol Neurobiol *39*, 1-9.

Chou, M. M., Hou, W., Johnson, J., Graham, L. K., Lee, M. H., Chen, C. S., Newton, A. C., Schaffhausen, B. S., and Toker, A. (1998). Regulation of protein kinase C zeta by PI 3-kinase and PDK-1. Curr Biol *8*, 1069-1077.

Chung, J., Grammer, T. C., Lemon, K. P., Kazlauskas, A., and Blenis, J. (1994). PDGF- and insulin-dependent pp70S6k activation mediated by phosphatidylinositol-3-OH kinase. Nature *370*, 71-75.

Cohen, P., and Frame, S. (2001). The renaissance of GSK3. Nat Rev Mol Cell Biol *2*, 769-776.

Conigrave, A. D., Quinn, S. J., and Brown, E. M. (2000). L-amino acid sensing by the extracellular Ca2+-sensing receptor. Proc Natl Acad Sci U S A *97*, 4814-4819.

Coughlin, M. D., and Collins, M. B. (1985). Nerve growth factor-independent development of embryonic mouse sympathetic neurons in dissociated cell culture. Dev Biol *110*, 392-401.

Creedon, D. J., Johnson, E. M., and Lawrence, J. C. (1996). Mitogen-activated protein kinase-independent pathways mediate the effects of nerve growth factor and cAMP on neuronal survival. J Biol Chem *271*, 20713-20718.

Cross, D. A., Alessi, D. R., Cohen, P., Andjelkovich, M., and Hemmings, B. A. (1995). Inhibition of glycogen synthase kinase-3 by insulin mediated by protein kinase B. Nature *378*, 785-789.

Crowley, C., Spencer, S. D., Nishimura, M. C., Chen, K. S., Pitts-Meek, S., Armanini, M. P., Ling, L. H., McMahon, S. B., Shelton, D. L., Levinson, A. D., and et al. (1994). Mice lacking nerve growth factor display perinatal loss of sensory and sympathetic neurons yet develop basal forebrain cholinergic neurons. Cell *76*, 1001-1011.

Dahl, E., Koseki, H., and Balling, R. (1997). Pax genes and organogenesis. Bioessays *19*, 755-765.

D'Amico-Martel, A., and Noden, D. M. (1983). Contributions of placodal and neural crest cells to avian cranial peripheral ganglia. Am J Anat *166*, 445-468.

Datta, S. R., Dudek, H., Tao, X., Masters, S., Fu, H., Gotoh, Y., and Greenberg, M. E. (1997). Akt phosphorylation of BAD couples survival signals to the cell-intrinsic death machinery. Cell *91*, 231-241.

Davies, A., and Lumsden, A. (1984). Relation of target encounter and neuronal death to nerve growth factor responsiveness in the developing mouse trigeminal ganglion. J Comp Neurol *223*, 124-137.

Davies, A. M. (1987). Molecular and cellular aspects of patterning sensory neurone connections in the vertebrate nervous system. Development *101*, 185-208.

Davies, A. M. (1989). Intrinsic differences in the growth rate of early nerve fibres related to target distance. Nature *337*, 553-555.

Davies, A. M. (1994). Intrinsic programmes of growth and survival in developing vertebrate neurons. Trends Neurosci *17*, 195-199.

Davies, A. M. (1997). Neurotrophin switching: where does it stand? Curr Opin Neurobiol *7*, 110-118.
Davies, A. M. (2000). Neurotrophins: more to NGF than just survival. Curr Biol *10*, R374-376.

Davies, A. M. (2003). Regulation of neuronal survival and death by extracellular signals during development. Embo J *22*, 2537-2545.

Davies, A. M., Bandtlow, C., Heumann, R., Korsching, S., Rohrer, H., and Thoenen, H. (1987). Timing and site of nerve growth factor synthesis in developing skin in relation to innervation and expression of the receptor. Nature *326*, 353-358.

Davies, A. M., Lee, K. F., and Jaenisch, R. (1993). p75-deficient trigeminal sensory neurons have an altered response to NGF but not to other neurotrophins. Neuron *11*, 565-574.

Davies, A. M., Minichiello, L., and Klein, R. (1995). Developmental changes in NT3 signalling via TrkA and TrkB in embryonic neurons. Embo J *14*, 4482-4489.

Davies, A. M., Thoenen, H., and Barde, Y. A. (1986). The response of chick sensory neurons to brain-derived neurotrophic factor. J Neurosci *6*, 1897-1904.

De Camilli, P., Emr, S. D., McPherson, P. S., and Novick, P. (1996). Phosphoinositides as regulators in membrane traffic. Science *271*, 1533-1539.

De Cesare, D., Fimia, G. M., and Sassone-Corsi, P. (1999). Signaling routes to CREM and CREB: plasticity in transcriptional activation. Trends Biochem Sci *24*, 281-285.

Deckwerth, T. L., Elliott, J. L., Knudson, C. M., Johnson, E. M., Jr., Snider, W. D., and Korsmeyer, S. J. (1996). BAX is required for neuronal death after trophic factor deprivation and during development. Neuron *17*, 401-411.

Dent, E. W., and Gertler, F. B. (2003). Cytoskeletal dynamics and transport in growth cone motility and axon guidance. Neuron *40*, 209-227.

Dhand, R., Hara, K., Hiles, I., Bax, B., Gout, I., Panayotou, G., Fry, M. J., Yonezawa, K., Kasuga, M., and Waterfield, M. D. (1994). PI 3-kinase: structural and functional analysis of intersubunit interactions. Embo J *13*, 511-521.

Dickson, B. J., and Gilestro, G. F. (2006). Regulation of commissural axon pathfinding by slit and its Robo receptors. Annu Rev Cell Dev Biol *22*, 651-675.

Egea, J., and Klein, R. (2007). Bidirectional Eph-ephrin signaling during axon guidance. Trends Cell Biol *17*, 230-238.

Eickholt, B. J., Walsh, F. S., and Doherty, P. (2002). An inactive pool of GSK-3 at the leading edge of growth cones is implicated in Semaphorin 3A signaling. J Cell Biol *157*, 211-217.

Enokido, Y., Wyatt, S., and Davies, A. M. (1999). Developmental changes in the response of trigeminal neurons to neurotrophins: influence of birthdate and the ganglion environment. Development *126*, 4365-4373.

Ernfors, P., Lee, K. F., and Jaenisch, R. (1994). Target derived and putative local actions of neurotrophins in the peripheral nervous system. Prog Brain Res *103*, 43-54.

Ernsberger, U., Edgar, D., and Rohrer, H. (1989). The survival of early chick sympathetic neurons in vitro is dependent on a suitable substrate but independent of NGF. Dev Biol *135*, 250-262.

Etienne-Manneville, S., and Hall, A. (2003). Cdc42 regulates GSK-3beta and adenomatous polyposis coli to control cell polarity. Nature *421*, 753-756.

Fagan, A. M., Zhang, H., Landis, S., Smeyne, R. J., Silos-Santiago, I., and Barbacid, M. (1996). TrkA, but not TrkC, receptors are essential for survival of sympathetic neurons in vivo. J Neurosci *16*, 6208-6218.

Fang, X., Yu, S. X., Lu, Y., Bast, R. C., Jr., Woodgett, J. R., and Mills, G. B. (2000). Phosphorylation and inactivation of glycogen synthase kinase 3 by protein kinase A. Proc Natl Acad Sci U S A *97*, 11960-11965.

Farinas, I., Yoshida, C. K., Backus, C., and Reichardt, L. F. (1996). Lack of neurotrophin-3 results in death of spinal sensory neurons and premature differentiation of their precursors. Neuron *17*, 1065-1078.

Favor, J., Sandulache, R., Neuhauser-Klaus, A., Pretsch, W., Chatterjee, B., Senft, E., Wurst, W., Blanquet, V., Grimes, P., Sporle, R., and Schughart, K. (1996). The mouse Pax2(1Neu) mutation is identical to a human PAX2 mutation in a family with renal-coloboma syndrome and results in developmental defects of the brain, ear, eye, and kidney. Proc Natl Acad Sci U S A *93*, 13870-13875.

Ferry, S., Traiffort, E., Stinnakre, J., and Ruat, M. (2000). Developmental and adult expression of rat calcium-sensing receptor transcripts in neurons and oligodendrocytes. Eur J Neurosci *12*, 872-884.

Flanagan, J. G. (2006). Neural map specification by gradients. Curr Opin Neurobiol *16*, 59-66.

Forgie, A., Wyatt, S., Correll, P. H., and Davies, A. M. (2003). Macrophage stimulating protein is a target-derived neurotrophic factor for developing sensory and sympathetic neurons. Development *130*, 995-1002.

Francis, N., Farinas, I., Brennan, C., Rivas-Plata, K., Backus, C., Reichardt, L., and Landis, S. (1999). NT-3, like NGF, is required for survival of sympathetic neurons, but not their precursors. Dev Biol *210*, 411-427.

Fukada, T., Hibi, M., Yamanaka, Y., Takahashi-Tezuka, M., Fujitani, Y., Yamaguchi, T., Nakajima, K., and Hirano, T. (1996). Two signals are necessary for cell proliferation induced by a cytokine receptor gp130: involvement of STAT3 in anti-apoptosis. Immunity *5*, 449-460.

Ganitkevich, V., Hasse, V., and Pfitzer, G. (2002). Ca2+-dependent and Ca2+-independent regulation of smooth muscle contraction. J Muscle Res Cell Motil *23*, 47-52.

Gillespie, L. N. (2003). Regulation of axonal growth and guidance by the neurotrophin family of neurotrophic factors. Clin Exp Pharmacol Physiol *30*, 724-733.

Glebova, N. O., and Ginty, D. D. (2004). Heterogeneous requirement of NGF for sympathetic target innervation in vivo. J Neurosci *24*, 743-751.

Goold, R. G., and Gordon-Weeks, P. R. (2005). The MAP kinase pathway is upstream of the activation of GSK3beta that enables it to phosphorylate MAP1B and contributes to the stimulation of axon growth. Mol Cell Neurosci *28*, 524-534.

Gordon, A. M., Homsher, E., and Regnier, M. (2000). Regulation of contraction in striated muscle. Physiol Rev *80*, 853-924.

Gordon-Weeks, P. R. (2004). Microtubules and growth cone function. J Neurobiol *58*, 70-83.
Graef, I. A., Wang, F., Charron, F., Chen, L., Neilson, J., Tessier-Lavigne, M., and Crabtree, G. R. (2003). Neurotrophins and netrins require calcineurin/NFAT signaling to stimulate outgrowth of embryonic axons. Cell *113*, 657-670.

Grimes, C. A., and Jope, R. S. (2001). CREB DNA binding activity is inhibited by glycogen synthase kinase-3 beta and facilitated by lithium. J Neurochem *78*, 1219-1232.

Gundersen, R. W., and Barrett, J. N. (1979). Neuronal chemotaxis: chick dorsal-root axons turn toward high concentrations of nerve growth factor. Science *206*, 1079-1080.

Hall, A., and Nobes, C. D. (2000). Rho GTPases: molecular switches that control the organization and dynamics of the actin cytoskeleton. Philos Trans R Soc Lond B Biol Sci *355*, 965-970.

Hamburger, V., and Levi-Montalcini, R. (1949). Proliferation, differentiation and degeneration in the spinal ganglia of the chick embryo under normal and experimental conditions. J Exp Zool *111*, 457-501.

Hammerland, L. G., Krapcho, K. J., Garrett, J. E., Alasti, N., Hung, B. C., Simin, R. T., Levinthal, C., Nemeth, E. F., and Fuller, F. H. (1999). Domains determining ligand specificity for Ca2+ receptors. Mol Pharmacol *55*, 642-648.

Hannigan, G. E., Leung-Hagesteijn, C., Fitz-Gibbon, L., Coppolino, M. G., Radeva, G., Filmus, J., Bell, J. C., and Dedhar, S. (1996). Regulation of cell adhesion and anchorage-dependent growth by a new beta 1-integrin-linked protein kinase. Nature *379*, 91-96.

Hari, A., Djohar, B., Skutella, T., and Montazeri, S. (2004). Neurotrophins and extracellular matrix molecules modulate sensory axon outgrowth. Int J Dev Neurosci *22*, 113-117.

Hawkins, P. T., Jackson, T. R., and Stephens, L. R. (1992). Platelet-derived growth factor stimulates synthesis of PtdIns(3,4,5)P3 by activating a PtdIns(4,5)P2 3-OH kinase. Nature *358*, 157-159.

He, T. C., Zhou, S., da Costa, L. T., Yu, J., Kinzler, K. W., and Vogelstein, B. (1998). A simplified system for generating recombinant adenoviruses. Proc Natl Acad Sci U S A *95*, 2509-2514.

Hellard, D., Brosenitsch, T., Fritzsch, B., and Katz, D. M. (2004). Cranial sensory neuron development in the absence of brain-derived neurotrophic factor in BDNF/Bax double null mice. Dev Biol *275*, 34-43.

Helmbacher, F., Schneider-Maunoury, S., Topilko, P., Tiret, L., and Charnay, P. (2000). Targeting of the EphA4 tyrosine kinase receptor affects dorsal/ventral pathfinding of limb motor axons. Development *127*, 3313-3324.

Hempstead, B. L. (2002). The many faces of p75NTR. Curr Opin Neurobiol *12*, 260-267.

Henderson, T. A., Johnson, E. M., Jr., Osborne, P. A., and Jacquin, M. F. (1994). Fetal NGF augmentation preserves excess trigeminal ganglion cells and interrupts whisker-related pattern formation. J Neurosci *14*, 3389-3403.

Heyeraas, K. J., Haug, S. R., Bukoski, R. D., and Awumey, E. M. (2008). Identification of a Ca2+-sensing receptor in rat trigeminal ganglia, sensory axons, and tooth dental pulp. Calcif Tissue Int *82*, 57-65.

Higgs, H. N., and Pollard, T. D. (2000). Activation by Cdc42 and PIP(2) of Wiskott-Aldrich syndrome protein (WASp) stimulates actin nucleation by Arp2/3 complex. J Cell Biol *150*, 1311-1320.

Hill, R. E., Favor, J., Hogan, B. L., Ton, C. C., Saunders, G. F., Hanson, I. M., Prosser, J., Jordan, T., Hastie, N. D., and van Heyningen, V. (1991). Mouse small eye results from mutations in a paired-like homeobox-containing gene. Nature *354*, 522-525.

Hoeflich, K. P., Luo, J., Rubie, E. A., Tsao, M. S., Jin, O., and Woodgett, J. R. (2000). Requirement for glycogen synthase kinase-3beta in cell survival and NF-kappaB activation. Nature *406*, 86-90.

Hofer, A. M., and Brown, E. M. (2003). Extracellular calcium sensing and signalling. Nat Rev Mol Cell Biol *4*, 530-538.

Hogan, B. L., Horsburgh, G., Cohen, J., Hetherington, C. M., Fisher, G., and Lyon, M. F. (1986). Small eyes (Sey): a homozygous lethal mutation on chromosome 2 which affects the differentiation of both lens and nasal placodes in the mouse. J Embryol Exp Morphol *97*, 95-110.

Howe, L. R., Leevers, S. J., Gomez, N., Nakielny, S., Cohen, P., and Marshall, C. J. (1992). Activation of the MAP kinase pathway by the protein kinase raf. Cell *71*, 335-342.

Hu, J., McLarnon, S. J., Mora, S., Jiang, J., Thomas, C., Jacobson, K. A., and Spiegel, A. M. (2005). A region in the seven-transmembrane domain of the human Ca2+ receptor critical for response to Ca2+. J Biol Chem *280*, 5113-5120.

Huang, E. J., and Reichardt, L. F. (2001). Neurotrophins: roles in neuronal development and function. Annu Rev Neurosci *24*, 677-736.

Huang, E. J., Wilkinson, G. A., Farinas, I., Backus, C., Zang, K., Wong, S. L., and Reichardt, L. F. (1999). Expression of Trk receptors in the developing mouse trigeminal ganglion: in vivo evidence for NT-3 activation of TrkA and TrkB in addition to TrkC. Development *126*, 2191-2203.

Hughes, K., Nikolakaki, E., Plyte, S. E., Totty, N. F., and Woodgett, J. R. (1993). Modulation of the glycogen synthase kinase-3 family by tyrosine phosphorylation. Embo J *12*, 803-808.
Jacobson, A. G. (1963a). The Determination and Positioning of the Nose, Lens and Ear. I. Interactions within the Ectoderm, and between the Ectoderm and Underlying Tissues. J Exp Zool *154*, 273-283.

Jacobson, A. G. (1963b). The Determination and Positioning of the Nose, Lens and Ear. Ii. The Role of the Endoderm. J Exp Zool *154*, 285-291.

Jacobson, A. G. (1963c). The Determination and Positioning of the Nose, Lens and Ear. Iii. Effects of Reversing the Antero-Posterior Axis of Epidermis, Neural Plate and Neural Fold. J Exp Zool *154*, 293-303.

Jeffrey, K. L., Camps, M., Rommel, C., and Mackay, C. R. (2007). Targeting dual-specificity phosphatases: manipulating MAP kinase signalling and immune responses. Nat Rev Drug Discov *6*, 391-403.

Ji, R. R., and Suter, M. R. (2007). p38 MAPK, microglial signaling, and neuropathic pain. Mol Pain *3*, 33.

Jiang, H., Guo, W., Liang, X., and Rao, Y. (2005). Both the establishment and the maintenance of neuronal polarity require active mechanisms: critical roles of GSK-3beta and its upstream regulators. Cell *120*, 123-135.

Jimbo, T., Kawasaki, Y., Koyama, R., Sato, R., Takada, S., Haraguchi, K., and Akiyama, T. (2002). Identification of a link between the tumour suppressor APC and the kinesin superfamily. Nat Cell Biol *4*, 323-327.

Jones, K. R., Farinas, I., Backus, C., and Reichardt, L. F. (1994). Targeted disruption of the BDNF gene perturbs brain and sensory neuron development but not motor neuron development. Cell *76*, 989-999.

Jope, R. S., and Johnson, G. V. (2004). The glamour and gloom of glycogen synthase kinase-3. Trends Biochem Sci *29*, 95-102.

Karni, R., Jove, R., and Levitzki, A. (1999). Inhibition of pp60c-Src reduces Bcl-XL expression and reverses the transformed phenotype of cells overexpressing EGF and HER-2 receptors. Oncogene *18*, 4654-4662.

Katada, T., and Ui, M. (1982). ADP ribosylation of the specific membrane protein of C6 cells by islet-activating protein associated with modification of adenylate cyclase activity. J Biol Chem *257*, 7210-7216.

Klein, R. (1994). Role of neurotrophins in mouse neuronal development. Faseb J *8*, 738-744.

Klein, R., Smeyne, R. J., Wurst, W., Long, L. K., Auerbach, B. A., Joyner, A. L., and Barbacid, M. (1993). Targeted disruption of the trkB neurotrophin receptor gene results in nervous system lesions and neonatal death. Cell *75*, 113-122.

Klesse, L. J., Meyers, K. A., Marshall, C. J., and Parada, L. F. (1999). Nerve growth factor induces survival and differentiation through two distinct signaling cascades in PC12 cells. Oncogene *18*, 2055-2068.

Klippel, A., Kavanaugh, W. M., Pot, D., and Williams, L. T. (1997). A specific product of phosphatidylinositol 3-kinase directly activates the protein kinase Akt through its pleckstrin homology domain. Mol Cell Biol *17*, 338-344.

Kruger, R. P., Aurandt, J., and Guan, K. L. (2005). Semaphorins command cells to move. Nat Rev Mol Cell Biol *6*, 789-800.

Kuruvilla, R., Zweifel, L. S., Glebova, N. O., Lonze, B. E., Valdez, G., Ye, H., and Ginty, D. D. (2004). A neurotrophin signaling cascade coordinates sympathetic neuron development through differential control of TrkA trafficking and retrograde signaling. Cell *118*, 243-255.

Kwon, H. J., and Riley, B. B. (2009). Mesendodermal signals required for otic induction: Bmp-antagonists cooperate with Fgf and can facilitate formation of ectopic otic tissue. Dev Dyn *238*, 1582-1594.

Le Douarin, N. M. (2004). The avian embryo as a model to study the development of the neural crest: a long and still ongoing story. Mech Dev *121*, 1089-1102.

Le Good, J. A., Ziegler, W. H., Parekh, D. B., Alessi, D. R., Cohen, P., and Parker, P. J. (1998). Protein kinase C isotypes controlled by phosphoinositide 3-kinase through the protein kinase PDK1. Science *281*, 2042-2045.

LeMaster, A. M., Krimm, R. F., Davis, B. M., Noel, T., Forbes, M. E., Johnson, J. E., and Albers, K. M. (1999). Overexpression of brain-derived neurotrophic factor enhances sensory innervation and selectively increases neuron number. J Neurosci *19*, 5919-5931.

Levi-Montalcini, R. (1987). The nerve growth factor 35 years later. Science *237*, 1154-1162.

Levi-Montalcini, R., and Booker, B. (1960). Destruction of the Sympathetic Ganglia in Mammals by an Antiserum to a Nerve-Growth Protein. Proc Natl Acad Sci U S A *46*, 384-391.

Li, M., Wang, X., Meintzer, M. K., Laessig, T., Birnbaum, M. J., and Heidenreich, K. A. (2000). Cyclic AMP promotes neuronal survival by phosphorylation of glycogen synthase kinase 3beta. Mol Cell Biol *20*, 9356-9363.

Li, X., Bijur, G. N., and Jope, R. S. (2002). Glycogen synthase kinase-3beta, mood stabilizers, and neuroprotection. Bipolar Disord *4*, 137-144.

Li, Y., Jia, Y. C., Cui, K., Li, N., Zheng, Z. Y., Wang, Y. Z., and Yuan, X. B. (2005). Essential role of TRPC channels in the guidance of nerve growth cones by brain-derived neurotrophic factor. Nature *434*, 894-898.

Liebl, D. J., Tessarollo, L., Palko, M. E., and Parada, L. F. (1997). Absence of sensory neurons before target innervation in brain-derived neurotrophic factor-, neurotrophin 3-, and TrkC-deficient embryonic mice. J Neurosci *17*, 9113-9121.

Liepinsh, E., Ilag, L. L., Otting, G., and Ibanez, C. F. (1997). NMR structure of the death domain of the p75 neurotrophin receptor. Embo J *16*, 4999-5005.

Lindsay, R. M., Barde, Y. A., Davies, A. M., and Rohrer, H. (1985a). Differences and similarities in the neurotrophic growth factor requirements of sensory neurons derived from neural crest and neural placode. J Cell Sci Suppl *3*, 115-129.

Lindsay, R. M., Thoenen, H., and Barde, Y. A. (1985b). Placode and neural crest-derived sensory neurons are responsive at early developmental stages to brain-derived neurotrophic factor. Dev Biol *112*, 319-328.

Litsiou, A., Hanson, S., and Streit, A. (2005). A balance of FGF, BMP and WNT signalling positions the future placode territory in the head. Development *132*, 4051-4062.

Loisel, T. P., Boujemaa, R., Pantaloni, D., and Carlier, M. F. (1999). Reconstitution of actin-based motility of Listeria and Shigella using pure proteins. Nature *401*, 613-616.

Lonze, B. E., and Ginty, D. D. (2002). Function and regulation of CREB family transcription factors in the nervous system. Neuron *35*, 605-623.

Lonze, B. E., Riccio, A., Cohen, S., and Ginty, D. D. (2002). Apoptosis, axonal growth defects, and degeneration of peripheral neurons in mice lacking CREB. Neuron *34*, 371-385.
Lu, B., Pang, P. T., and Woo, N. H. (2005). The yin and yang of neurotrophin action. Nat Rev Neurosci *6*, 603-614.

Lucas, F. R., Goold, R. G., Gordon-Weeks, P. R., and Salinas, P. C. (1998). Inhibition of GSK-3beta leading to the loss of phosphorylated MAP-1B is an early event in axonal remodelling induced by WNT-7a or lithium. J Cell Sci *111 (Pt 10)*, 1351-1361.

Maina, F., and Klein, R. (1999). Hepatocyte growth factor, a versatile signal for developing neurons. Nat Neurosci *2*, 213-217.

Manoukian, A. S., and Woodgett, J. R. (2002). Role of glycogen synthase kinase-3 in cancer: regulation by Wnts and other signaling pathways. Adv Cancer Res *84*, 203-229.

Mansouri, A., Hallonet, M., and Gruss, P. (1996). Pax genes and their roles in cell differentiation and development. Curr Opin Cell Biol *8*, 851-857.

Markus, A., Patel, T. D., and Snider, W. D. (2002). Neurotrophic factors and axonal growth. Curr Opin Neurobiol *12*, 523-531.

Martin, K., and Groves, A. K. (2006). Competence of cranial ectoderm to respond to Fgf signaling suggests a two-step model of otic placode induction. Development *133*, 877-887.

Masuda, T., Watanabe, K., Sakuma, C., Ikenaka, K., Ono, K., and Yaginuma, H. (2008). Netrin-1 acts as a repulsive guidance cue for sensory axonal projections toward the spinal cord. J Neurosci *28*, 10380-10385.

Mazzoni, I. E., Said, F. A., Aloyz, R., Miller, F. D., and Kaplan, D. (1999). Ras regulates sympathetic neuron survival by suppressing the p53-mediated cell death pathway. J Neurosci *19*, 9716-9727.

Menesini Chen, M. G., Chen, J. S., and Levi-Montalcini, R. (1978). Sympathetic nerve fibers ingrowth in the central nervous system of neonatal rodent upon intracerebral NGF injections. Arch Ital Biol *116*, 53-84.

Mettling, C., Gouin, A., Robinson, M., el M'Hamdi, H., Camu, W., Bloch-Gallego, E., Buisson, B., Tanaka, H., Davies, A. M., and Henderson, C. E. (1995). Survival of newly postmitotic motoneurons is transiently independent of exogenous trophic support. J Neurosci *15*, 3128-3137.

Miller, F. D., and Kaplan, D. R. (2001). Neurotrophin signalling pathways regulating neuronal apoptosis. Cell Mol Life Sci *58*, 1045-1053.

Mukai, F., Ishiguro, K., Sano, Y., and Fujita, S. C. (2002). Alternative splicing isoform of tau protein kinase I/glycogen synthase kinase 3beta. J Neurochem *81*, 1073-1083.

Mullins, R. D., Heuser, J. A., and Pollard, T. D. (1998). The interaction of Arp2/3 complex with actin: nucleation, high affinity pointed end capping, and formation of branching networks of filaments. Proc Natl Acad Sci U S A *95*, 6181-6186.

Murphy, M., Dutton, R., Koblar, S., Cheema, S., and Bartlett, P. (1997). Cytokines which signal through the LIF receptor and their actions in the nervous system. Prog Neurobiol *52*, 355-378.

Nemeth, E. F., Delmar, E. G., Heaton, W. L., Miller, M. A., Lambert, L. D., Conklin, R. L., Gowen, M., Gleason, J. G., Bhatnagar, P. K., and Fox, J. (2001). Calcilytic compounds: potent and selective Ca2+ receptor antagonists that stimulate secretion of parathyroid hormone. J Pharmacol Exp Ther *299*, 323-331.

Nemeth, E. F., Steffey, M. E., Hammerland, L. G., Hung, B. C., Van Wagenen, B. C., DelMar, E. G., and Balandrin, M. F. (1998). Calcimimetics with potent and selective activity on the parathyroid calcium receptor. Proc Natl Acad Sci U S A *95*, 4040-4045.

Ng, J., and Luo, L. (2004). Rho GTPases regulate axon growth through convergent and divergent signaling pathways. Neuron *44*, 779-793.

Nguyen, T., and Di Giovanni, S. (2008). NFAT signaling in neural development and axon growth. Int J Dev Neurosci *26*, 141-145.

Nieuwkoop, P. D. (1985). Inductive interactions in early amphibian development and their general nature. J Embryol Exp Morphol *89 Suppl*, 333-347.

Ninkina, N., Adu, J., Fischer, A., Pinon, L. G., Buchman, V. L., and Davies, A. M. (1996). Expression and function of TrkB variants in developing sensory neurons. Embo J *15*, 6385-6393.

Nishizuka, Y. (1992). Intracellular signaling by hydrolysis of phospholipids and activation of protein kinase C. Science *258*, 607-614.

Nobes, C. D., and Hall, A. (1995). Rho, rac, and cdc42 GTPases regulate the assembly of multimolecular focal complexes associated with actin stress fibers, lamellipodia, and filopodia. Cell *81*, 53-62.

Nobes, C. D., and Tolkovsky, A. M. (1995). Neutralizing anti-p21ras Fabs suppress rat sympathetic neuron survival induced by NGF, LIF, CNTF and cAMP. Eur J Neurosci *7*, 344-350.

Nusser, N., Gosmanova, E., Zheng, Y., and Tigyi, G. (2002). Nerve growth factor signals through TrkA, phosphatidylinositol 3-kinase, and Rac1 to inactivate RhoA during the initiation of neuronal differentiation of PC12 cells. J Biol Chem *277*, 35840-35846.

Nykjaer, A., Lee, R., Teng, K. K., Jansen, P., Madsen, P., Nielsen, M. S., Jacobsen, C., Kliemannel, M., Schwarz, E., Willnow, T. E., *et al.* (2004). Sortilin is essential for proNGF-induced neuronal cell death. Nature *427*, 843-848.

O'Connor, R., and Tessier-Lavigne, M. (1999). Identification of maxillary factor, a maxillary process-derived chemoattractant for developing trigeminal sensory axons. Neuron *24*, 165-178.

Oppenheim, R. W. (1991). Cell death during development of the nervous system. Annu Rev Neurosci *14*, 453-501.

Orike, N., Thrasivoulou, C., Wrigley, A., and Cowen, T. (2001). Differential regulation of survival and growth in adult sympathetic neurons: an in vitro study of neurotrophin responsiveness. J Neurobiol *47*, 295-305.

Owen, R., and Gordon-Weeks, P. R. (2003). Inhibition of glycogen synthase kinase 3beta in sensory neurons in culture alters filopodia dynamics and microtubule distribution in growth cones. Mol Cell Neurosci *23*, 626-637.

Pak, C. W., Flynn, K. C., and Bamburg, J. R. (2008). Actin-binding proteins take the reins in growth cones. Nat Rev Neurosci *9*, 136-147.

Pap, M., and Cooper, G. M. (1998). Role of glycogen synthase kinase-3 in the phosphatidylinositol 3-Kinase/Akt cell survival pathway. J Biol Chem *273*, 19929-19932.

Parker, P. J., Caudwell, F. B., and Cohen, P. (1983). Glycogen synthase from rabbit skeletal muscle; effect of insulin on the state of phosphorylation of the seven phosphoserine residues in vivo. Eur J Biochem *130*, 227-234.

Patel, T. D., Jackman, A., Rice, F. L., Kucera, J., and Snider, W. D. (2000). Development of sensory neurons in the absence of NGF/TrkA signaling in vivo. Neuron *25*, 345-357.

Patel, T. D., Kramer, I., Kucera, J., Niederkofler, V., Jessell, T. M., Arber, S., and Snider, W. D. (2003). Peripheral NT3 signaling is required for ETS protein expression and central patterning of proprioceptive sensory afferents. Neuron *38*, 403-416.

Petruska, J. C., and Mendell, L. M. (2004). The many functions of nerve growth factor: multiple actions on nociceptors. Neurosci Lett *361*, 168-171.

Pezet, S., Malcangio, M., and McMahon, S. B. (2002). BDNF: a neuromodulator in nociceptive pathways? Brain Res Brain Res Rev *40*, 240-249.

Pinon, L. G., Minichiello, L., Klein, R., and Davies, A. M. (1996). Timing of neuronal death in trkA, trkB and trkC mutant embryos reveals developmental changes in sensory neuron dependence on Trk signalling. Development *122*, 3255-3261.

Pollack, S. J., and Harper, S. J. (2002). Trk Neurotrophin Receptor Activators. Drug News Perspect *15*, 268-277.

Pollard, T. D., and Borisy, G. G. (2003). Cellular motility driven by assembly and disassembly of actin filaments. Cell *112*, 453-465.

Postigo, A., Calella, A. M., Fritzsch, B., Knipper, M., Katz, D., Eilers, A., Schimmang, T., Lewin, G. R., Klein, R., and Minichiello, L. (2002). Distinct requirements for TrkB and TrkC signaling in target innervation by sensory neurons. Genes Dev *16*, 633-645.

Pruyne, D., Evangelista, M., Yang, C., Bi, E., Zigmond, S., Bretscher, A., and Boone, C. (2002). Role of formins in actin assembly: nucleation and barbed-end association. Science *297*, 612-615.

Qi, M., and Elion, E. A. (2005). MAP kinase pathways. J Cell Sci *118*, 3569-3572.

Quest, A. F. (1996). Regulation of protein kinase C: a tale of lipids and proteins. Enzyme Protein *49*, 231-261.

Quinlan, M. E., Heuser, J. E., Kerkhoff, E., and Mullins, R. D. (2005). Drosophila Spire is an actin nucleation factor. Nature *433*, 382-388.

Quinn, S. J., Kifor, O., Trivedi, S., Diaz, R., Vassilev, P., and Brown, E. (1998). Sodium and ionic strength sensing by the calcium receptor. J Biol Chem *273*, 19579-19586.
Raftopoulou, M., and Hall, A. (2004). Cell migration: Rho GTPases lead the way. Dev Biol *265*, 23-32.

Ramón y Cajal (1890). Sobre ciertos elementos bipolares del cerebelo y algunos delas mas sobre el crecimiento y evolucion de las fibras cerebelosas. Gac. Sanit. Barc. ano II nos. 5 y 7: 208-217

Ray, L. B., and Sturgill, T. W. (1987). Rapid stimulation by insulin of a serine/threonine kinase in 3T3-L1 adipocytes that phosphorylates microtubule-associated protein 2 in vitro. Proc Natl Acad Sci U S A *84*, 1502-1506.

Reichardt, L. F. (2006). Neurotrophin-regulated signalling pathways. Philos Trans R Soc Lond B Biol Sci *361*, 1545-1564.
Robinson, M., Adu, J., and Davies, A. M. (1996). Timing and regulation of trkB and BDNF mRNA expression in placode-derived sensory neurons and their targets. Eur J Neurosci *8*, 2399-2406.

Robles, E., Woo, S., and Gomez, T. M. (2005). Src-dependent tyrosine phosphorylation at the tips of growth cone filopodia promotes extension. J Neurosci *25*, 7669-7681.

Rodriguez-Tebar, A., Jeffrey, P. L., Thoenen, H., and Barde, Y. A. (1989). The survival of chick retinal ganglion cells in response to brain-derived neurotrophic factor depends on their embryonic age. Dev Biol *136*, 296-303.

Rodriguez-Viciana, P., Warne, P. H., Dhand, R., Vanhaesebroeck, B., Gout, I., Fry, M. J., Waterfield, M. D., and Downward, J. (1994). Phosphatidylinositol-3-OH kinase as a direct target of Ras. Nature *370*, 527-532.

Rohrer, H., Heumann, R., and Thoenen, H. (1988). The synthesis of nerve growth factor (NGF) in developing skin is independent of innervation. Dev Biol *128*, 240-244.
Rosenquist, G. C. (1981). Epiblast origin and early migration of neural crest cells in the chick embryo. Dev Biol *87*, 201-211.

Round, J., and Stein, E. (2007). Netrin signaling leading to directed growth cone steering. Curr Opin Neurobiol *17*, 15-21.

Rusakov, D. A., and Fine, A. (2003). Extracellular Ca2+ depletion contributes to fast activity-dependent modulation of synaptic transmission in the brain. Neuron *37*, 287-297.

Sato, N., L, Meier, et al (2004) Maintainence of pluripotency in human and mouse embryonic stem cells through activation of Wnt signaling by a pharmacological GSK-3-specific inhibitor Nat Med 10 (1): 55-63

Sayas, C. L., Avila, J., and Wandosell, F. (2002). Regulation of neuronal cytoskeleton by lysophosphatidic acid: role of GSK-3. Biochim Biophys Acta *1582*, 144-153.

Schimmang, T., Minichiello, L., Vazquez, E., San Jose, I., Giraldez, F., Klein, R., and Represa, J. (1995). Developing inner ear sensory neurons require TrkB and TrkC receptors for innervation of their peripheral targets. Development *121*, 3381-3391.

Schotte, P., Van Loo, G., Carpentier, I., Vandenabeele, P., and Beyaert, R. (2001). Lithium sensitizes tumor cells in an NF-kappa B-independent way to caspase activation and apoptosis induced by tumor necrosis factor (TNF). Evidence for a role of the TNF receptor-associated death domain protein. J Biol Chem *276*, 25939-25945.

Schwamborn, J. C., and Puschel, A. W. (2004). The sequential activity of the GTPases Rap1B and Cdc42 determines neuronal polarity. Nat Neurosci *7*, 923-929.
Scott, S. A., and Davies, A. M. (1993). Age-related effects of nerve growth factor on the morphology of embryonic sensory neurons in vitro. J Comp Neurol *337*, 277-285.
Selleck, M. A., and Bronner-Fraser, M. (1995). Origins of the avian neural crest: the role of neural plate-epidermal interactions. Development *121*, 525-538.

Shi, S. H., Jan, L. Y., and Jan, Y. N. (2003). Hippocampal neuronal polarity specified by spatially localized mPar3/mPar6 and PI 3-kinase activity. Cell *112*, 63-75.

Sitaramayya, A. (2002). Calcium-dependent activation of guanylate cyclase by S100b. Adv Exp Med Biol *514*, 389-398.

Smeyne, R. J., Klein, R., Schnapp, A., Long, L. K., Bryant, S., Lewin, A., Lira, S. A., and Barbacid, M. (1994). Severe sensory and sympathetic neuropathies in mice carrying a disrupted Trk/NGF receptor gene. Nature *368*, 246-249.

Smith, C. L., Afroz, R., Bassell, G. J., Furneaux, H. M., Perrone-Bizzozero, N. I., and Burry, R. W. (2004). GAP-43 mRNA in growth cones is associated with HuD and ribosomes. J Neurobiol *61*, 222-235.
Smith, L. G., and Li, R. (2004). Actin polymerization: riding the wave. Curr Biol *14*, R109-111.

Spencer, G. E., Lukowiak, K., and Syed, N. I. (2000). Transmitter-receptor interactions between growth cones of identified Lymnaea neurons determine target cell selection in vitro. J Neurosci *20*, 8077-8086.

Sperber, B. R., Leight, S., Goedert, M., and Lee, V. M. (1995). Glycogen synthase kinase-3 beta phosphorylates tau protein at multiple sites in intact cells. Neurosci Lett *197*, 149-153.

Stambolic, V., and Woodgett, J. R. (1994). Mitogen inactivation of glycogen synthase kinase-3 beta in intact cells via serine 9 phosphorylation. Biochem J *303 (Pt 3)*, 701-704.

Stephens, L. R., Hughes, K. T., and Irvine, R. F. (1991). Pathway of phosphatidylinositol(3,4,5)-trisphosphate synthesis in activated neutrophils. Nature *351*, 33-39.

Stokoe, D. (2005). The phosphoinositide 3-kinase pathway and cancer. Expert Rev Mol Med *7*, 1-22.

Stokoe, D., Engel, K., Campbell, D. G., Cohen, P., and Gaestel, M. (1992). Identification of MAPKAP kinase 2 as a major enzyme responsible for the phosphorylation of the small mammalian heat shock proteins. FEBS Lett *313*, 307-313.

Stone, L.S (1924) Experiments on the transplantation of placodes of the cranial ganglia in the amphibian embryo. I. Heterotopic transplantations of the ophthalmic placode upon the head of Amblystoma punctatum. J. Comp. Neurol. 38, 73-105.

Stone, L.S (1928) Experiments on the transplantation of placodes of the cranial ganglia in the amphibian embryo. II. Heterotopic transplantations of the ophthalmic placode upon the head and body of Amblystoma punctatum. J. Comp. Neurol. 47, 91-116.

Stone, L.S (1929) Experiments on the transplantation of placodes of the cranial ganglia in the amphibian embryo. IV. Heterotopic transplantations of the postauditory placodal material upon the head of Amblystoma punctatum. J. Comp. Neurol. 48, 311-330

Streit, A. (2001). Origin of the vertebrate inner ear: evolution and induction of the otic placode. J Anat *199*, 99-103.

Streit, A. (2002). Extensive cell movements accompany formation of the otic placode. Dev Biol *249*, 237-254.

Streit, A. (2004). Early development of the cranial sensory nervous system: from a common field to individual placodes. Dev Biol *276*, 1-15.
Streit, A. (2007). The preplacodal region: an ectodermal domain with multipotential progenitors that contribute to sense organs and cranial sensory ganglia. Int J Dev Biol *51*, 447-461.

Stull, J. T., Kamm, K. E., Krueger, J. K., Lin, P., Luby-Phelps, K., and Zhi, G. (1997). Ca2+/calmodulin-dependent myosin light-chain kinases. Adv Second Messenger Phosphoprotein Res *31*, 141-150.

Sun, S. K., Dee, C. T., Tripathi, V. B., Rengifo, A., Hirst, C. S., and Scotting, P. J. (2007). Epibranchial and otic placodes are induced by a common Fgf signal, but their subsequent development is independent. Dev Biol *303*, 675-686.

Svoboda, K., Denk, W., Kleinfeld, D., and Tank, D. W. (1997). In vivo dendritic calcium dynamics in neocortical pyramidal neurons. Nature *385*, 161-165.

Toker, A., and Cantley, L. C. (1997). Signalling through the lipid products of phosphoinositide-3-OH kinase. Nature *387*, 673-676.

Trivedi, N., Marsh, P., Goold, R. G., Wood-Kaczmar, A., and Gordon-Weeks, P. R. (2005). Glycogen synthase kinase-3beta phosphorylation of MAP1B at Ser1260 and Thr1265 is spatially restricted to growing axons. J Cell Sci *118*, 993-1005.

Vassilev, P. M., Mitchel, J., Vassilev, M., Kanazirska, M., and Brown, E. M. (1997). Assessment of frequency-dependent alterations in the level of extracellular Ca2+ in the synaptic cleft. Biophys J *72*, 2103-2116.

Virdee, K., and Tolkovsky, A. M. (1996). Inhibition of p42 and p44 mitogen-activated protein kinase activity by PD98059 does not suppress nerve growth factor-induced survival of sympathetic neurones. J Neurochem *67*, 1801-1805.

Vizard, T. N., O'Keeffe, G. W., Gutierrez, H., Kos, C. H., Riccardi, D., and Davies, A. M. (2008). Regulation of axonal and dendritic growth by the extracellular calcium-sensing receptor. Nat Neurosci *11*, 285-291.

Vogel, K. S., Brannan, C. I., Jenkins, N. A., Copeland, N. G., and Parada, L. F. (1995). Loss of neurofibromin results in neurotrophin-independent survival of embryonic sensory and sympathetic neurons. Cell *82*, 733-742.

Vogel, K. S., and Davies, A. M. (1991). The duration of neurotrophic factor independence in early sensory neurons is matched to the time course of target field innervation. Neuron *7*, 819-830.

Vogel, K. S., and Davies, A. M. (1993). Heterotopic transplantation of presumptive placodal ectoderm changes the fate of sensory neuron precursors. Development *119*, 263-276.
Voigt, J., and Papalopulu, N. (2006). A dominant-negative form of the E3 ubiquitin ligase Cullin-1 disrupts the correct allocation of cell fate in the neural crest lineage. Development *133*, 559-568.

Volinia, S., Hiles, I., Ormondroyd, E., Nizetic, D., Antonacci, R., Rocchi, M., and Waterfield, M. D. (1994). Molecular cloning, cDNA sequence, and chromosomal localization of the human phosphatidylinositol 3-kinase p110 alpha (PIK3CA) gene. Genomics *24*, 472-477.
Wang, Y., Awumey, E. K., Chatterjee, P. K., Somasundaram, C., Bian, K., Rogers, K. V., Dunn, C., and Bukoski, R. D. (2003). Molecular cloning and characterization of a rat sensory nerve Ca2+-sensing receptor. Am J Physiol Cell Physiol *285*, C64-75.
Ward, D. T. (2004). Calcium receptor-mediated intracellular signalling. Cell Calcium *35*, 217-228.

Watcharasit, P., Bijur, G. N., Zmijewski, J. W., Song, L., Zmijewska, A., Chen, X., Johnson, G. V., and Jope, R. S. (2002). Direct, activating interaction between glycogen synthase kinase-3beta and p53 after DNA damage. Proc Natl Acad Sci U S A *99*, 7951-7955.

White, F. A., Keller-Peck, C. R., Knudson, C. M., Korsmeyer, S. J., and Snider, W. D. (1998). Widespread elimination of naturally occurring neuronal death in Bax-deficient mice. J Neurosci *18*, 1428-1439.

Wilkinson, G. A., Farinas, I., Backus, C., Yoshida, C. K., and Reichardt, L. F. (1996). Neurotrophin-3 is a survival factor in vivo for early mouse trigeminal neurons. J Neurosci *16*, 7661-7669.

Willis, D., Li, K. W., Zheng, J. Q., Chang, J. H., Smit, A., Kelly, T., Merianda, T. T., Sylvester, J., van Minnen, J., and Twiss, J. L. (2005). Differential transport and local translation of cytoskeletal, injury-response, and neurodegeneration protein mRNAs in axons. J Neurosci *25*, 778-791.

Wu, K. Y., Hengst, U., Cox, L. J., Macosko, E. Z., Jeromin, A., Urquhart, E. R., and Jaffrey, S. R. (2005). Local translation of RhoA regulates growth cone collapse. Nature *436*, 1020-1024.

Wyatt, S., and Davies, A. M. (1993). Regulation of expression of mRNAs encoding the nerve growth factor receptors p75 and trkA in developing sensory neurons. Development *119*, 635-648.

Wyatt, S., Shooter, E. M., and Davies, A. M. (1990). Expression of the NGF receptor gene in sensory neurons and their cutaneous targets prior to and during innervation. Neuron *4*, 421-427.

Xing, J., Ginty, D. D., and Greenberg, M. E. (1996). Coupling of the RAS-MAPK pathway to gene activation by RSK2, a growth factor-regulated CREB kinase. Science *273*, 959-963.

Xing, J., Kornhauser, J. M., Xia, Z., Thiele, E. A., and Greenberg, M. E. (1998). Nerve growth factor activates extracellular signal-regulated kinase and p38 mitogen-activated protein kinase pathways to stimulate CREB serine 133 phosphorylation. Mol Cell Biol *18*, 1946-1955.

Yano, S., Brown, E. M., and Chattopadhyay, N. (2004). Calcium-sensing receptor in the brain. Cell Calcium *35*, 257-264.

Yip, H. K., Rich, K. M., Lampe, P. A., and Johnson, E. M., Jr. (1984). The effects of nerve growth factor and its antiserum on the postnatal development and survival after injury of sensory neurons in rat dorsal root ganglia. J Neurosci *4*, 2986-2992.

Yoshimura, T., Kawano, Y., Arimura, N., Kawabata, S., Kikuchi, A., and Kaibuchi, K. (2005). GSK-3beta regulates phosphorylation of CRMP-2 and neuronal polarity. Cell *120*, 137-149.

Zampieri, N., and Chao, M. V. (2006). Mechanisms of neurotrophin receptor signalling. Biochem Soc Trans *34*, 607-611.

Zhou, F. Q., and Snider, W. D. (2006). Intracellular control of developmental and regenerative axon growth. Philos Trans R Soc Lond B Biol Sci *361*, 1575-1592.

Zhou, F. Q., Zhou, J., Dedhar, S., Wu, Y. H., and Snider, W. D. (2004). NGF-induced axon growth is mediated by localized inactivation of GSK-3beta and functions of the microtubule plus end binding protein APC. Neuron *42*, 897-912.

Zvelebil, M. J., MacDougall, L., Leevers, S., Volinia, S., Vanhaesebroeck, B., Gout, I., Panayotou, G., Domin, J., Stein, R., Pages, F., and et al. (1996). Structural and functional diversity of phosphoinositide 3-kinases. Philos Trans R Soc Lond B Biol Sci *351*, 217-223.

Zweifel, L. S., Kuruvilla, R., and Ginty, D. D. (2005). Functions and mechanisms of retrograde neurotrophin signalling. Nat Rev Neurosci *6*, 615-625.